

1

REPORT DOCUMENTATION PAGE

Form Approved
OMB No. 0704-0188

1a. REPORT SECURITY CLASSIFICATION UNCLASSIFIED			1b. RESTRICTIVE MARKINGS NONE		
2a. SECURITY CLASSIFICATION AUTHORITY AD-A218 183			3. DISTRIBUTION/AVAILABILITY OF REPORT APPROVED FOR PUBLIC RELEASE; DISTRIBUTION UNLIMITED.		
6a. NAME OF PERFORMING ORGANIZATION AFIT STUDENT AT Indiana Univ			6b. OFFICE SYMBOL (If applicable)		7a. NAME OF MONITORING ORGANIZATION AFIT/CIA
6c. ADDRESS (City, State, and ZIP Code)			7b. ADDRESS (City, State, and ZIP Code) Wright-Patterson AFB OH 45433-6583		
8a. NAME OF FUNDING / SPONSORING ORGANIZATION		8b. OFFICE SYMBOL (If applicable)	9. PROCUREMENT INSTRUMENT IDENTIFICATION NUMBER		
8c. ADDRESS (City, State, and ZIP Code)			10. SOURCE OF FUNDING NUMBERS		
			PROGRAM ELEMENT NO.	PROJECT NO.	TASK NO.
			WORK UNIT ACCESSION NO.		
11. TITLE (Include Security Classification) (UNCLASSIFIED) DETECTION ACUITY IN THE PERIPHERAL RETINA					
12. PERSONAL AUTHOR(S) FRANK E. CHENEY, JR.					
13a. TYPE OF REPORT THESIS/DISSERTATION		13b. TIME COVERED FROM _____ TO _____		14. DATE OF REPORT (Year, Month, Day) 1989	
15. PAGE COUNT 158					
16. SUPPLEMENTARY NOTATION APPROVED FOR PUBLIC RELEASE IAW AFR 190-1 ERNEST A. HAYGOOD, 1st Lt, USAF Executive Officer, Civilian Institution Programs					
17. COSATI CODES			18. SUBJECT TERMS (Continue on reverse if necessary and identify by block number)		
FIELD	GROUP	SUB-GROUP			
19. ABSTRACT (Continue on reverse if necessary and identify by block number)					
<div style="text-align: center;">DTIC ELECTE S FEB 15 1990 D D a</div> <div style="text-align: right;">*Original contains color plates: All DTIC reproductions will be in black and white.</div> <div style="text-align: center; font-size: 2em; margin-top: 20px;">90 02 14 004</div>					
20. DISTRIBUTION / AVAILABILITY OF ABSTRACT <input checked="" type="checkbox"/> UNCLASSIFIED/UNLIMITED <input type="checkbox"/> SAME AS RPT. <input type="checkbox"/> DTIC USERS			21. ABSTRACT SECURITY CLASSIFICATION UNCLASSIFIED		
22a. NAME OF RESPONSIBLE INDIVIDUAL ERNEST A. HAYGOOD, 1st Lt, USAF			22b. TELEPHONE (Include Area Code) (513) 255-2259		22c. OFFICE SYMBOL AFIT/CI

**DETECTION ACUITY
IN THE PERIPHERAL RETINA**

BY

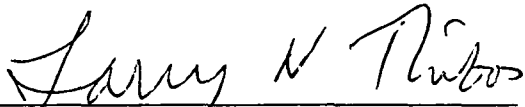
FRANK E. CHENEY, JR.

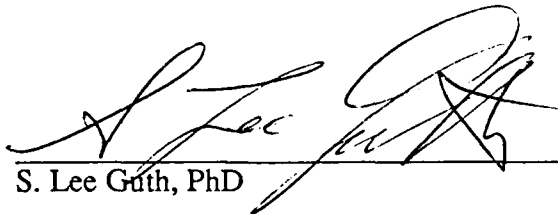
Submitted to the faculty of the Graduate School
in partial fulfillment of the requirements
for the degree of Master of Science
in the Department of Visual Sciences,
Indiana University
September, 1989

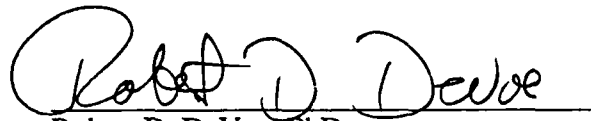
Accession For	
NTIS CRA&I	<input checked="checked" type="checkbox"/>
DTIC TAB	<input type="checkbox"/>
Unannounced	<input type="checkbox"/>
Justification	
By	
Distribution/	
Availability Codes	
Dist	Avail and/or Special
A-1	

RECEIVED
SEP 1989

Accepted by the faculty of the Graduate School Committee for Physiological Optics,
Indiana University, in partial fulfillment of the requirements of the degree of Master of
Science.


Larry N. Thibos, PhD, Chairman


S. Lee Guth, PhD


Robert D. DeVoe, PhD

ACKNOWLEDGEMENT

This project has been a long time coming to fruition and it is only through the assistance and encouragement of many individuals that, despite a couple unexpected scientific detours, it finally got completed.

My appreciation to the Air Force Institute of Technology for giving me this opportunity to pursue a graduate degree and to Dr Farrer and Lt Col Cartledge for allowing me to take an extended period of leave from work to finish writing this report

To my wife Heidi goes a debt of gratitude for her continual support and encouragement.

My thanks to Steve Gregory and Marcia Wilkins who so ably assisted in being subjects and in the collection of data.

I am grateful to Drs David Walsh and David Still whose worked on related research was so helpful to this project.

My appreciation to Dr Arthur Bradley for his participation as a subject, but even more for his many insights and his support.

My thanks goes to my committee members, Drs. Lee Guth and Robert Devoe for their time, effort, and counsel, not only for this thesis but during the entire graduate program.

I am especially indebted to Dr Larry Thibos who not only was the main subject and chairman of my committee, but was the person who kept putting this project back on course. His willingness to share his knowledge, to listen and take a real interest in a student's idea, and to get down in the trenches to give assistance, made it a privilege to be his student.


TABLE OF CONTENTS

Introduction.....	1
A. Isolating Roles of Successive Parts of Visual System.....	1
B. Basis for Current Investigation.....	1
1. Selective Filtering - A Way to Explore Peripheral Vision.....	1
2. Resolution Meridionally (Radially) Tuned in the Periphery.....	1
3. Aliasing in the Periphery (Detection of Gratings-like Percepts Above the Resolution Limit).....	3
4. Reports of Aliasing with Central Viewing.....	7
C. The Investigation Begins- Quantifying Detection Acuity Above the Resolution Limit for the Peripheral Retina Using Aliasing Percepts of Gratings Generated Interferometrically.....	8
1. The Horizontal Meridia in the Periphery.....	8
2. The Eight Primary Meridia in the Periphery.....	9
Methods.....	14
A. Apparatus.....	14
B. Procedure.....	15
1. White Light Experiment.....	15
2. 550 nm Interference Filter Control Experiments.....	16
3. Control Session with a Dilated Pupil.....	17
4. Further 550 nm Interference Filter Experiments.....	18
5. Analysis Of Data.....	19
6. Training Subjects.....	21
C. Rationale For Methods Used.....	21
1. The Lotmar Visometer and Optical Aberrations.....	21
2. Method of Adjustment.....	22
3. Constant Presence of Peripheral Target.....	22
Results.....	26
A. White Light Experiments.....	26
1. The Effect of Stimulus Orientation on Grating Detection.....	26
2. Quantative Analysis of the Meridional Effect.....	28
3. Quantative Analysis of the Oblique Effect.....	28
B. 550 nm Interference Filter Control Experiments.....	29
C. Control Session with a Dilated Pupil.....	30
D. Further 550 nm Interference Filter Control Experiments At 30 Degrees Eccentricity.....	31
E. Contrast Threshold Determination for LT for Horizontal Nasal Meridian at 30 Degrees Eccentricity.....	32
Discussion.....	61
A. Approach.....	61
B. Quantifying Detection Acuity Above the Resolution Limit Using Aliasing Percepts of Gratings Generated Interferometrically.....	61
1. Further Evidence that Aliasing Exists.....	61
2. Radial Tuning.....	62
3. How Do Detection Acuities Compare to Those Predicted by Cone Inner Segment Diameter?.....	63
4. Comparing Experimental Results at 30 Degrees Along The Horizontal Meridia with Theoretical Predictions of Contrast Degradation Due to Lateral Chromatic Aberration And Spatial Summation By Cones.....	67

5. Protective Effect of Longitudinal Aberration (Personal Communication; Zhang, Bradley, and Thibos)	74
6. Other Evidence of Aliasing in the Periphery Using Interferometric Techniques.....	75
C. Detection Above the Resolution Limit for Natural Viewing.....	75
1. Human Psychophysical Studies Using Natural Viewing	75
2. Quantifying Detection Acuity and Peripheral MTF at 30 Degrees in the Periphery (PhD Thesis by David Still).....	76
D. Overview.....	76
E. Conclusions	78
References	95
Appendix I.....	99
Appendix II.....	100
Appendix III.....	101
Appendix IV.....	102
Appendix V.....	123
Appendix VI.....	142
Vita	

INTRODUCTION

A. ISOLATING ROLES OF SUCCESSIVE PARTS OF VISUAL SYSTEM

— One of the goals in exploring vision is to isolate the role each successive part of the visual system plays in transforming an external visual stimulus into a visual percept. This requires that methods be used which can separately test the pre-retinal, retinal and post-retinal contributions. New electrophysiological and psychophysical techniques are enabling us to probe more accurately these individual components. By integrating and correlating these findings with known anatomical and psychophysical findings, investigators attempt to form a consistent model which can describe how the visual system functions. However, the information gained from investigating separate components, though essential to our total understanding of the system, will frequently seem misleading until the interactions of all the other components have been determined. This certainly has been true for this experiment. (K T) 

B. BASIS FOR CURRENT INVESTIGATION

1. Selective Filtering - A Way to Explore Peripheral Vision

For years researchers have been trying to determine the different contributions of peripheral visual function to our overall visual performance, to define what limits or modifies these inputs and to determine where in the visual pathway, pre-retinal, retinal or neural that the information is in some way altered or selectively filtered. Naturally they look for findings that show that selective filtering has occurred so they can begin to isolate the process which caused the change. This experiment was an example of that process in action.

2. Resolution Meridionally (Radially) Tuned in the Periphery

a. Extracellular recording from Cat ganglion cells

Levick and Thibos (1980) when doing extracellular recordings from cat ganglion cell located in the peripheral retina noticed that the response of a good proportion of ganglion cells seemed to be radially or meridionally tuned. This means that gratings which were oriented parallel (or nearly parallel) to the meridian tested frequently gave a more substantial response during these recordings than the non-meridionally oriented gratings. Care was taken to make sure the lines-of-sight for these stimuli were normal to the corneal surface. Levick and Thibos surmised that there was good reason to believe that the stimuli which reach the retina have all been equally filtered by the pre-retinal system and that an orientation bias might exist at the level of the retina. Previously all evidence of orientation bias had pointed toward a cortical origin.

b. Human Psychophysical Studies-Early Studies Using Natural Viewing

This meridional bias found in the cat peripheral retina may have prompted investigators to redirect their attention toward the question of whether horizontal and vertical gratings had a lower threshold than oblique gratings (commonly called the Oblique Effect) in the human periphery as they do in central foveal viewing. (See Appelle 1972 for summary) Rovamo et al. (1982), in a human psychophysical study which used natural viewing (therefore viewed through the eye's own peripheral optics) and a white light grating resolution task, found a meridional bias starting at 20 degrees eccentricity. Temme et al. (1982) also found a definite meridional bias for grating resolution at 30 degrees eccentricity. In order to rule out pre-retinal selective filtering as a possible cause for these findings, Rovamo et al, corrected peripheral refractive error and Temme et al. viewed the target through a pinhole, but the meridional effect remained. They concluded that the meridional effect appeared to have a neural as opposed to pre-retinal origin.

The supposition that this finding was due to retinal or post-retinal filtering seemed to be further supported by the work of Jennings and Charming (1984). They concluded that the optical quality of a dilated pupil using white light "changes relatively slowly with peripheral angle" and that spatial frequencies far above that resolved by the periphery reached the retinal surface. Therefore, the tremendous decrease in visual acuity with increasing eccentricity probably has a neural origin.

c. Human Psychophysical Studies using Achromatic Moire Interferometric viewing

Intrigued by the findings of meridional bias for resolution in the periphery by Rovamo et al, Temme et al, and Holt et al. (unpublished data), in 1985 Walsh and Thibos started to explore this phenomenon by making a systematic evaluation of the effect of different grating orientations on resolution. But instead of using natural viewing they used a Lotmar visometer (see description in Methods) , which gave them the unique opportunity to essentially bypass the peripheral refractive error and the majority of the other optical aberrations except for lateral chromatic aberration. Their results also showed a reduction of the oblique effect and an increase in the meridional effect with increasing eccentricity but the changeover was slower and a mixture of the two effects still remained at 30 degrees eccentricity for all subjects. (See Walsh, 1985, for complete summary.)

3. Aliasing in the Periphery (Detection of Gratings-like Percepts Above the Resolution Limit)

a. Discovery and Brief Description of Aliasing in Human Psychophysical Studies Using Achromatic Moire Interferometry

During the peripheral resolution experiment (Walsh and Thibos) using the Lotmar Visometer, Thibos noticed at very high frequencies, random noise which became interspersed with brief percepts of grating-like patterns as the spatial frequency was

reduced. As he continued to reduce the spatial frequency toward the resolution limit, (Thibos and Walsh, 1985) the grating percepts became more persistent but remained unstable, consisting of a sequence of gratings of rapidly changing orientation and relatively low spatial frequency. The apparent spatial frequency and orientation of the percept was frequently quite different from that of the grating actually present. This phenomenon is called aliasing is very compelling near the resolution limit.

Additionally, informal experiments convinced these researchers that aliasing could also be seen by natural viewing in the periphery, though this had never been observed in previous peripheral vision experiments using natural viewing such as those by Rovamo et al. and Temme et al. or even by LT, the first of our subjects to notice this phenomenon interferometrically.

b. Theory of Alias Production

Since a sinusoidal grating contains only one harmonic, the retina alone could account for equal limits for resolution and detection. It would require that the individual cell receptive field area, which dictates if a cell can detect a grating, and the spacing between receptive fields (the matrix), which can resolve the grating, be well-matched. In order to determine if this requirement is met, the limiting factors for both resolution and detection acuity must be determined and the possible ramifications of not being well-matched must be evaluated. Aliasing is one of the possible ramifications.

To resolve a grating, according to Shannon's sampling theory, the matrix would require one cell per bar of a cycle. To detect a grating requires a luminance difference between cells in the matrix. If we assume that the cell, as a detector, simply uniformly averages the light it receives, and that its output depends on this averaged light, then the less the difference in the output between cells, the less will be the modulation of the output signal. For example a 100% contrast sinusoidal grating with a period equal to the diameter of the cell would be reduced to a maximum of 18% modulation between the output of the cells

(see discussion section on Sombbrero function). When the threshold modulation for detection is reached (receptive field is too large to detect grating), the stimulus look as if it has a uniform luminance.

So what are the possible effects if resolution and detection are not well matched. If the cell receptive field size is too small the cells would be able to detect that a grating was present (visual noise, perhaps even an alias would occur) before the matrix could resolve it, but it would be a non-veridical representation of the stimulus. If the cell receptive field size were too large, the matrix would have the capability to resolve the grating before the individual receptive fields could detect it. If detection and resolution are matched, they will perfectly complement each other and have equal acuity thresholds.

Fig. I1 shows a square wave grating stimulus, which is a more complex stimulus than a sinusoidal grating, but it can still demonstrate how an alias could be produced by a regular matrix. The circles indicate the size of the receptive field of each cell. Assuming the area of the square is 1 deg squared the matrix could resolve 2 cycles per degree. Obviously, the receptive field, which does not reach 0% modulation for a square wave (for the first time) until the square wave grating has a period equal to the diameter of the receptive field, can detect a grating which is considerably smaller than the matrix can resolve. The stimulus, which is 4 cycles per degree, is above the resolution limit but well within the detection limit of the receptive field and produces an alias of a different spatial frequency and different orientation. As the spatial frequency of the stimulus increases in Fig. I2, it is possible the percept could even be that of a pair of crossed gratings.

c. Trying to Correlate Peripheral Aliasing with Known Anatomical and Psychophysical Findings

The results of Jennings and Charming indicated that the optical quality of the eye would permit the passage of spatial frequencies well above the resolution limit of the peripheral retina. (See Still, 1989 for a thorough discussion of this experiment.) However, many

scientists felt that what was known about the organizational interaction of the cones and ganglion cells would not support the detection of a grating above its resolution limit.

The peripheral retina has many interactions occurring between each layer and between subsequent layers which affect how the overall retina selectively filters and samples the signal as it recodes the physical light stimulus into a neural signal. The two most critical components of this process are the cones, which transduce the light into a neural signal, and the ganglion cells which receive this signal from the cone via the bipolar cells and send a signal to the brain. There are many types of ganglion cells in the retina, some with large dendritic fields which receive input from many cones (high convergence factor), some with smaller dendritic fields such as beta cells and some with a very small dendritic field called midget ganglion cells. It is conceivable that some midget ganglion cells may receive input from only one cone and form what Polyak (1941) describes as a "monosynaptic" pathway. Presumably each different type ganglion cell has a different function. Each cone-ganglion cell type forms its own network which has a resolution capability defined by the spacing between ganglion cells which is probably irregular and a detection capability defined in part by its receptive field size. Unlike a circular receptive field of a cone which should act linearly, the receptive field of the ganglion cells with all the complex interactions (amacrine and horizontal cells) in the retina may contain non-linear subunits which may amplify the contribution of certain inputs and improve its detection capability. This diversity of ganglion types plus the many possible interactions within and between each type greatly complicates the ability to predict resolution and detection thresholds from known retinal structure. Therefore, considering the large receptive fields of many of the ganglion cells (along with no substantiated "monosynaptic pathway"), the predicted irregularity of their spacing which would scatter frequencies above the resolution limit into broadband noise (Yellot, 1984), and the complete absence of any prior psychophysical evidence, it is not surprising that scientists found aliasing in the periphery unlikely.

4. Reports of Aliasing with Central Viewing

About the same time Williams (1983; 1985) was exploring the aliasing phenomenon centrally using a helium-neon laser interferometer and was actively seeking possible alternative explanations for what he was observing. Centrally, possible observations of aliasing had been observed earlier; (Helmoltz, 1962; Byram, 1944; Bergman, 1858), but these reports were the rare exception and could have had other possible explanations.

Centrally it was known that the eye's pre-retinal optics, its MTF, acted as a low pass filter and severely attenuated spatial frequencies above the resolution capability of the eye (Campbell and Gubisch, 1966) so that there was little chance that foveal aliasing would be a problem. In fact it had seemed likely that even if the higher spatial frequencies had reached the retina, that several additional factors (Williams, 1985) could prevent aliasing from occurring.

Even though Polyak (1941) demonstrated the "monosynaptic" pathway in the fovea, Yellot (1982) had felt the irregularity of the cone mosaic would cause aliases to be formed simultaneously for a wide range of orientations which would be extremely noisy and hard to interpret. However, this conclusion was basis on a spectral analysis of human foveal outer cone segments. Yellot (1984) reevaluated this position and agreed with Miller and Bernard (1983) who felt the more regular inner cone segment was the key cone component and that this regularity could permit foveal aliasing to occur. However, the cone's receptive field size still needed to be considered. Miller and Bernard (1983) felt that the cones may act as a low pass filter, attenuating the higher spatial frequencies and complementing the pre-retinal optics. Lastly, fixation instability could cause higher temporal frequencies that could blur and attenuate the high spatial frequencies, again acting as a low pass filter.

Williams used a damped first order Bessel function (Sombbrero), suggested by Miller and Bernard (1983), to describe the loss of contrast for the detection of a sinusoidal grating

caused by the cone aperture. The function predicts that the contrast of 100% sinusoidal grating would be reduced to zero percent (reach its first zero crossover) when the spatial frequencies period was 1.22 times the aperture diameter. Using his experimental findings, Williams data indicated that the limiting aperture to detection was approximately 2.32 microns. This agreed nicely with the estimate Miller and Bernard (1983) for the inner cone segment diameter of 2.4 microns based on the anatomical data. Thus, for the first time the aliasing percept was validated and was beginning to be examined more closely.

C. THE INVESTIGATION BEGINS- Quantifying Detection Acuity Above the Resolution Limit for the Peripheral Retina Using Aliasing Percepts of Gratings Generated Interferometrically

1. The Horizontal Meridia in the Periphery

Continuing to use the Lotmar Visometer, Walsh and Thibos started the job of quantifying the upper detection limit in order to determine the width of the aliasing zone. Since the percepts at the very high spatial frequencies were fleeting, and erratic, using these percepts as detection criteria would make the endpoint very unstable. Thus, the detection acuity was defined as the highest spatial frequency which produced the percept of a persistent grating-like pattern. Using the method of adjustment and proceeding from non-seeing to seeing, they studied detection as a function of stimulus frequency and orientation along the horizontal nasal meridian for six eccentricities between 10 and 35 degrees. They found that for eccentricities of 20 degrees or greater there was a definite meridional effect for detection. Fig. I2 and Fig. I3 show the results for LT at 20 and 30 degrees in the periphery. They are plotted on a logarithmic scale so that the magnitude of the difference between the meridional grating and the other orientations is substantial. The width of the aliasing zone between detection and resolution has increased at 30 degrees, mainly due to the decrease in resolution acuity. But the most striking result was that the subject seems to have the ability to detect a 20/20 grating as far as 35 degrees into the periphery. Thibos

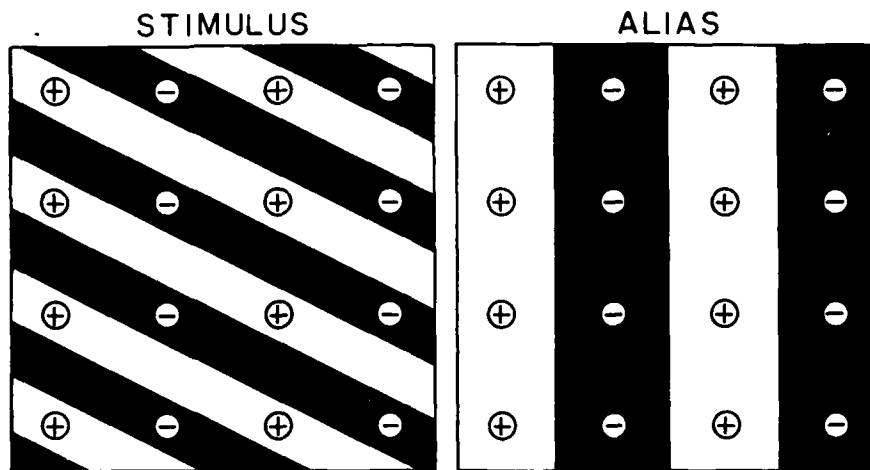
and Cheney finished the temporal field, and Fig I4 from (Thibos, Walsh, and Cheney, 1987) shows the magnitude of the difference between resolution and detection limits for horizontal (meridional) gratings for LT for the two horizontal meridia. It is also plotted on a logarithmic scale so that the greater width of the aliasing zone with increasing eccentricity indicates a larger detection to resolution ratio which reaches 10 at 35 degrees. The data separate the spectrum of visible spatial frequencies into a zone of veridical perception, which lies beneath the resolution limit, and a zone of aliasing which extends from the resolution limit to the detection limit. The detection value for central viewing was taken from Williams (1985).

2. The Eight Primary Meridia in the Periphery

The experiments described in this thesis went on to explore whether this meridional effect was found in the other primary meridia as well; to quantify using a narrowband 550 filter whether lateral chromatic aberration, which is the major uncorrected aberration in this experiment, had any affect on this radial tuning; to examine the receptive field characteristics of the combined retinal and post-retinal visual pathway; and to relate our findings to the aliasing results for natural viewing which were being explored by other researchers during this four year time span.

FIG. 11. UNDERSAMPLING CAUSING AN ALIAS PERCEPT.

A



B

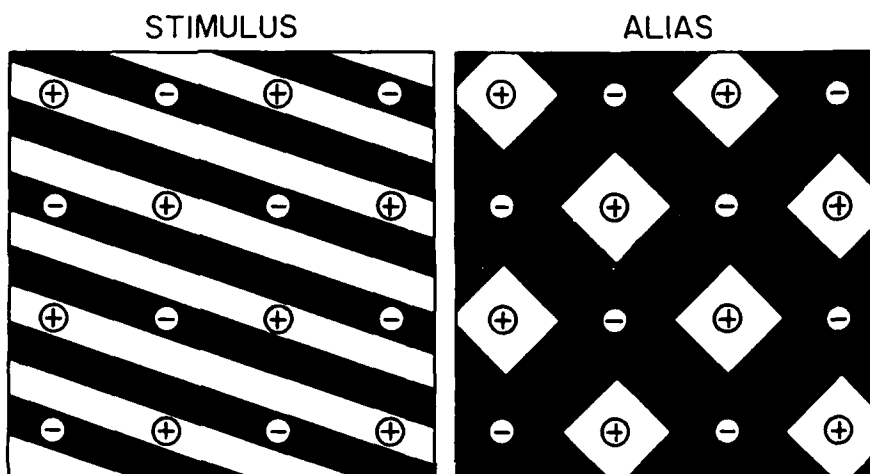


FIG. 12. ALIASING ZONE FOR LT AT 20 DEG ECCENTRICITY

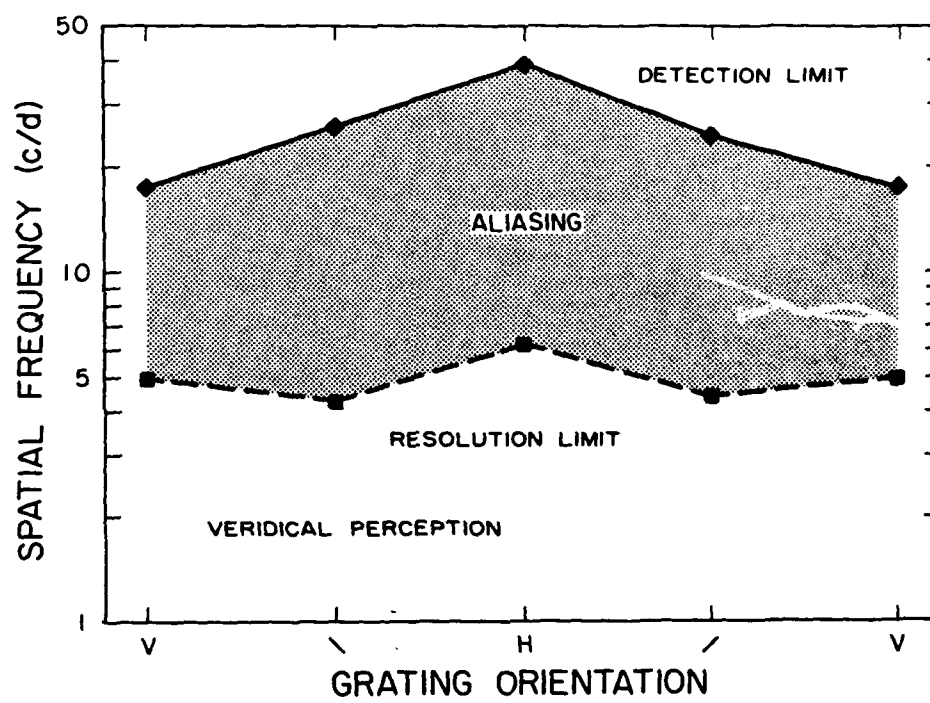


FIG. 13. ALIASING ZONE FOR LT AT 30 DEG ECCENTRICITY

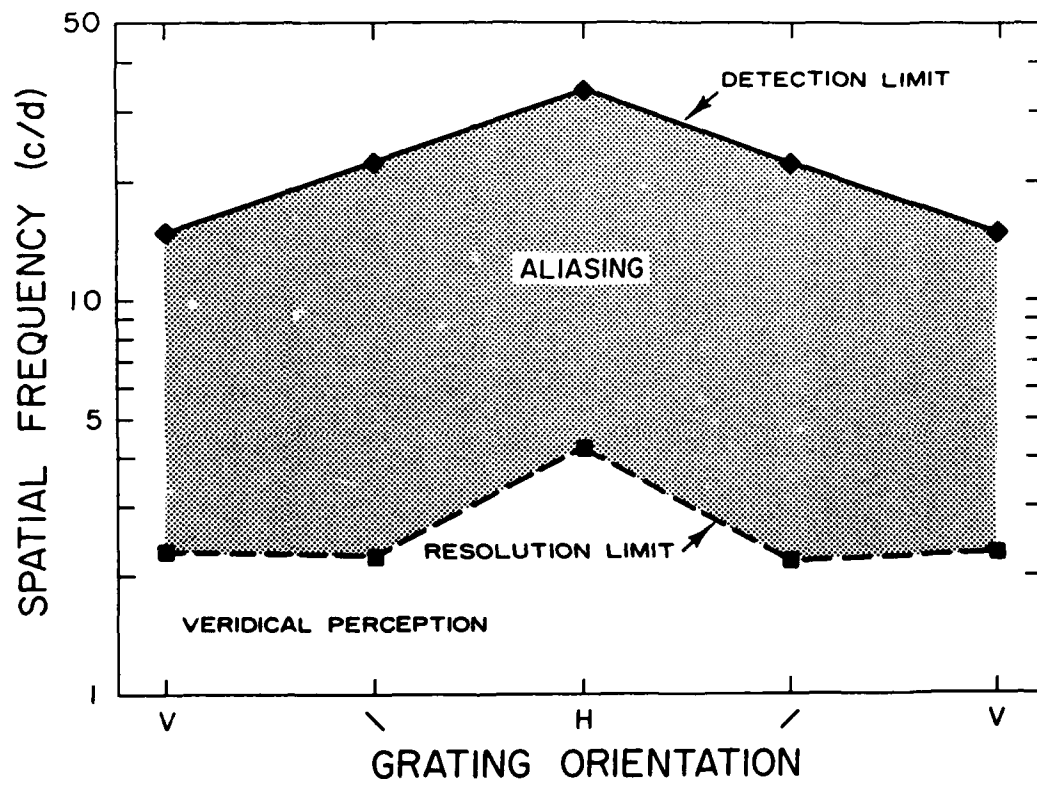
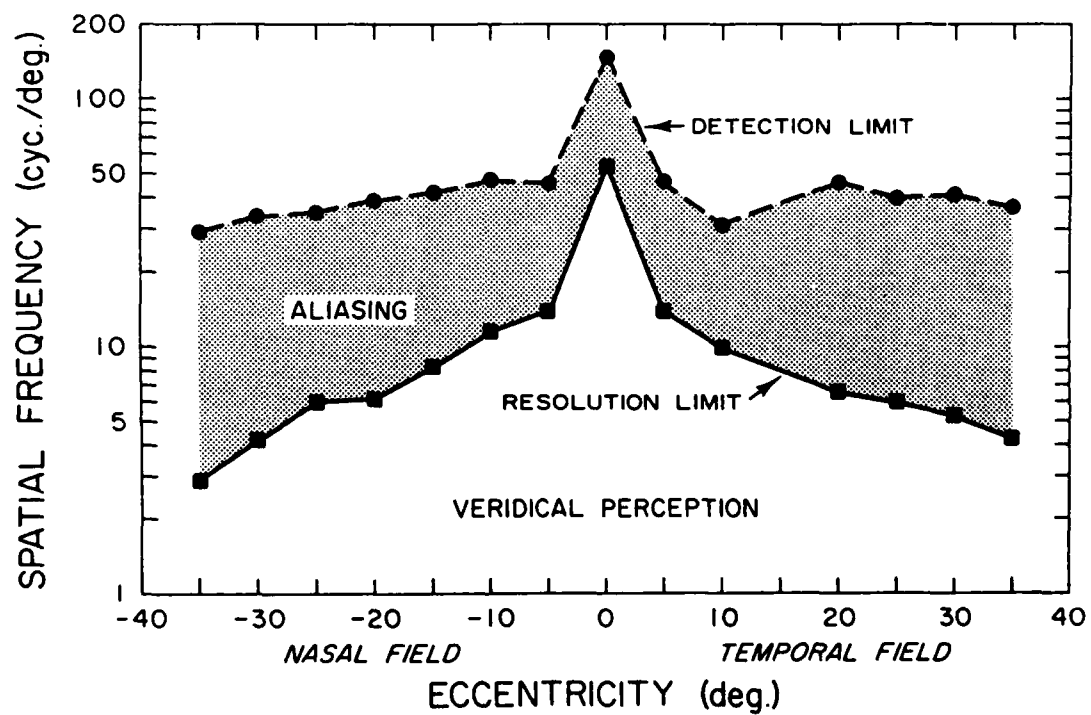


FIG. 14. ALIASING ZONE FOR HORIZONTAL GRATINGS FOR LT IN
HORIZONTAL MERIDIAN



METHODS

A. APPARATUS

The apparatus was a commercially available clinical instrument, the Lotmar Visometer (Lotmar, 1970), manufactured by Haag Streit, Berne, Switzerland and described by Thibos and Walsh (OSA, Digest Tech papers, 1985) and by Walsh (1985). It was installed on a modified gimbal by Dr. Walsh and could be rotated around the entrance pupil of the eye and positioned at the required eccentricity and meridian. The gimbal is secured on a wooden base which is set in a track that allows movement backwards and forwards to maintain a fixed distance from the instrument to the cornea.

All experiments were done on the subject's right eye. The naming convention for visual meridians labels the temporal field as 0 and proceeds counterclockwise until we end with numbering the inferior temporal as 315. The absolute stimulus orientation labels reflects (or derives from) the meridian to which the grating is parallel (e.g. a 45 degree grating is parallel to the 45 degree. superior temporal meridian). Relative orientation of the grating is measured counterclockwise from the visual meridian. See Fig. M1. With the left eye patched, the right fixated a 0.86 degree illuminated astigmatic dial which was seen at a distance of 6 meters. The subject's head was held erect and his gaze was in the primary position. A bite bar, which could be adjusted both horizontally and vertically, allowed the subject to maintain critical alignment.

The achromatic moire interferometer generates two spatially-coherent, white quasi-point sources, which enter the eye in Maxwellian view, and form high contrast interference fringes on the retina. The separation of the two points determines the grating's spatial frequency and was controlled by a knob calibrated in a 0.6 cycle/degree divisions but which could easily be read to the nearest 0.3 cycle/degree. The manufacturer's calibrations were verified photographically (Walsh, 1985). Additional verification involved measurement of the separation of the individual color components of the point source. The

two sources were viewed with a compound microscope (15x eyepiece, 4x objective) by removing the condensing lens and light source and substituting the Visometer. Calibrated interference filters were placed between the visometer and objective to isolate, in turn, different spectral components. Test separation was measured with a calibrated graticule and results are shown in Appendix I. The red end of the spectrum needs to be separated a greater distance than the blue end to achieve the same spatial frequency. Therefore, microscopically the two point sources looked like a rainbow (see Fig. M2). The measured results were all within 5% of their nominal values.

The target size was normally 3.5 degrees, but occasionally a 2.5 or 1.5 degree target was used. The retinal illuminance of the gratings were measured by Walsh (1985) using a Pritchard photometer and the method described by Westheimer (1966). The result was 3.2 log Trolands with the 0.5 Neutral density filter in place. I repeated this measurement and found the value without the neutral density filter to be 3.64 log Trolands. In addition, I calibrated the instrument by placing an interference filter in the *light path* so as to provide monochromatic light. The values obtained are given in Appendix II.

The grating stimulus was surrounded by a white field. This included a white cap which had been installed to the the black annulus inside the instrument which surrounded the grating and a large piece of white cardboard which provided a large, uniform field with luminance adjusted to match that of the grating. (See Fig. M3 for photograph of experimental setup.)

B. PROCEDURE

1. White Light Experiment

LT, SG, AB, and FC served as subjects. SG wore soft contact lens which left uncorrected 0.75 diopters of astigmatism. Refractive errors of all other subjects were near plano with 1.00 diopter of astigmatism or less. Since the design of the instrument

minimizes the effect of small refractive errors, no other correction other than the soft contact lens were worn.

Using the Method of Adjustment, subjects reduced the spatial frequency until a pattern-like percept was perceived to be consistently present. This spatial frequency will be referred to as the detection acuity.

Each session consisted of taking five readings in a pseudorandom order at each of four stimulus orientations (0, 45, 90, 135 degrees). Sessions were done at various eccentricities ranging from 5 to 35 degrees. Subjects FC and AB were only tested in the horizontal nasal meridian while subjects LT and SG were test in the eight primary meridians with special emphasis at 20 and 30 degrees eccentricity. Each session lasted from 1/2 to 1 hour. Subjects were then asked to comment on their opinion of the consistency of their criterion and for a description of their subjective percepts seen during that session.

2. 550 nm Interference Filter Control Experiments

To eliminate the influence of the eye's chromatic aberration on our experiments, a 550 nm interference filter was inserted between the instrument's light source and its 0.15 mm entrance pupil. The filter made the stimulus more temporally coherent and had a half bandwidth of approximately 9 nm as calibrated with a Beckman spectrophotometer (Appendix III) while reducing the the luminance of the stimulus to 2.4 log Trolands. The luminance of the fixation target and the illuminance of the the background were matched to the reduced stimulus luminance.

Because of the reduced light levels, the eye's pupils was larger than for the white light experiment. This along with the fact that only green light was entering the subject's eye increased his chance of undetected alignment error. He no longer had the colored fringes to tell him that the stimulus may be getting partially blocked by the pupil's edge causing a reduction in contrast. Also even if the subject's pupil was not blocking the stimulus, the larger pupil made it more difficult to judge when he was centrally aligned in the pupil. For

one subject, SG, who had a larger average pupil size than the other subjects, alignment was accomplished by centering the white light stimulus first before adding the 550 nm filter.

This experiment was limited to the horizontal meridian. Otherwise the experimental protocol was the same as for the white light experiment.

3. Control Session with a Dilated Pupil

As a control to investigate whether the meridional effect could be caused by the oval shape of the pupil as viewed off axis, subject LT's pupil was dilated with 1% cyclogel. The machine's 0.5 ND filter was used to reduce the luminance level from 3.64 to 3.13 log Trolands. However, this light level is still 0.7 log units brighter than the 550 nm experiments.

The eccentricity was set at 30 degrees into the temporal meridian which had shown a definite meridional effect in earlier white light experiments and the two point sources were positioned in the center of the entrance pupil. A preliminary trial was run after dilation to familiarize the subject with the task and to get background luminances adjusted. Also during this preliminary trial, detection acuities were recorded for all four orientations to check if the horizontal gratings still gave the highest detection acuity and the vertical gratings the lowest acuity. Once it was determined that the meridional effect was still present, it was assumed that if the vertical and horizontal detection acuities became similar that this would be true for the oblique meridians as well. Therefore, a regular trial was run in which only horizontal and vertical gratings were tested.

The bite bar was then adjusted a few millimeters horizontally and vertically to determine the location that gave the highest detection acuity for vertical gratings. Horizontal and vertical gratings were again tested.

Next, leaving the machine's location fixed, the 550 narrow band filter was swapped with the 0.5 neutral density filter and changes in the background illuminance and fixation target luminance were made. The horizontal and vertical gratings were retested.

Since the subject felt his percept of the alias was different than in previous experiments, the subject then returned the next morning with his accommodation almost completely returned to normal but with his pupil still well dilated at 7 mm. A control session then repeated the previous day's trial run and the results were recorded.

4. Further 550 nm Interference Filter Experiments

a. Continuation of Other Meridia at 30 Degrees Eccentricity

Since the first 550 nm interference filter experiment was limited to the horizontal meridian, three years later another experiment was run on all eight primary meridia at 30 degrees eccentricity on our most consistent subject, LT. However, the original Lotmar visometer had already been converted so that it could vary contrast as well as spatial frequency. Therefore to make this experimental setup as similar as possible to the original, a second Lotmar visometer which was the same model as the original was substituted. A less formal check than the initial experiments was made by matching the brightness of the Lotmar field to that of a CRT. This check yielded approximately 2.2 log Trolands for the target. Two meridia 225 and 270 were run at all four orientations. However, since in the white light experiments the meridional grating at 30 degrees eccentricity had always given the highest detection acuity and the tangential grating the lowest detection acuity, only the meridional and tangential gratings were tested in the other 6 meridia.

b. Determination of Contrast Thresholds for Several Spatial Frequencies for the Horizontal Nasal Meridian at 30 Degrees Eccentricity.

This experiment used the original Lotmar visometer which had been modified by Still to vary contrast by adding an extra light channel. In order to get a homogeneous field the target diameter was reduced to 2.5 degrees (3.5 degree was used in most of the previous experiments) and to get enough light the entrance pupil was changed from 0.15 to 0.5 mm.

He then added stepper motors so that both the contrast and spatial frequency could be accurately monitored and controlled by a Macintosh II computer (Still, 1989). The experiment used method of adjustment and averaged the non-seeing to seeing trials (subject increases contrast until aliasing appears) and the seeing to non-seeing trials (subject decreases contrast sensitivity until aliasing disappears). This was done for vertical gratings of 10, 15, 20, 25, and 30 cycle per degree. Our target was approximately 2.6 log Trolands. Still had run a similar experiment, but his method employed two-alternative forced choice.

5. Analysis Of Data

a. Simple Grouping of Trends

The variation of highest detectable spatial frequency with grating orientation will be referred to as an "orientation tuning curve". Each tuning curve was defined by 4 points corresponding to horizontal, vertical, left oblique and right oblique gratings. Specific attention was focused on grouping the data based on both absolute and relative orientations. Relative orientations reorganized all the data relative to the grating parallel to the meridian being tested. Major trends found in the data were evaluated by determining the simple probability of that grouping occurring by chance.

b. Fourier Analysis

Each orientation tuning curve was analyzed using Fourier analysis. With four data points the results can be fit by a Fourier series with 4 coefficients, the mean ($A_0/2$), the cosine (A_1) and the sine (B_1) components of the first harmonic and the cosine (A_2) of the second harmonic. Since the maximum amplitude of a component is determined by the session's mean, I computed the modulation of each Fourier component by dividing each coefficient by the mean for their session. But comparing the modulations for A_1 's, B_1 's, and A_2 's of the different meridians only gives us the absolute modulation of each

component. This is valuable information but relationships that occur that revolve around the meridian being tested are more difficult to appreciate. Using the relative orientation tuning curves, I equated the A_1 component (A_1 meridionally shifted) to the grating parallel to the meridian being tested. This organized the results to more easily evaluate similarities due to radial tuning.

Summary of Interpretations For Absolute and Relative Fourier Coefficients

Absolute Tuning Curves

1. A_1/mean = Modulation of fundamental cosine component
2. B_1/mean = Modulation of fundamental sine component
3. A_2/mean = Modulation of second harmonic cosine component

(Direct measure of the magnitude of the oblique effect for detection)

Relative tuning Curves

1. $A_1(\text{meridionally-shifted})/\text{mean}$ = Modulation of fundamental of cosine component relative to meridian being tested.
(direct measure of the magnitude of a meridional effect)
2. $B_1(\text{meridionally-shifted})/\text{mean}$ = Modulation of fundamental of sine component relative to meridian being tested.
(Check for deviation of results from meridional effect and demonstrate if there is any difference between the two stimuli that are 45 degrees to either side of the meridional stimulus.)
3. $A_2(\text{meridionally-shifted})/\text{mean}$ = Modulation of the second harmonic of the cosine component relative to the meridian being tested.
(Checks for systematic variation between the meridional-tangential gratings and the gratings 45 degrees to either side. A meridionally-induced oblique effect)

c. Statistical Method

An attractive method of assessing the statistical significance of these results is ANOVA especially designed for Fourier data by Hartley (1949). One program evaluated the significance of the combined meridional effect $(A_1^{**2} + B_1^{**2})^{**}(1/2) = M_1$ and the significance of the one secondary harmonic component. This will show the presence or absence of a significant fundamental component and / or a secondary harmonic component but does not directly relate the fundamental to a specific orientation unless an angular component is also included. However, another program evaluates the contribution of the A_1 and B_1 components independently and has been modified to list the results in terms of the meridionally shifted A_1 component (A_1_MS), in addition to the meridionally shifted B_1 component (B_1_MS) and both the meridionally and non meridionally shifted A_2 components. Any significant systematic meridional variation of the data becomes readily apparent and allows the examination of possible influences of chromatic aberration which would be directly related to radial tuning.

6. Training Subjects

LT and AB were experienced subjects who had participated in numerous prior experiments requiring accurate peripheral judgments. LT, in fact, had been a subject in similar experiments for about 1/2 year and was the individual who first noticed the aliasing phenomenon while he was doing a resolution task. FC and SG required more extensive training to achieve steady fixation centrally while attending to a very demanding peripheral task.

C. RATIONALE FOR METHODS USED

1. The Lotmar Visometer and Optical Aberrations

The Lotmar Visometer enables us to separate the pre-retinal influence from that of the neural retina. Minor refractive errors are relatively unimportant. Spherical aberration is not

a problem since only two point sources are used. For the same reason coma is not a problem for the oblique rays. Lateral chromatic aberration can be a problem but is controlled by passing the stimulus through a narrow band-pass filter. Using an interference filter with a peak transmission at 550 nm, we make the stimulus more temporally coherent and eliminate most of the effects of chromatic aberration while we still obtain almost a 100 percent contrast. Therefore this interferometer combined with a narrow band filter seems to be able to bypass the optics of the eye and investigate the functioning of the neural retina. Removing the 550 filter introduces lateral chromatic aberrations and enables us to study its additional effect on peripheral vision.

2. Method of Adjustment

From an engineering standpoint at the time of these experiments were initiated, the current design of the Lotmar Visometer precluded the use of two-alternative forced-choice and made the Method of Adjustment the only feasible alternative. Normally, two-alternative forced choice is the preferred method since it is said to be criterion-free (Blackwell, 1963). However, it is also data-intensive and is not an efficient method for parametric, exploratory experiments. We were investigating an aliasing phenomenon which from previous analysis of retinal structure and function was considered highly improbable. Therefore, subjective input on the percept and how it changed sequentially with spatial frequency was critically important.

3. Constant Presence of Peripheral Target

The Troxler phenomenon, fading of peripheral vision with prolonged viewing, can be a definite problem. It bothered one subject much more than the other three subjects, but since sessions were not timed, a subject could rest his eyes between presentations. Only for one subject at 30 degrees eccentricity did the fading seem to directly affect the results.

FIG. M1. CONVENTIONS FOR SPECIFYING MERIDIAN AND ORIENTATION OF STIMULUS. ANATOMICAL REFERENCES ARE FOR VISUAL FIELD OF RIGHT EYE.

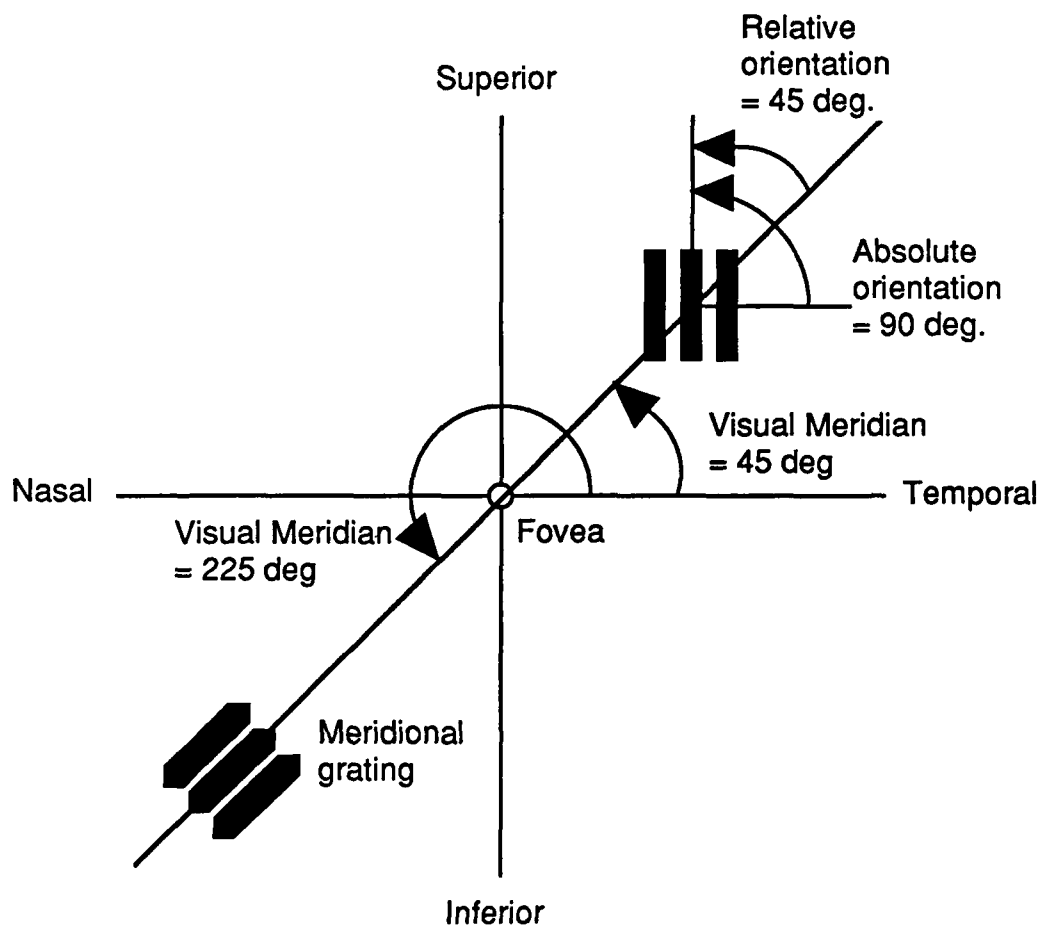


FIG. M2. QUASI-POINT SOURCES OF INTERFEROMETER

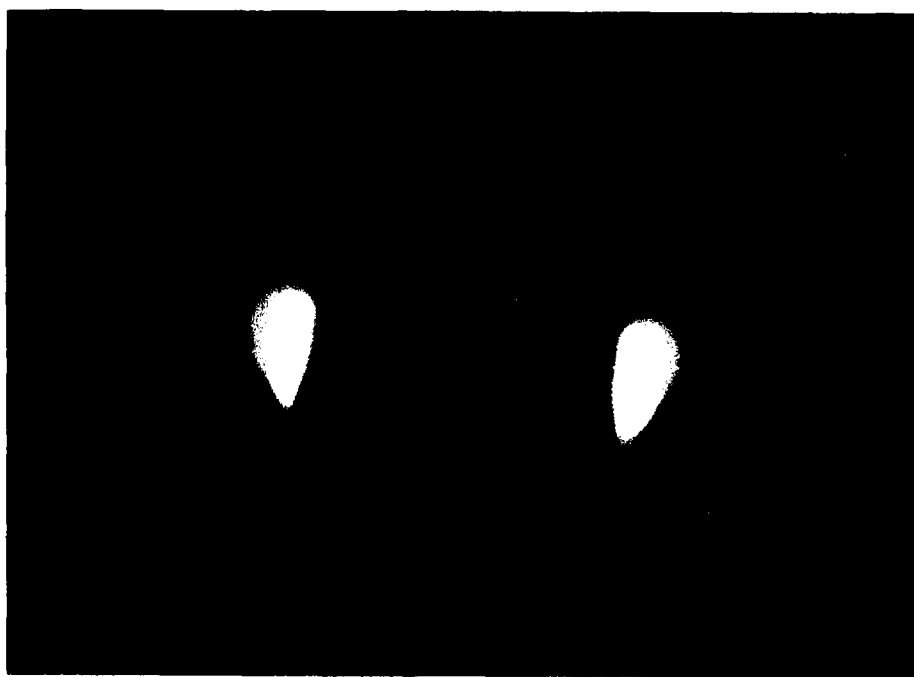
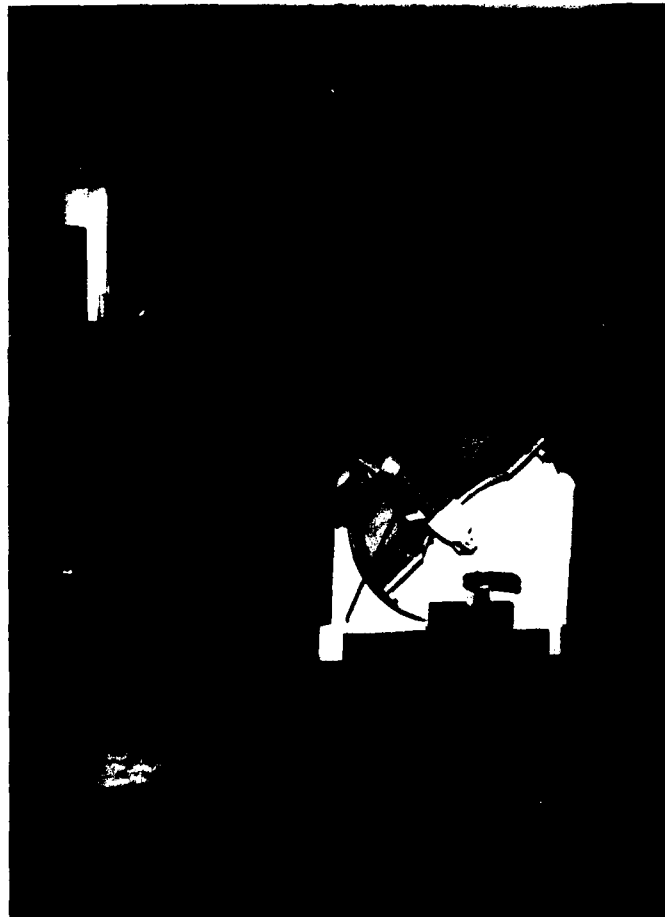


FIG. M3. EXPERIMENTAL SETUP



RESULTS

A. WHITE LIGHT EXPERIMENTS

1. The Effect of Stimulus Orientation on Grating Detection

a. Absolute Tuning Curves - Detection Varies with Orientation

The raw data for subjects LT, SG, and FC for all eccentricities and meridia tested are displayed in Appendix IV, Figs. A1 - A17. For each of these absolute tuning curves, the abscissa shows the absolute grating orientation of the stimulus and the ordinate shows the average of five determinations of the highest detectable spatial frequency. The main impression gained from the raw data is that detection acuity varies significantly with the meridian tested and the stimulus orientation. The error bars demonstrate that despite the difficulty of the detection task, the within session results are remarkably consistent especially for our most experienced subject, LT. To reveal the major systematic trends which emerged from this study, the data were replotted as functions of relative orientation as described in Methods (see section A, and Fig. M1) and grouped either by eccentricity or by meridian as described below.

b. Meridional Gratings Give Best Detection Acuity as Target Eccentricity Increases.

For an eccentricity of 15 degrees or greater, the orientational anisotropy becomes both more pronounced and more systematic. When the data of LT and SG are regraphed on a relative orientation axis across meridia for a specific eccentricity (Figs R1 - R5), it becomes readily apparent that the grating orientation that yielded the highest detection limit was normally the one whose bars were parallel to the meridian being tested and were defined as zero orientation. We call this orientation "meridional". Since FC was only tested in the horizontal nasal meridian his data are regraphed on a relative orientation axis across eccentricities (Fig. R6). Therefore, in his case the horizontal grating is always the

meridional orientation. The results for gratings oriented perpendicular to the test meridian are plotted twice at both 90 and -90. There is a clear tendency for the curves to peak in the middle and slope like a roof toward the 90 and -90 values. We call this systematic elevated performance for gratings zero relative orientation the "meridional effect". For FC and LT this was true for all their sessions at those eccentricities (26 out of 26, the probability of this occurring by chance is less than one in a trillion). For SG this was true 13 out of 15 times and the two times it wasn't the highest it was second best. For an eccentricity of less than 15 degrees, the meridional grating was the best only 3 out of 11 sessions.

To summarize the data still further, the data from the relative orientation curves were averaged across meridians for each eccentricity. The mean results for LT and SG are shown in Figs. R7 - R8. For SG the seven meridians at 12 1/2 degrees and the one meridian at 10 degrees (temporal, necessary due to optic disk) eccentricity average out to almost a straight line. For both subjects at 20 and 30 degrees eccentricity there is a prominent meridional effect across meridians. For SG, the average meridional detection acuity at 30 degrees would have been considerably higher if he had not had a major difficulty with the stimulus "blacking-out" at meridians 135, 270 and 315. Meridian 90 at 30 degrees was not able to be done due to obstruction of the stimulus by the upper lashes and lid.

c. Tangential Gratings Give Worst Detection Acuity as Target Eccentricity Increases

For the same eccentricities, subjects generally had the poorest detection readings for gratings which were oriented perpendicular to the meridian being tested. We will call this orientation "tangential". This was true for LT 19 out of 21 times, for FC 5 out of 5 times, for SG 12 out of 15 times.

d. Fourier Data Analysis - Consistent with Better Detection Acuity for Meridional Gratings as Target Eccentricity Increases.

(1) Eccentricities Less than 15 Degrees

Hartley's ANOVA for Fourier data evaluated M_1 for the three sessions in which the meridional grating gave the best detection threshold values. Only one of those sessions showed a significant effect at the $p=0.05$ level.

(2) Eccentricities 15 Degrees or Greater

Hartley's ANOVA for those 39 out of the 41 sessions which showed the meridional grating as the best-detected orientation further demonstrated the significance of this trend. The combined meridional component (M_1) was significant at the $p=0.05$ level 37 of 39 sessions. The meridionally shifted A_1 component was significant at the $p=0.05$ level 38 of 39 sessions.

The significance grew as the eccentricity increased so that all 21 sessions for eccentricities 25 or greater were significant for both M_1 and A_{1_MS} . Both M_k and A_{1_MS} were significant at the $p=0.001$ level 19 of the 21 sessions and at the $p=0.0001$ level 16 of 21 sessions.

2. Quantative Analysis of the Meridional Effect

To quantify the amount of orientational bias found at each location in the visual field, Fourier analysis was done on the relative orientational curves of Figs. R1 - R5. The modulation of the fundamental cosine component (A_{1_MS}) is then a direct measure of the meridional effect. Figs. R9 -R10 plot modulation against meridian for several eccentricities. The trend is for the strength of the meridional effect to increase with eccentricity along all 8 meridia tested.

Figs. R11 - R12 plot the modulation of the fundamental sine component (B_{1_MS}) versus meridian categorized by eccentricity. With two exceptions it seems to vary almost randomly about 0 which is consistent with the notion of a meridional bias. For SG, 12 out of 23 turning curves had positive B_{1_MS} s and LT had 11 out of 23 positive B_{1_MS} s. The variation does not seem to be systematically related to meridian or eccentricity. This is consistent with the overall effect of the B_{1_MS} /mean component being minimal.

3. Quantative Analysis of the Oblique Effect

The Cosine component of the second harmonic (absolute A_2/mean) is also plotted versus meridian categorized by eccentricity (R13 R14). These graphs show that the oblique effect is weak; for only 22 out of 35 (17.5 out of 35 is chance level) of the sessions for eccentricities 20 degrees or greater have an A_2/mean value that is positive.

However, if the A_2 component is meridionally shifted (A_{2_MS}), which would compare whether the average detection acuity of the gratings that are parallel and perpendicular to the meridian being tested were higher than the average of the two gratings oriented to 45 degrees to either side of the meridian, then the A_{2_MS}/mean for eccentricities 20 degrees or greater is positive for 30 out of the 35 sessions.

Comparing Figs. R9 - R10 with Figs R15 - R16, it can be seen that the amplitudes of the A_{1_MS}/mean are on the average much greater than A_{2_MS}/mean which shows the overall dominance of the meridional components.

In summary, the Fourier analysis shows an increasing A_{1_MS} component and to a much lesser degree A_{2_MS} component with increasing eccentricity. The overall effect of the B_{1_MS} component appears to be minimal. FC's data, graphed across eccentricity (Fig. R17), shows these trends very well. Since his results are for the horizontal meridian only, there is no meridional shift necessary (i.e. $A_1/\text{mean} = A_{1_MS}/\text{mean}$, $B_1/\text{mean} = B_{1_MS}/\text{mean}$ and $A_2 = A_{2_MS}/\text{mean}$).

B. 550 NM INTERFERENCE FILTER CONTROL EXPERIMENTS

Results obtained with white light showed a significant systematic superiority of the detection limit for meridional gratings. Although the interferometric technique using white light avoids focusing errors, it is not immune to lateral chromatic aberration. Therefore, to test the hypothesis that the meridional effect is due to chromatic aberration, selected loci along the horizontal meridian of the peripheral visual field were retested in three subjects using a narrow band green filter (550 nm).

Figs. R18 - R20 show the comparison between the detection acuity for white light and 550 nm light at 20 degrees along the horizontal nasal meridian for subjects SG, AB, and LT. With the 550 filter the meridional effect is clearly gone. Fourier analysis reveals no statistically significant components and the curves are essentially flat. Figs. R21 - R22 show that the same is close to being true for LT in the horizontal temporal and horizontal nasal meridian at 30 degrees eccentricity. However, even though there is a tremendous reduction in the meridional effect in the horizontal temporal meridian, a small but significant meridional effect still remains.

Although these results apply only to the horizontal meridian, they indicate that chromatic aberration (probably lateral) plays a large role in causing contrast reduction in the aliasing zone for high spatial frequency gratings that are non-meridional. However, since the green filter reduced the target luminance by 1.2 log Trolands to 2.4 log Trolands, there was the slim possibility that the smaller pupil diameter in the brighter white light experiment may have been a factor.

C. CONTROL SESSION WITH A DILATED PUPIL

In the above experiments, the pupil diameters were at least 2.5 mm. With eccentric stimuli, the pupil appears elongated with the short axis aligned with the visual meridian. Consequently, it is possible that one or the other of the coherent spots of light in the brighter white light experiments might have been obscured by the iris, thus reducing the image contrast. This would be most pronounced for spots which are destined to form gratings orthogonal to the visual meridian. In short, it is conceivable that a meridional effect is caused by the oval shape of the pupil as viewed off axis.

Two aspects of the earlier experiment suggest that the pupil size did not cause the meridional effect, though it did make lining up very critical. First a 2.5 mm diameter pupil would have a small axis of 2.0 mm at 30 degrees into the periphery. This could still pass a

spatial frequency of over 50 cycles per degree. Second, subjects noticed that colored fringes would begin to appear when the iris began to obscure the spots.

Nevertheless, to be absolutely sure that pupil size was not the main cause of the meridional effect, the following control experiment was done on one subject, LT. His pupil was dilated with 1% cyclogel and was put through a practice run. However, even though his data seemed reasonable, he felt his percept of the alias pattern was different than usual and was therefore uncertain about his criteria. The experiment was then repeated the next morning when his pupils were still well dilated and his accommodation had returned to normal. The eccentricity was set at 30 degrees into the temporal meridian which had shown a definite meridional effect in the earlier white light experiments. The point sources were positioned in the center of the entrance pupil, and the meridional (horizontal) grating and its tangential counterpart (vertical grating) were tested to determine the highest detectable spatial frequency which produced an alias pattern. The results in Fig. R23 indicate that even with a well dilated pupil, which could not possibly block the quasi-point sources, the aliasing pattern of the horizontal grating could still be detected at a much higher spatial frequency. Next the bite bar was adjusted horizontally by the subject to maximize detection acuity of the vertical grating. The amount of horizontal displacement of the subject's head was 1.5 mm in the nasal direction. This time when the detection task was repeated, Fig. R23 shows that the meridional effect disappeared. Geometrical analysis of the new decentered position of the visometer indicated that the quasi-point sources for the vertical grating were much closer to the nodal point axes. Fig. R23 also shows that adding a 550 nm narrowband filter gave similar detection values.

D. FURTHER 550 NM INTERFERENCE FILTER CONTROL EXPERIMENTS AT 30 DEGREES ECCENTRICITY

These experiments were done three years after the original 550 results to complement the data for the horizontal nasal and temporal meridia previously done at 30 degrees

eccentricity. Firstly, they were to test whether the meridional effect was also eliminated for all four stimulus orientations using the 550 nm filter for a selected oblique and vertical meridian. Secondly, they were to fill in the gaps for the other primary meridians at 30 degrees eccentricity but testing only the meridional and tangential gratings. These test parameters were chosen since both 30 degrees eccentricity and these two relative grating orientations had shown the most pronounced meridional effect in the white light experiments.

The two meridians chosen to test all 4 orientations were 225 (an oblique) and 270 (a vertical). However, these experiments were done on the same model but different Lotmar visometer than the experiments performed three years earlier. The original visometer had been modified by Still to include variable contrast but was now limited to only the horizontal meridians. The results depicted in Figs. R24 - R25 include the white light data taken with the other visometer. As in the previous 550 data the current experiments show an elimination of the meridional effect. The 550 data for 270 also shows a higher detection value for the meridional grating than in the white light data. Possible explanations for this type of finding is addressed in the discussion.

In order to allow a direct comparison the remaining six meridians, which include both of the horizontal meridians, were tested using the meridional grating and its tangential counterpart. Fig. R26 displays the detection data for these two relative orientations for all eight primary meridians. Except for 0 degrees, the horizontal temporal meridian, not only is the meridional effect eliminated, the detection results across meridians are very similar. Possible implications of these results and comparisons with white light data are included in the discussion.

E. CONTRAST THRESHOLD DETERMINATION FOR LT FOR HORIZONTAL NASAL MERIDIAN AT 30 DEGREES ECCENTRICITY

The results above demonstrate that in most instances for 30 degrees in the periphery when chromatic aberration is eliminated and the four different gratings orientations reach the receptors with equal contrast, the spatial frequency at which aliasing can be perceived is identical. This experiment used the original Lotmar visometer which included the 550 filter and had been modified by Still to vary contrast. The experiment tested the contrast thresholds for 10, 15, 20, 25, and 30 cycle per degree vertical gratings for the horizontal nasal meridian at 30 degrees eccentricity for LT. Method of adjustment was employed and the results reflect the average ascending and average descending limits. A yet to be explained finding is that the ascending and descending limits did not always overlap, yet the aliasing phenomenon though faint was clearly present at these thresholds. The results shown in Fig. R27 demonstrate the lack of precision within a spatial frequency. However there is a general trend that higher spatial frequencies require greater contrast at the retinal surface in order for the alias pattern to be seen.

FIG. R1. DETECTION ACUITY TUNING CURVE RELATIVE
TO MERIDIAN TESTED FOR LT AT
20 DEGREES ECCENTRICITY

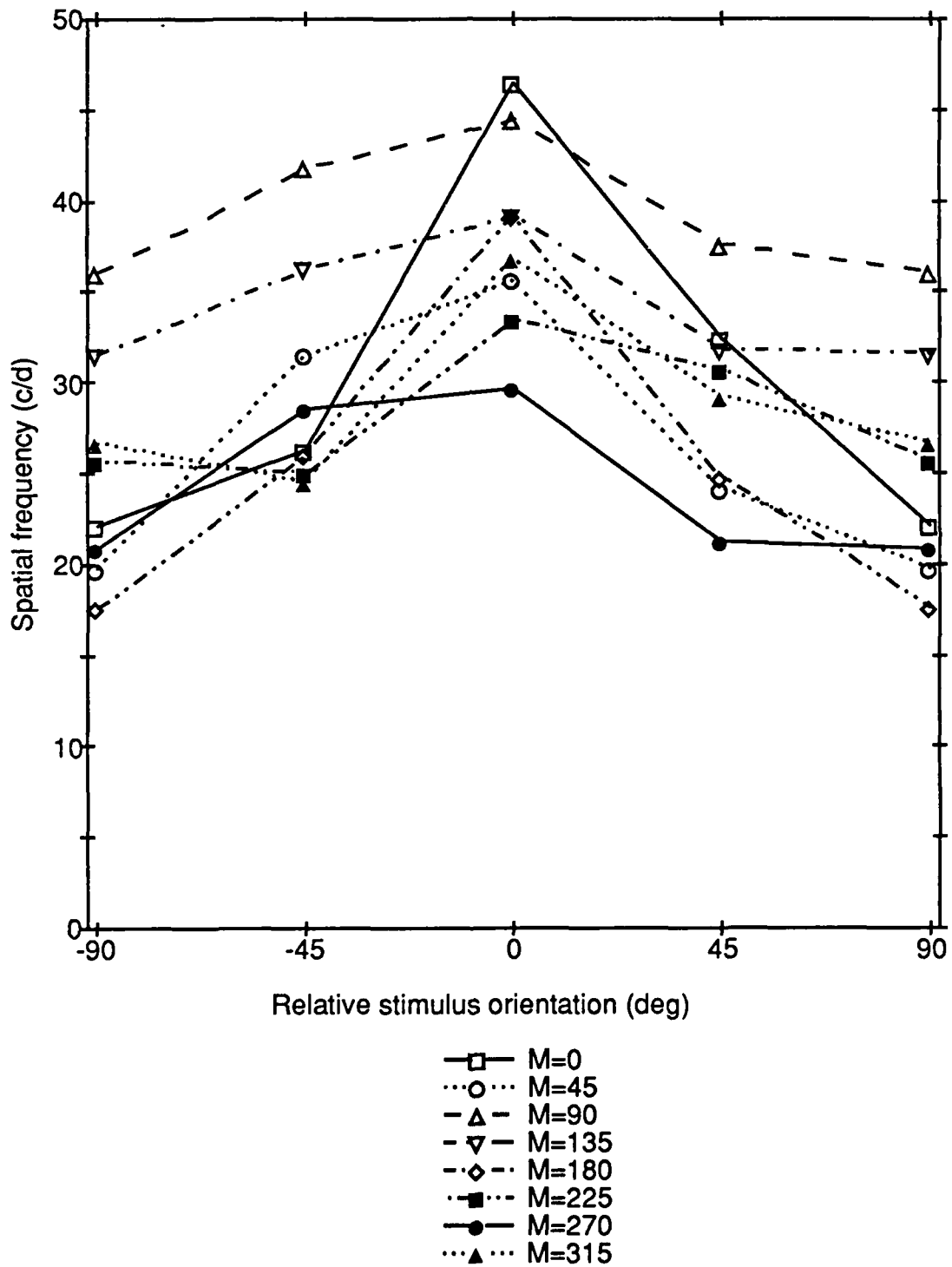


FIG. R2. DETECTION ACUITY TUNING CURVE RELATIVE
TO MERIDIAN TESTED FOR LT AT
30 DEGREES ECCENTRICITY

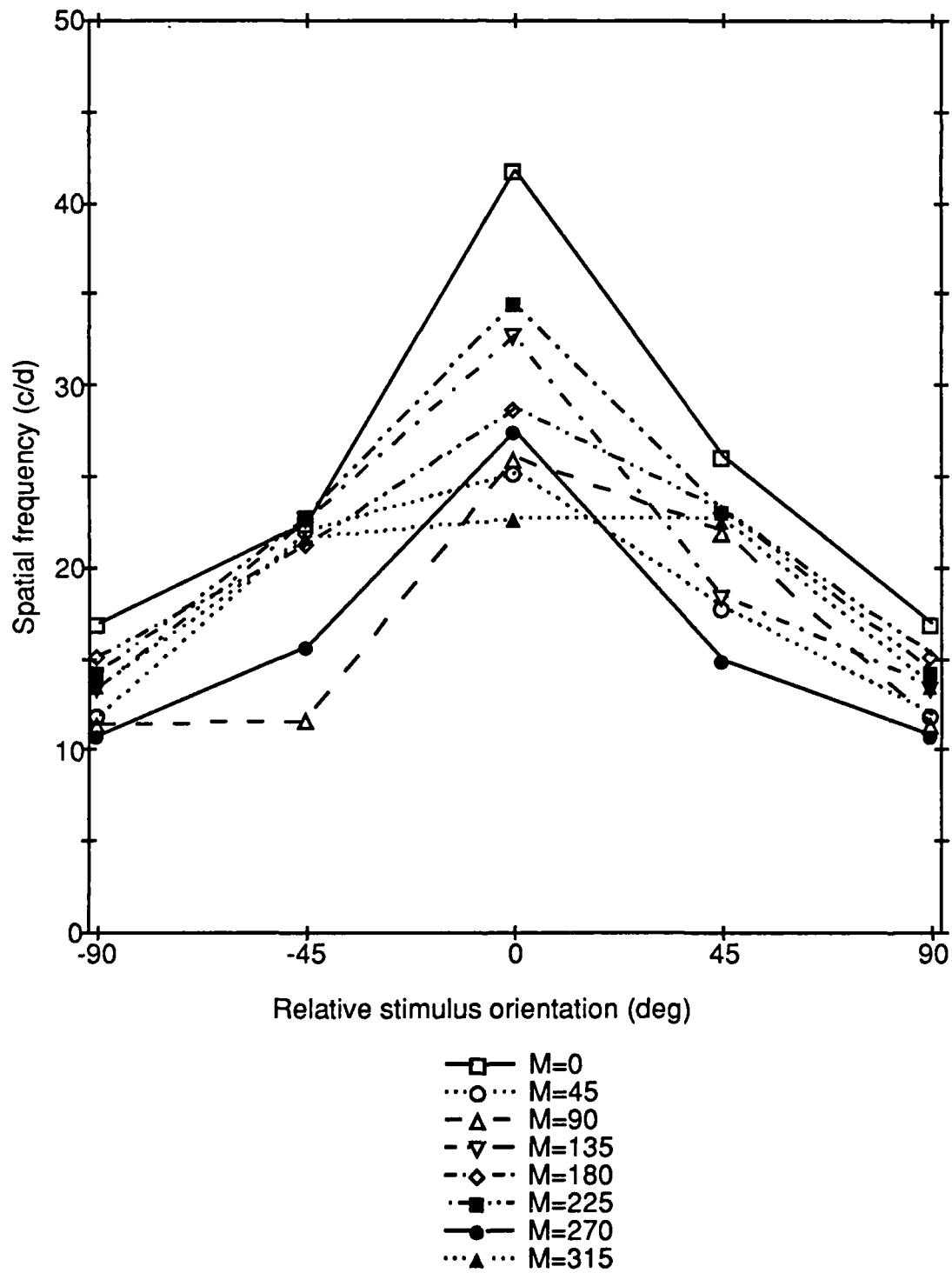


FIG. R3. DETECTION ACUITY TUNING CURVE RELATIVE
TO MERIDIAN TESTED FOR SG AT
12.5 DEGREES ECCENTRICITY

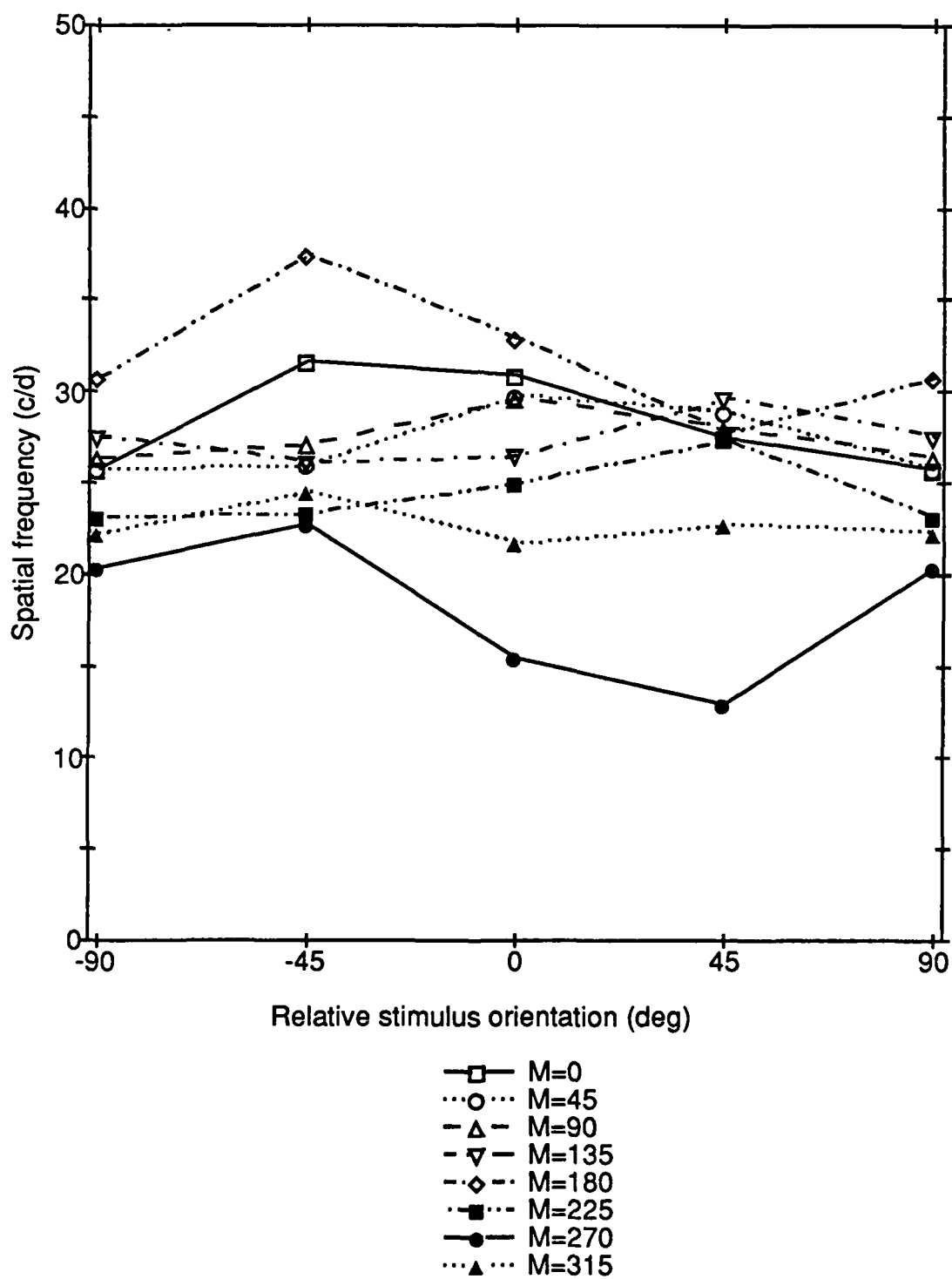
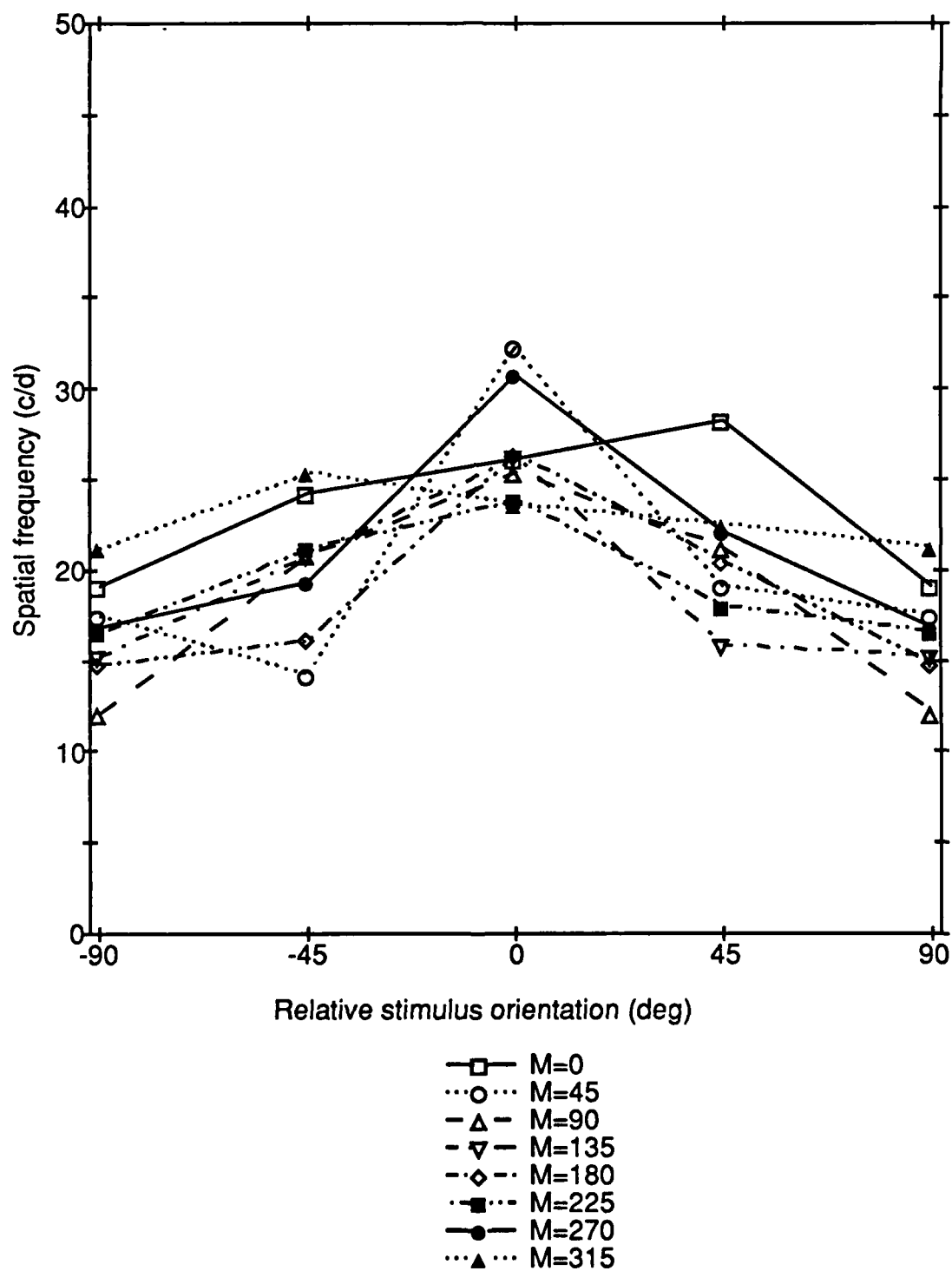


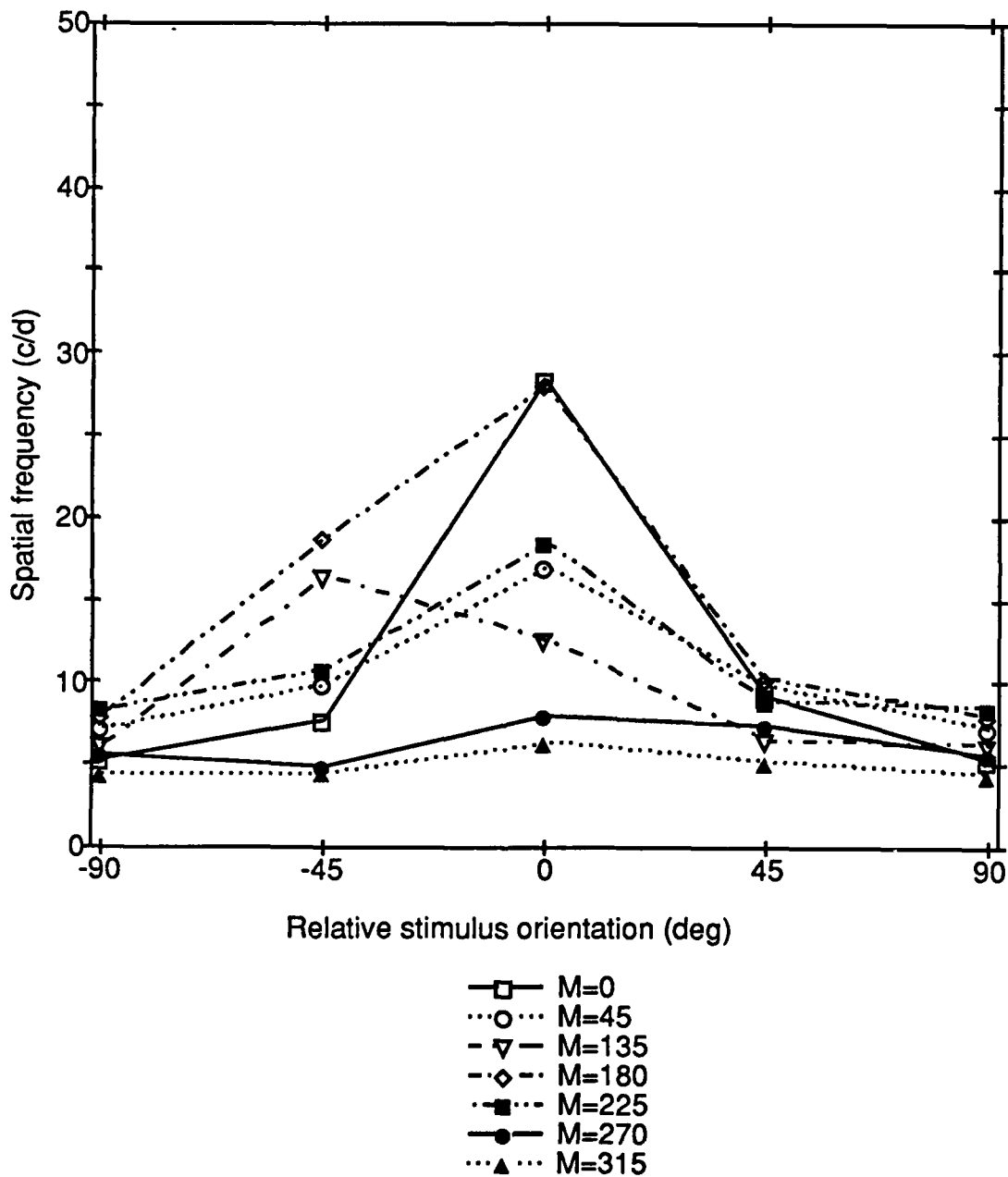
FIG. R4. DETECTION ACUITY TUNING CURVE RELATIVE
TO MERIDIAN TESTED FOR SG AT
20 DEGREES ECCENTRICITY



G_TUN_REL_SGD30

04-SEP-89 19:14 Page 1

FIG. R5. DETECTION ACUITY TUNING CURVE RELATIVE
TO MERIDIAN TESTED FOR SG AT
30 DEGREES ECCENTRICITY

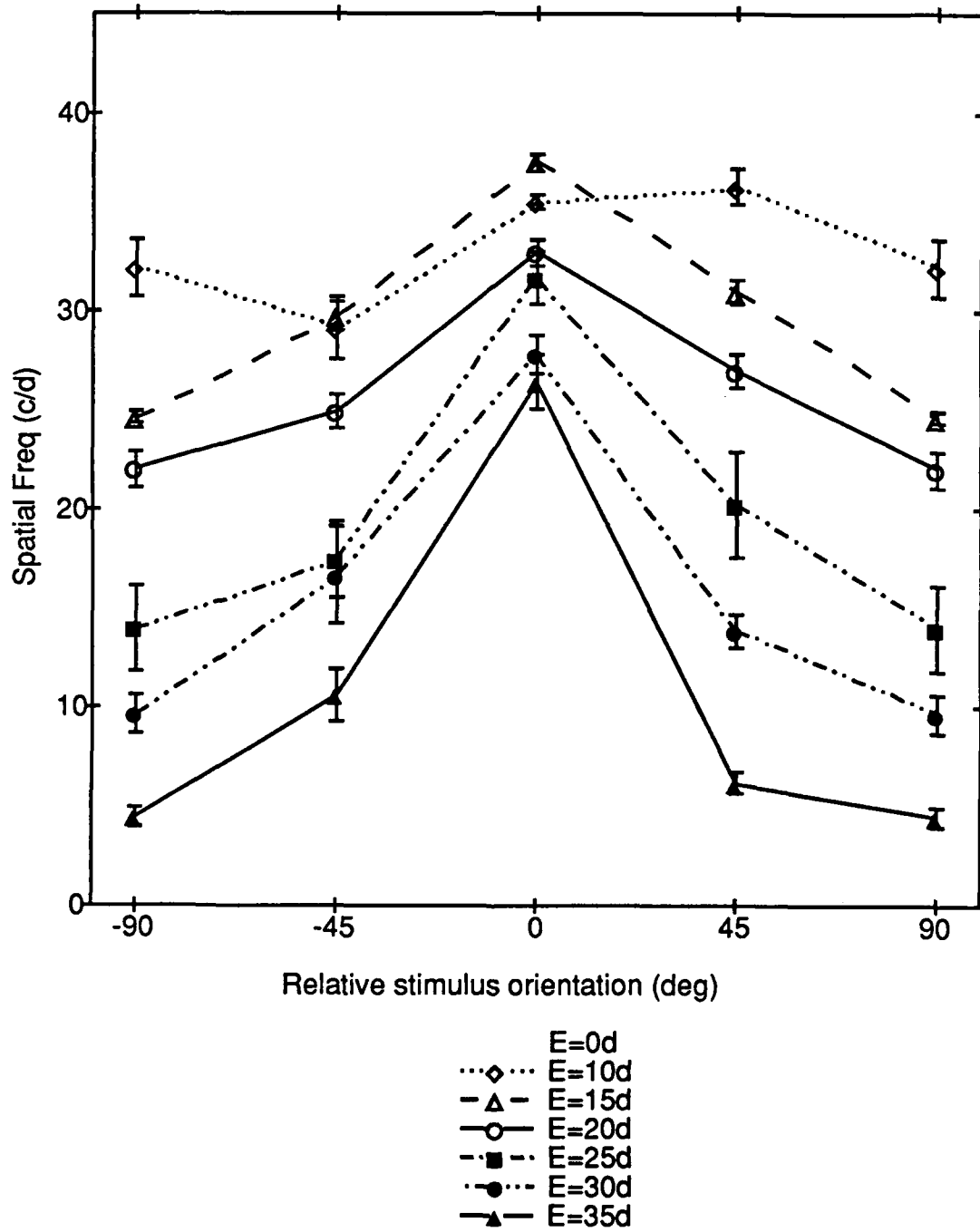


MERIDIAN 90 WAS TOO DIFFICULT TO GET RELIABLE RESULTS
DUE TO INTERFERENCE FROM UPPER LID
MERIDIANS 135, 270 AND 315 WERE ALSO VERY DIFFICULT DUE TO
SIMULUS BLACKING OUT

G_FCREL

04-SEP-89 19:26 Page 1

FIG. R6. DETECTION ACUITY TUNING CURVE RELATIVE
TO ECCENTRICITY TESTED FOR FC
ALONG THE HORIZONTAL NASAL
MERIDIAN

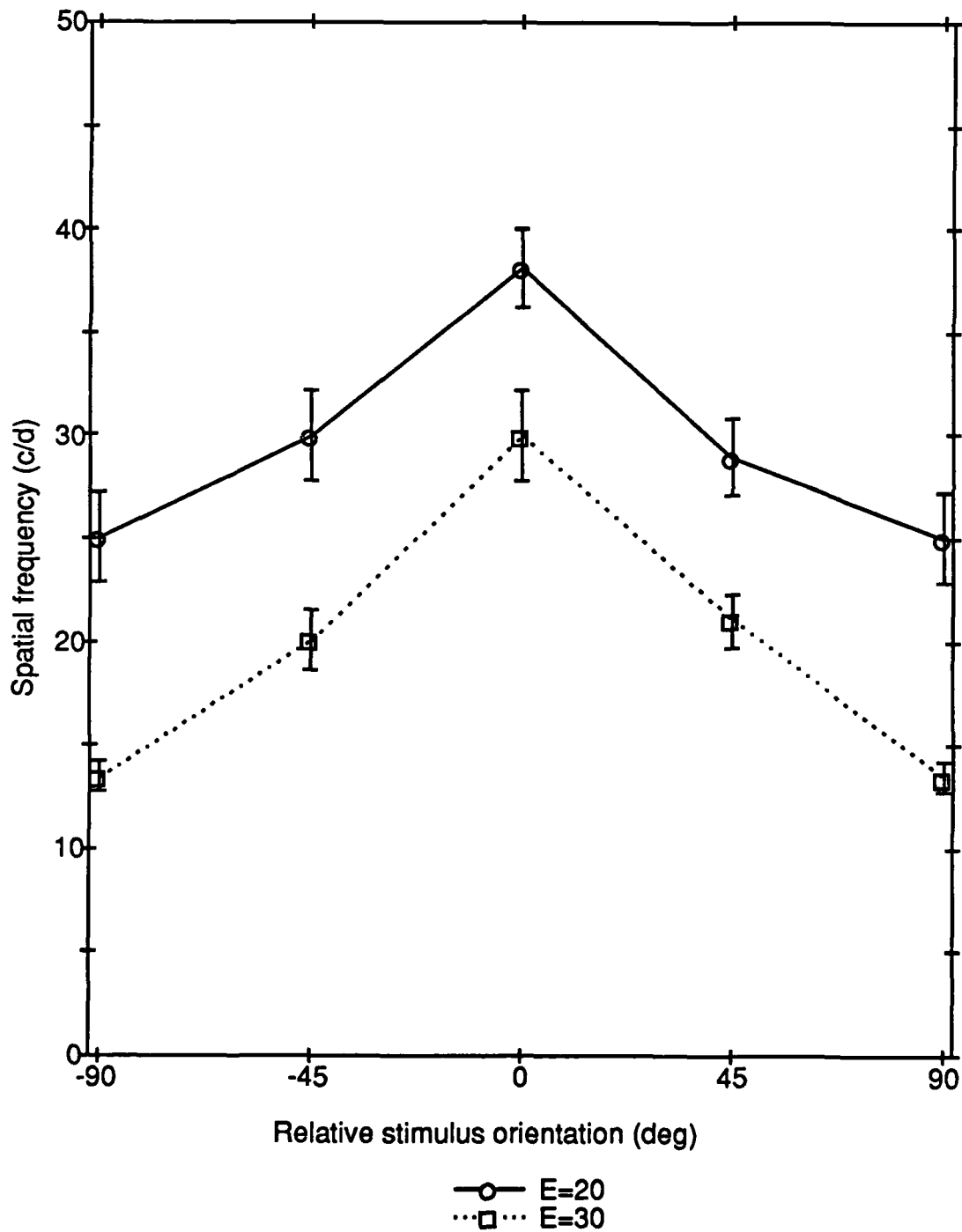


Error bars are ± 1 s.e.m.

G_TUN_LT_MER

04-SEP-89 19:36 Page 1

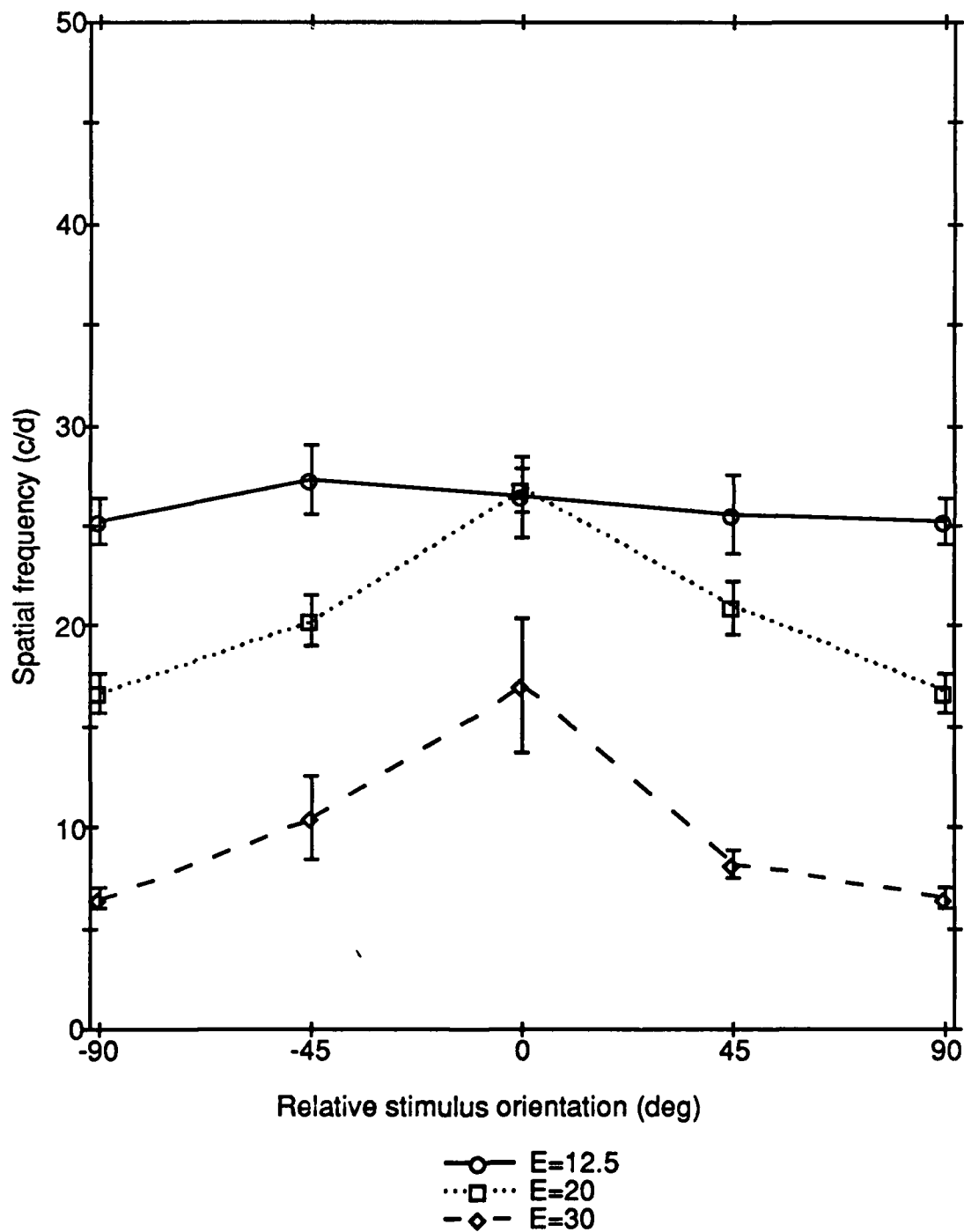
FIG. R7. AVERAGE OF DETECTION ACUITY RELATIVE
TUNING CURVES TO SHOW AVERAGE
MERIDIONAL EFFECT AT 20 AND
30 DEGREES ECCENTRICITY
FOR LT



G_TUN_SG_MER

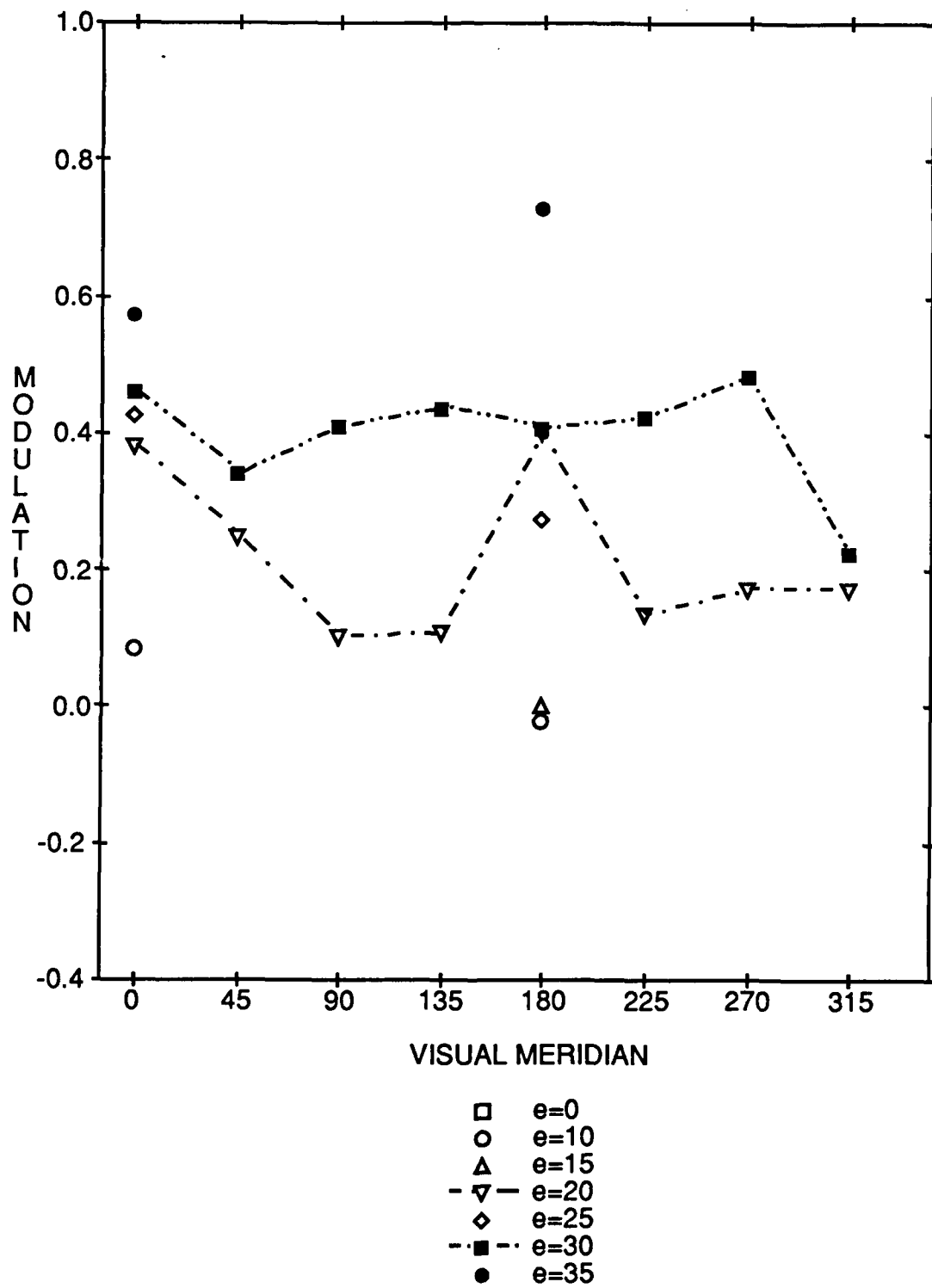
04-SEP-89 19:56 Page 1

FIG. R8. AVERAGE OF DETECTION ACUITY RELATIVE
TUNING CURVES TO SHOW AVERAGE
MERIDIONAL EFFECT AT 12.5, 20,
AND 30 DEGREES ECCENTRICITY
FOR SG



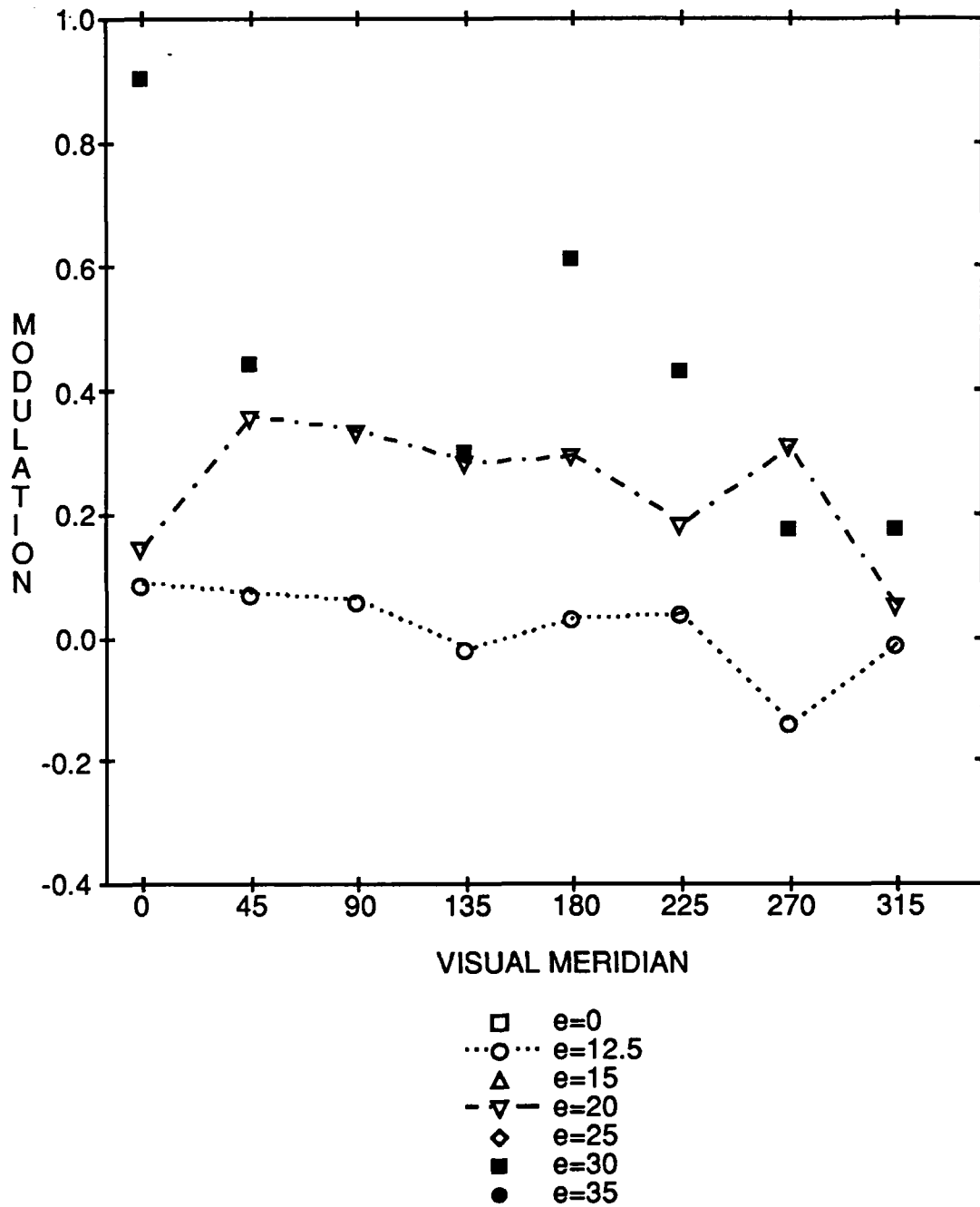
LT_A1_MER_SHIFT

04-SEP-89 20:21 Page 1

FIG. R9. MERIDIONAL EFFECT FOR LT, DETECTION TASK
(A1 MERIDIONALLY SHIFTED/MEAN)

SG_A1_MER_SHIFT

04-SEP-89 20:56 Page 1

FIG. R10. MERIDIONAL EFFECT FOR SG, DETECTION TASK
(A1 MERIDIONALLY SHIFTED/MEAN)

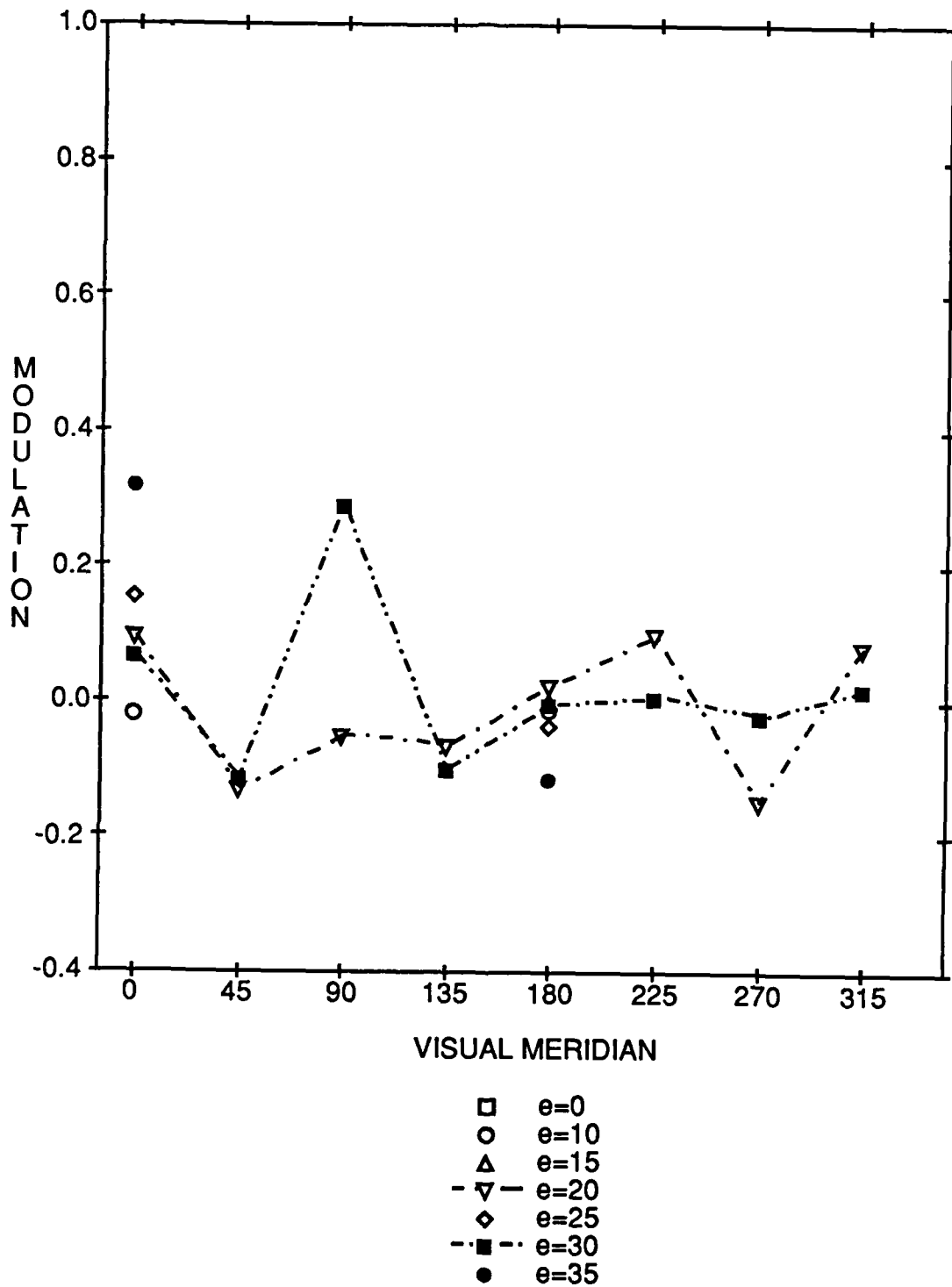
-MERIDIAN 90 AT 30 DEGREES WAS TOO DIFFICULT TO GET
RELIABLE RESULTS

-MERIDIANS 135, 270 AND 315 WERE ALSO VERY DIFFICULT

LT_B1_MER_SHIFT

04-SEP-89 20:32 Page 1

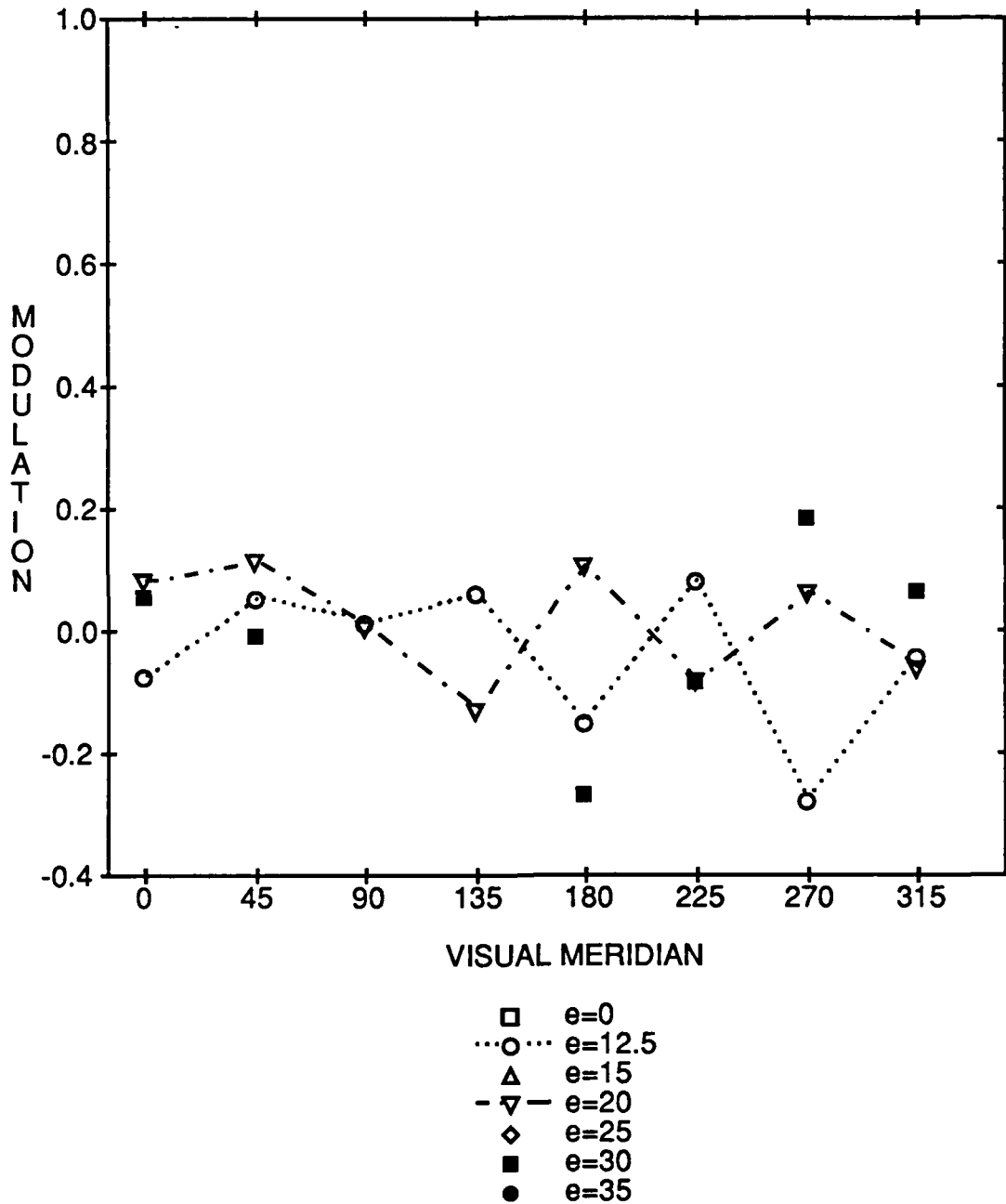
FIG. R11. FIRST HARMONIC EFFECT ORTHOGONAL TO
MERIDIAN FOR LT, DETECTION TASK
(B1 MERIDIONALLY SHIFTED/MEAN)



SG_B1_MER_SHIFT

04-SEP-89 21:05 Page 1

FIG. R12. FIRST HARMONIC EFFECT ORTHOGONAL TO
MERIDIAN FOR SG, DETECTION TASK
(B1 MERIDIONALLY SHIFTED/MEAN)

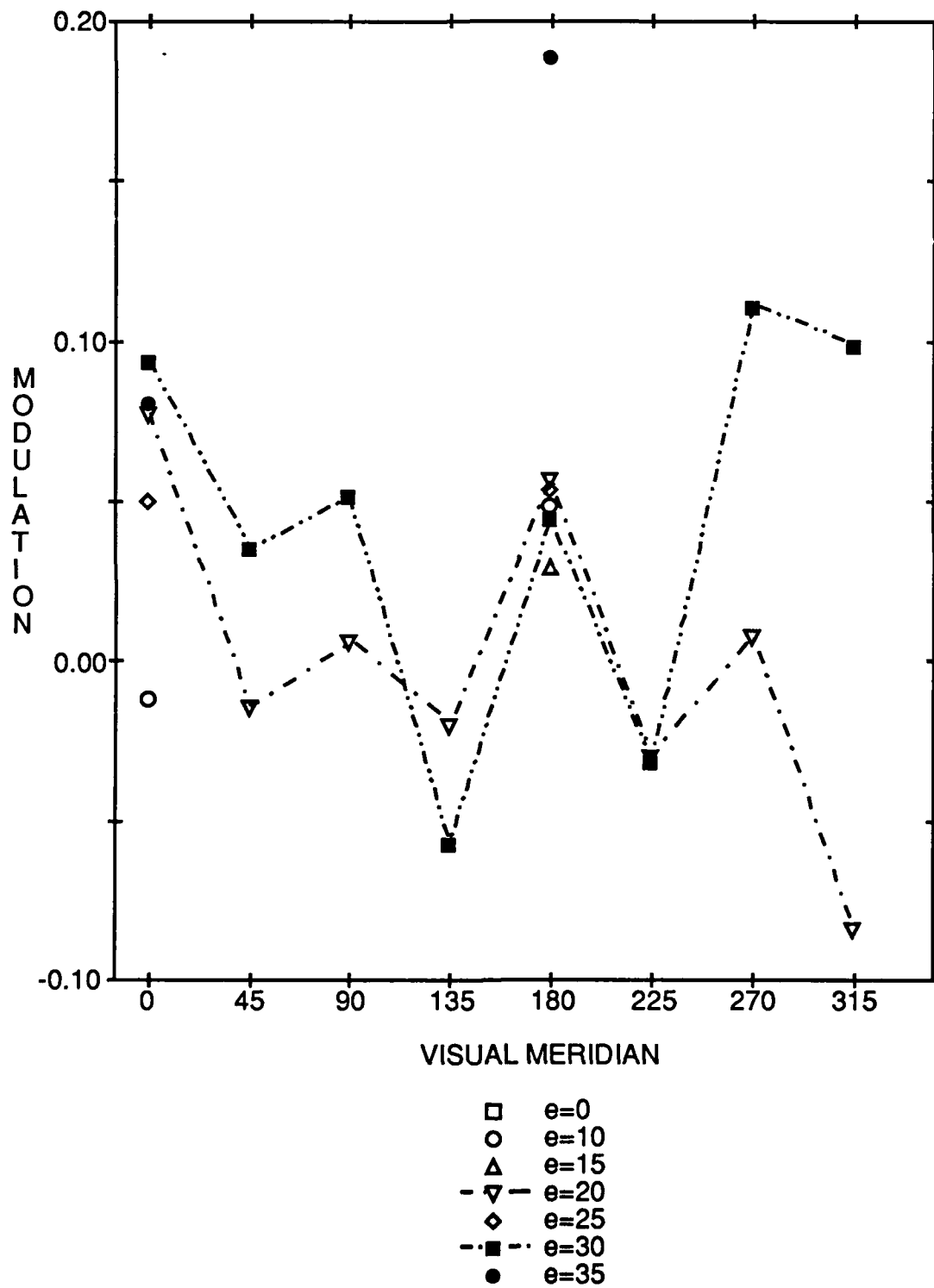


-MERIDIAN 90 AT 30 DEGREES WAS TOO DIFFICULT TO GET
RELIABLE RESULTS

-MERIDIANS 135, 270 AND 315 AT 30 DEGREES WERE ALSO DIFFICULT

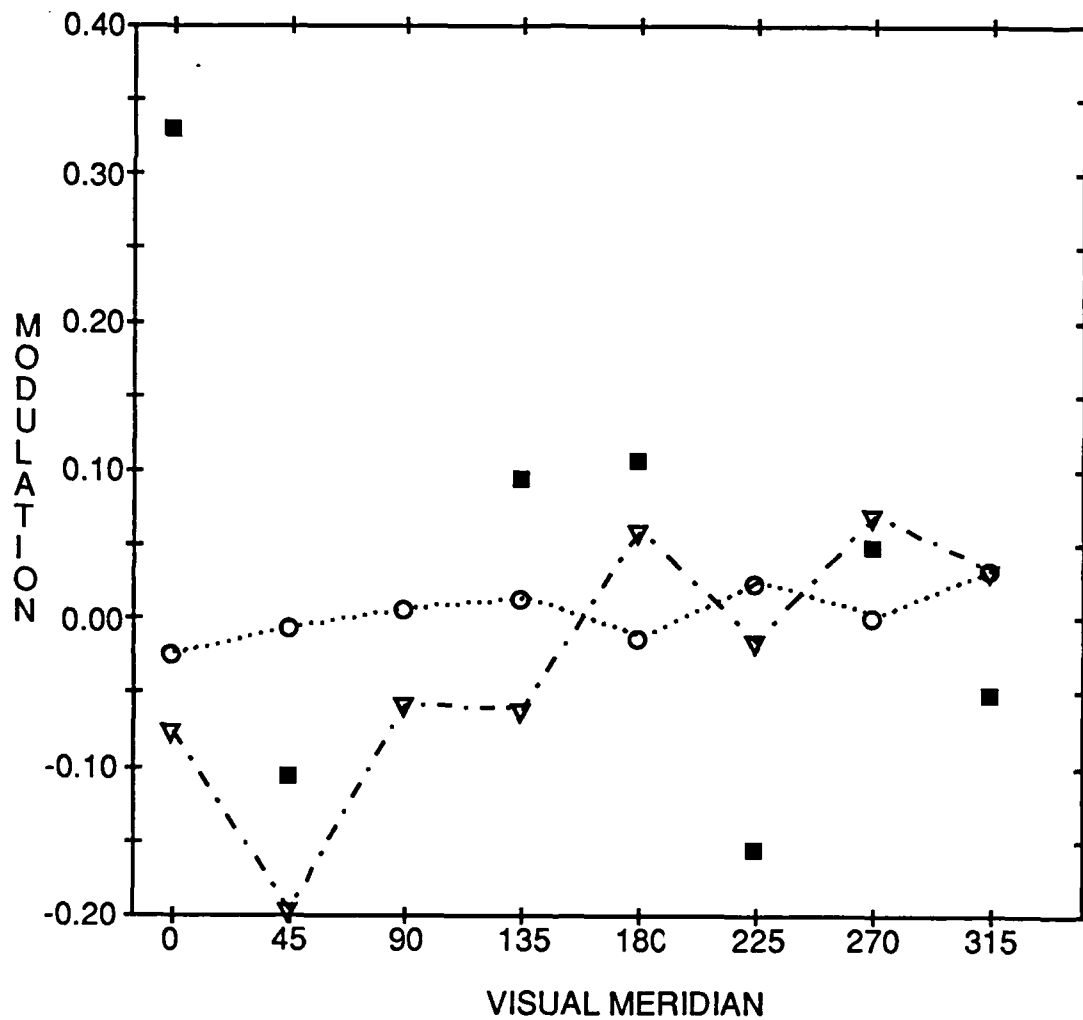
LT_A2

04-SEP-89 21:11 Page 1

FIG. R13. OBLIQUE EFFECT FOR LT, DETECTION TASK
(A2/MEAN)

SG_A2

04-SEP-89 21:24 Page 1

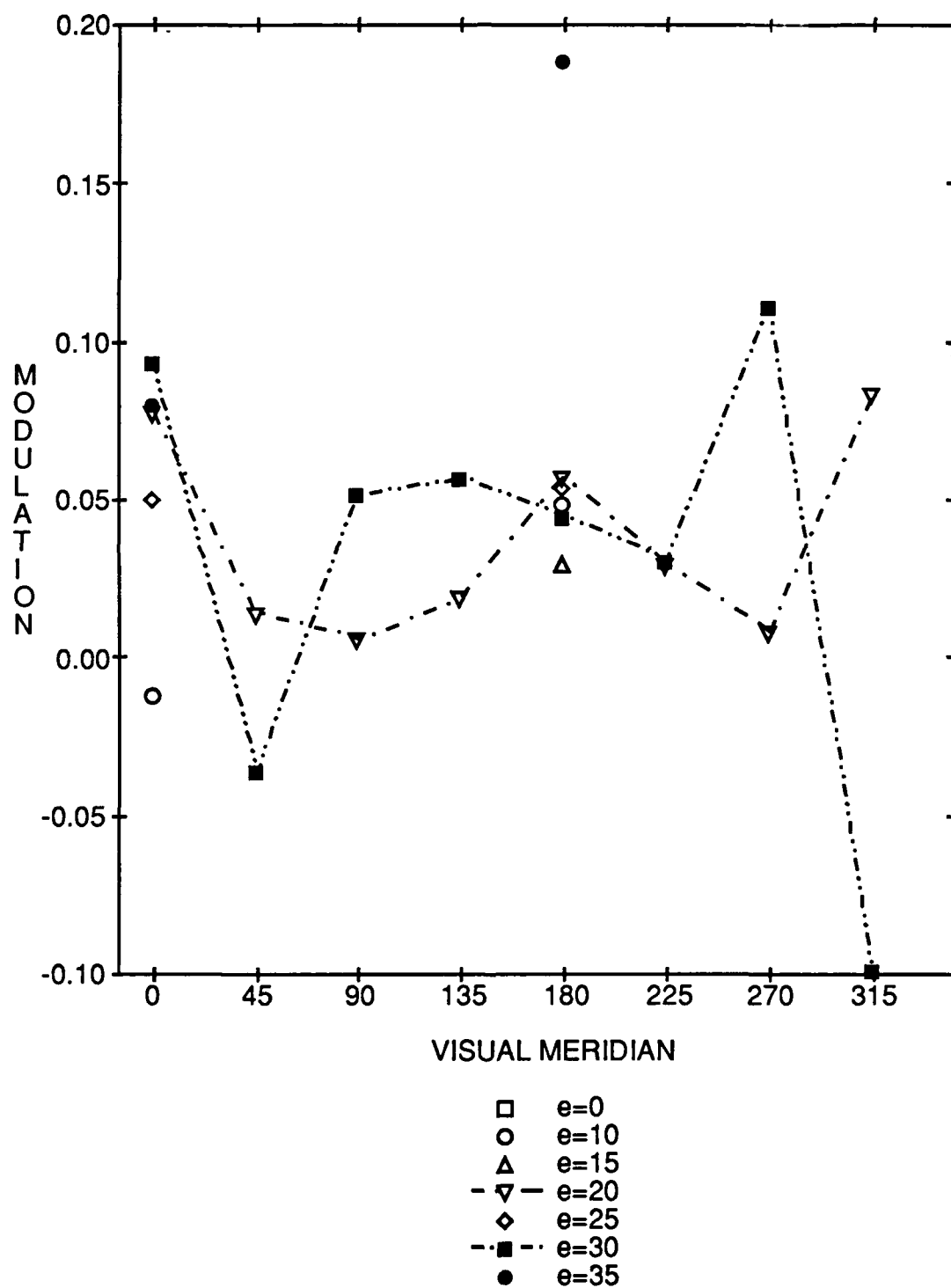
FIG. R14. OBLIQUE EFFECT FOR SG, DETECTION TASK
(A2/MEAN)

-MERIDIAN 90 AT 30 DEGREES WAS TOO DIFFICULT TO GET
RELIABLE RESULTS
-MERIDIANS 135, 270 AND 315 WERE ALSO DIFFICULT
-MERIDIAN 0 (12.5 DEG ECC) WAS DONE AT 10 DEG ECC
DUE TO OPTIC DISC

LT_A2MER_SHIFT

04-SEP-89 21:38 Page 1

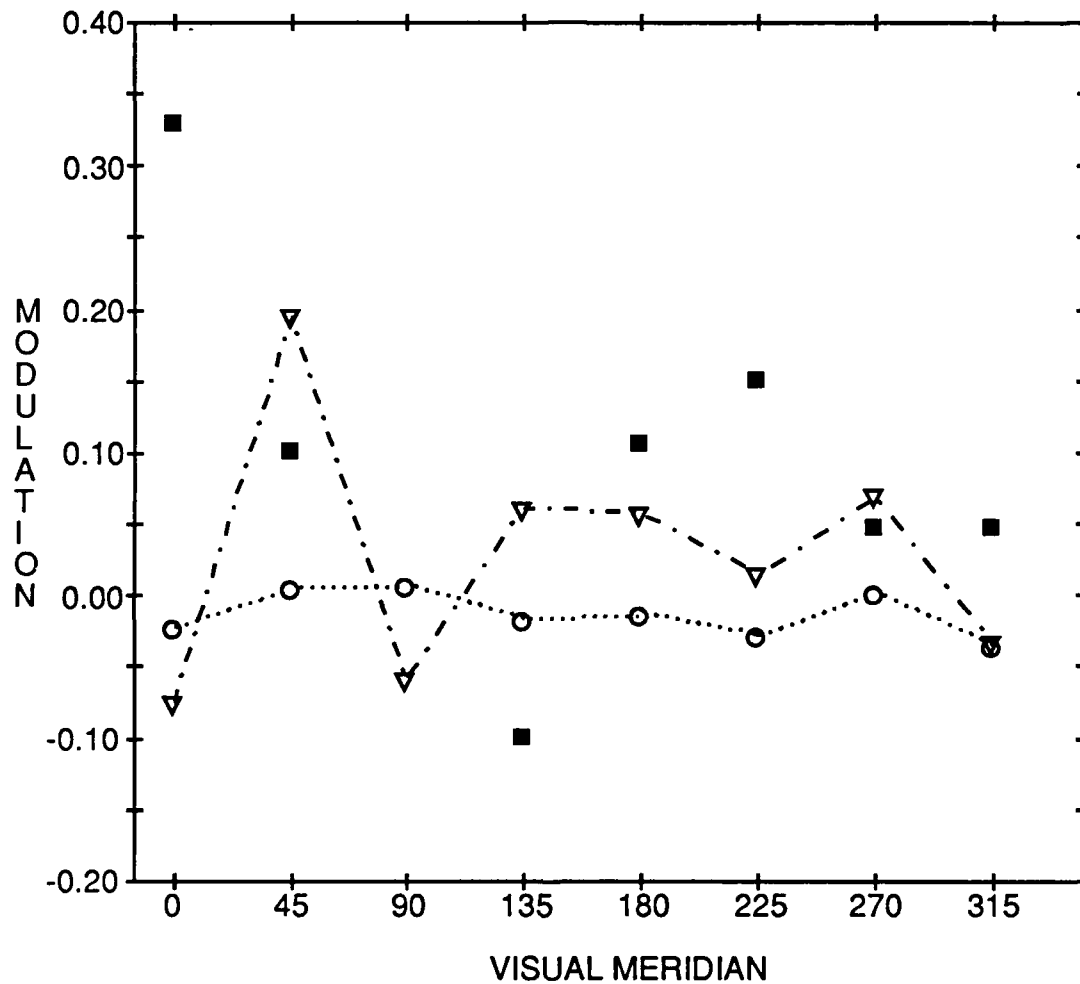
FIG. R15. SECOND HARMONIC EFFECT FOR LT RELATIVE
TO MERIDIAN TESTED, DETECTION TASK
(A2 MERIDIONALLY SHIFTED/MEAN)



SG_A2_MER_SHIFT

04-SEP-89 21:50 Page 1

FIG. R16. SECOND HARMONIC EFFECT FOR SG, RELATIVE
TO MERIDIAN TESTED, DETECTION TASK
(A2 MERIDIONALLY SHIFTED/MEAN)



-MERIDIAN 90 AT 30 DEGREES WAS TOO DIFFICULT TO GET
RELIABLE RESULTS
-MERIDIANS 135, 270 AND 315 WERE ALSO DIFFICULT
-MERIDIAN 0 (12.5 DEG ECC) WAS DONE AT 10 DEG ECC
DUE TO OPTIC DISC

G_FC_A1B1A2

04-SEP-89 22:11 Page 1

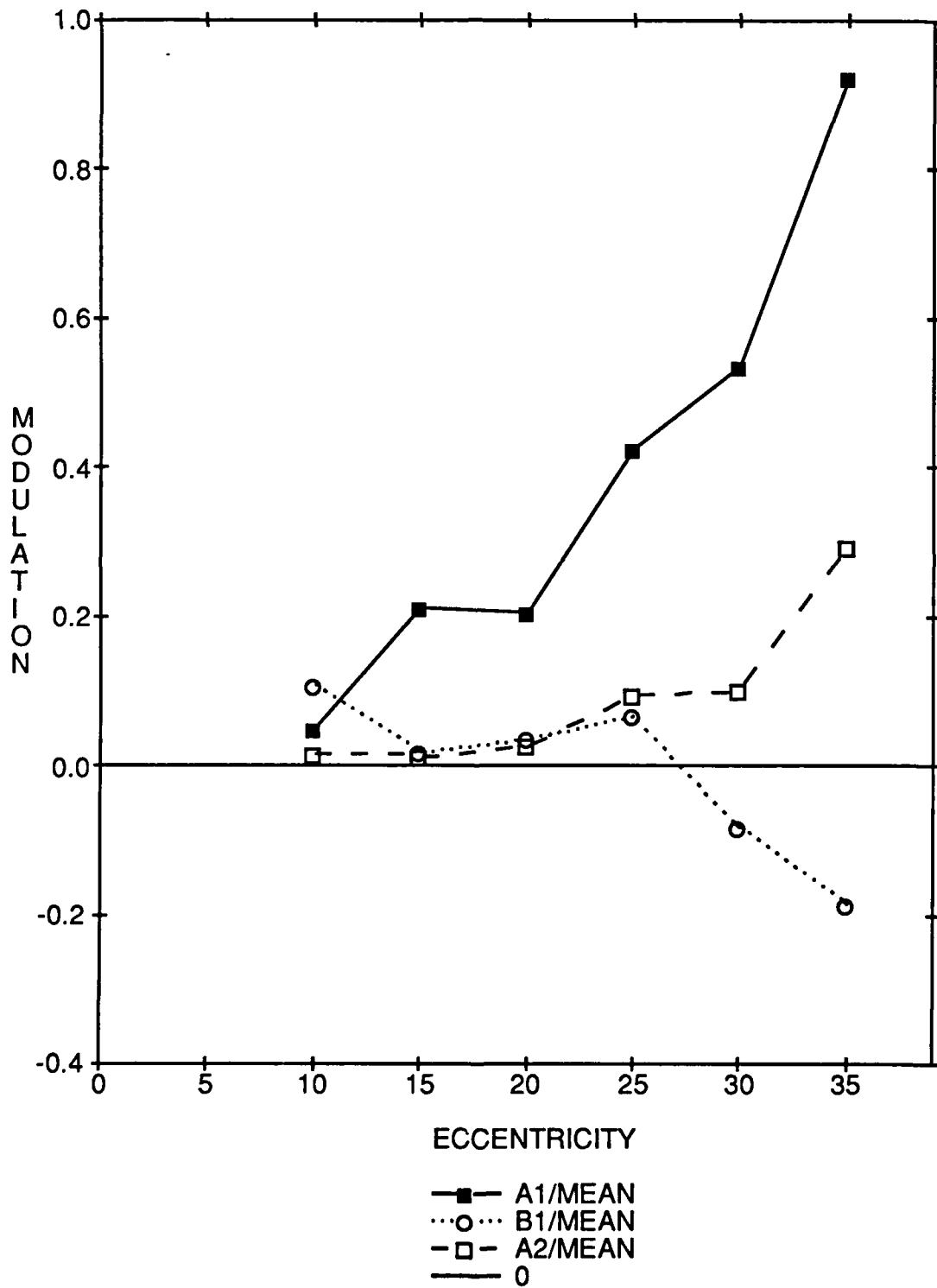
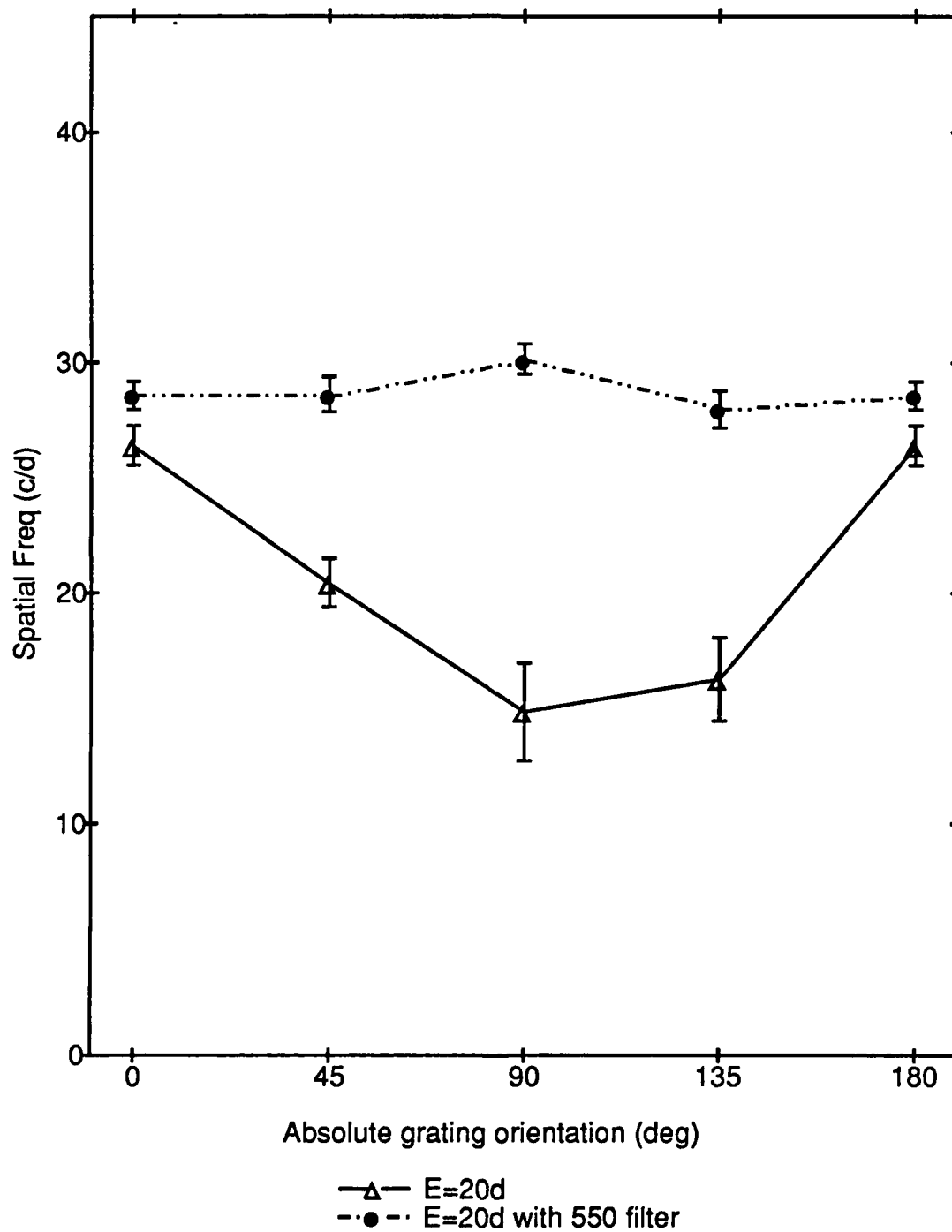
FIG. R17. COMPARISON OF A1, B1, AND A2 FOR FC FOR
HORIZONTAL NASAL MERIDIAN

FIG. R18. DETECTION ACUITY FOR WHITE LIGHT AND 550 FILTER
FOR SG IN THE HORIZONTAL NASAL MERIDIAN
AT 20 DEGREES ECCENTRICITY

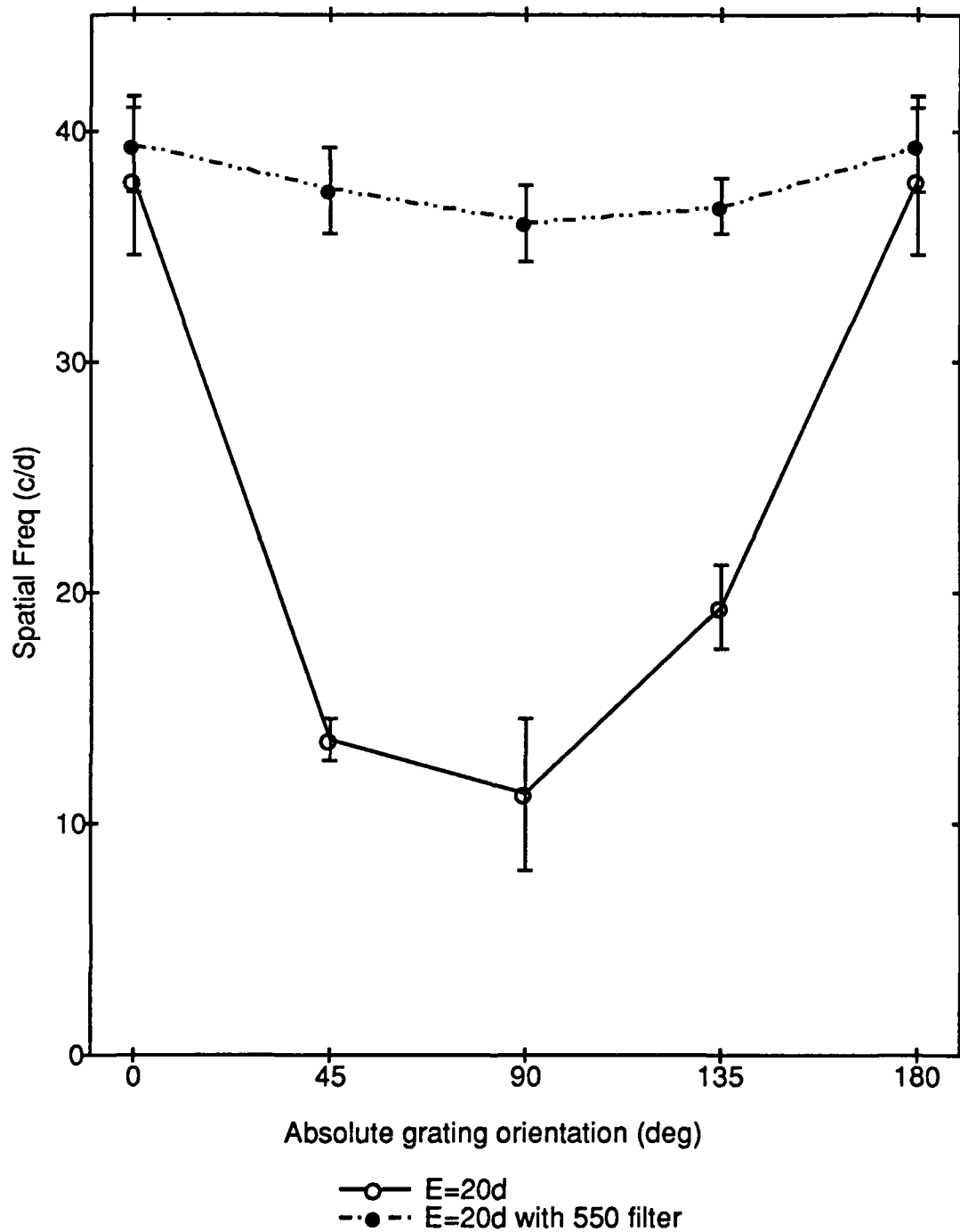


Error bars are ± 1 s.e.m.

G_TUNING_AB180D20_W_550

04-SEP-89 22:26 Page 1

FIG. R19. DETECTION ACUITY FOR WHITE LIGHT AND 550 FILTER
FOR AB IN THE HORIZONTAL NASAL MERIDIAN
AT 20 DEGREES ECCENTRICITY

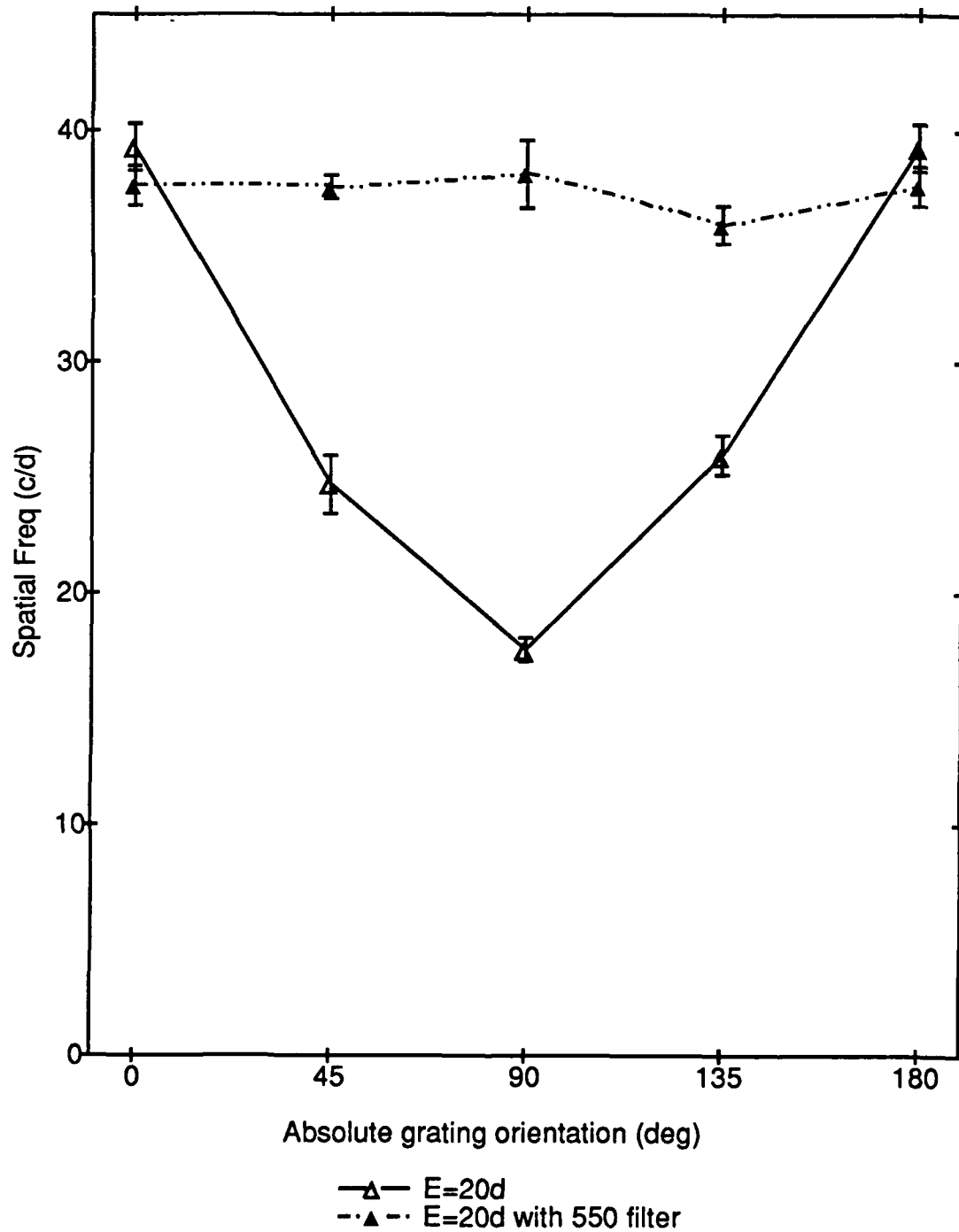


Error bars are +/- 1 s.e.m.

G_TUN_LT180D20_W_550

04-SEP-89 22:59 Page 1

FIG. R20. DETECTION ACUITY FOR WHITE LIGHT AND 550 FILTER
FOR LT IN THE HORIZONTAL NASAL MERIDIAN
AT 20 DEGREES ECCENTRICITY

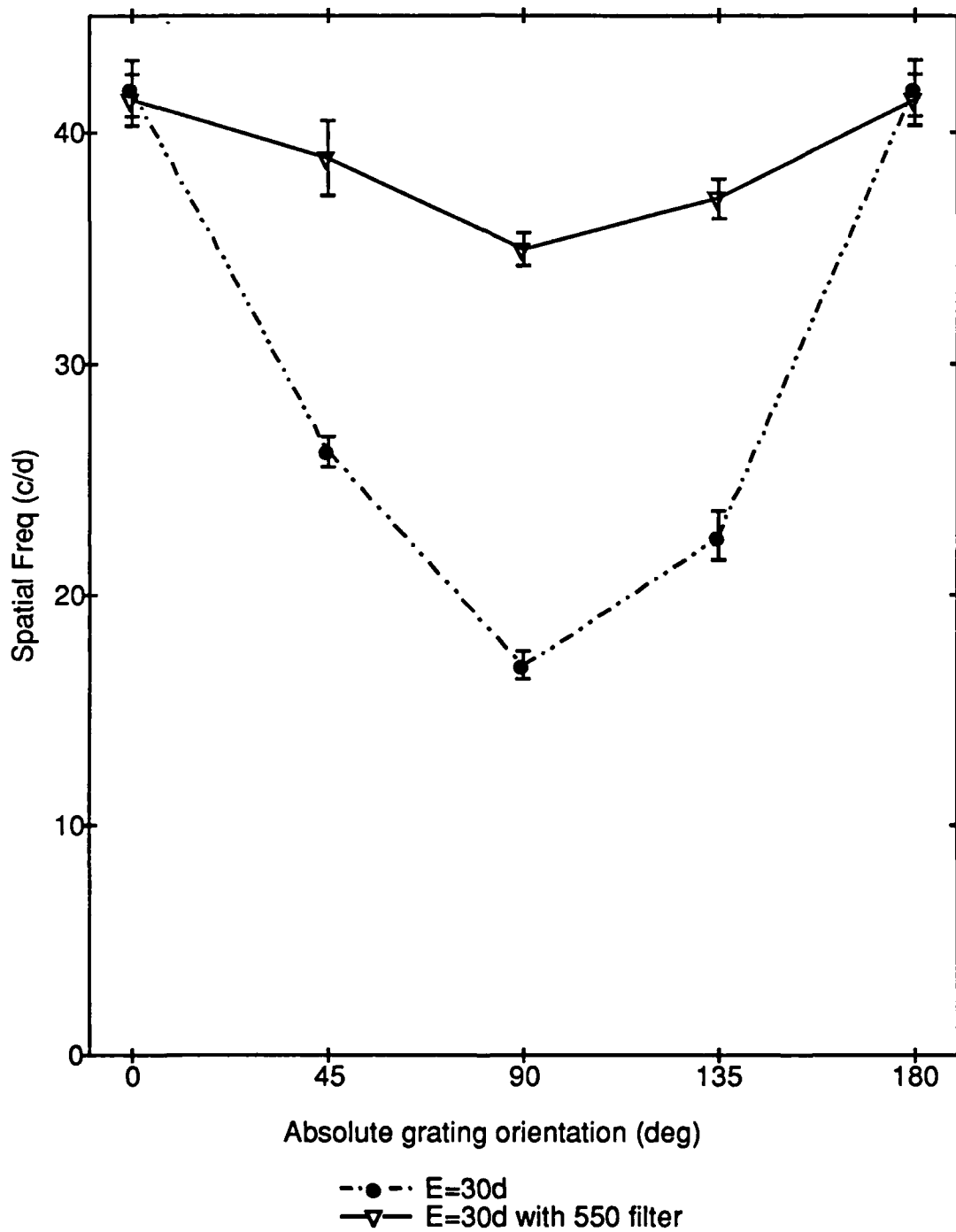


Error bars are +/- 1 s.e.m.

G_LT0D30_W_550

04-SEP-89 22:52 Page 1

FIG. R21. DETECTION ACUITY FOR WHITE LIGHT AND 550 FILTER
FOR LT IN THE HORIZONTAL TEMPORAL MERIDIAN
AT 30 DEGREES ECCENTRICITY

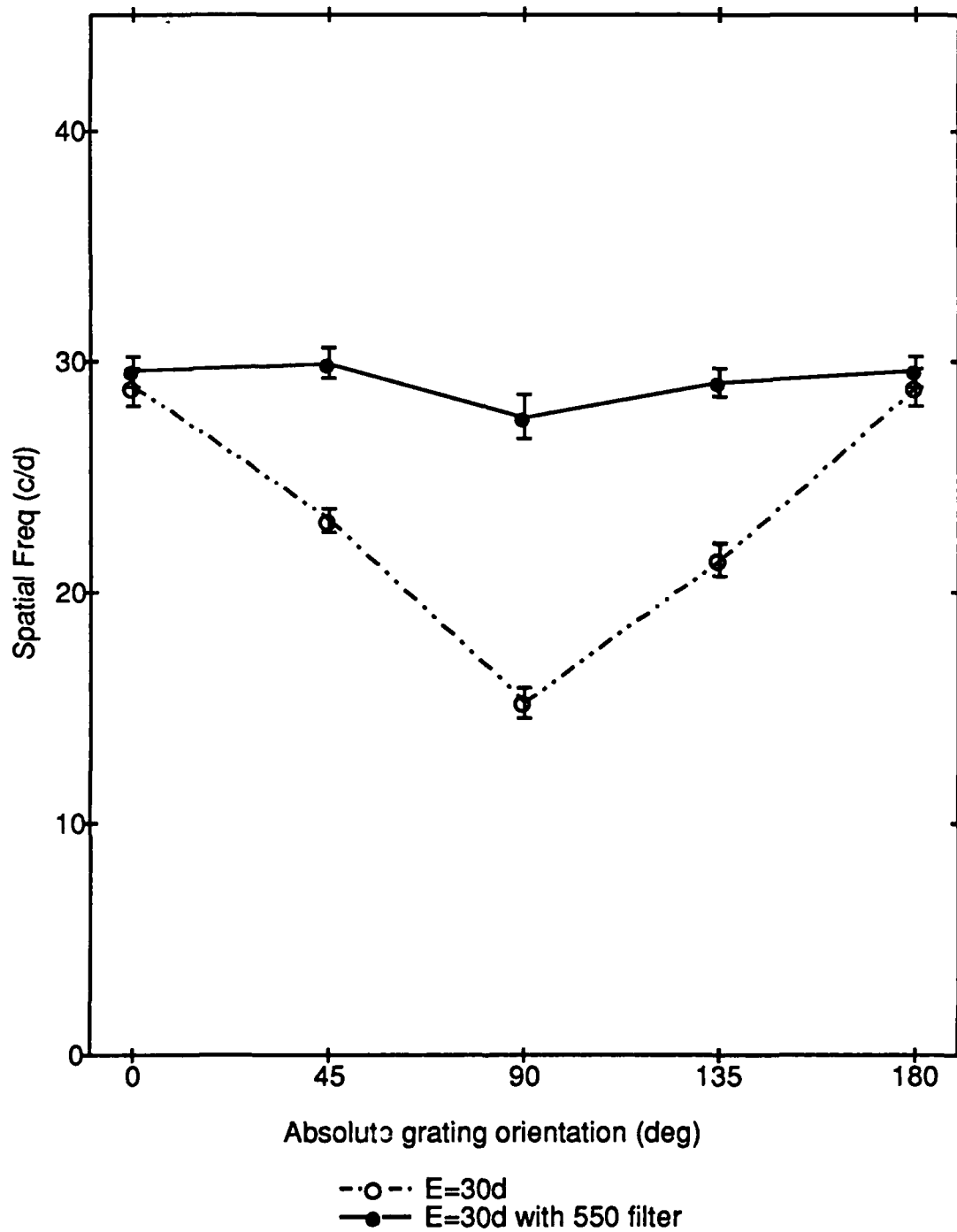


Error bars are +/- 1 s.e.m.

G_TUN_LT180D30_W_550

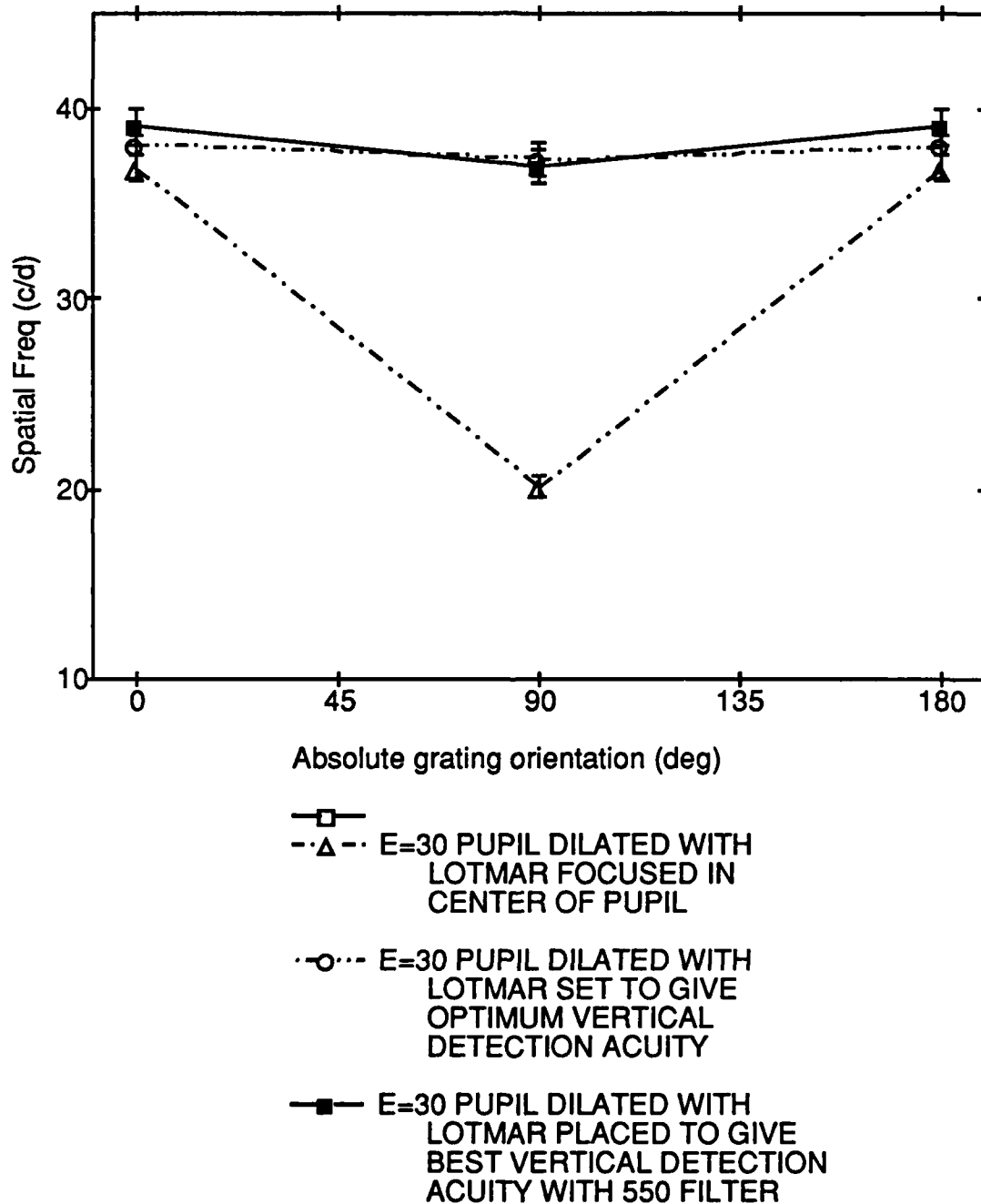
04-SEP-89 23:06 Page 1

FIG. R22. DETECTION ACUITY FOR WHITE LIGHT AND 550 FILTER
FOR LT IN HORIZONTAL NASAL MERIDIAN
AT 30 DEGREES ECCENTRICITY



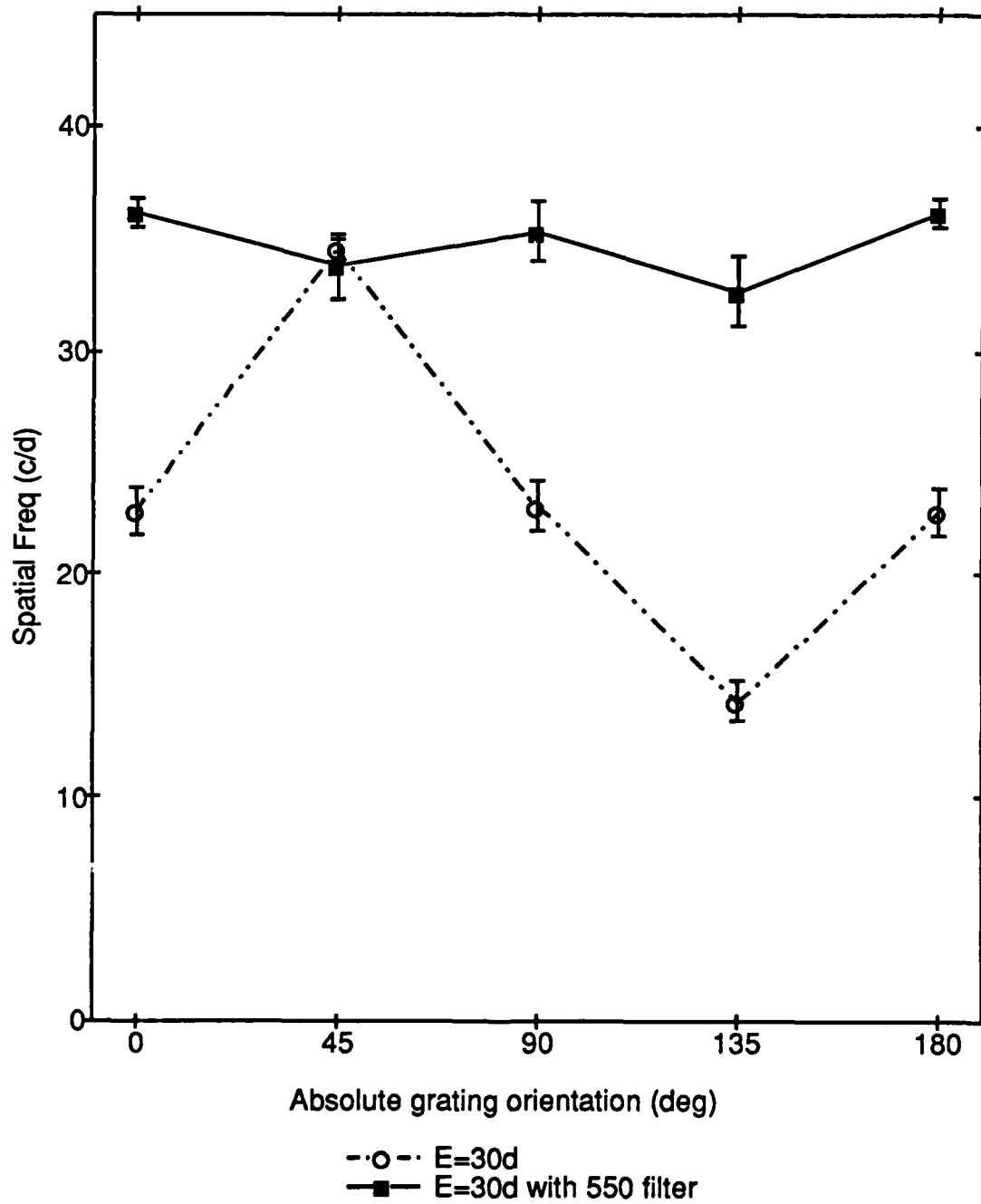
Error bars are +/- 1 s.e.m.

FIG. R23. EFFECT OF MOVING LOTMAR VISOMETER FROM CENTER OF PUPIL TO POSITION GIVING OPTIMUM DETECTION ACUITY FOR LT FOR TANGENTIAL GRATINGS



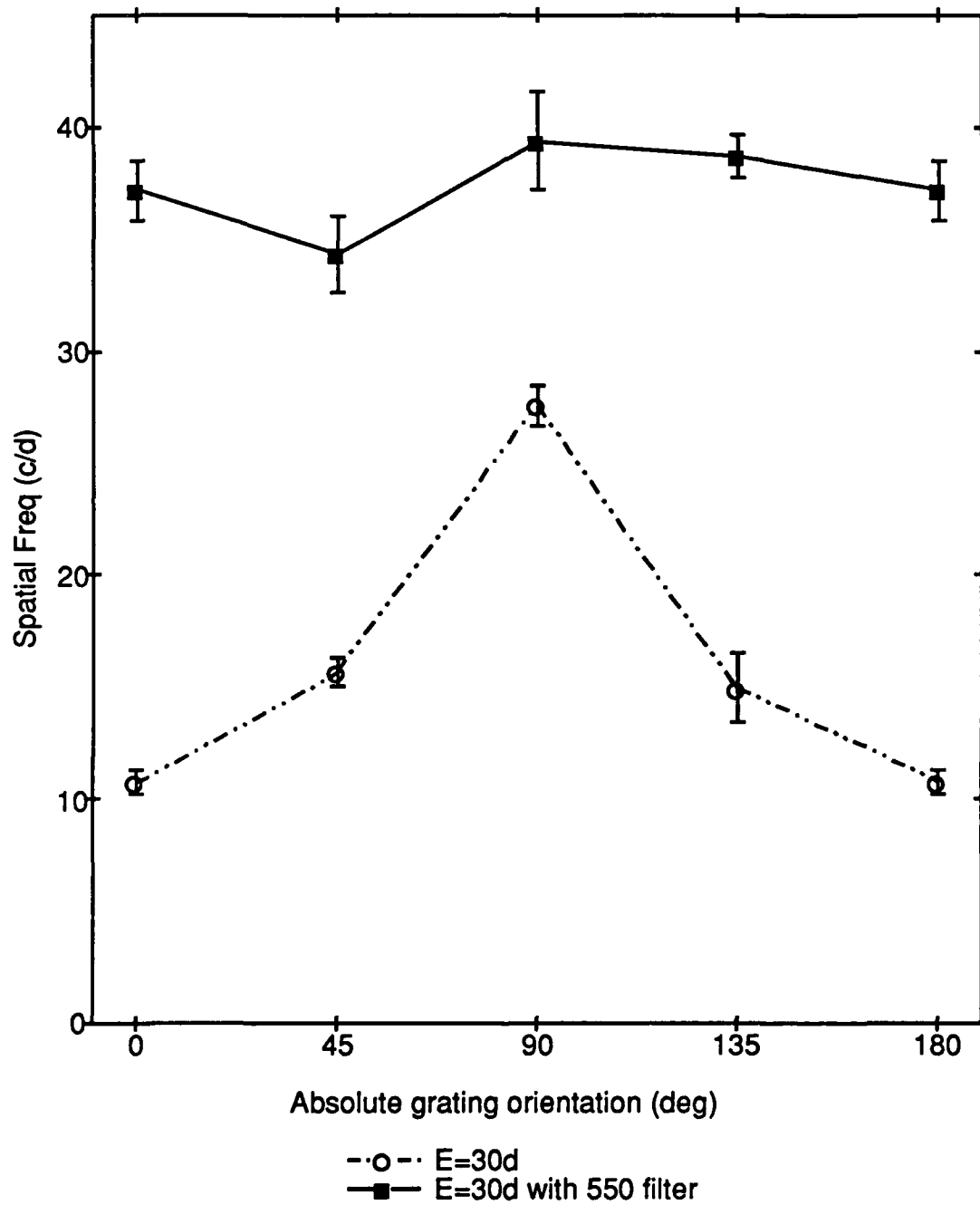
Error bars are +/- 1 s.e.m.

FIG. R24. DETECTION ACUITY FOR WHITE LIGHT USING
VISOMETER #1 AND FOR 550 FILTER
USING VISOMETER #2 FOR LT IN THE
INFERIOR NASAL MERIDIAN AT
30 DEGREES ECCENTRICITY



Error bars are +/- 1 s.e.m.

FIG. R25. DETECTION ACUITY FOR LT FOR WHITE LIGHT USING VISOMETER #1 AND FOR 550 FILTER USING VISOMETER #2 FOR LT IN THE INFERIOR MERIDIAN AT 30 DEGREES ECCENTRICITY

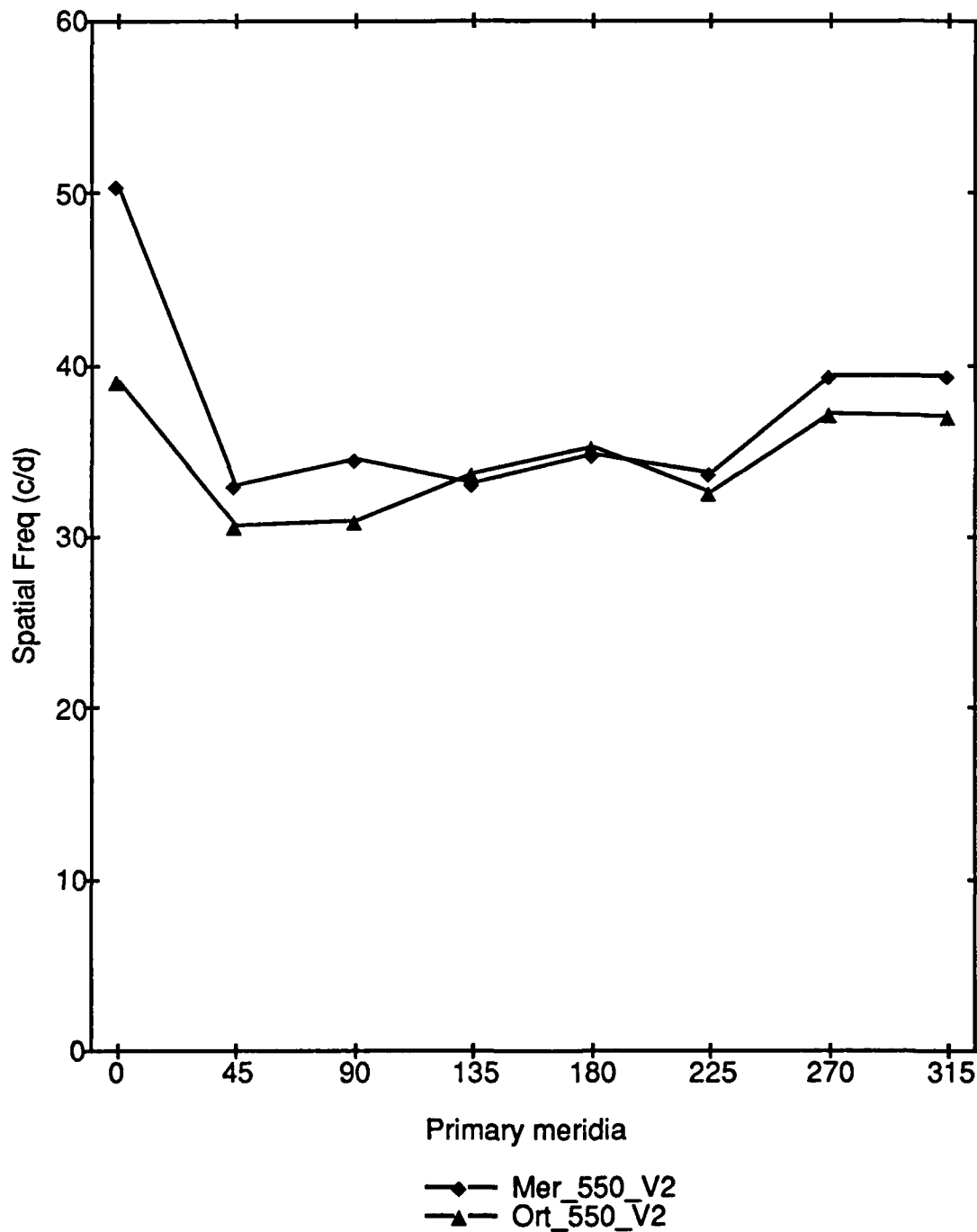


Error bars are +/- 1 s.e.m.

DETECT30_550VIS2

05-SEP-89 1:15 Page 1

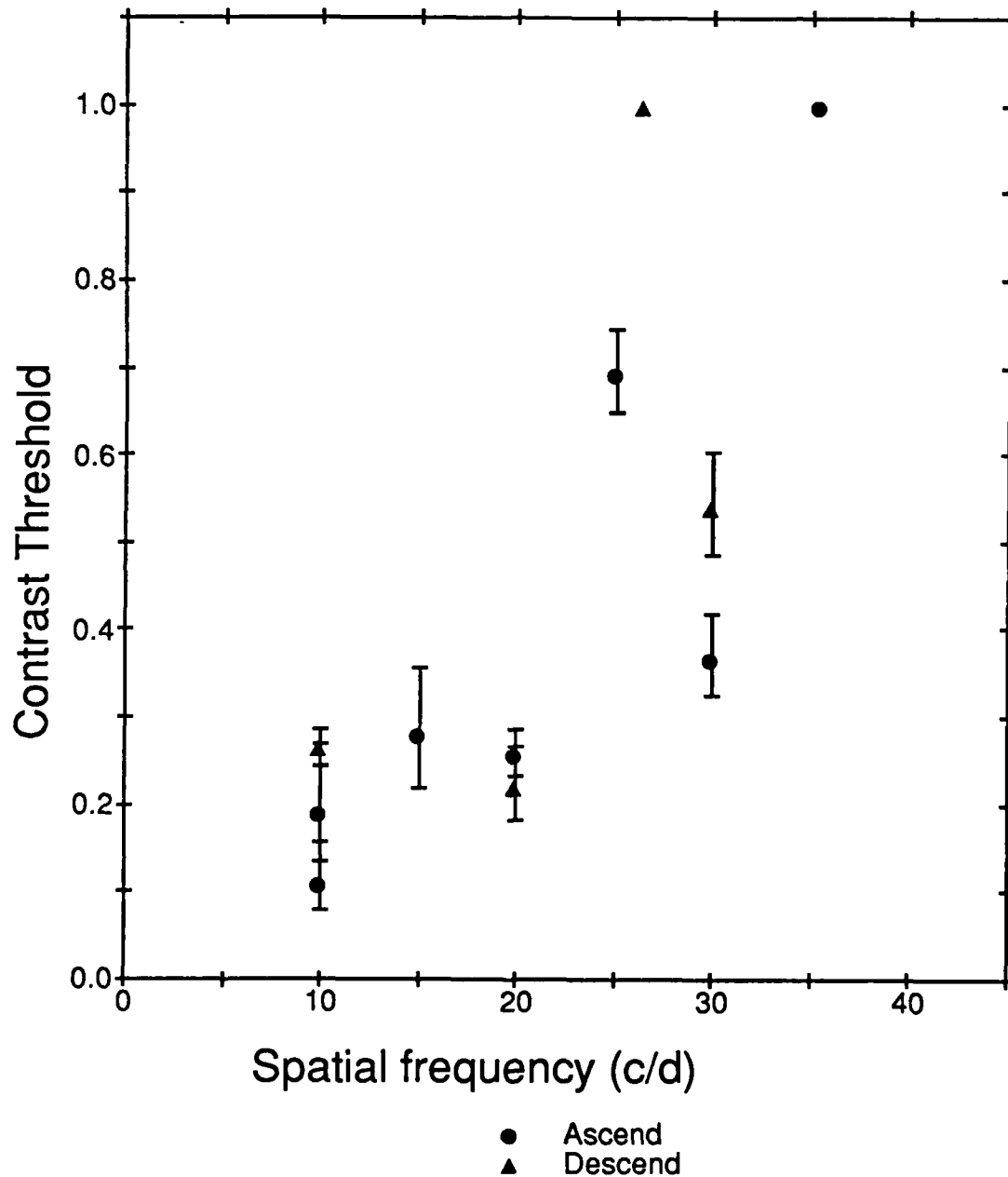
FIG. R26. DETECTION ACUITY USING VISOMETER #2 FOR LT FOR EACH MERIDIAN AT 30 DEGREE ECCENTRICITY FOR NARROWBAND 550 nm FILTERED LIGHT FOR MERIDIONALLY-ORIENTED GRATINGS AND TANGENTIAL COUNTERPARTS AS A FUNCTION OF SPATIAL FREQUENCY



R27

06-SEP-89 13:59 Page 1

FIG. R27. CONTRAST THRESHOLD OF SUBJECT LNT
AT 30 DEG ECCENTRICITY,
HORIZONTAL NASAL FIELD



Psychophysical determination of contrast threshold for narrowband (550nm) interference fringes. Thresholds for seeing-to-nonseeing trials are shown by triangles and thresholds for nonseeing-to-seeing trials are shown by circles. Error bars show ± 1 s.e.m. (n=5).

DISCUSSION

A. APPROACH

These experiments were done over a four year timeframe. Our perspectives of the experimental results and the discussion section that I would have written in May of 1986 is drastically different than that of August of 1986, and August of 1986 is considerably different from that of August 1989. Therefore, this discussion presents the progression of our thoughts as new findings occurred and the effect these findings had on the interpretation of our results.

B. QUANTIFYING DETECTION ACUITY ABOVE THE RESOLUTION LIMIT USING ALIASING PERCEPTS OF GRATINGS GENERATED INTERFEROMETRICALLY

1. Further Evidence that Aliasing Exists

In order to use a method to quantify a threshold, the method must have gained some validity. Therefore, one of our initial goals was to convince a skeptical scientific world that aliasing truly does exist in the periphery.

First of all, to make sure the aliasing percept was repeatable in more than just subject LT, the three other subjects in our experiment were tested for resolution as well as detection acuity at 20 degrees eccentricity along the horizontal nasal meridian. Figs. A.18 - 20 of Appendix 4 shows that the detection acuity are distinctly different from the resolution acuity for all stimuli.

Secondly, to make sure that the aliasing percept was not just a repeatable artifact or entoptic phenomenon, several observations were made. If the aliasing percept is the result of undersampling of interference fringes which are a higher spatial frequency than the resolution limit, then naturally the aliasing percept can only appear when the fringes are present on the retina. For the interference fringe to appear it is necessary to have both point sources enter through the pupil. We verified that the aliasing percept disappears when one

point source is prevented from entering the eye. If aliasing were an entoptic phenomenon which depended on total luminance, then the changes in orientation for the white light grating which change the retinal contrast of the stimulus but not its mean luminance should still have the same thresholds. They obviously do not.

Lastly, later experiments by other investigators confirmed the presence of aliasing in the periphery by using both natural (Smith and Cass, 1987; Still and Thibos, 1987) viewing and different interferometric techniques (Williams and Coletta, 1987). These experiments will be discussed later.

2. Radial Tuning

a. Meridional Effect which Includes Effects of Lateral Chromatic Aberration

The white light experimental results clearly indicated that all eight primary meridians demonstrated a highly significant meridional effect for 20 and 30 degrees eccentricity (Cheney and Thibos, 1986). The achromatic moire interferometer effectively bypassed all the retinal optics except lateral chromatic aberration. The initial consensus of opinion was that lateral chromatic aberration was predicted to have a minimal effect on the results and that there was a strong indication that the neural retinal fields were elongated. The strength of the meridional effect increased with eccentricity as indicated by the increase in the meridionally shifted component in the Fourier analysis curves in Figs. R9 - R10. In trying to account for the meridional effect we centered our attention on eccentricity 30 degrees where it had its greater effect rather than 20 degrees. Fig. D1 shows the detection threshold at 30 degrees eccentricity for LT for meridional gratings and their tangential counterparts. Though there is some variation across meridians, especially for 0 and 315, the majority of the results for the meridional gratings are around 30 cycles per degree and the majority of the tangential counterparts are around 15 cycles per degree. Possible explanations for the variation in results will be discussed later. At Arvo 1986, it was suggested that we go the final step and also eliminate lateral chromatic aberration. The

stimulus would then essentially bypass all of the eyes optics and give an even better estimate of the retinal receptive fields.

b. Elimination of Meridional Effect Using Narrowband Interference Filter and its Comparison with White Light Data

Placing a narrowband 550 nm filter in the Lotmar Visometer, we repeated many of the data points done in the white light experiment along the horizontal meridia. A comment frequently heard from the subjects was that the aliasing looked a lot cleaner with the addition of the narrowband filter even for the meridional gratings. Except for a small but significant residual meridional effect at 30 degrees eccentricity in the temporal meridian, results indicated that using the narrowband filter eliminated the meridional effect (Cheney and Thibos, 1987) as demonstrated in Figs. R18 - R22. Later experiments at 30 degrees eccentricity for subject LT verified that this finding was true for all meridia at 30 degrees eccentricity (Figs. R23 - R26). Fig. D2 plots the detection threshold at 30 degrees eccentricity for both white and narrowband (550 nm) filtered light for meridionally and tangentially oriented gratings as a function of spatial frequency. It shows that the difference in detection acuity between 315 and the other meridia except for 0 has disappeared. Even remembering that the earlier results were done on the same model but different visometer (V1) than the later data (V2), the main result is that meridional effect disappears or at least is drastically reduced. Therefore, the neural receptive fields now appear to be round rather than elongated. For orientations which were replicated using both visometers, V2 (done three years later) seems to have results about 5 cycles per degree higher than the earlier results with V1.

3. How Do Detection Acuities Compare to Those Predicted by Cone Inner Segment Diameter?

a. Background

Anatomists and researchers (Miller, 1983; Yellot, 1984) seem to now agree that the inner cone segment diameter is the critical limiting aperture in the cone. Even though it is

larger than the cone outer segment diameter, it is the aperture through which light enters the cone. The waveguide theory (Enoch, 1961; Miller, 1983) advocates that the collected light will then be guided through the smaller outer cone segment aperture where it is absorbed by photopigments.

Once the grating is through the cone aperture it is summated. Therefore, the important question is how much modulation is needed between the cones for the subject to judge that contrast is present and not just a uniform field. Assuming the cone absorbs light equally across a circular aperture, the modulation between cones is predicted by the Sombbrero function and is dependent on the product of spatial frequency and the inner cone segment diameter. The spatial frequency increases until the luminance readings at all cones of equal aperture size is the same and the modulation between cones is 0%. Theoretically, 0% modulation for a sinusoidal grating occurs when the period of the grating is 1.22 times the cone inner segment diameter. Beyond that point there is a negative contrast which can increase to about 13% and then decrease and make another 0 crossover (see Fig. D3). These peaks of positive and negative contrast continue as the spatial frequency increases, but each time the maximum contrast obtainable decreases.

Williams (1985a) in exploring foveal aliasing used his results to determine an upper limit for the cone inner segment diameter. His logic was that his subjects saw continuous aliasing until they reached a specific spatial frequency where the aliasing suddenly disappeared. If the subject's contrast threshold should really be almost 0%, the cone inner segment diameter could be calculated by dividing the period of the grating divided by 1.22. If the contrast threshold was really greater than 0%, the first crossover would occur at a higher spatial frequency and the cone diameter would be smaller. Therefore, even though a precise inner cone diameter could not be calculated, it could not be greater than the period of the threshold spatial frequency divided by 1.22.

b. Our Experiments

Our experimental approach was slightly different since our subjects went from non-seeing to seeing (high spatial frequency to low spatial frequency). However, periodically using the highest detection acuity, we would have our subjects continue to reduce the spatial frequency to see if a break in the aliasing pattern occurred. Since the pattern was always continuous, we assumed the subjects were at a spatial frequency lower than the first crossover. The only meridian which was at all unusual was the temporal meridian for LT. Here at very high spatial frequencies LT would get low contrast noise fading in and out before he reached his criteria of dynamic high-contrast aliases. But even with LT trying to be consistent with his criteria, his detection acuity was still higher than those for the other meridia.

Initially, we had looked at detection acuity values for the white light data along the horizontal nasal meridian and tried to make a reasonable prediction of receptive field size. We made the assumption that the contrast threshold would be reached when the period of the detection threshold frequency was equal to the diameter of the receptive field. This threshold is equivalent to an 18% modulation of the output from the cones (as calculated using the Sombbrero function). Using this assumption the detection acuities were very close to the expected diameter of a cone inner segment (based on extrapolation of Polyak's data, 1941) at these eccentricities in the peripheral retina (Fig. D4 from Thibos, Cheney, and Walsh, 1987). Note, that in Fig. D4 that the minimum angle of detection is compared to the radius (not the diameter) of the receptive field. The figure further shows that at 30 degrees eccentricity, the smallest receptive field size other than a cone is for a human ganglion cell with a 2 min radius (4 min diameter). This ganglion cell receptive field radius is more than double Polyak's estimate of 0.9 min radius for the inner cone segment diameter and also double our estimate of the size needed for an equally weighted receptive field to account for our detection acuity results.

Miller (1983) had expressed some concerns about some previous measurements on cone inner segment diameter being underestimated due to shrinkage and other factors in tissue

preparation. Recently, Curcio (1987) has published data on cone inner segment diameters for different retinal eccentricities. It was reassuring to see that Curcio's data which matched Miller's data for the foveal inner cone diameter was very close to our extrapolation of Polyak's data.

In a recently concluded narrowband 550 nm experiment on subject LT at 30 degrees eccentricity, his maximum detection acuity was just below 40 cycles per degree (except the temporal meridian which was 50.5 cycles per degree) and averaged about 35 cycles per degree. Using 40 cycles per degree as the maximum value cutoff would translate into a maximum cone inner segment diameter of 1.8 min (using Williams' criteria, 1985) which has a 0 crossing at about 40.6 cycles/degree. (1.45 min inner cone segment diameter would be maximum for the temporal meridia; other possibilities for this higher detection acuity are discussed in section "Possible reasons for deviations from expected values"). These values for a maximum receptive field diameter which integrates uniformly over its diameter are obviously much smaller than the 4.0 min diameter of the smallest human ganglion cell.

At 30 degrees eccentricity we had extrapolated a inner cone diameter of 1.8 min while Curcio's data indicates that the diameter may be closer to 1.7 min. Using a 1.7 min inner cone segment diameter at 30 degrees eccentricity in the evaluation of LT's white light and narrowband data (average detection acuity of about 35 cycles/degree) would make his average threshold modulation between cones to be about 19%. Therefore (except for possibly horizontal gratings at 30 degree in the temporal meridia), the detection acuities are consistent with those detection acuities which would be predicted by the cone inner segment diameter and are inconsistent with a ganglion cell population with a 4 min diameter receptive field which averages uniformly across cones. The predicted average detection threshold of 19% for LT (using 1.7 cone inner segment diameter) at 30 degrees eccentricity would make seeing beyond the zero crossing (except possibly temporal meridian) unlikely and is consistent with subjects reports that after the aliasing pattern disappears, it does not reappear again at higher spatial frequencies.

Overall, our detection acuity data indicates that detection information at the cone level is being reliably mediated centrally. Therefore it seems probable that either information from the cones is being processed nonlinearly or there are ganglion cells with "monosynaptic" pathways which have yet to be described anatomically in the periphery.

4. Comparing Experimental Results at 30 Degrees Along The Horizontal Meridia with Theoretical Predictions of Contrast Degradation Due to Lateral Chromatic Aberration And Spatial Summation By Cones

a. Approach

Having shown experimentally that detection acuity varies with the orientation of white light interference fringes but not for narrowband fringes, we ask whether this effect can be quantitatively accounted for by the lateral chromatic aberration of the eye. The argument is as follows. As the spatial frequency increases for a tangentially-oriented, white grating, the retinal contrast falls due to chromatic aberration. Eventually, the contrast will fall below threshold and the corresponding spatial frequency is thus the cutoff spatial frequency for contrast detection. To employ this line of reasoning to predict experimental results we need two items of information: the optical MTF for white interference fringes and retinal threshold contrast for our subjects.

b. Optical MTF - Accounting for Lateral Chromatic Aberration

Why should the meridional gratings be effected the least and the tangential gratings the most?

Fig. D5. shows how the two spatially coherent point light sources for the tangential grating no longer symmetrically straddles the eye's optical axis. As was seen in Fig. M2, the two point sources look like rainbows. The key in Fig. D5 shows the separation of the red and blue parts of the spectrum. Since the red end of the spectrum needs to be separated a greater distance than the blue end of the spectrum to achieve the same spatial frequency, the red is on the outside of the two points of light and the blue is on the inside. To determine the magnitude of the effect caused by the non-symmetry of the point sources, Dr

Thibos calculated fringe contrast as a function of spatial frequency by using a water eye model (Thibos, 1987). Fig. D5 further shows how the non-symmetric entrance causes the two point sources to go through non corresponding refractive surfaces and travel different path lengths. The blue light is refracted more than the red so that it is further away from the red light in the top point source and closer to the red light in the bottom light source. The two point sources are no longer symmetrical, and the individual wavefronts are at different angles. The result is a minor change in spatial frequency but a major shift in phase which varies with wavelength. As these different wavelengths have become out of phase with each other, destructive interference has occurred which drastically reduces the grating's contrast. For meridional orientations the two points are still able to travel close to symmetric paths and thus avoid the phase shifts which are the major cause of contrast loss from lateral chromatic aberration. The results for three different grating orientations at 30 degrees eccentricity are shown by the dashed curves in Fig. D6. The tangential grating is affected the most.

Fig. D7 shows that the effect of lateral chromatic aberration parallels the meridional effect in that they both increase with increasing eccentricity.

A further demonstration of the importance of the two point sources entering the eye symmetrically located about the eye's optic axis is shown by the dilated pupil experiment. Shifting the point sources which formed the tangential grating to a location where they were more symmetric to the eye's optical axis also eliminated the meridional effect.

c. Predicted Interaction of Optical MTF with Retinal Contrast Threshold for Fringes for LT and Comparison with Experimental Results.

Retinal contrast thresholds were measured for narrowband (550) fringes and were presented in Fig. R26 and are replotted in Fig. D8. To predict detection acuity for tangential, white gratings, for example, we need to identify in Fig D8 that spatial frequency for which the optical contrast falls below psychophysical threshold. There is some uncertainty as to the exact answer because of the variability in the psychophysical data. To

overcome this problem we constructed confidence bounds by linking the upper extent of the error bars and also the lower extent. This envelope, shown by the shaded area in Fig. D8, captures the uncertainty of the psychophysical data and allows us to estimate an upper and lower limit to the predicted cutoff spatial frequency, as shown by the arrows. Similar predictions were obtained for the other two grating orientations (45 degrees, 0 degrees) and the results are plotted on Fig. D9 along with the experimental measurements of two sets of white light data for LT at this retinal position. The quality of the match is extraordinary.

d. Modeling Experimental Results

(1) Basis for Calculating Neural Contrast Threshold

Fig. D10 is a model which may put the selective filtering effects that have been described into perspective. The stimulus enters the eye and is affected by the eye's optical MTF which alters the stimulus so that the fringe at the retinal surface has a different contrast. In case of the achromatic interferometer, lateral chromatic aberration is essentially the only remaining aberration affecting this MTF. (Using the narrowband filter with the achromatic interferometer essentially makes the optical MTF equal to 1 and the stimulus and the fringe contrast are equal.) The fringe is then sampled by the cones. The cone density in the matrix in the diagram is too low to faithfully represent the fringe's spatial frequency. Each cone averages the light that enters its aperture. In order for the cones to differentiate the fringe from a uniform field, there must be a difference in output between the cones which is above threshold. As the spatial frequency of the fringe increases the difference in the output between the cones decreases as demonstrated by the Sombbrero function Fig. D3. By the time the spatial frequency of a 100% fringe contrast grating has a period equal to the diameter of the cone inner segment, the Sombbrero function calculates that the modulation of the output from the cones is reduced to about 18%. This is similar to the modulation threshold predicted for LT for a 1.7 min cone. In the diagram the period of the fringe is greater than the diameter of the cone. Therefore, if the fringe contrast in the diagram was

100%, LT should be able to detect a contrast difference between the cones and since there is undersampling by the cone matrix, he may see an alias as a neural output.

In Fig. D10 and in the discussion on comparing detection acuities to those predicted by inner cone segment diameters, the only factors which are mentioned as affecting the final modulation between the cones are the optical MTF and the cone inner cone segment diameter. The question then arises: is it reasonable to assume that the contrast modulation between cones for detection of a fringe grating is the same for all grating orientations and for all spatial frequencies? If so, then the difference in fringe contrast thresholds for different spatial frequencies in Fig. D8 is due to the degradation of the higher spatial frequencies by the cone aperture.

If this assumption is true, knowing the threshold modulation between the cones and the cone inner segment diameter, we should be able to predict what fringe contrast would be required at each spatial frequency to produce the necessary threshold modulation.

Rearranging the equation in Fig. D10 gives:

$$\text{fringe contrast} = \frac{\text{Modulation between cones}}{\text{somb}(\text{Spatial frequency} \bullet \text{cone dia})} \quad (1)$$

To obtain a value for cone aperture size we can use the prediction by Curcio (1987) that a cone inner segment diameter is approximately 1.7 min (.0283 deg) at 30 degree in the periphery.

To obtain an estimate for the modulation between the cones we need to know one fringe contrast value. The question now becomes: what is the most accurate way to determine this value so that it will have the most predictive value for our white light and narrowband filtered light experiments? These experiments involved determining detection acuity from non-seeing to seeing (high spatial frequency to low spatial frequency). There is only one data point done precisely that way and that is the point on the curve for 100% fringe contrast for the ascending contrast data. The detection acuity for that point is 35.4 cycles per degree which matches very well with the narrowband data done previously. We now

can determine the modulation threshold by substituting into equation 1. Since this data point agrees so well with the previous narrowband data, the modulation threshold value is the same as in those experiments 18%.

We now use the 18% modulation value and the 0.0283 deg inner cone segment diameter and determine a predictive fringe contrast for different spatial frequencies and place the curve which shows the results of these calculations on Fig. D11, which contains the non-seeing to seeing (ascending contrast) data from Fig. D8.

Now using this predicted retinal fringe contrast threshold curve, the procedure is the same as with the envelope. Points of intersection with lateral chromatic aberration curves are determined so that predictions can be made for the cutoff detection acuities for the tangential, oblique and meridional gratings. These predictions, along with the data from Fig. D9, are plotted in Fig. D12. The fit is reasonably good indicating that for this data the model which uses a constant modulation threshold value for all spatial frequencies was a good indicator of the experimental value.

But this is only a measurement of one individual at a specific location in the visual field. Can the same technique (strictly for purposes of comparison) be applied to the other subjects' data? If so, than it would give an opportunity to compare the data against a given theory, to talk about possible sources of variability in collecting our data and hopefully put the results of the experiment for all subjects into a better prospective. The main key is the same as for LT; to obtain an accurate estimate of the threshold modulation between the cones. Since the experiments used Method of Adjustment, the threshold modulation values will vary depending on the criteria of the subjects. For LT, we used his detection acuity for narrowband 550 nm filtered light to determine the threshold modulation. However, since a properly aligned meridional grating should not be significantly attenuated by lateral chromatic aberration, a reliably accurate threshold modulation can be determined from the meridional detection acuity by using the Sombbrero function for the predicted cone aperture size at that eccentricity (1.7 at 30 degrees). The rest of procedure is the same as was done

for LT. Knowing this modulation between the cones and using the Sombrero function, equation (1) can be used to determine a curve which would show a predicted fringe contrast threshold for each spatial frequency and would be analogous to the curve generated for LT assuming a threshold modulation between cones of 18%. The intersection of predicted fringe contrast threshold curve with the appropriate attenuation curves for lateral chromatic aberration would give the projected detection acuity threshold for the white light experiments.

(2) Comparing Predictions with Experimental Data

Both FC and SG had a detection acuity of approximately 28 cycles per degree for the meridional grating for the horizontal nasal meridian at 30 degrees eccentricity (same retinal position as done for LT above). For a 1.7 mm cone inner segment diameter this translates into a modulation between cones threshold of about 40% (more conservative threshold than LT). Fig. D13 shows the predicted retinal fringe contrast threshold curve using a modulation between cones of 40%. Fig. D14 show these projected values for threshold spatial frequencies for the oblique and tangential gratings as compared with their white light data.

Since the predicted values for threshold detection for the oblique and tangential gratings for LT, SG, and FC are fairly close to the experimental white light data, the Fourier analysis of the predicted curves might give some insight to the other white light data at 30 degrees eccentricity as well. Since these predictions are for gratings along the horizontal nasal meridian, no meridional shifting of the A_1 , B_1 , and A_2 results are necessary, but when comparing other meridians the important values are $A_{1_mer_shift}/mean$, $B_{1_mer_shift}/mean$, and $A_{2_mer_shift}/mean$. First of all, looking at the predicted curves what values would be expected for the A_1 , B_1 and A_2 coefficients? Since the obliques have equal predicted detection acuity, the $B_1/mean$ component will be zero. There is a large difference between the meridional and tangential gratings, therefore a large $A_1/mean$ component is expected. For the model for LT $A_1/mean$ equaled 49% modulation and for

FC and SG it equaled 55 %. With increasing eccentricity the predicted detection acuity of the obliques becomes much lower than the average of the meridional and tangential gratings due to lateral chromatic aberration, therefore it would be expected that a positive A_2/mean would be needed to add to the A_1_{MS} to predict lateral chromatic aberration's effect. For the model for LT A_2/mean equaled 14% modulation and for FC and SG it equaled 16% modulation. Looking at the Fourier analysis on the white light data for data LT, SG, and FC, (Figs. R9 - R12 and Figs. R15 - R17), the overall trend seems to follow a similar pattern.

(3) Possible Reasons for Deviation from Expected

Overall, the experimental detection acuities from LT, SG, and FC along the horizontal meridian at 30 degrees eccentricity fit the predictions of the model fairly well. But not all the data would give that good a fit.

There are three different general areas from which deviations could arise.

The first area is that the model may not hold across meridians and therefore is not a good predictor of the data. This could be because the conditions that determined the model were done with a dimmer target which was narrowband, and a smaller target size (2.5 deg vs 3.5 deg) than the white light experiments. Another possibility is the hypothesis that the threshold modulation between cones for detection is the same for all grating orientation and for all spatial frequencies is incorrect. It could also be that the cone diameter is different from 1.7 min or that it even varies for different meridians at same eccentricity. For example a cone inner segment diameter of 1.4 min could account for the high detection acuity for LT along the temporal meridian. A third possibility is that the water eye model calculations for lateral chromatic aberration may deviate from the amounts of lateral chromatic aberration really present in an actual eye.

The second area is variability due to the subject. The subject's criteria or even his attention may vary between trials or even between orientations. Although the subject could take as long as he wished and rest when necessary, each trial required from 30 to 45

minutes of intensive work. Even if the subject's criteria stay relatively constant, his results may be variable due to fading as a result of the Troxler Phenomenon. This was a major complaint of subjects AB and SG particularly at 30 degrees eccentricity. The subjects may be misaligned enough to throw off their detection acuities for the different orientations. For instance if the point sources which generate the tangential gratings are aligned closer to the normal to the corneal surface, this would increase the tangential detection acuity and possibly decrease the meridional grating detection acuity due to loss of contrast from pupillary interference. This was a distinct possibility for subject LT who initially tried to get the best detection acuity at all times. He was particularly frustrated at meridian 315 at 30 degrees eccentricity where he never felt properly aligned. His meridional grating detection acuity was unusually low, especially compared to the gratings which were oblique to the meridian which almost had the same detection acuities. This is particularly true for the oblique meridia which presented a much more difficult alignment challenge. Narrowband 550 light alignment was more of a problem since subjects no longer had the rainbows appear when they were not aligned.

The third area is a possible influence from other factors. The possibility was proposed by Dr Thibos that perhaps the nerve fiber layer was regular enough at certain spots on the retina to interact with the fringe grating and form a moire fringe with a lower spatial frequency component which might enable detection of gratings at higher spatial frequencies. This suggestion is an attempt to explain the high detection acuity found in the temporal meridian for subject LT at 30 degrees eccentricity.

5. Protective Effect of Longitudinal Aberration (Personal Communication; Zhang, Bradley and Thibos). Interaction Offers Explanation for Negation of Large Lateral Chromatic Effect

Our results in the white light and narrow band experiments demonstrated the enormous isolated effect that lateral chromatic aberration has on the contrast of non meridional

gratings in the peripheral retina. Our initial reaction was to expect that in combination with the other optical aberrations that lateral chromatic aberration would act as an orientation sensitive filter and drastically affect the contrast of the grating before it reaches the retinal surface.

However at the same time the different wavelengths are becoming out of phase with respect to each other due to lateral chromatic aberration, they are also being focused at different planes in the eye due to longitudinal chromatic aberration. Therefore, when the eye focuses one wavelength of light, the others are out of focus and this causes a reduction in contrast of these out of focus wavelengths. Now these wavelengths instead of causing destructive interference are merely reducing the contrast equally for the grating as whole.

6. Other Evidence of Aliasing in the Periphery Using Interferometric Techniques.

Williams (1987) described an aliasing effect out to 20 to 25 degrees in the periphery. By observing the alias pattern his subjects were able to estimate cone spacing by determining what spatial frequency caused an orientation reversal of the stimulus grating. This reversal is predicted to occur when the period of the interference fringe equals the average spacing between cones. Beyond 25 degrees the orientation reversal effect disappeared but spatial noise continued until far into the periphery.

C. DETECTION ABOVE THE RESOLUTION LIMIT FOR NATURAL VIEWING

1. Human Psychophysical Studies Using Natural Viewing

At ARVO (Cheney and Thibos, 1986) we set up a demonstration which permitted many individuals to experience aliasing using natural viewing.

Smith et Cass (1987) demonstrated under controlled experimental conditions an aliasing percept at 4.5 and 7 degrees in the periphery. They found that an equi-luminant surround which matched the mean luminance of the grating and a bright high contrast grating stimulus greatly enhanced the alias percept. This enhancement they felt may explain

why Virsu and Rovamo (1979) who used a low contrast relatively dim stimulus with a dark surround did not notice any difference between the resolution and detection acuity.

2. Quantifying Detection Acuity and Peripheral MTF at 30 Degrees in the Periphery (PhD Thesis by David Still)

Still and Thibos (1987) also were able to detect peripheral aliasing using natural viewing as far out as 30 degrees in the periphery. Still, having modified the Lotmar visometer to vary contrast as well as spatial frequency and using the narrowband 550 filter, now had available the capability to measure the contrast sensitivity threshold for detection for both natural and interferometric viewing conditions. His thesis (1989) demonstrates that for 30 degrees in the periphery on the horizontal nasal meridian that the peripheral MTF is experimentally indistinguishable from the foveal MTF.

Since Still did his experiment for both horizontal and vertical gratings, it becomes an interesting test case for the protective effect of longitudinal chromatic aberration. One would expect that if lateral chromatic aberration were to play a significant role as an orientation sensitive filter that along the horizontal meridian aliasing for horizontally-oriented gratings should be able to be perceived at significantly higher spatial frequencies while if longitudinal aberration significantly reduced the effect of lateral chromatic aberration the detection thresholds for horizontal and vertical gratings would be closer together. The results for detection thresholds for horizontal and vertical gratings were approximately the same.

D. OVERVIEW

Interferometric viewing has provided us with a direct psychophysical measure of the detection capability for the combined retinal and post-retinal parts of the visual system. This has allowed researchers to isolate the pre-retinal attenuation of the visual stimulus and to calculate both foveal and peripheral MTF's. Knowing these detection capabilities gives

researchers a starting point for unraveling the selective filtering attributes and function of the retinal and post-retinal parts of the visual system.

We know from natural viewing experiments that spatial frequencies up to 30 cycles per degree are detected in the peripheral retina at 30 degrees eccentricity if peripheral refractive error is accurately corrected. From the experiments that bypass the eye's optics, the neural visual system is able to still perceive a persistent alias pattern for that spatial frequency and up to almost the limit of the cone aperture.

Yet aliasing in the periphery is not a problem in everyday life. To see aliasing requires a trained subject in a specialized noise-free environment with specialized stimuli for the targets. In fact, individuals need to be well trained to even resolve a grating up to the Nyquist limit. Frequently, untrained subjects can only resolve gratings of much lower spatial frequency and higher contrast. Therefore they are not even demonstrably using all the information available to them as far as resolution is concerned even under specialized conditions.

Clearly, even though we now know that spatial frequencies way above the resolution limit are perceived by the retina, we have not explained of what value these percepts have to peripheral visual function.

E. CONCLUSIONS

1. We duplicated the initial aliasing phenomenon, found in subject LT by Walsh, in three other subjects.

2. The achromatic moire interferometer essentially eliminates all optical aberrations, except lateral chromatic aberration. The interferometer was used to test up to five different eccentricities from 10 to 35 degrees in the eight primary meridians. The results indicated that eccentricities greater than 15 degrees showed a predominant meridional effect for detection acuity which became increasingly pronounced as the eccentricity increased.

3. Using a narrowband interference filter (550 nm) which made the light much more nearly monochromatic, the meridional effect disappeared in the meridians tested (except for a small residual amount in the temporal meridian at 30 degrees eccentricity. This indicated that the meridional effect was purely optically-induced with chromatic aberration acting as the selective filter. This also reduced the possibility that the oblique viewing angle of the pupil was not allowing the quasi-point sources to fit within the pupil. (Note with the filter there was a reduction in illumination that increased pupil size.)

4. Dilating the pupil and viewing the fringe through the center of the entrance pupil gave the same meridional effect. Therefore the meridional effect was not due to obscuration of the quasi-point sources by the pupil. However, moving the stimulus so the quasi-point sources from the peripheral target were more nearly normal to the corneal surface eliminated the meridional effect. This elimination of the meridional effect is consistent with calculations that the effect of lateral chromatic aberration should be reduced as the point sources enter the eye more nearly normal to the corneal surface.

5. Values for detection acuity using the narrowband 550 filter were relatively consistent at 30 degrees across meridians. The horizontal grating in the horizontal temporal meridian at 30 degrees eccentricity did seem to give a higher detection acuity though the reason for the increase in acuity is purely speculative.

6. These detection acuities are similar to values predicted by measured cone inner segment diameters. Subject LT's detection acuity for the horizontal nasal meridian at 30 degrees eccentricity equates to a modulation between receptive fields of approximately 18% for the predicted cone inner segment diameter of 1.7 min.

7. Reductions in detection acuities for meridionally tangential and meridionally oblique gratings for LT for the horizontal meridian at 30 degrees eccentricity for the white light experiments are understandable based upon the predictions from lateral chromatic aberration calculations and its intersection with the threshold envelope of contrast limits for different spatial frequencies?

8. A model which assumes that threshold modulation needed between cones is the same for all spatial frequencies makes it possible to predict a fringe contrast threshold for the various spatial frequencies. Predictions made by the model for the white light data of SG and FC at 30 degrees eccentricity using a 1.7 min inner cone segment diameter as one of its parameters, match the experimental data fairly closely. These subjects, with an apparently more conservative criterion than subject LT, had a predicted modulation threshold between the receptive fields which equated to approximately 40%.

9. Our detection acuity data indicates that information at the cone level is being reliably mediated centrally. It appears that either the information from the cones is being handled non-linearly by the ganglion cells or there are ganglion cells with a "monosynaptic" pathway which have yet to be anatomically described in the periphery.

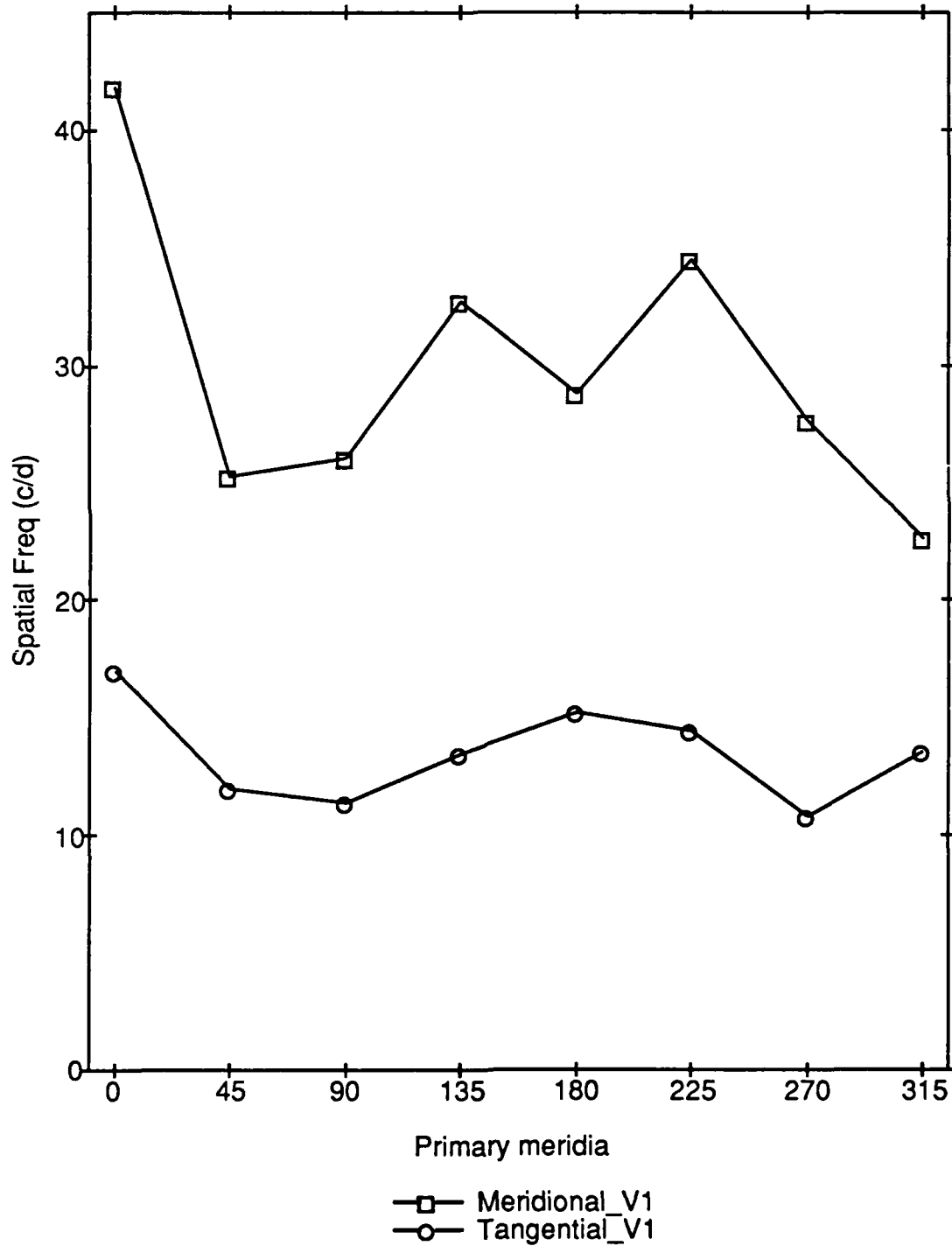
10. Using the isolated pre-retinal optical information gathered about lateral chromatic aberration can be misleading. Alone it would seem to indicate that lateral chromatic aberration acts as an orientation sensitive tuner which enables the meridional gratings to be selectively perceived at higher spatial frequencies. However, this effect appears to be true if only lateral but not longitudinal aberration is taken into account. Per personnel communication (Zhang, Bradley, and Thibos) the longitudinal aberration acts as

a protective mechanism which counteracts a good portion of the deleterious effects of lateral chromatic aberration. The result of Still's thesis for natural viewing supports their theory.

DETECT30

03-SEP-89 18:24 Page 1

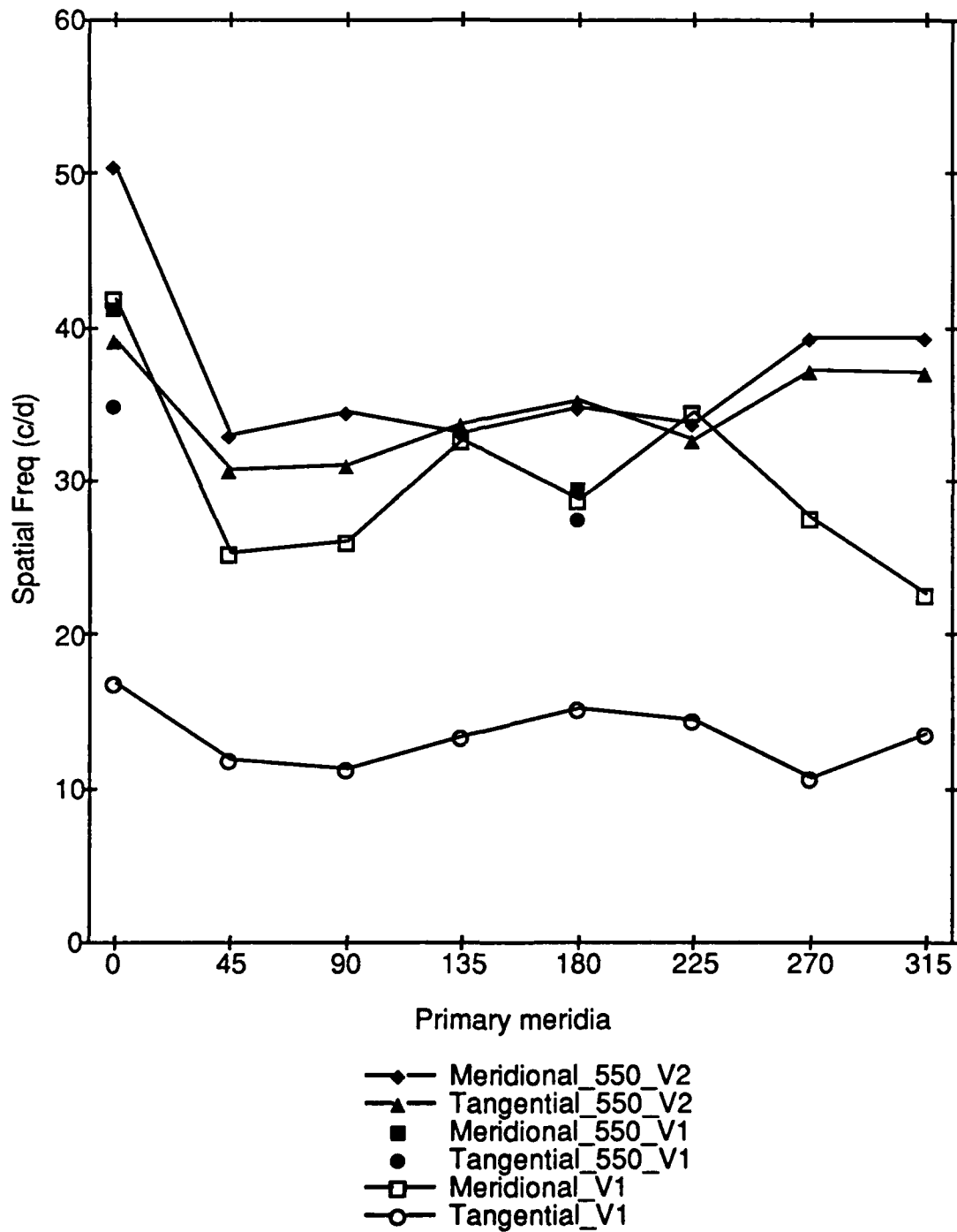
FIG. D1. DETECTION ACUITY FOR LT FOR WHITE
LIGHT AT 30 DEGREE ECCENTRICITY FOR
MERIDIONAL AND TANGENTIAL GRATINGS
AS A FUNCTION OF SPATIAL FREQUENCY



DETECT30_W_550

03-SEP-89 18:43 Page 1

FIG. D2. DETECTION ACUITY FOR LT FOR BOTH WHITE AND NARROWBAND 550 nm FILTERED LIGHT AT 30 DEGREES ECCENTRICITY FOR MERIDIONAL AND TANGENTIAL GRATINGS AS A FUNCTION OF SPATIAL FREQUENCY



SOMBRERO

03-SEP-89 19:24 Page 1

FIG. D3. SOMBRERO FUNCTION FOR A 1.7 MINUTE CONE
INNER SEGMENT DIAMETER AS A FUNCTION
OF SPATIAL FREQUENCY

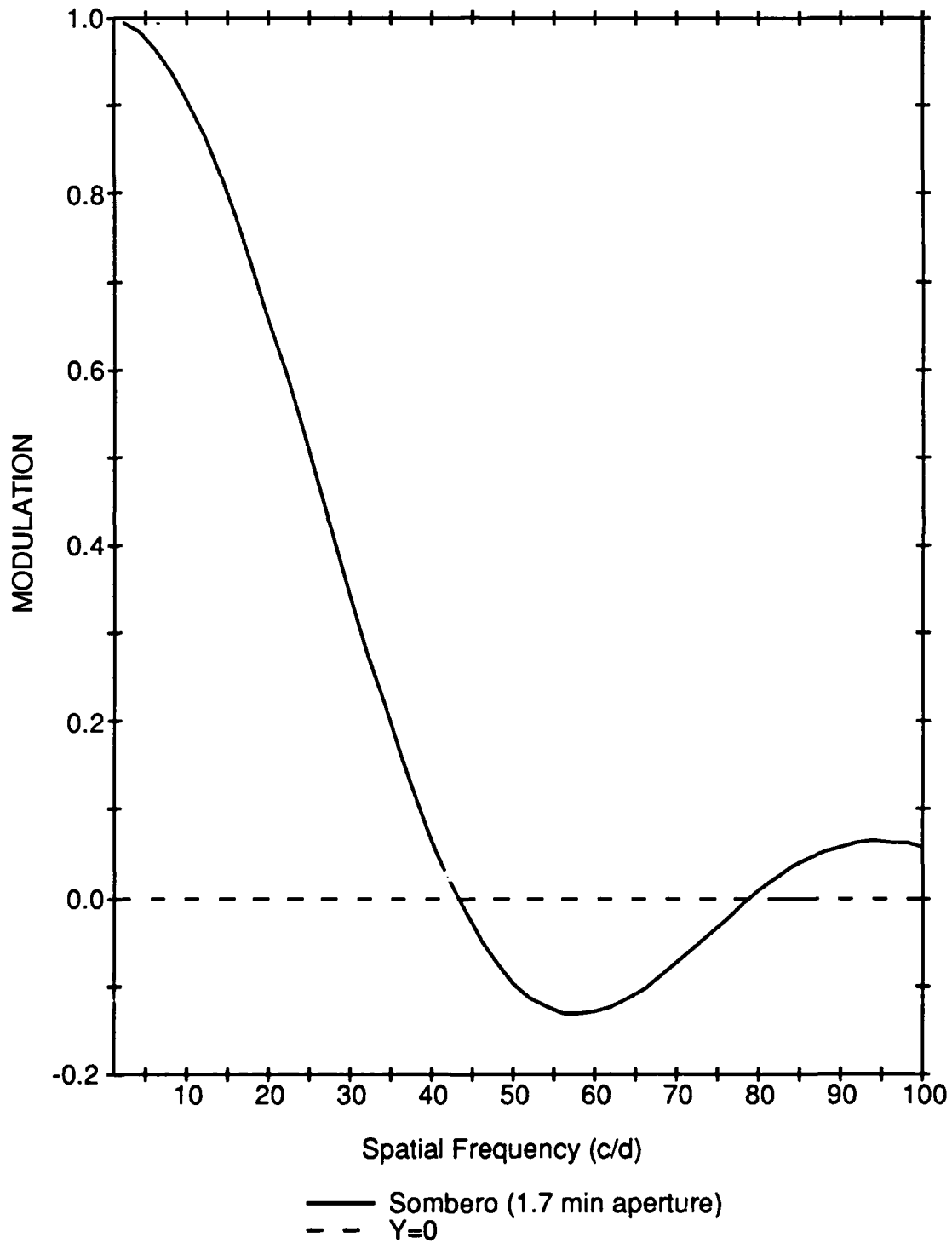


FIG. D4. COMPARISON OF RECEPTIVE FIELD SIZE FOR DETECTION WITH ANATOMICAL RECEPTIVE FIELDS

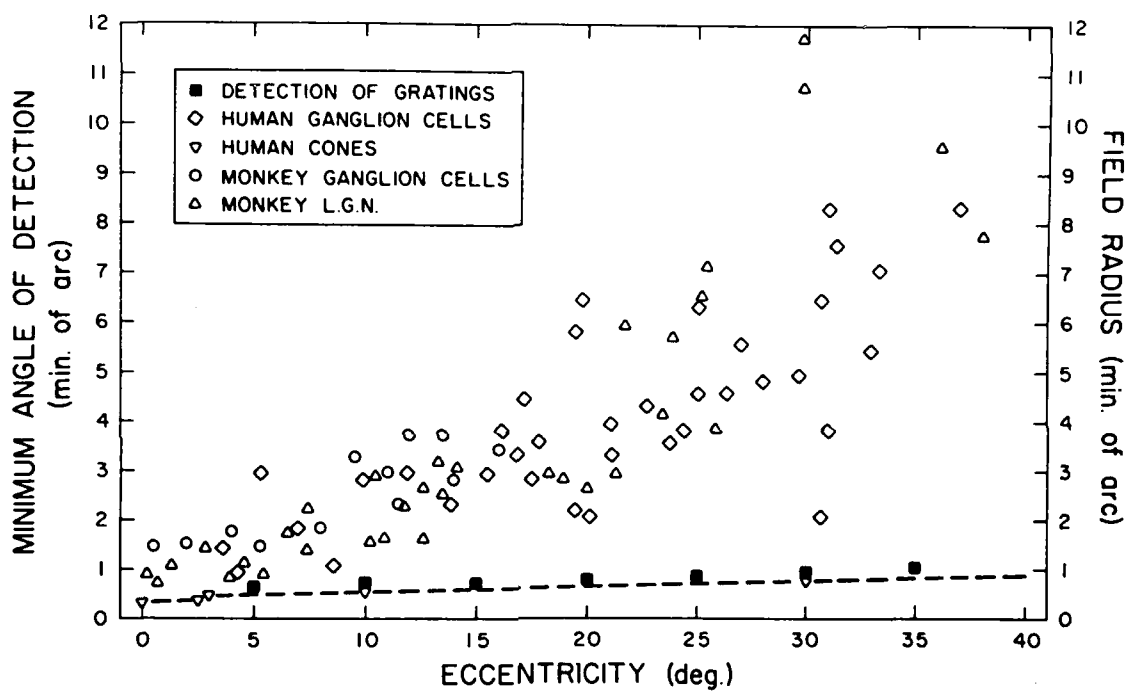
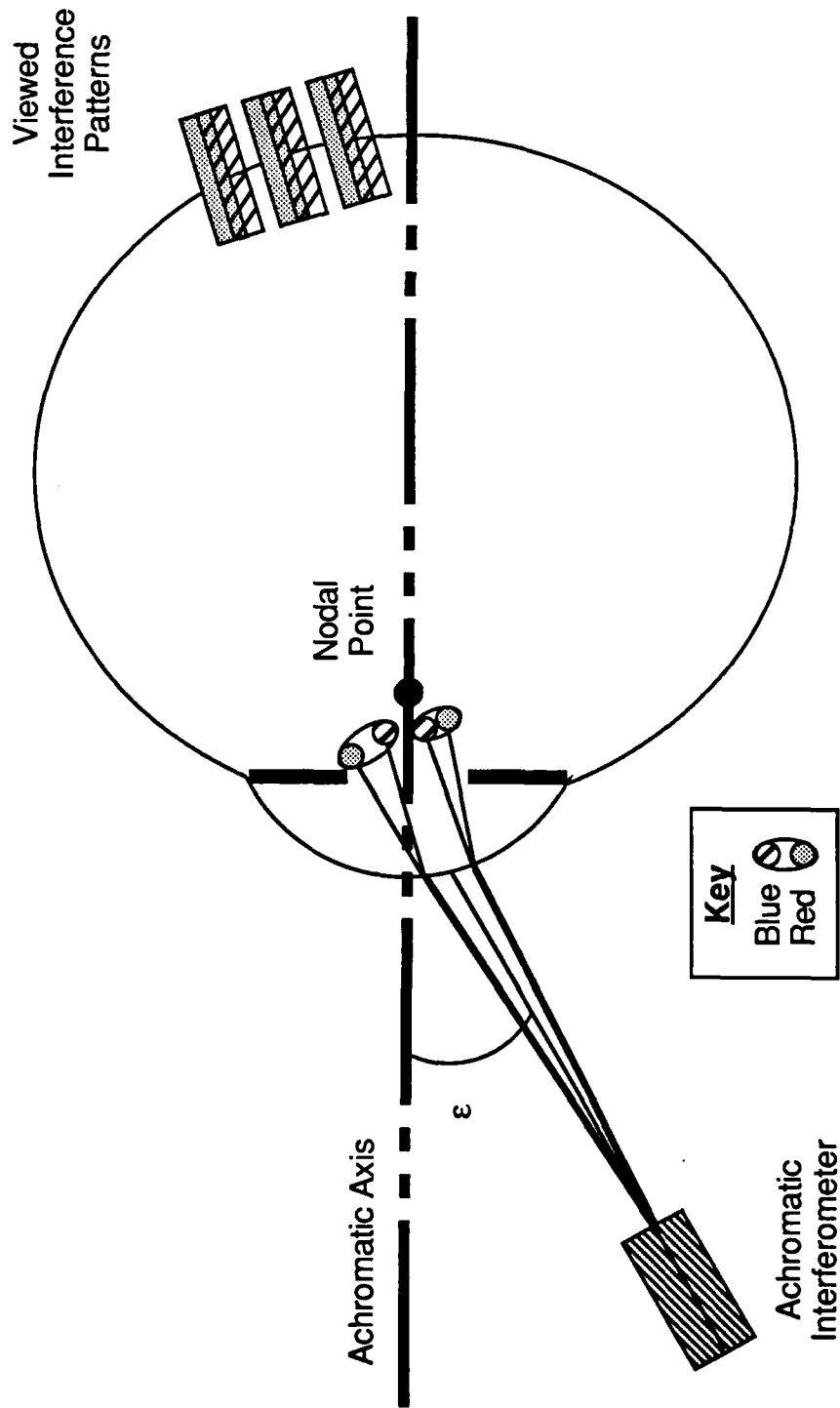


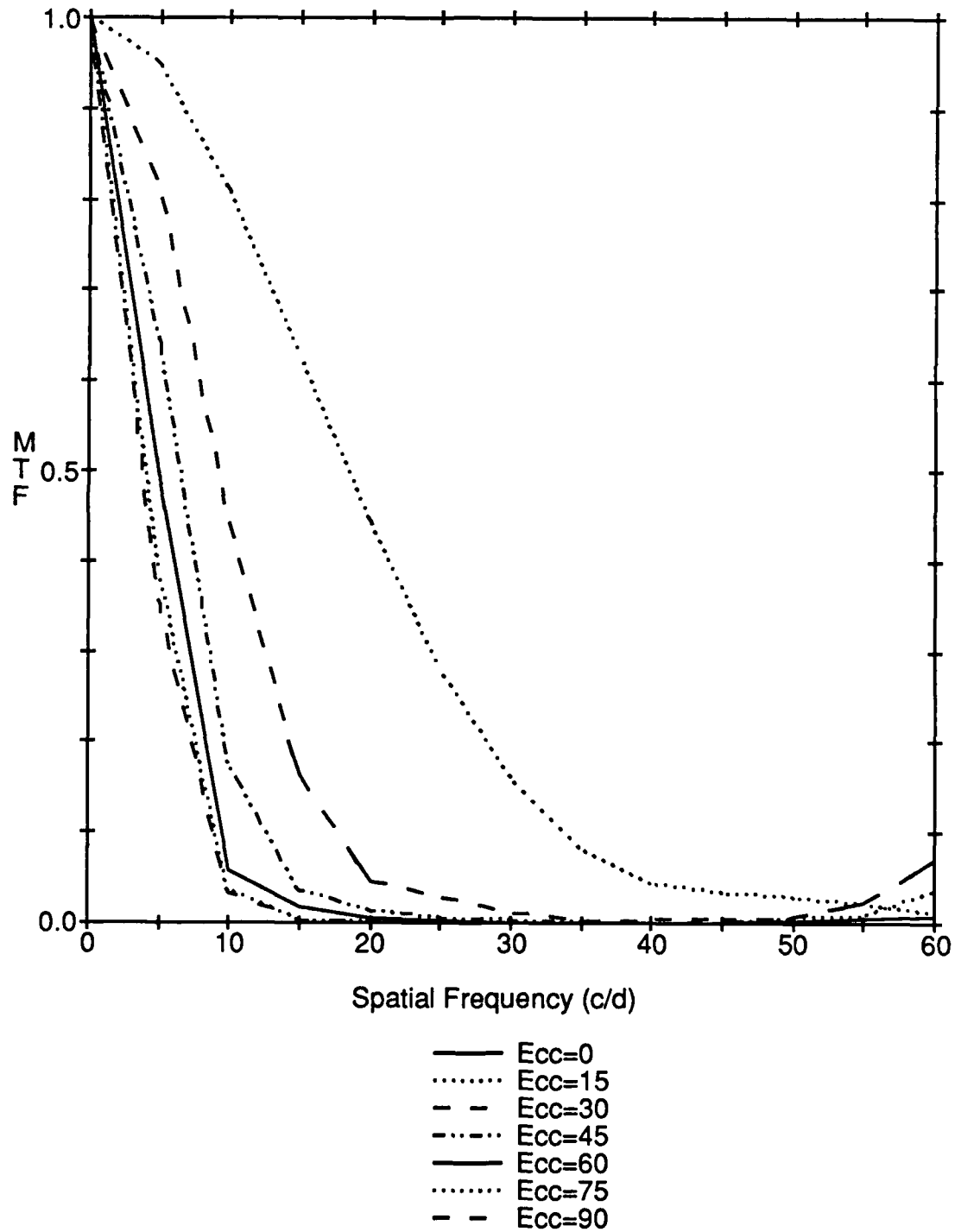
FIG. D5. LATERAL CHROMATIC ABERRATION OF THE EYE CAUSES GREATER DEMODULATION OF INTERFERENCE FRINGES WITH INCREASING STIMULUS ECCENTRICITY (ϵ).



LOT_MTF_ECC

03-SEP-89 20:03 Page 1

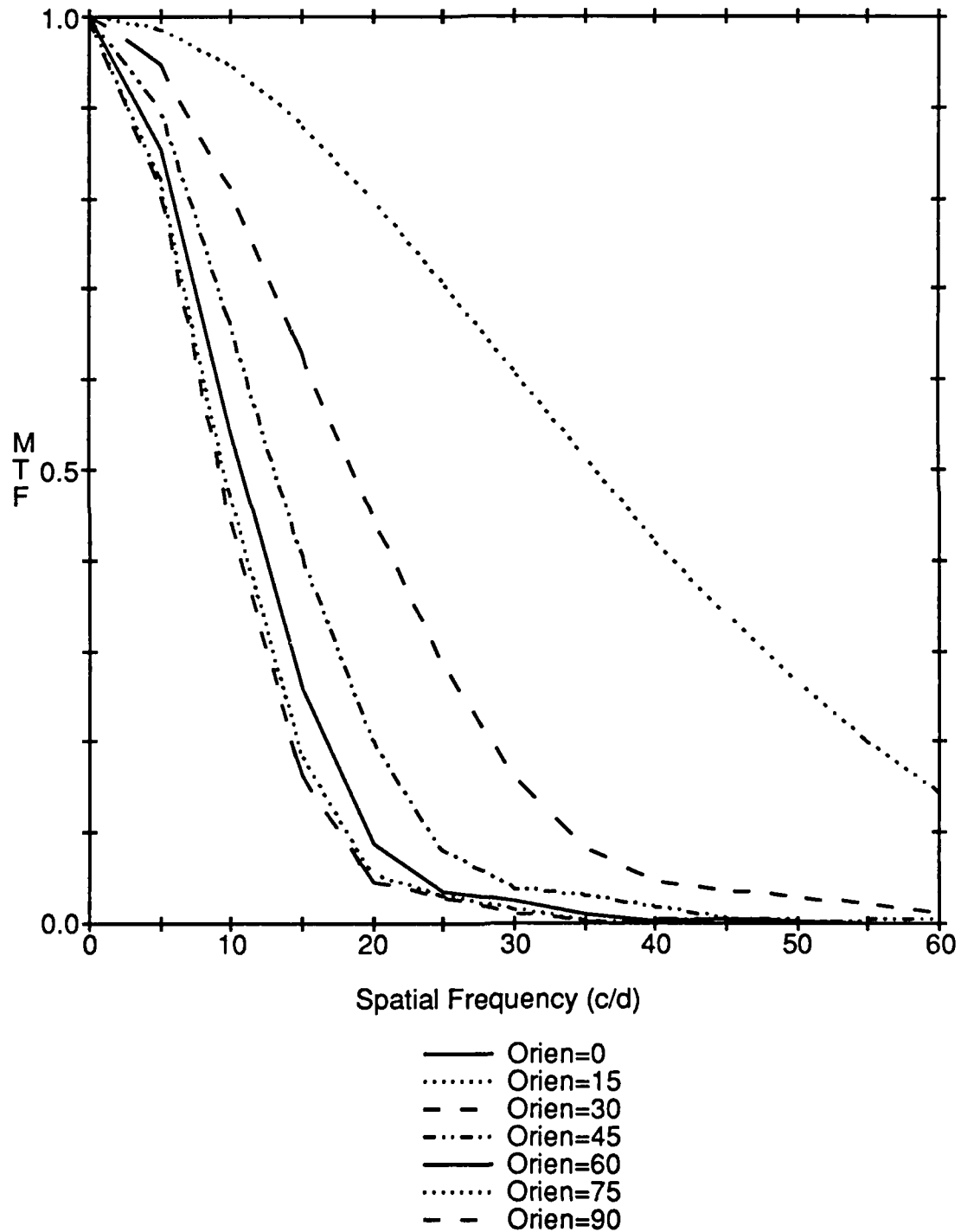
FIG. D6. MTF OF THE WHITE LIGHT (ACHROMATIC)
INTERFEROMETER IN THE PERIPHERAL
FIELD FOR TANGENTIAL GRATINGS
(2798K TUNGSTEN)



LOT_MTF_OR

03-SEP-89 19:54 Page 1

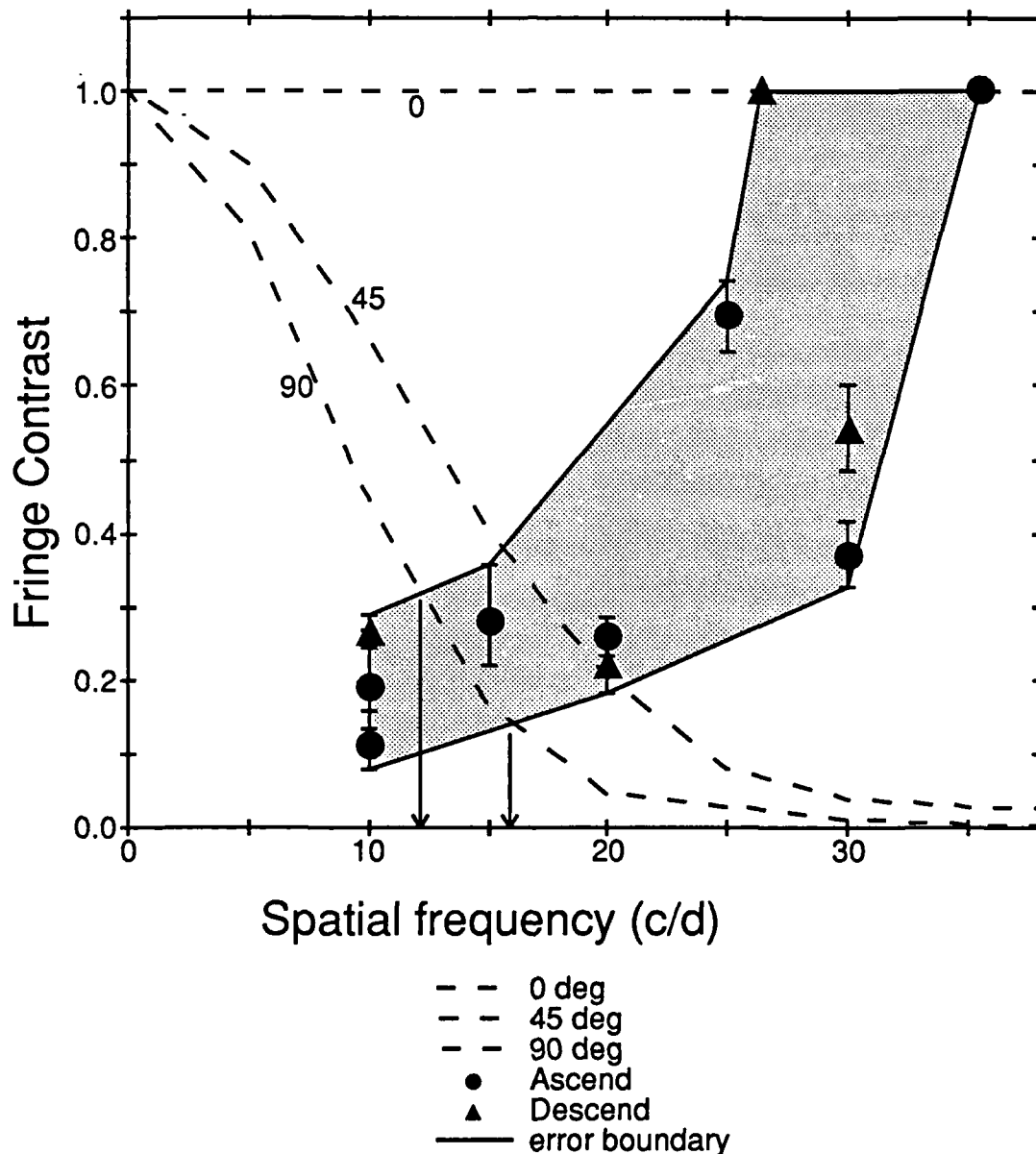
FIG. D7. MTF OF THE WHITE LIGHT (ACHROMATIC)
INTERFEROMETER AT 30 DEGREES
ECCENTRICITY (2798K TUNGSTEN)



D8

11-SEP-89 9:55 Page 1

FIG. D8. PREDICTION OF DETECTION ACUITY FOR LT



NOTE: Prediction of detection acuity based on measurements of contrast threshold (symbols) and the computed loss of retinal contrast due to ocular chromatic aberration (dashed lines) for three different stimulus orientations (indicated by number next to curve). Lower and upper limits to contrast threshold were estimated by forming the envelope of error bars (shaded region). Intersection of this threshold envelope with optical MTFs provides lower and upper estimates of the highest detectable spatial frequency for different stimulus orientations (shown for the 90deg case by arrows).

D9

05-SEP-89 20:48 Page 1

FIG. D9. PREDICTION OF ORIENTATION TUNING CURVES FOR
SUBJECT LT FOR WHITE FRINGES,
HORIZONTAL NASAL MERIDIAN,
30 DEGREES ECCENTRICITY

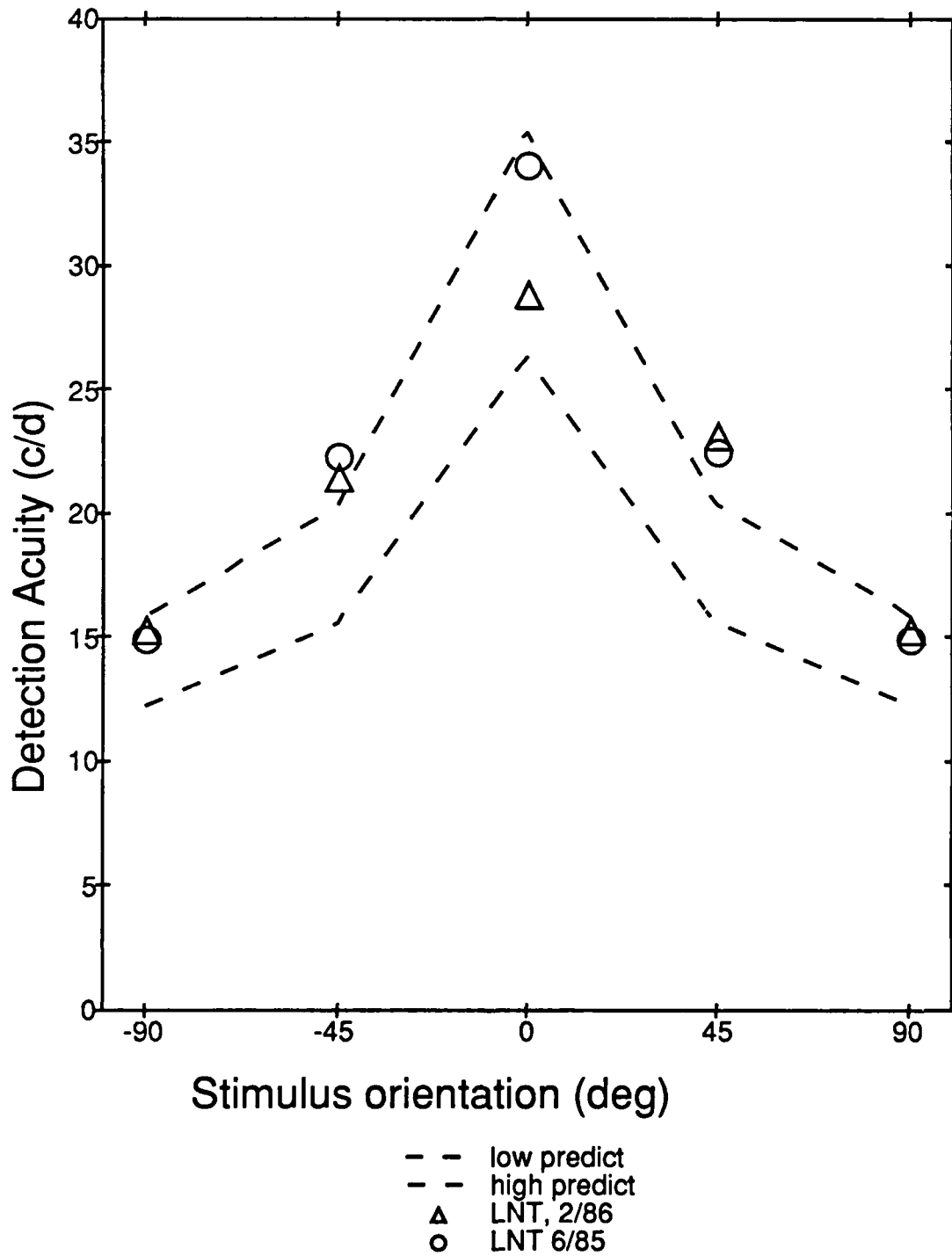
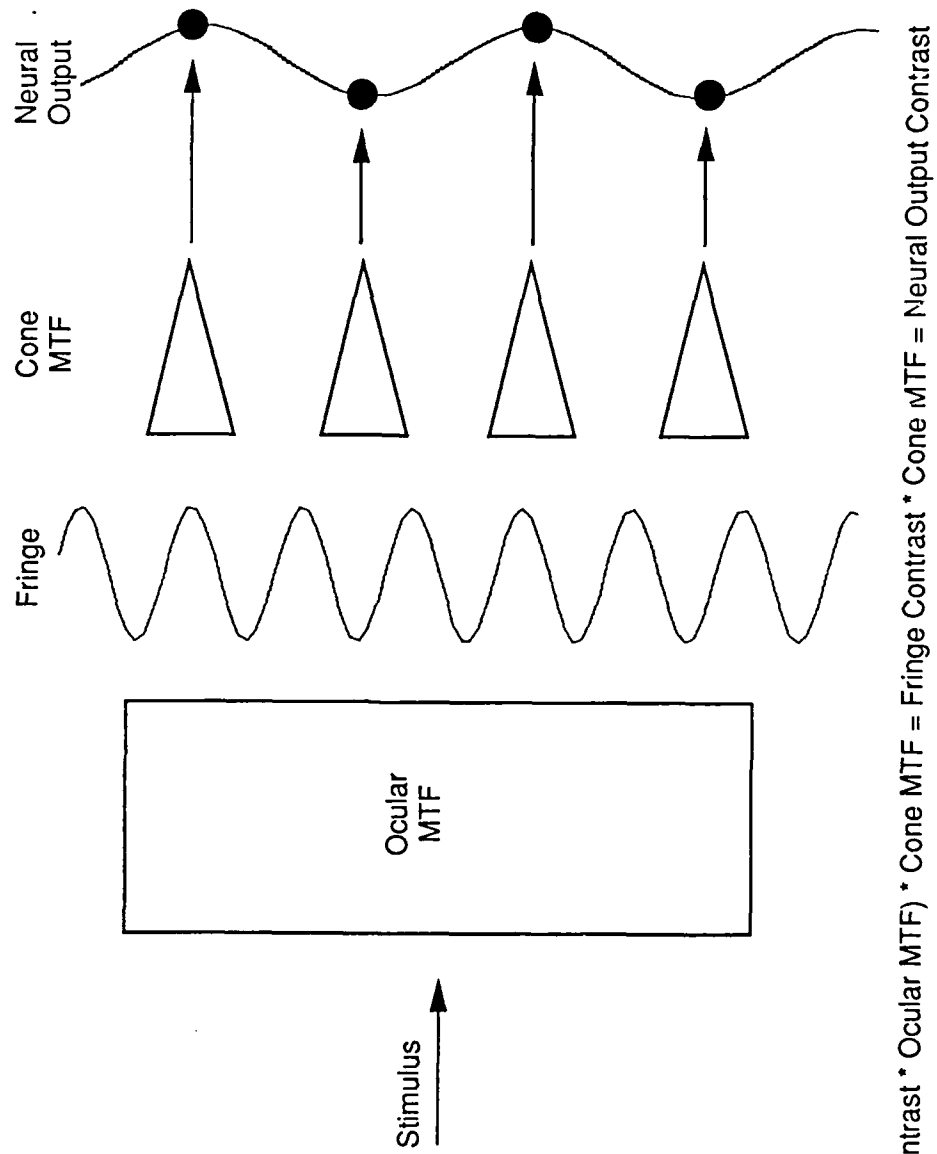


FIG. D10. MODEL OF CONTRAST DETECTION

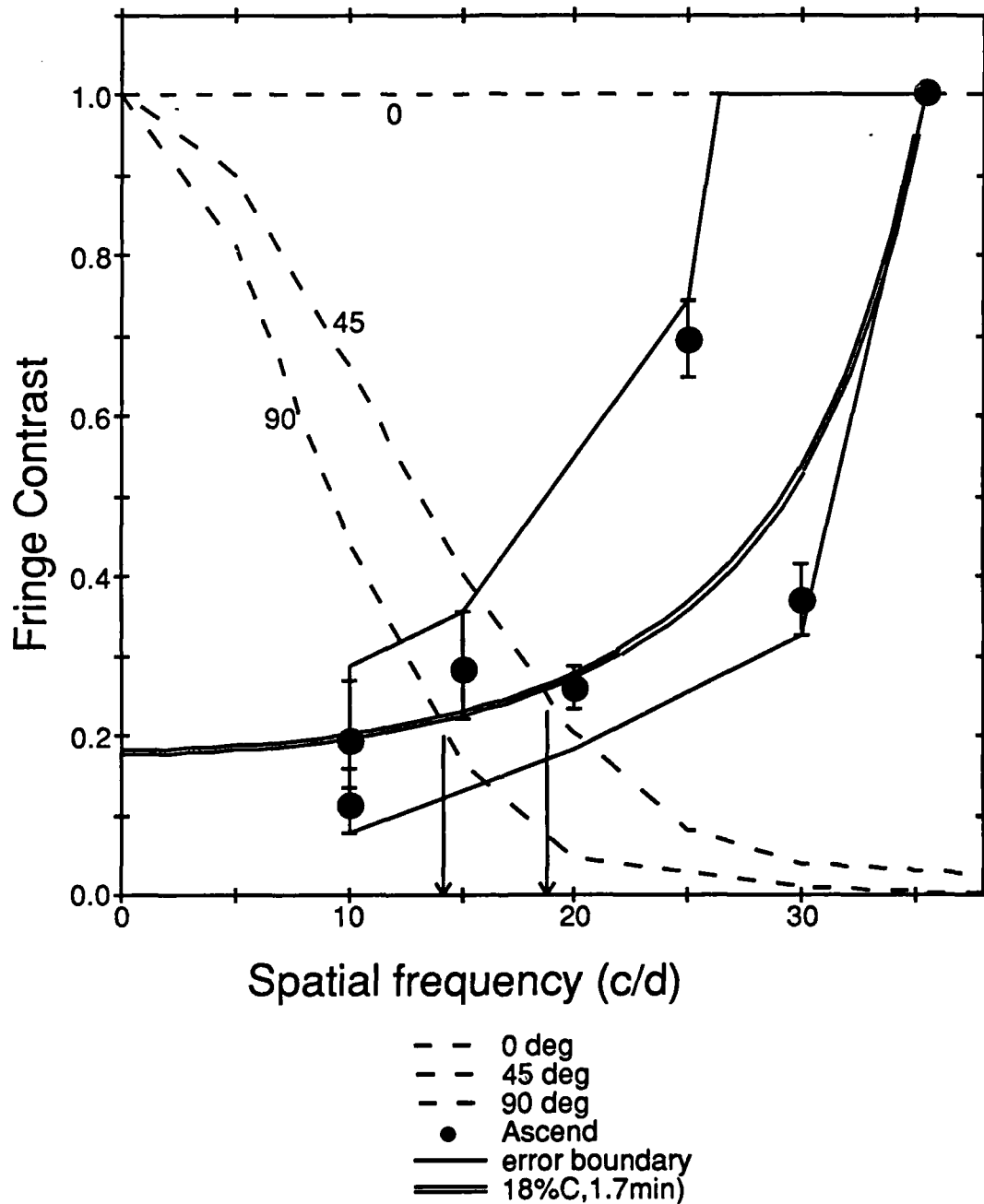


$$(\text{Stimulus Contrast} * \text{Ocular MTF}) * \text{Cone MTF} = \text{Fringe Contrast} * \text{Cone MTF} = \text{Neural Output Contrast}$$

D11

11-SEP-89 11:21 Page 1

FIG. D11. PREDICTION OF DETECTION ACUITY FOR LT (#2)

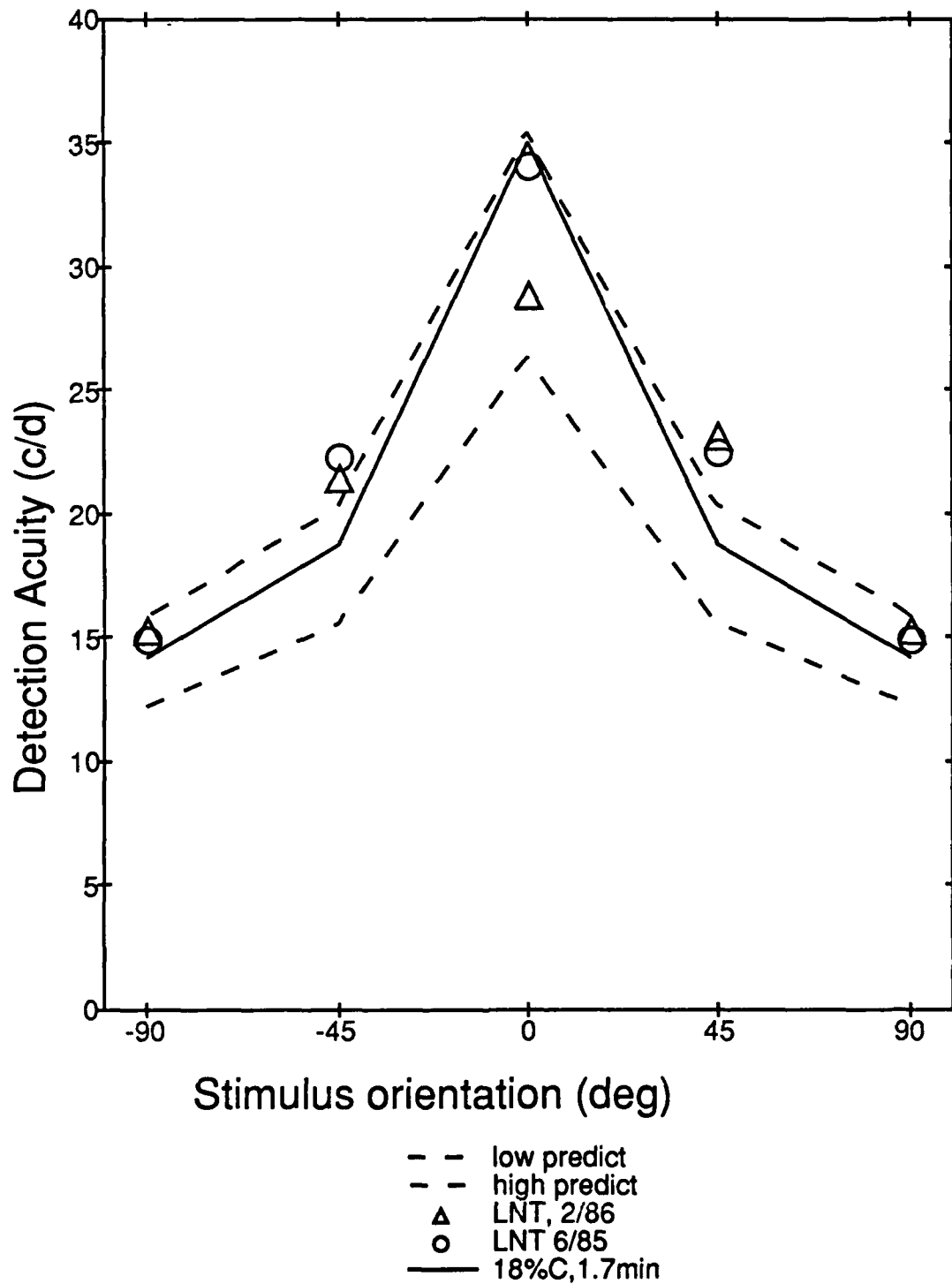


NOTE: Prediction of detection acuity for model of contrast detection of Fig. D10 is compared with similar predictions for subject LT (ascending limits) redrawn from Fig. D8. Double line shows the fringe contrast required to achieve 18% modulation in the output of a homogeneous array of cones (1.7 arcmin diameter).

D12

05-SEP-89 20:53 Page 1

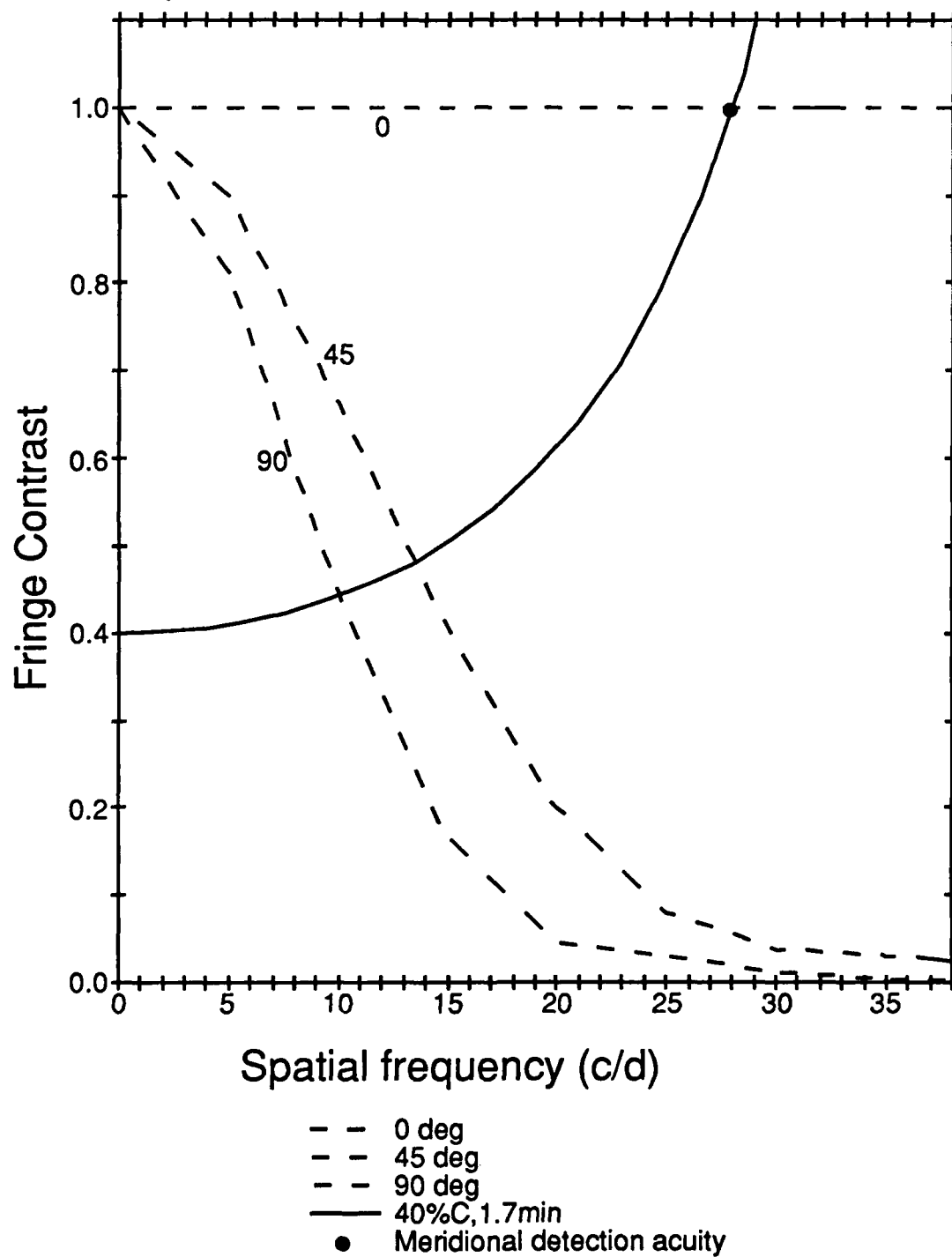
FIG. D12. PREDICTION OF ORIENTATION TUNING CURVES FOR SUBJECT LT FOR WHITE FRINGES, HORIZONTAL NASAL MERIDIAN, 30 DEGREE ECCENTRICITY (#2)



D13 *

05-SEP-89 20:25 Page 1

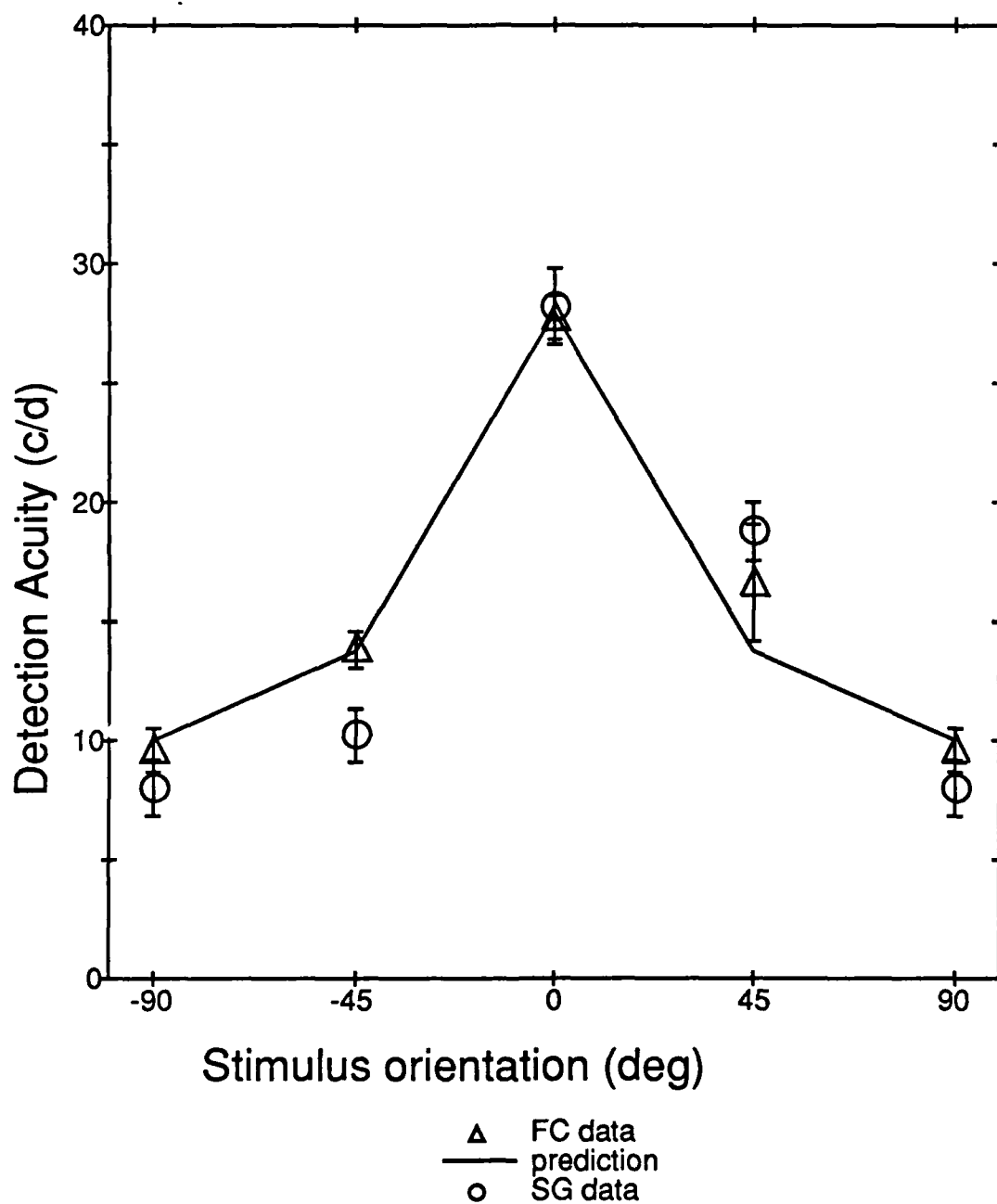
FIG. D13. PREDICTION OF DETECTION ACUITY FOR FC AND SG
FOR WHITE FRINGES, HORIZONTAL NASAL
MERIDIAN, 30 DEGREES ECCENTRICITY



D14

05-SEP-89 20:36 Page 1

FIG. D14. PREDICTION OF ORIENTATION TUNING CURVES FOR
SUBJECTS FC AND SG FOR WHITE FRINGES,
HORIZONTAL NASAL MERIDIAN,
30 DEGREES ECCENTRICITY



NOTE: Prediction is based on the assumption that contrast threshold occurs when output modulation of a 1.7 arcmin cone falls to 40%.

REFERENCES

- Appelle S. (1972)** Perception and discrimination as a function of stimulus orientation: The "oblique effect" in man and animals. *Psychol. Bull.* **78**, 266-278.
- Bergmann C. (1858)** Anatomisches und Pysiologisches uber die Netzhaut des Auges. *Z. ration. Medicin.* **2**, 83-108.
- Blackwell H. R. (1963)** Neural theories of simple visual discriminations. *J. opt. Soc. Am.* **53**, 129-159.
- Byram G. M. (1944)** The physical and photochemical basis of visual resolving power. Part II Visual acuity and the photochemistry of the retina. *J. opt. Soc. Am.* **34**, 718-738.
- Campbell F. W. and Gubish R. W. (1966)** Optical quality of the human eye. *J. Physiol., Lond.* **186**, 558-578.
- Cheney F. E., Still D. L., Thibos L.N. and Walsh D. J. (1987)** What limits faithful encoding of spatial patterns in human peripheral vision? *Physiol. Soc.* **396**, 139P
- Cheney F. E and Thibos L. N. (1986)** Evidence of elongated receptive fields in human peripheral retina. *Invest. Ophthal. visual Sci. Supp.;* **27**, 341.
- Coletta N. J. and Williams D. R. (1987)** Psychophysical estimate of extrafoveal cone spacing. *J. opt. Soc. Am.* **4**, 1503-1513.
- Curcio, C. (1987)** Diameters of presumed cone apertures in human retina. *J. opt. Soc. Am.* **A4(13)**, P70.
- Enoch J. M. (1961)** Nature of transmission of energy in the retinal receptors. *J. opt. Soc. Am.* **51**, 1122-1126
- Green D. G. (1970)** Regional variation in visual acuity for interference fringes on the retina. *J. Physiol.* **207**, 351-356

- Hartley, H. O. (1949) Tests of significance in harmonic analysis. *Biometrika*. 36, 194-201.
- Helmholtz H. von (1911) *Treatise on Physiological Optics Vol 2*. (Edited by Southall J. P. C.). Opt. Soc. Am. 1924.
- Hiltz R. and Cavanaugh C. R. (1974) Functional organization of the peripheral retina: sensitivity to periodic stimuli. *Vision Res.* 14, 1333-1338.
- Holt T., Levick W. R., Ross J., and Thibos L. N. (unpublished) Anisotropy of human vision.
- Jennings J. A. M. and Charman W. N. (1981) Off-axis image quality in the human eye. *Vision Res.* 21, 445-455.
- Levick W. R. and Thibos L. N. (1980) Orientation bias of cat retinal ganglion cells. *Nature* 286, 389-390.
- Lotmar W. (1972) Use of moire fringes for testing visual acuity of the retina. *Applied Optics* 11, 1266-1268.
- Lotmar W. (1980) Apparatus for the measurement of retinal acuity by moire' fringes. *Invest. Ophthalmol. visual Sci.* 19, 393-400
- Miller W. H. Intraocular filters. In *Handbook of Sensory Physiology* (edited by Autrum H.), Vol VII/6A, Chap. 3. Springer, Berlin.
- Miller W. H. and Bernard G. D. (1983) Averaging over the foveal receptor aperture curtails aliasing. *Vision Res.* 23, 1365-1369.
- Perry V. H. and Cowey A. (1985) The ganglion cell and cone distributions in the monkey's retina: implications for central magnification factors. *Vision Res.* 25, 1795-1810.
- Polyak S. (1941) *The Retina*. Univ of Chicago Press, Chicago, Illinois.
- Rovamo J., Virsu V., Laurinen P. and Havarinen L. (1982) Resolution of gratings oriented along and across meridians in peripheral vision. *Invest. Ophthalmol. visual Sci.* 23, 666-670.

- Shannon C.E. (1949) Communication in the presence of noise. *Proc. I.R.E.* 37, 10-21.
- Smith R. A. and Cass P. (1987) Aliasing in the parafovea with incoherent light. *J. opt Soc. Am.* A4, 1530-1534.
- Still D. L. and Thibos L. N. (1987) Detection of peripheral aliasing for gratings seen in newtonian view. *J. Opt.Soc. Am.* A4, (13), 92.
- Still D. L. (1989) Optical limits to contrast sensitivity in human peripheral vision. PhD Thesis.
- Temme L. A., Malcus L. and Noell W. K. (1982) Perception of grating orientation in the peripheral field. *Invest. Ophthalmol. Vis Sci (Supp.)* 22, 253
- Thibos L. N. (1987) Calculation of the influence of lateral chromatic aberration on image quality across the visual field. *J. opt Soc. Am.* 4, 1673-1680
- Thibos L. N., Bradley A., Still D. L., Zhang X. X. and Howarth P. (1989) Theory and measurement of ocular chromatic aberration. *Vision Res.* In Press.
- Thibos L. N., Cheney F. E. and Walsh D. J. (1987) Retinal limits to detection and resolution of gratings. *J. opt Soc. Am.* A4, 1524-1529
- Thibos L. N. and Walsh D. J. (1985) Detection of high frequency gratings in the periphery. *J. opt. Soc. Am.* A2, P64.
- Thibos L. N., Walsh D. J. and Cheney F. E. (1987) Vision beyond the resolution limit: aliasing in the periphery. *Vision Res.* 27, 2193-2197.
- van Meeteren A. and Dunnewold C. J. W. (1983) Image quality of the human eye for eccentric entrance pupils. *Vision Res.* 23, 573-579.
- Virsu V. and Rovamo J. (1979) Visual resolution, contrast sensitivity, and the cortical magnification factor. *Exp. Brain Res.* 37, 475-494.
- Walsh D. (1985) Peripheral visual acuity: Oblique and meridional effects. MS Thesis
- Westheimer G. (1960) Modulation for sinusoidal light distribution on the retina. *J. Physiol. Lond.* 152, 67-74.

- Westheimer G. (1966)** The Maxwellian view. *Vision Res.* **6**, 669-682.
- Williams D. R. (1983)** Consequences of spatial sampling by a human photoreceptor mosaic. *Science, N.Y.* **221** 385-387
- Williams D. R. (1985a)** Aliasing in human foveal vision. *Vision Res.* **25**, 195-205
- Williams D. R. (1985b)** Visibility of interference fringes near the resolution limit. *J. opt. Soc. Am.* **A2**, 1087-1093.
- Williams D. R. and Coletta N. J. (1987)** Cone spacing and the visual resolution limit *J. Opt. Soc. Am.* **A4**, 1414-1522.
- Yellot J. I. Jr (1982)** Spectral analysis of spatial sampling by photoreceptors: Topological disorder prevents aliasing. *Vision Res.* **22**, 1205-1210.
- Yellot J. I. Jr. (1984)** Image sampling properties of photoreceptors: a reply to Miller and Bernard. *Vision Res.* **24**, 281-282.

APPENDIX I**Measurement of Separation of Spectral Components
of the Two Point Sources**

Wavelength (nm)	Measured spot Separation (mm)	Calculated Spectral Frequency (Snellen Fraction)	Calibrated Grating Spatial Frequency (Snellen Fraction)	Percent Difference
450	1.5	1.933	1.975	2.3
505	1.7	1.952	"	1.2
550	1.83	1.925	"	2.6
600	1.975	1.909	"	3.3
650	2.125	1.896	"	4.0
450	1.875	2.417	2.475	2.3
505	2.075	2.383	"	3.8
550	2.25	2.373	"	4.1
600	2.5	2.417	"	2.3

Calculation

Snellen Fraction = Separation * (580/wavelength)

Measurements

Measurements done using Nikon Alphaphot microscope with 15X eyepiece and 4X objective using narrowband interference filters (Appendix III)

APPENDIX II

Calculation of Retinal Illuminance of Gratings
Using Light Measurements from the Pritchard Photometer

Formula

$$E(\text{Trolands}) = 10^{**7} * (B) * (x^{**2} / r)$$

B = Illuminance off reflecting plate in milliLamberts

r = Reflectance of Minolta Lambertian surface

x = Distance past focus in pupil in meters

Light	Entrance Pupil	B(mL)	x(meters)	r	Trolands	Log Trolands
-------	-------------------	-------	-----------	---	----------	-----------------

White	.15	.00715	.2375	.921	4378.9	3.64
-------	-----	--------	-------	------	--------	------

White	.5	.0948	.2375	.921	58034.1	4.76
-------	----	-------	-------	------	---------	------

	.5	.0411	.365	.921	59396	4.77
--	----	-------	------	------	-------	------

550	.5	.00565	.365	.921	3459.3	3.54
-----	----	--------	------	------	--------	------

White	.5	.0292	.365	.921	17865	4.25
-------	----	-------	------	------	-------	------

.5 ND

Filter

Calculations

1. ND filter = $4.76 - 4.25 = .51$ Neutral density

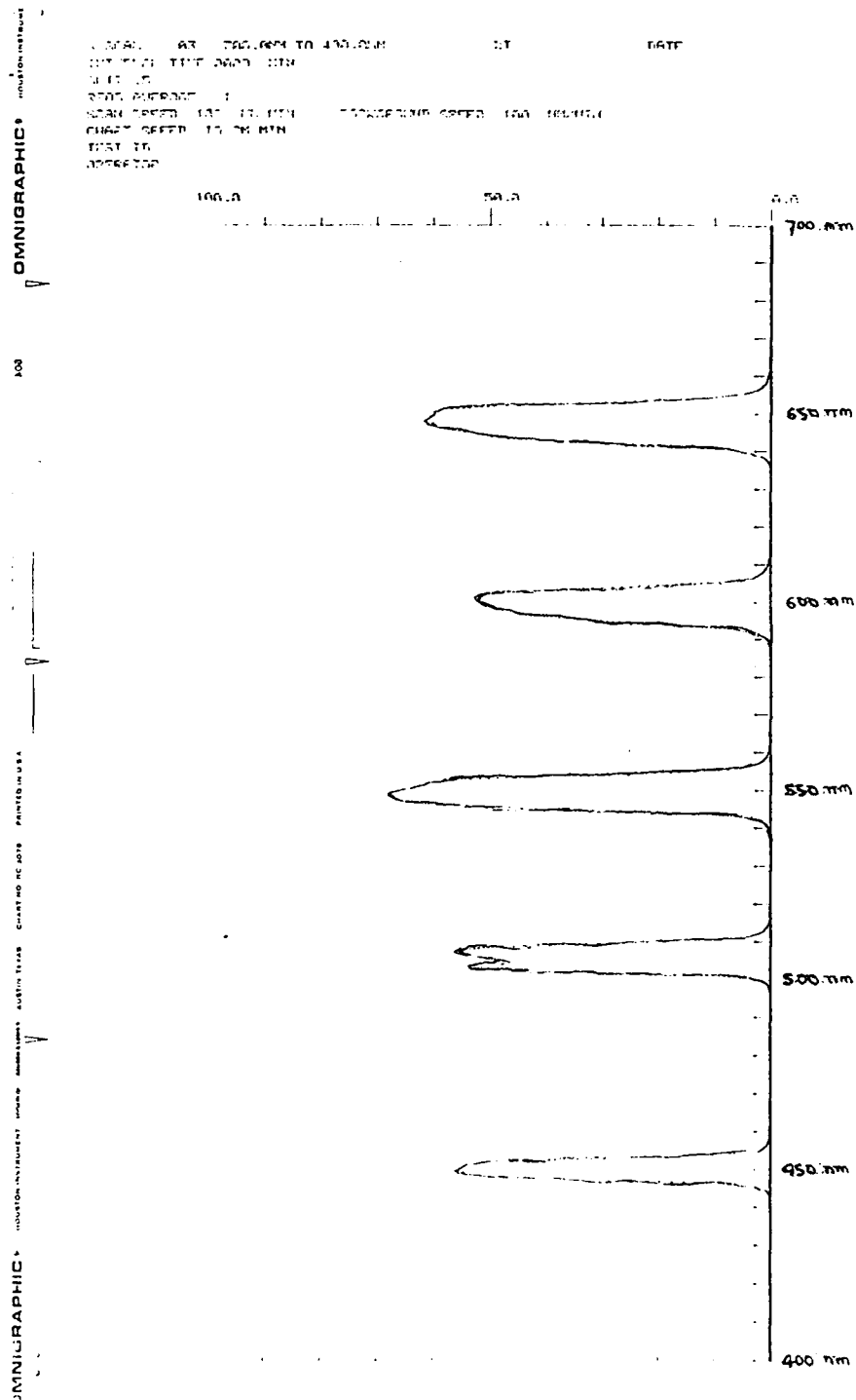
2. White light with 0.5 ND filter = $3.64 - 0.51 = 3.13$ log Trolands
and 0.15 entrance pupil

3. 550 filter = $4.76 - 3.54 = 1.22$ ND

4. 550 light with = $3.64 - 1.22 = 2.42$ log Trolands
0.15 entrance pupil

APPENDIX III

Measurement of Interference Filters by Beckman Photometer

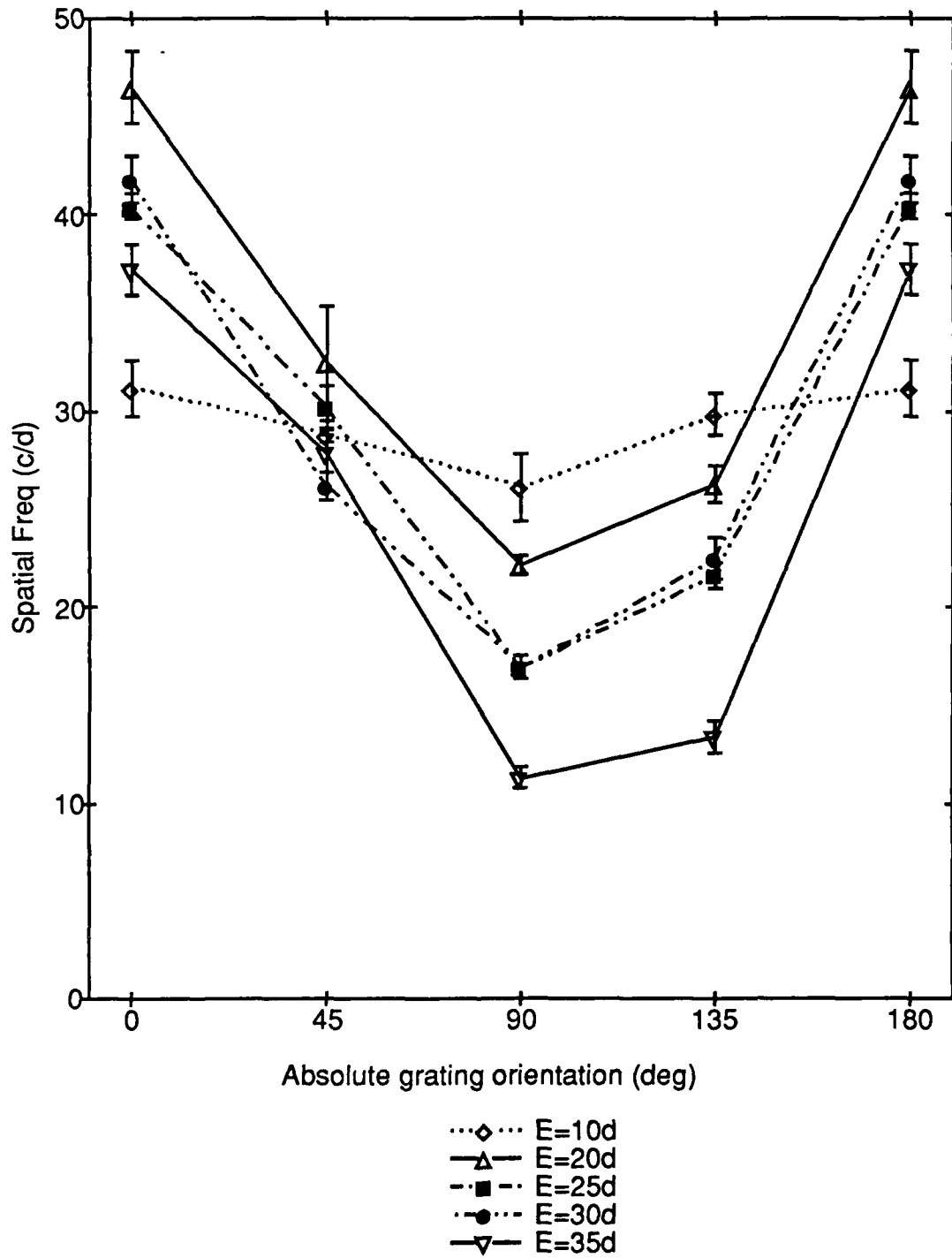


APPENDIX IV

The Following Figures are Referenced in the Main Body of the Thesis

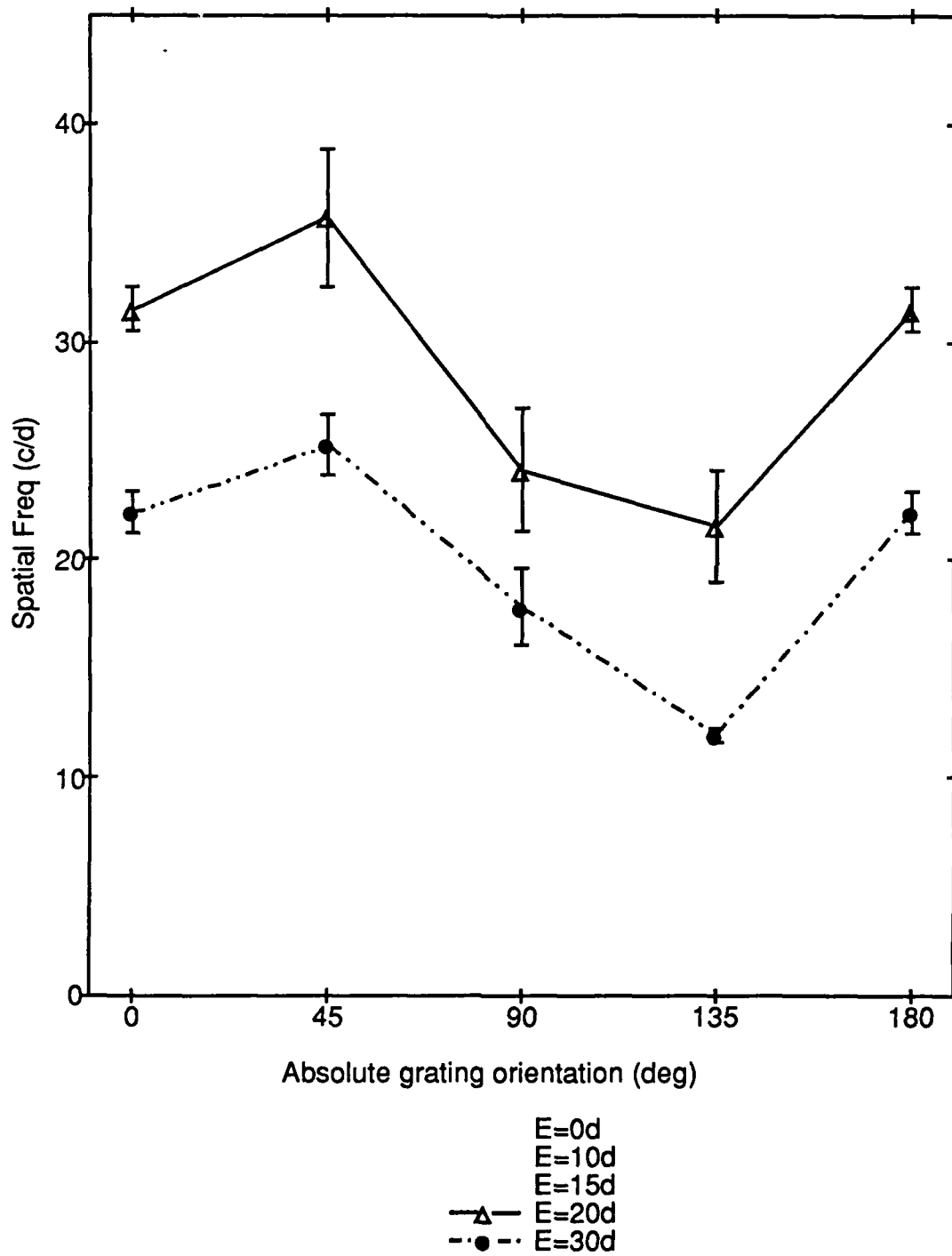
G_TUN_LT0D

02-SEP-89 15:34 Page 1

FIG. A1. DETECTION ACUITY FOR LT FOR
HORIZONTAL TEMPORAL MERIDIANError bars are ± 1 s.e.m.

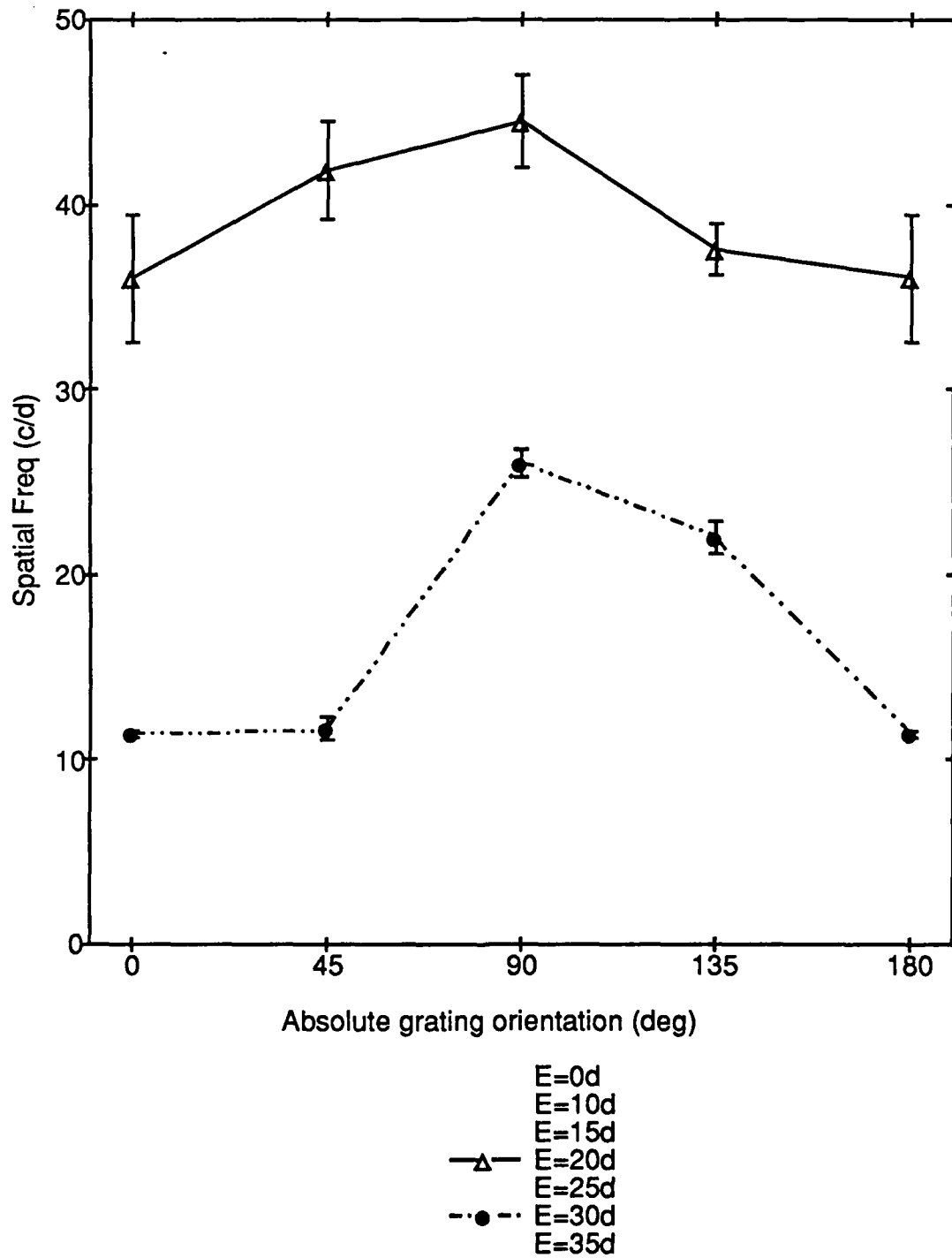
G_TUN_LT45D

02-SEP-89 15:42 Page 1

FIG. A2. DETECTION ACUITY FOR LT FOR
SUPERIOR TEMPORAL MERIDIANError bars are ± 1 s.e.m.

G_TUN_LT90D

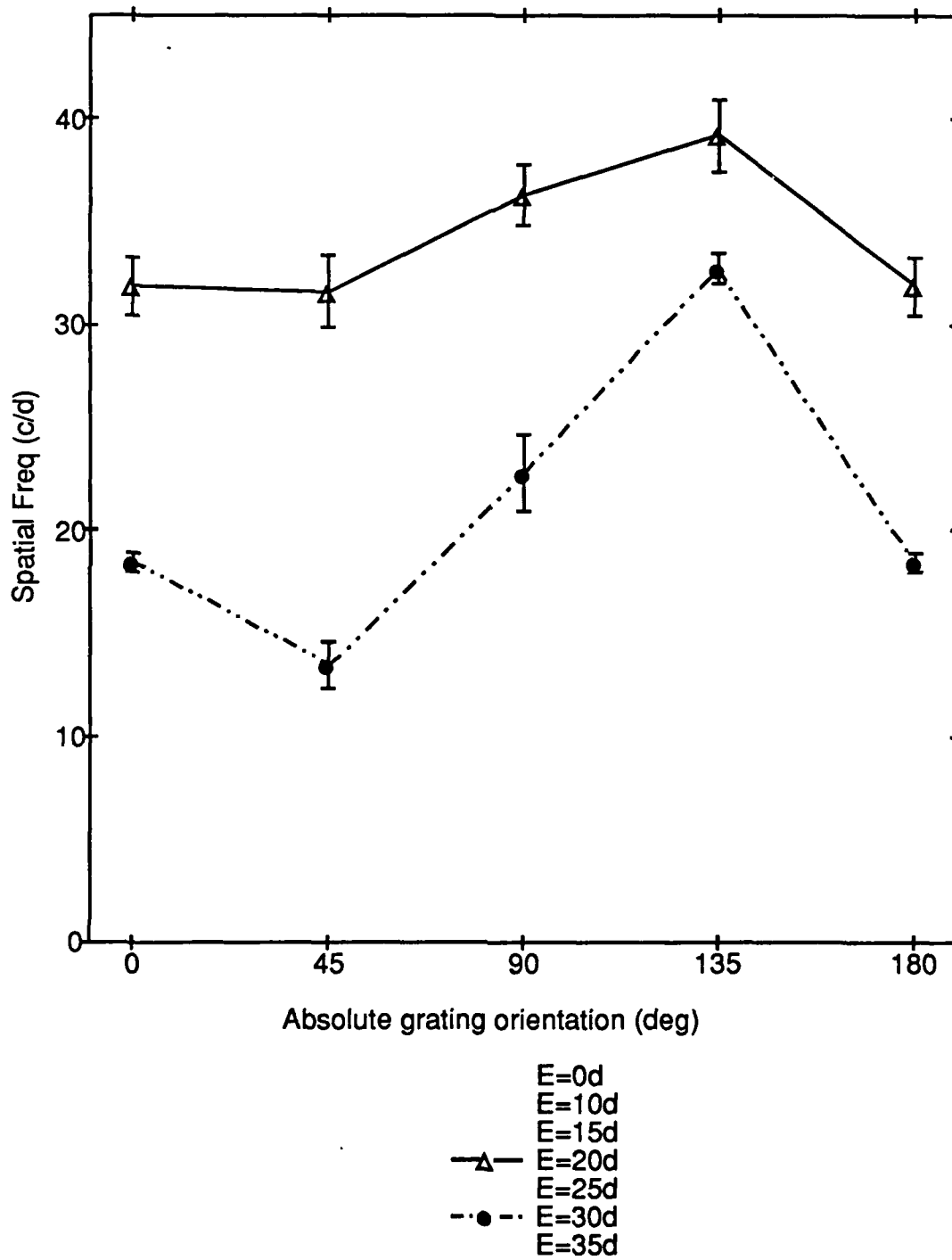
02-SEP-89 15:38 Page 1

Fig. A3. DETECTION ACUITY FOR LT
FOR SUPERIOR MERIDIAN

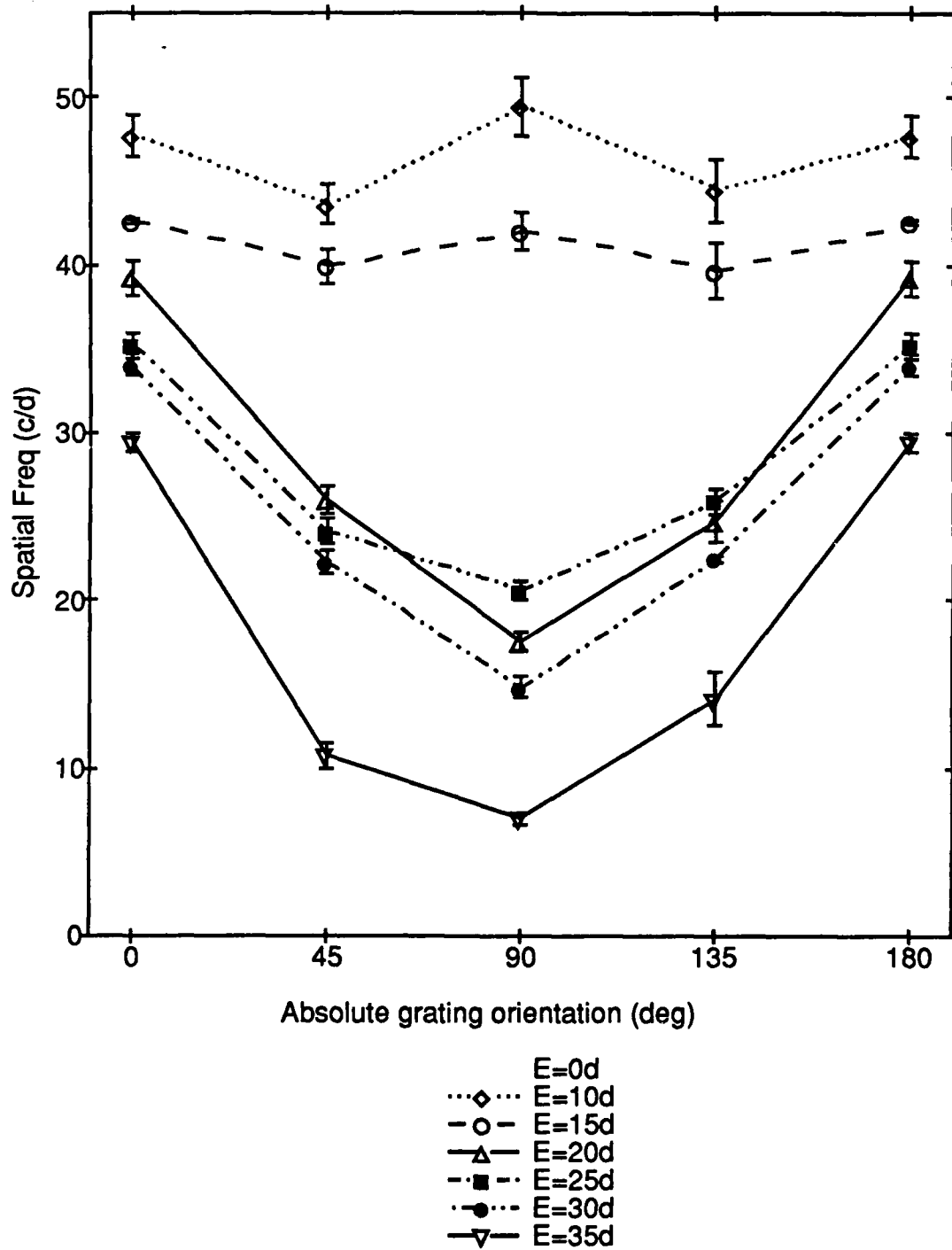
Error bars are +/- 1 s.e.m.

G_TUN_LT135D

02-SEP-89 15:48 Page 1

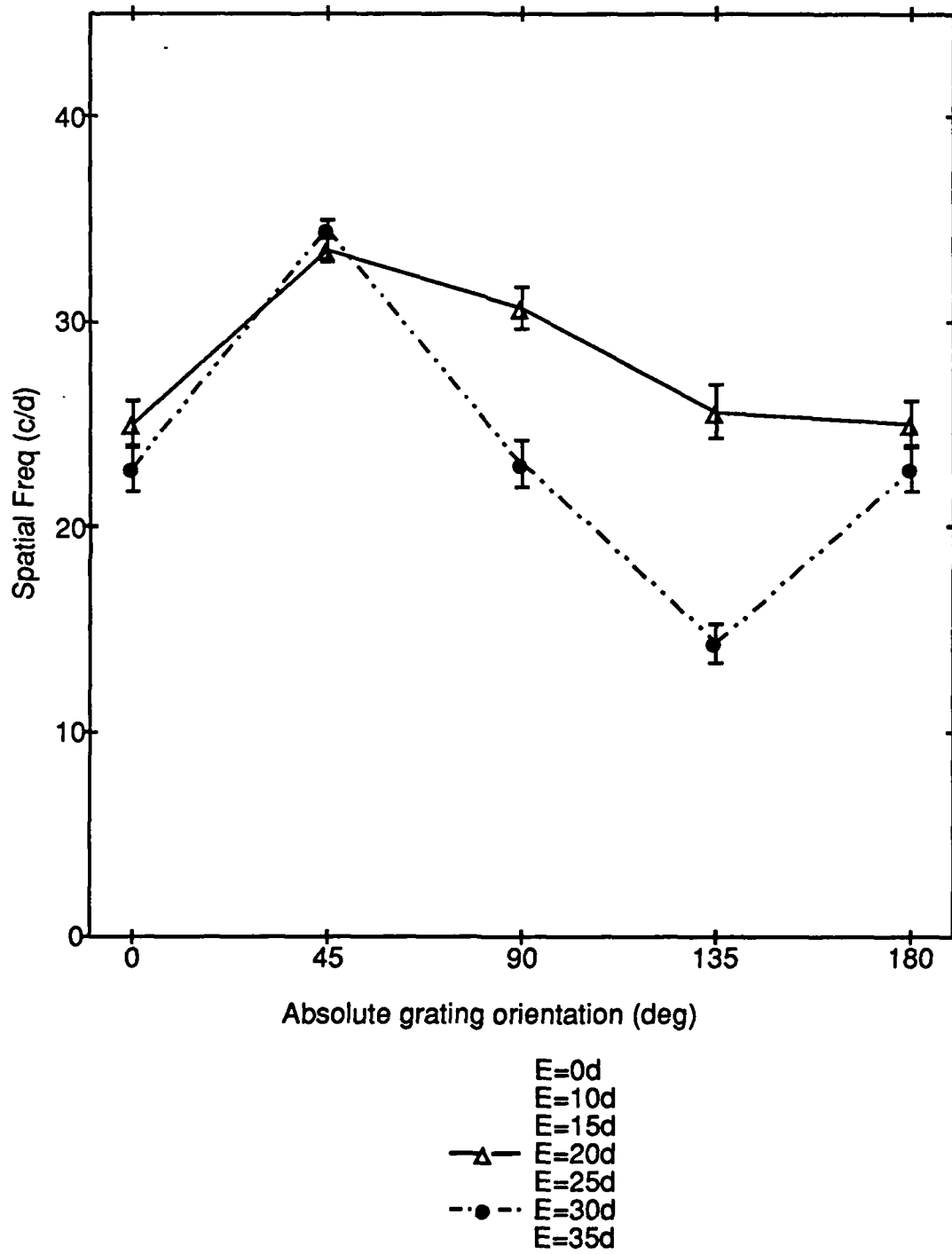
FIG. A4. DETECTION ACUITY FOR LT FOR
SUPERIOR NASAL MERIDIAN

Error bars are +/- 1 s.e.m.

FIG. A5. DETECTION ACUITY FOR LT FOR
HORIZONTAL NASAL MERIDIAN

G_TUN_LT225D

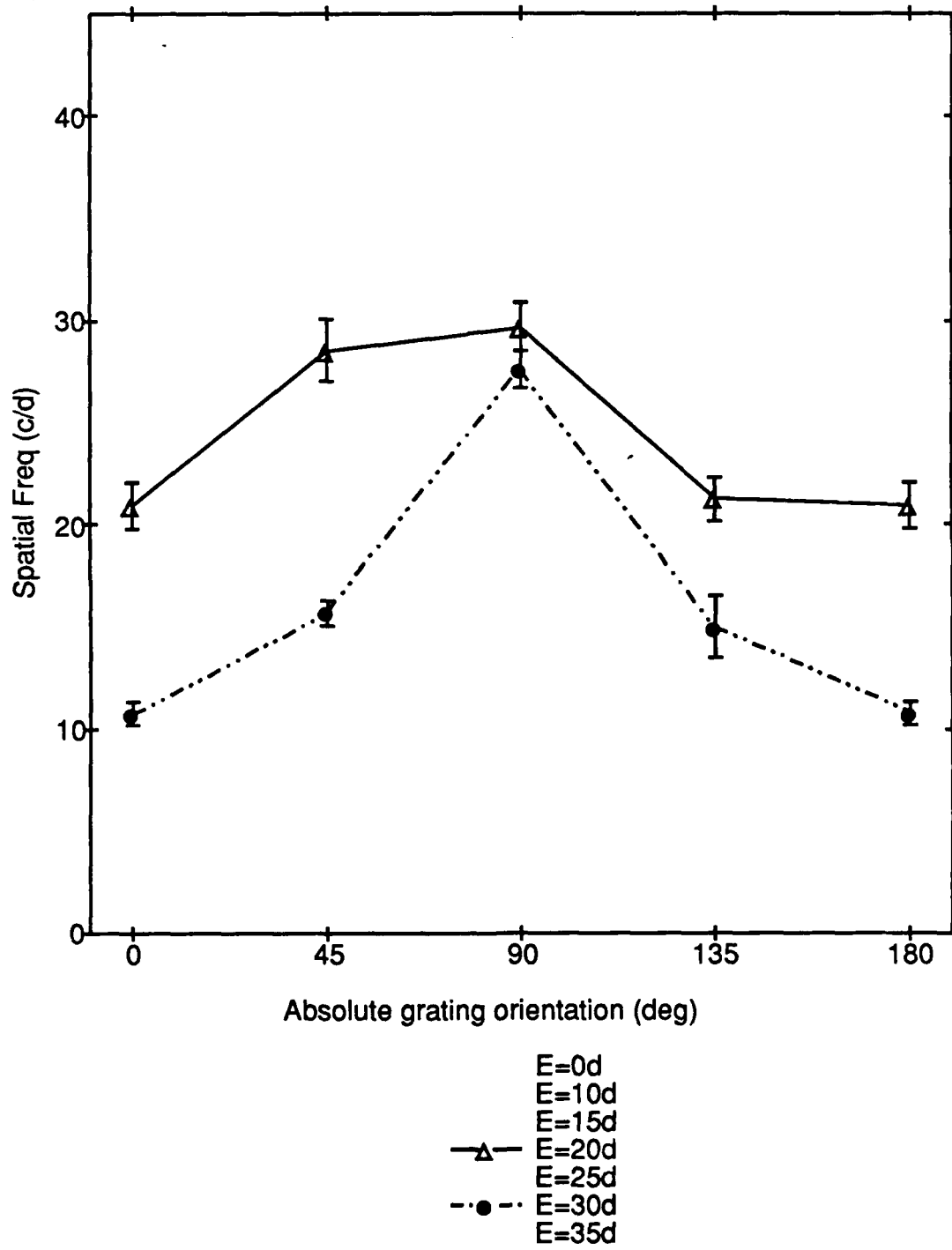
03-SEP-89 15:12 Page 1

FIG. A6. DETECTION ACUITY FOR LT FOR
INFERIOR NASAL MERIDIAN

Error bars are +/- 1 s.e.m.

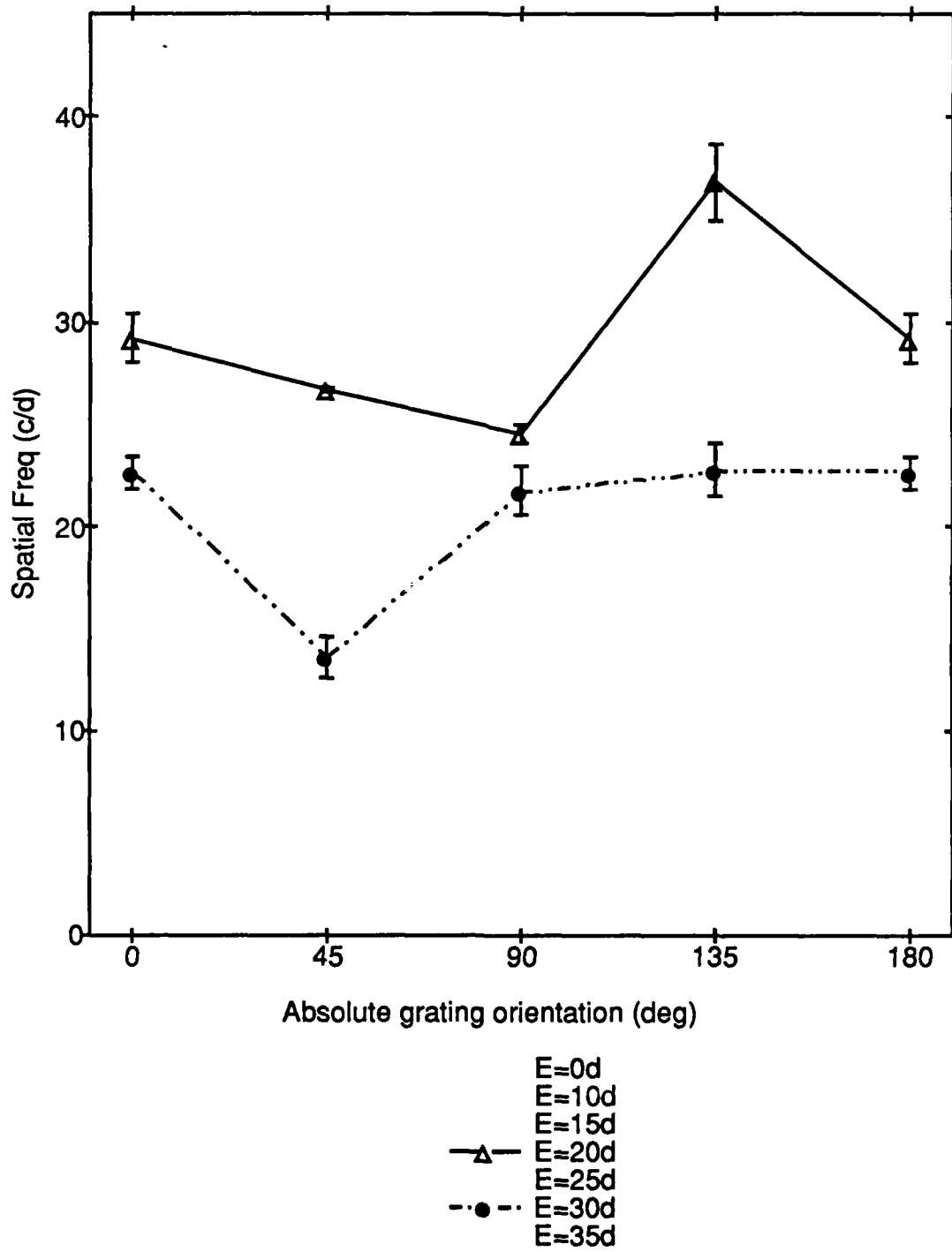
G_TUN_LT270D

03-SEP-89 15:20 Page 1

FIG. A7. DETECTION ACUITY FOR LT
FOR INFERIOR MERIDIANError bars are ± 1 s.e.m.

G_TUN_LT315D

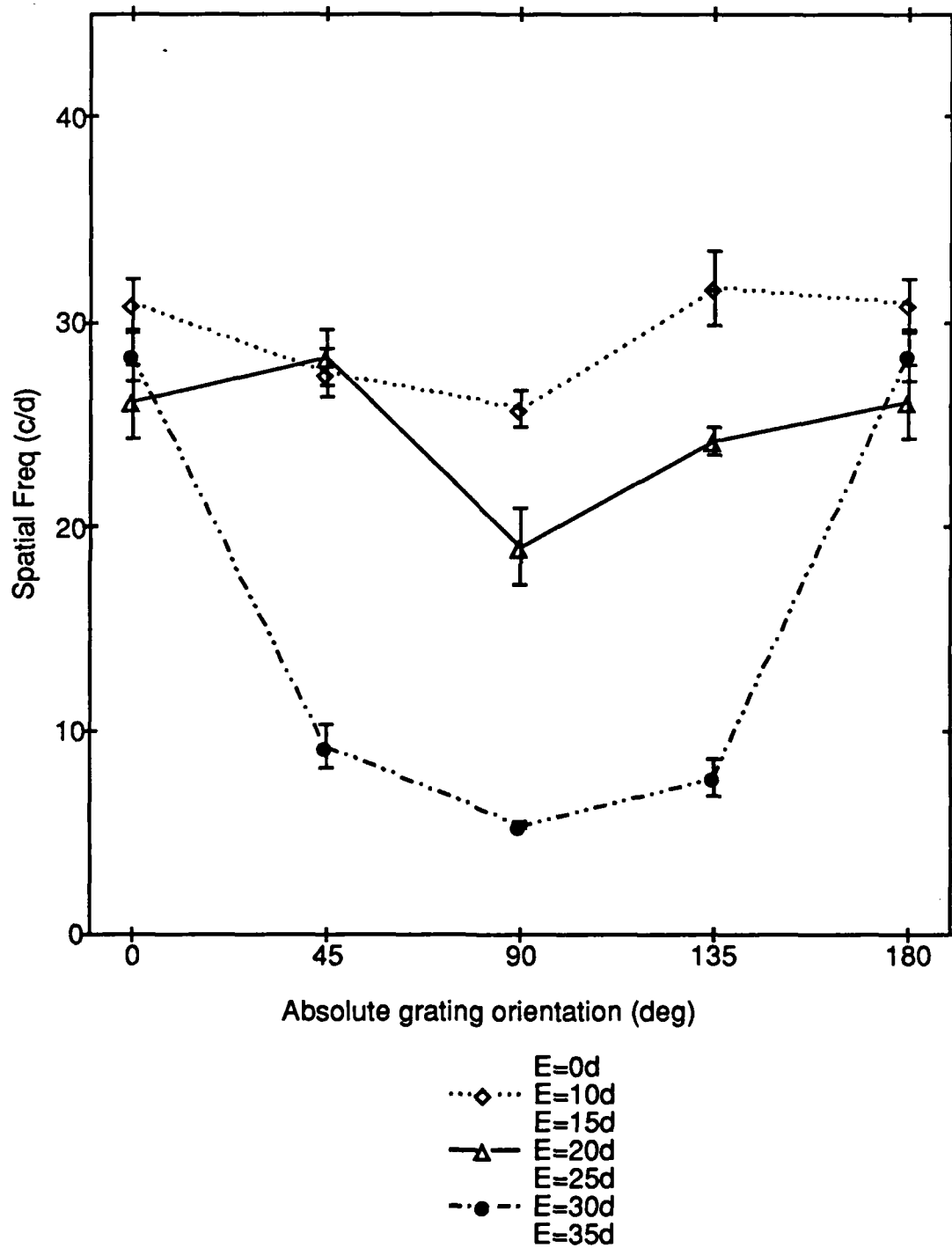
03-SEP-89 15:28 Page 1

FIG. A8. DETECTION ACUITY FOR LT FOR
INFERIOR TEMPORAL MERIDIAN

Error bars are +/- 1 s.e.m.

G_TUN_SG0D

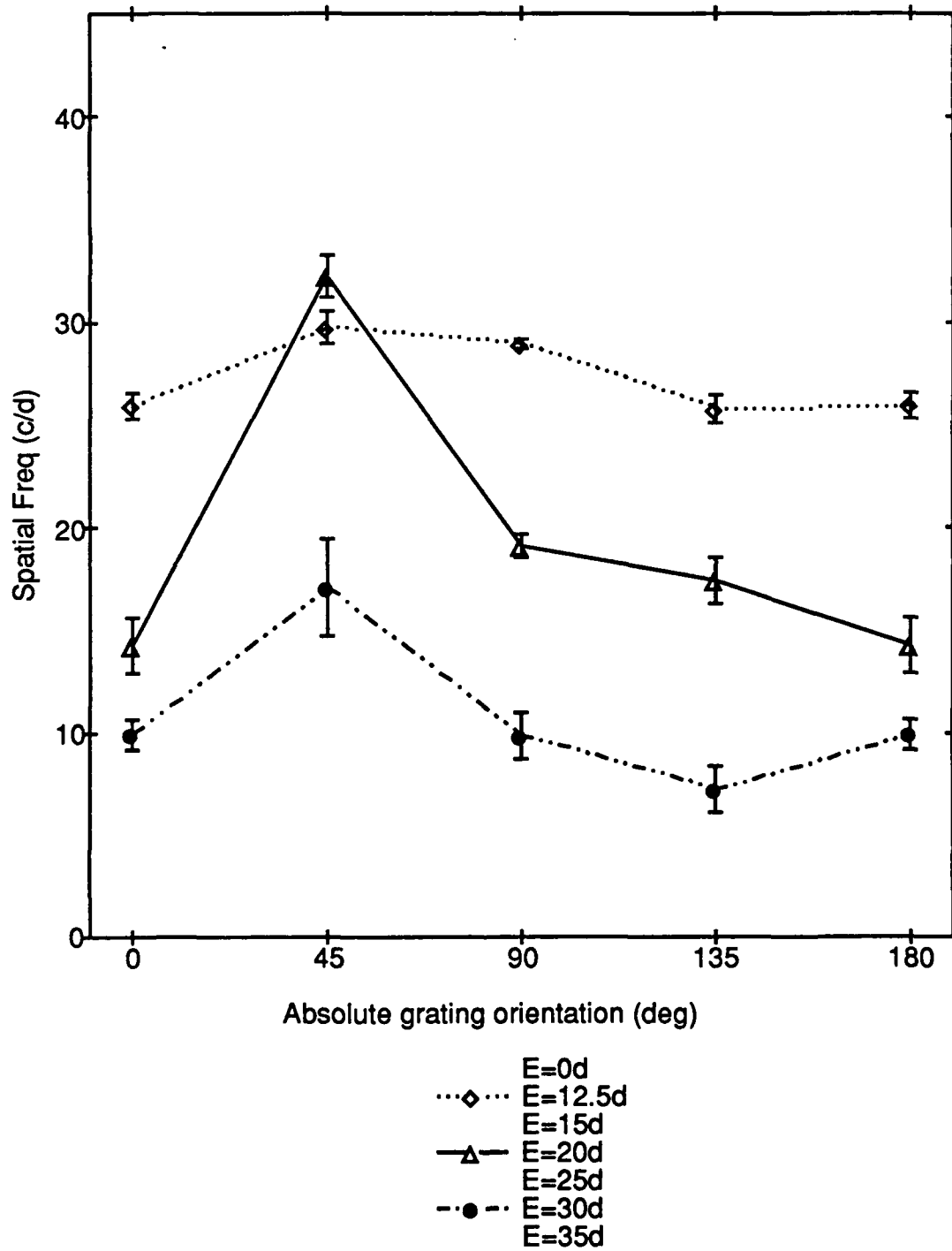
03-SEP-89 15:36 Page 1

FIG. A9. DETECTION ACUITY FOR SG FOR
HORIZONTAL TEMPORAL MERIDIAN

Error bars are +/- 1 s.e.m.

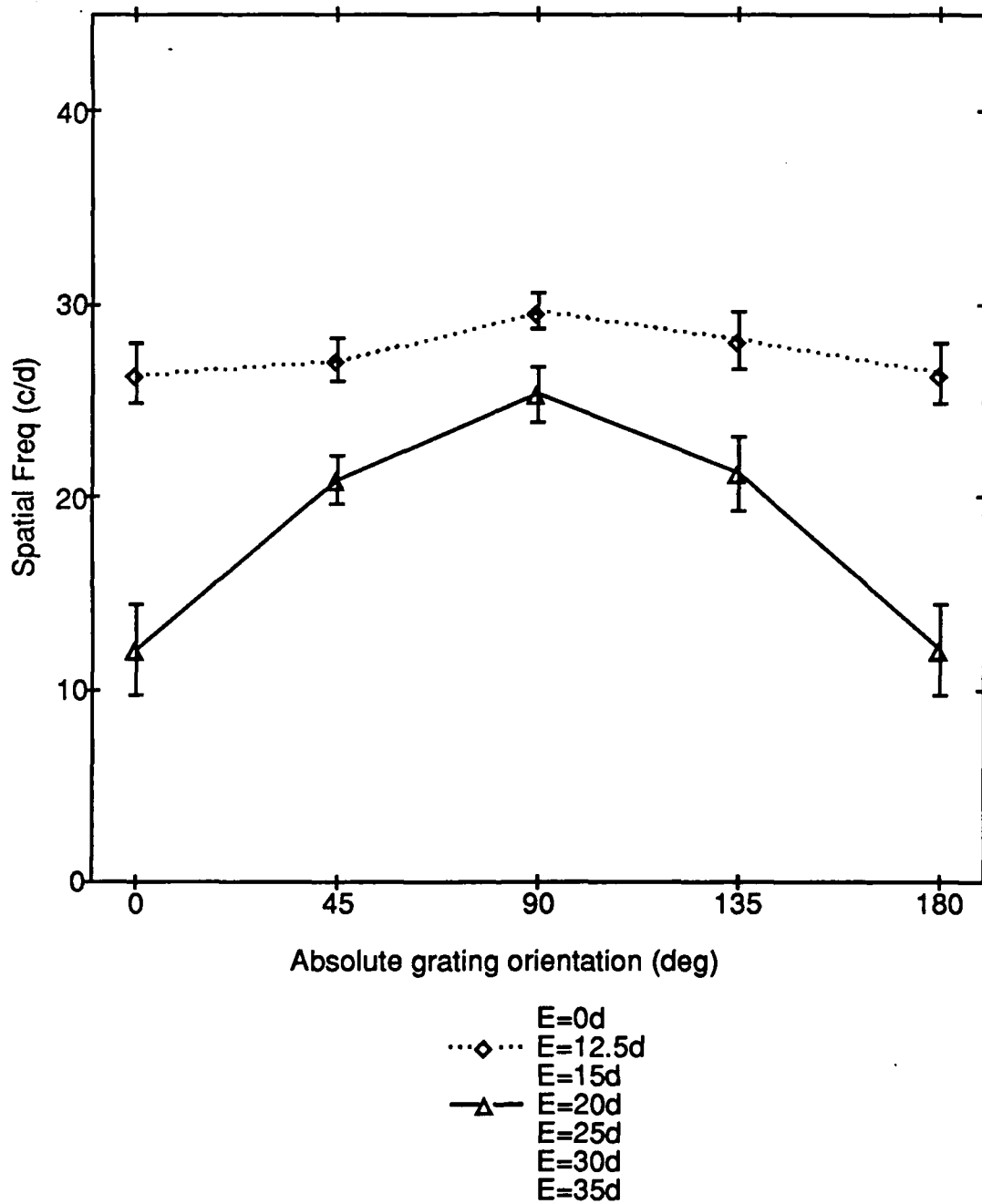
G_TUN_SG45D

03-SEP-89 15:42 Page 1

FIG. A10. DETECTION ACUITY FOR SG FOR
SUPERIOR TEMPORAL MERIDIANError bars are ± 1 s.e.m.

G_TUN_SG90D

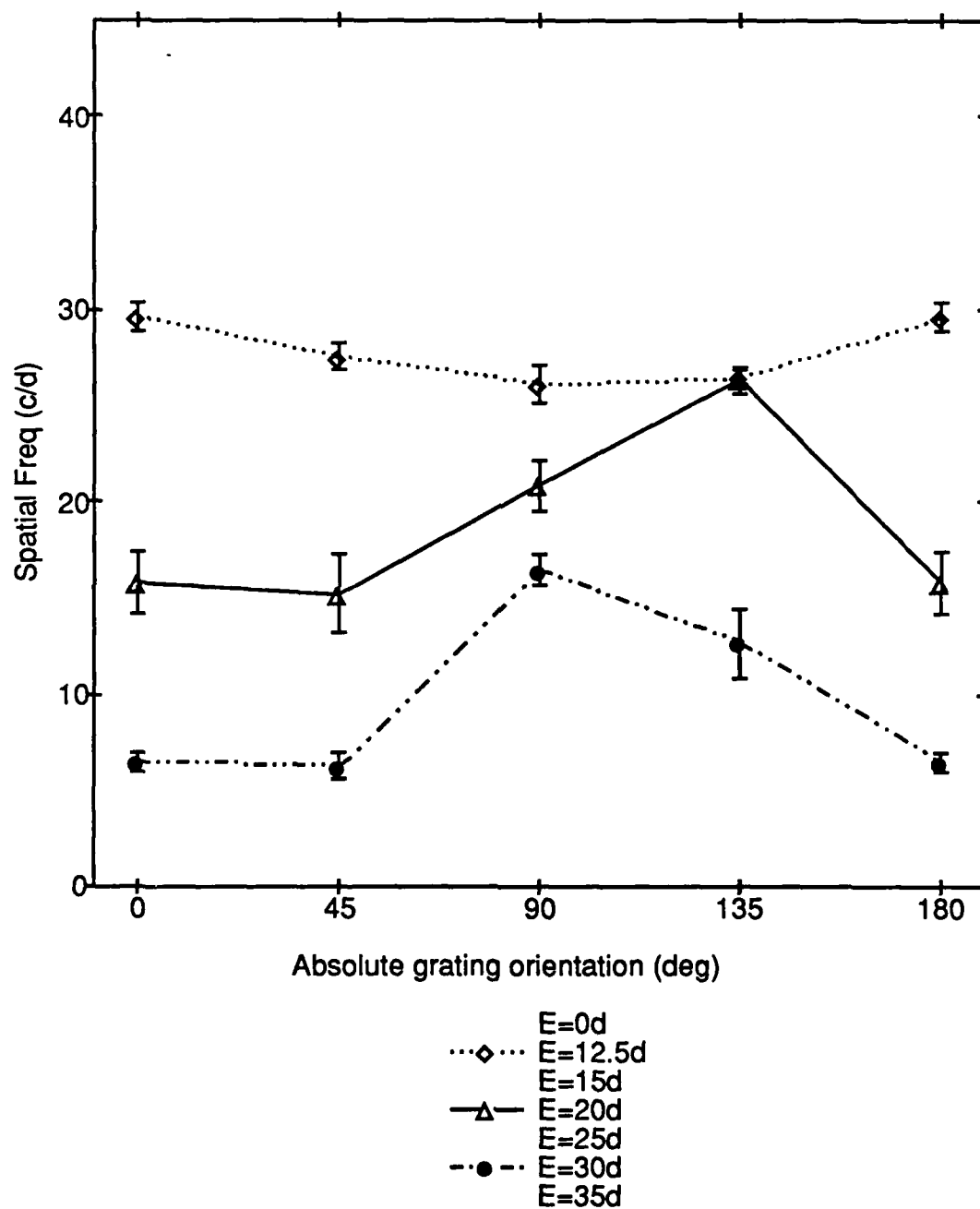
03-SEP-89 15:51 Page 1

FIG. A11. DETECTION ACUITY FOR SG
FOR SUPERIOR MERIDIAN

Error bars are +/- 1 s.e.m.
MERIDIAN 90 AT 30 DEGREES ECCENTRICITY WAS TOO DIFFICULT
TO GET RELIABLE RESULTS DUE TO INTERFERENCE BY UPPER LID

G_TUN_SG135D

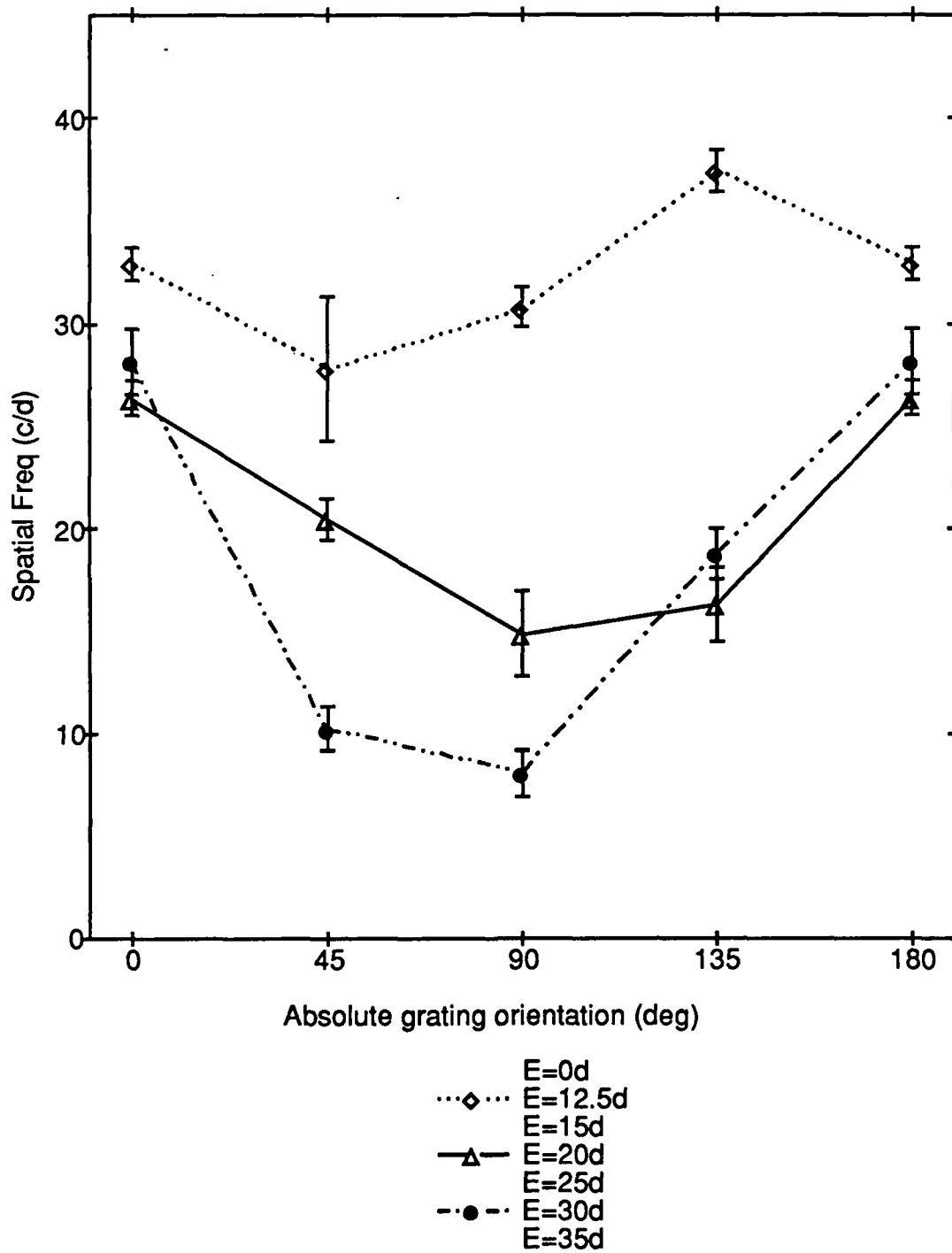
03-SEP-89 16:06 Page 1

FIG. A12. DETECTION ACUITY FOR SG FOR
SUPERIOR NASAL MERIDIAN

Error bars are ± 1 s.e.m.
ECCENTRICITY 30 DEGREES WAS VERY DIFFICULT DUE
TO "BLACKING-OUT" OF GRATING

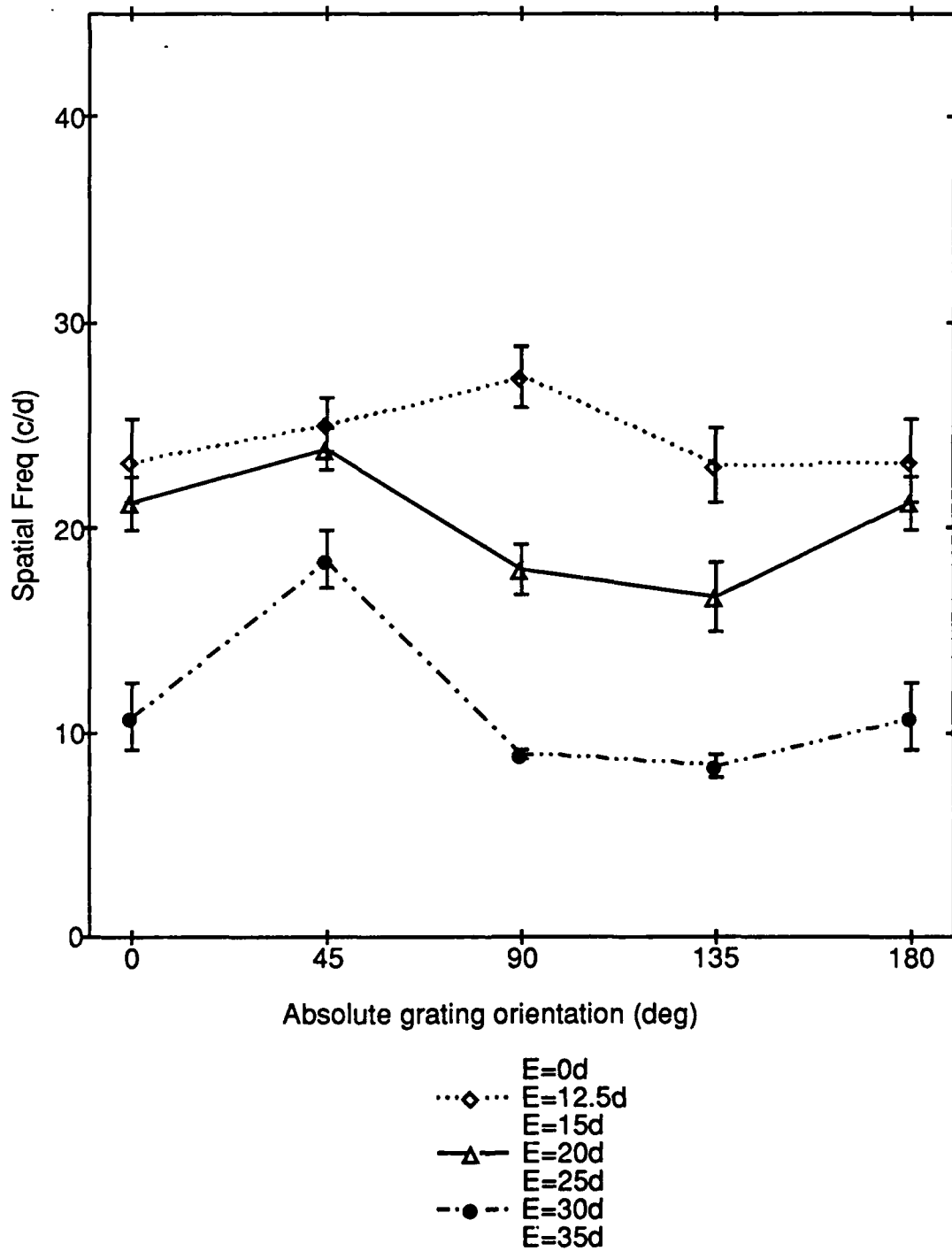
G_TUN_SG180D

03-SEP-89 16:33 Page 1

FIG. A13. DETECTION ACUITY FOR SG FOR
HORIZONTAL NASAL MERIDIANError bars are ± 1 s.e.m.

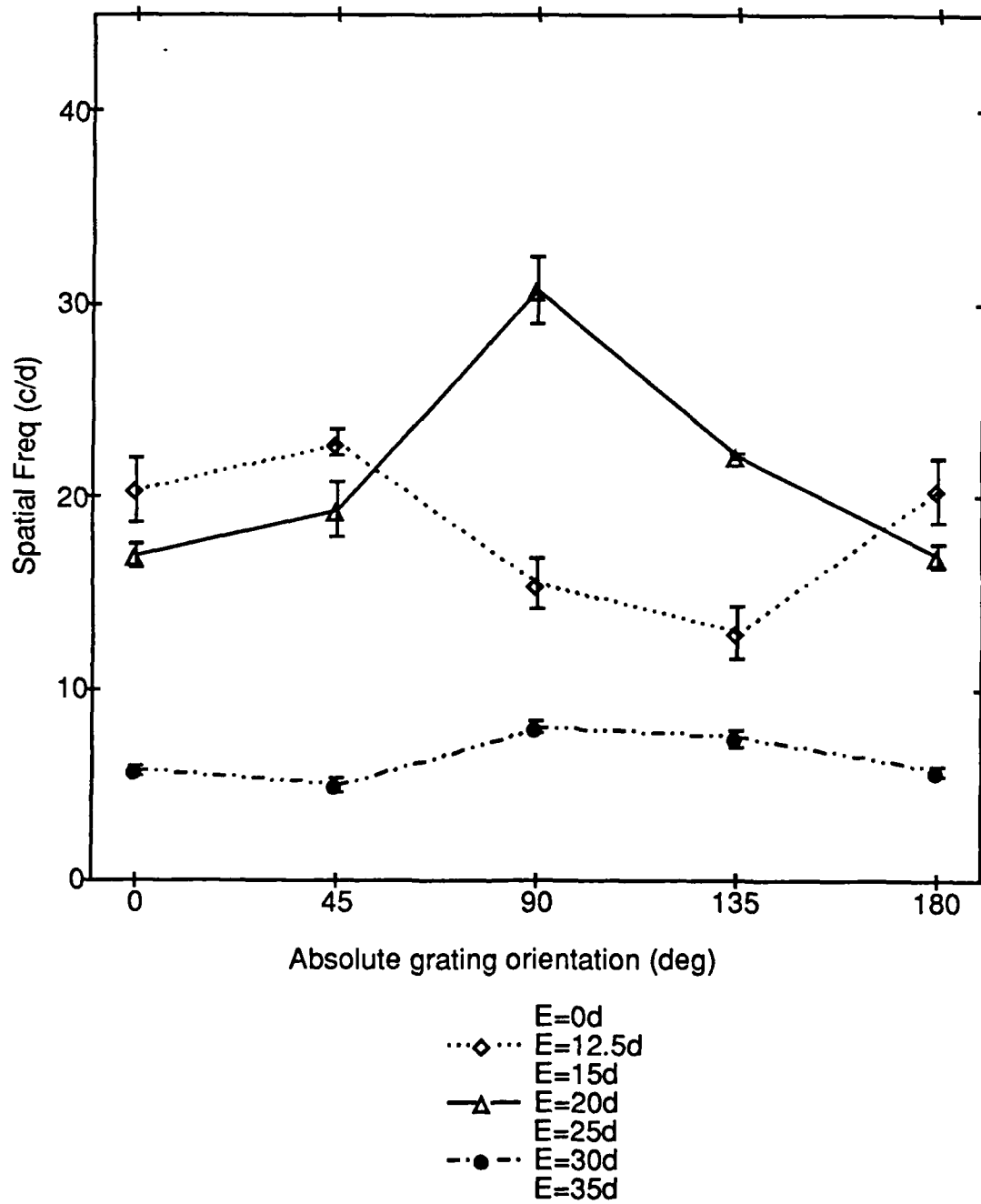
G_TUN_SG225D

03-SEP-89 16:40 Page 1

FIG. A14. DETECTION ACUITY FOR SG FOR
INFERIOR NASAL MERIDIANError bars are ± 1 s.e.m.

G_TUN_SG270D

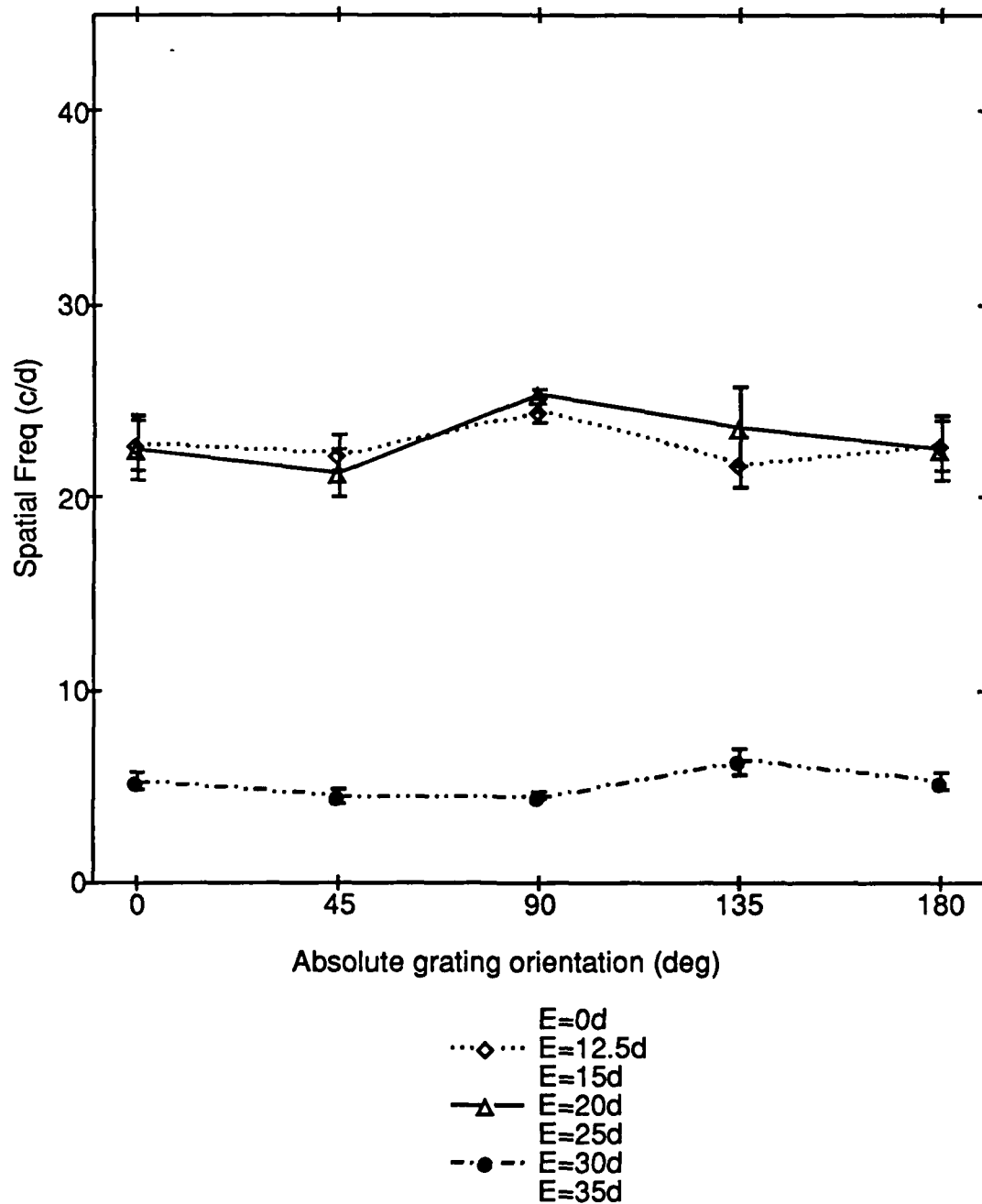
03-SEP-89 16:46 Page 1

FIG. A15. DETECTION ACUITY FOR SG
FOR INFERIOR MERIDIAN

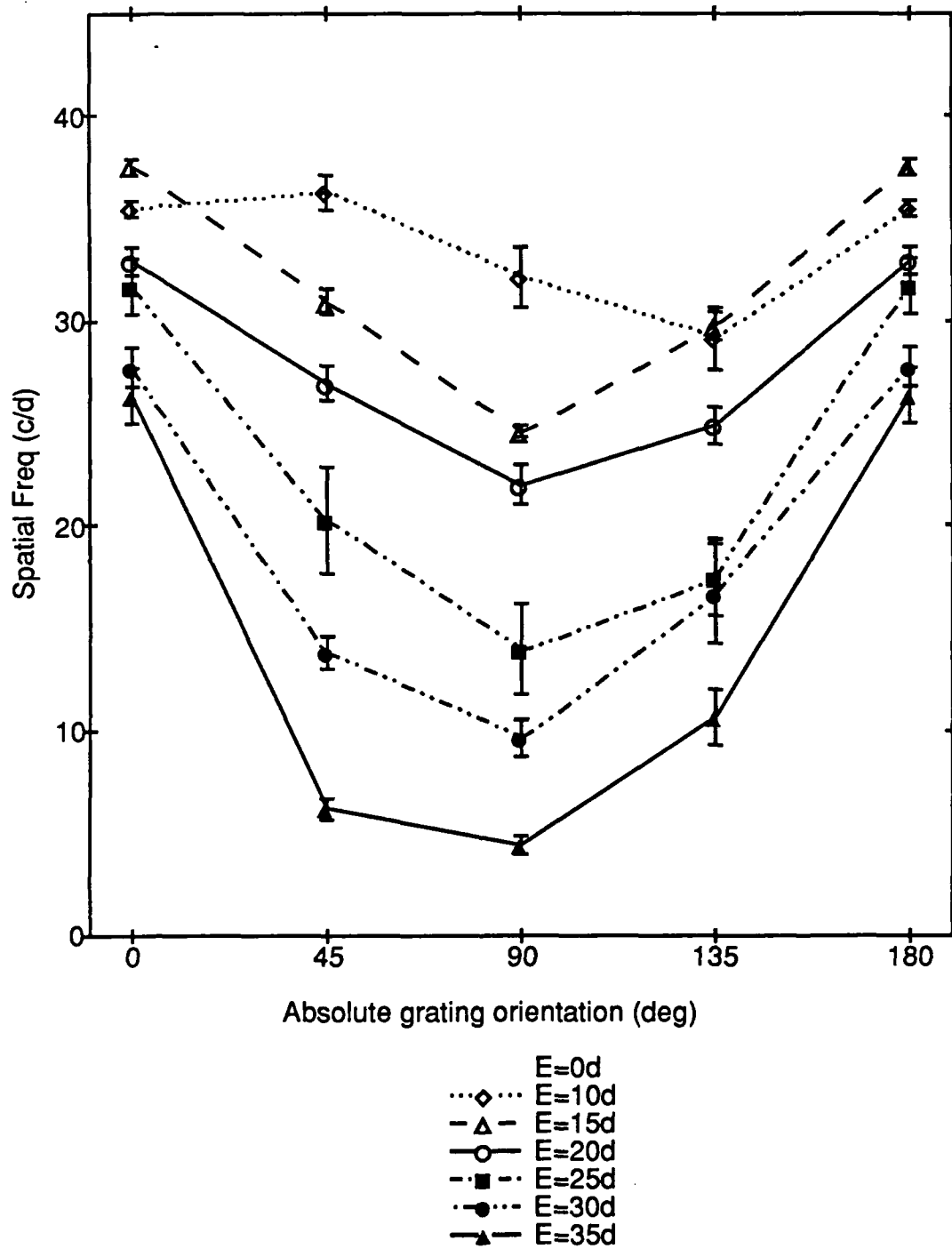
Error bars are ± 1 s.e.m.
 E=30d WAS VERY DIFFICULT DUE TO "BLACKING-OUT"
 OF GRATING

G_TUN_SG315D

03-SEP-89 16:53 Page 1

FIG. A16. DETECTION ACUITY FOR SG FOR
INFERIOR TEMPORAL MERIDIAN

Error bars are +/- 1 s.e.m.
 E=30d WAS VERY DIFFICULT DUE TO "BLACKING-OUT"
 OF GRATING

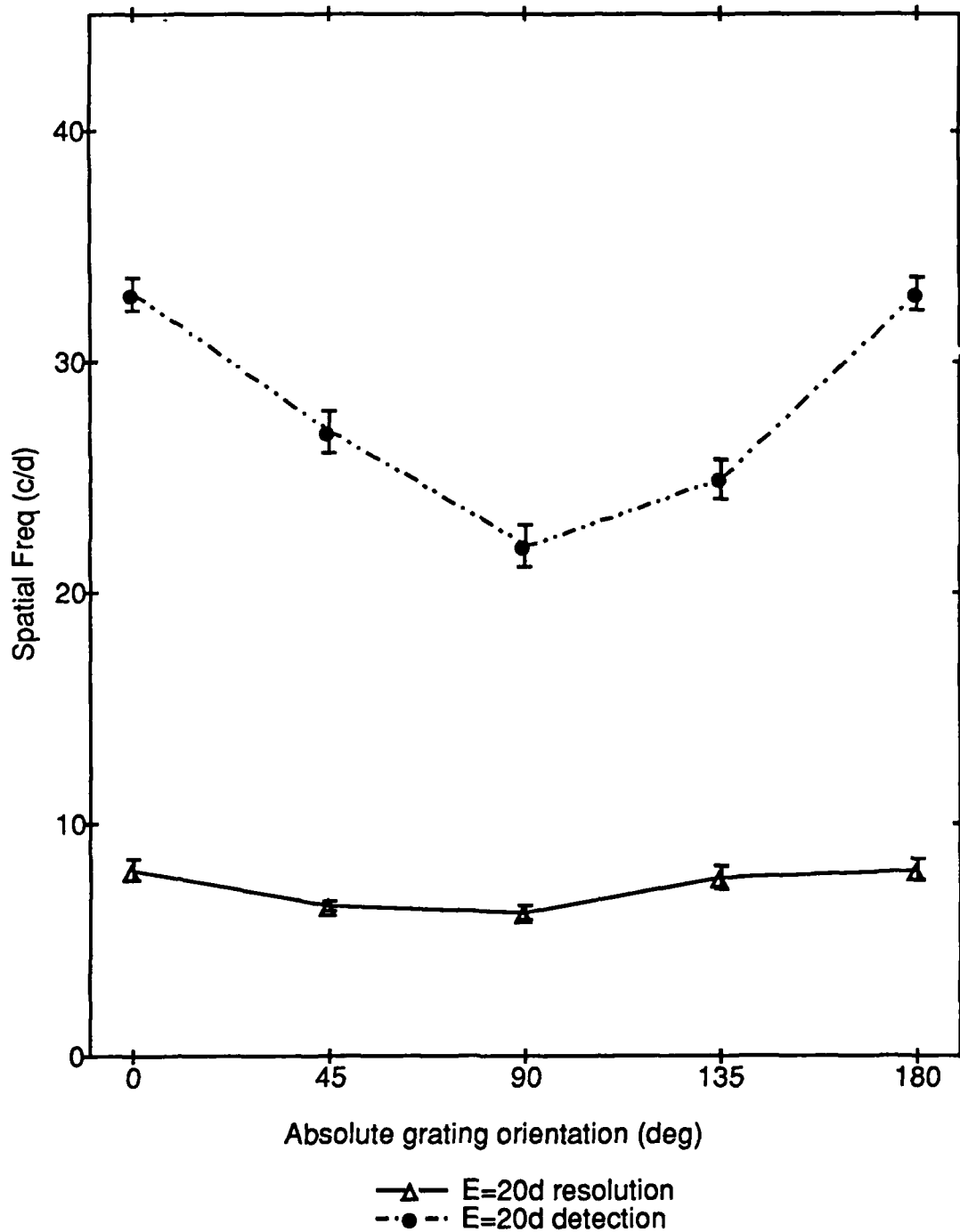
FIG. A17. DETECTION ACUITY FOR FC FOR
HORIZONTAL NASAL MERIDIAN

Error bars are +/- 1 s.e.m.

G_TUNING_FC180DR20

03-SEP-89 17:16 Page 1

FIG. A18. DETECTION AND RESOLUTION ACUITY FOR FC
IN HORIZONTAL NASAL MERIDIAN
AT 20 DEGREES ECCENTRICITY

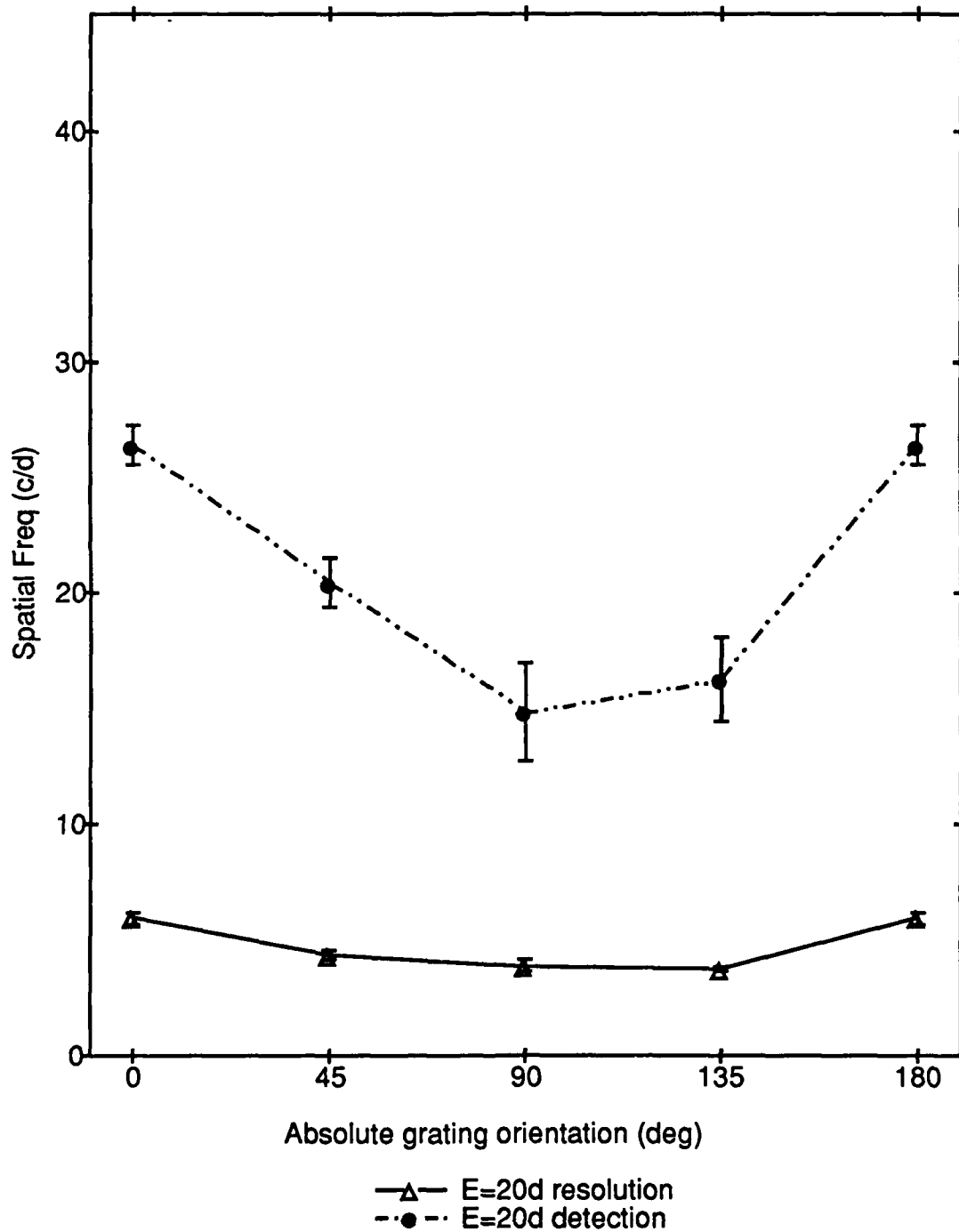


Error bars are +/- 1 s.e.m.

G_TUNING_SG180DR20

03-SEP-89 17:23 Page 1

FIG. A19. DETECTION AND RESOLUTION ACUITY FOR SG
IN HORIZONTAL NASAL MERIDIAN
AT 20 DEGREES ECCENTRICITY

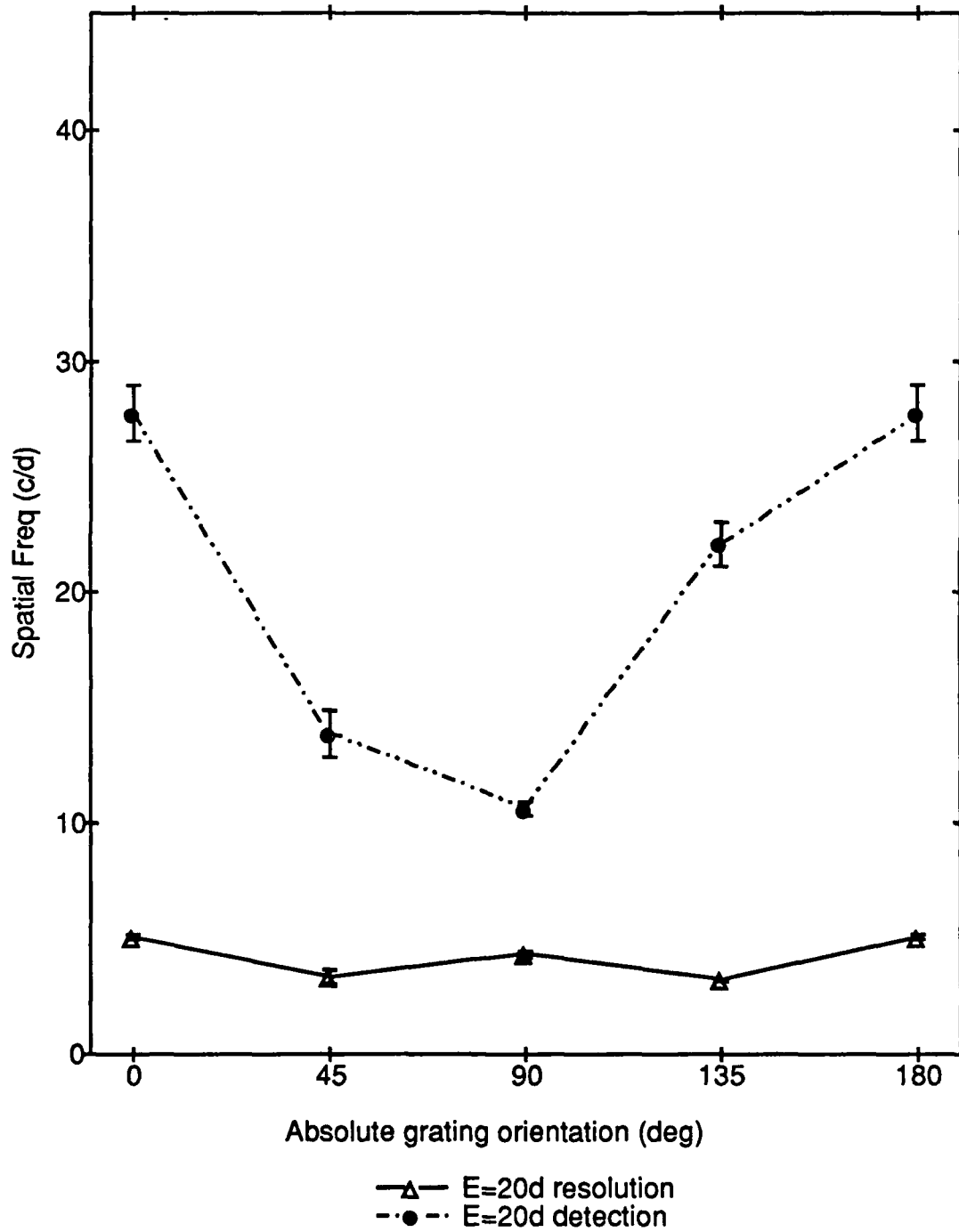


Error bars are +/- 1 s.e.m.

G_TUNING_AB180DR20

03-SEP-89 17:31 Page 1

FIG. A20. DETECTION AND RESOLUTION ACUITY FOR AB
IN HORIZONTAL NASAL MERIDIAN
AT 20 DEGREES ECCENTRICITY



Error bars are +/- 1 s.e.m.

APPENDIX V

TABLE:16386 11R x 1C

09-SEP-89 18:19 Page 1

Frank's Thesis Procedures

0 Name	1 Definition	
1 FA2_T	/*A2 FOURIER ANGLE FOR TUNING CURVE	
2 RAWSTATS	/*STATS OF RAW PSYCHOPHYSICAL DATA.	V
3 FC1_T	/*C1 FOURIER COEF FOR TUNING CURVE	
4 DATA_TO_T	/*FORMAT TUNING CURVES FROM ORIENTATION DATA TABLES	
5 T_TO_E	/*GRAPH FORMAT CONVERSION: TUNING TO ECCENTRICITY	
6 FA1_T	/*A1 FOURIER ANGLE FOR TUNING CURVE	
7 PROCESS_DATA	/*PROCESS ORIENTATION DATA TABLES FROM PSYCHOPHYSICAL EXPERIMENTS	
8 DATA_TO_BIAS	/*FORMAT ORIEN BIAS CURVES FROM DATA TABLES	
9 F_ANOVA	/*ANOVA for Fourier Coefficients.	LNT 17dec85
10 FC2_T	/*C2 FOURIER COEF FOR TUNING CURVE	v12sep86
11 MAKE_REL_TUN	/*construct a table of relative tuning curves	10jul86

Variable

09-SEP-89 18:30 Page 1

```

/*A2 FOURIER ANGLE FOR TUNING CURVE          */
/*PROCEDURE NAME = FA2_T                      */
/*USAGE: X = FA2_T(T,R,C)                    */
/*ARGUMENTS:  T = TABLE NAME                */
/*           R = CURRENT ROW                  */
/*           C = CURRENT COLUMN               */

/*LNT 18JUL85  same method as procedure A1CT */

PROCEDURE(T,R,C);

ta2 = (T[R,1]+T[R,3]-T[R,2]-T[R,4]);

/* For the case of just 4 orientations tested, B2=0 and phase can only */
/* be either 0deg or 45deg (recall, second harmonic is quadrimodal on 360d*/
/* So, value of angle depends solely on sign of ta2                      */

IF ta2=EMPTY THEN RETURN EMPTY;
IF (ta2<0) THEN RETURN 45.0; /*means preferred orientation is oblique */
ELSE RETURN 0.0;           /*means pref. orien is horizontal or vertical */
END;

```

Variable

09-SEP-89 18:31 Page 1

```

/*STATS OF RAW PSYCHOPHYSICAL DATA.                                V12SEP86
  USAGE: CALL RAWSTATS('TABLENAME',N,'MODELNAME',YESCOPY,SEP)
  TABLENAME= source of raw snellen scores
  N = number of data rows in TABLENAME
  MODELNAME = destination model for storing mean and sem results
              Can be set to "NONE" to skip saving results in a model.
  YESCOPY = TRUE for non-interactive printing of table.
              FALSE for non-interactive display of table on terminal.
              EMPTY to skip display of results.
  SEP = TRUE to separately analyze A & B components, FALSE to combine A&B

  LNT 16JUL85; 31JUL85 add parameter N=#data rows
  LNT 8AUG85; Change def of row n1, col 5 to allow for variable
              number of values per orientation.
  LNT 31OCT85; Add auto tranfer of results into model tables
  LNT 19NOV85; Save source table name
  LNT 05DEC85; Correct for small calibration error, add YESCOPY switch.
  LNT 17DEC85; Add F-test for significance of harmonic amplitudes.
  LNT 31DEC85; Make F-ratio negative if harmonic amplitude is insignificant.
  LNT 6JAN86; Include expansion of model by 3 columns automatically
  MODIFY CALL TO F_ANOVA TO HANDLE NEW PARAMETER
*/

PROCEDURE(T,N,MODEL_NAME,COPYTYPE); /* proc name = RAWSTATS */

IF MODEL_NAME >< EMPTY THEN MODEL_NAME=CAPS(MODEL_NAME);
IF T = EMPTY THEN T = GETTABLE("Name of table containing raw data: ");
IF N = EMPTY THEN N = GETNUMBER(
  "Number of data rows (can do !DIS ".T." to refresh your memory)? ",
  FALSE,5,);

IF COPYTYPE >< EMPTY THEN COPYTYPE=CAPS(COPYTYPE);
IF COPYTYPE><'P' AND COPYTYPE><'D' AND COPYTYPE><'S' THEN COPYTYPE=EMPTY;
IF COPYTYPE=EMPTY THEN COPYTYPE=GETRESPONSE(
  "Do you want results printed (P), displayed (D) or suppressed (S)? ",
  FALSE,'P','D','S');
IF COPYTYPE='P' THEN YESCOPY=TRUE;
IF COPYTYPE='D' THEN YESCOPY=FALSE;
IF COPYTYPE='S' THEN YESCOPY=EMPTY;

N1 = N+1;      /* means in Snellen fraction */
N2 = N+2;      /* sem in Snellen fraction */
N3 = N+3;      /* mean in cyc/deg */
N4 = N+4;      /* sem in cyc/deg */
N7 = N+7;      /* I.D. row */

TYPE NOCR 'Calculating ...';

SET COL 5 OF TABLE(T) TO ROWMEAN OF COLS 1 TO 4 OF ROWS 1 TO N OF TABLE(T);

SET ROW N1 OF TABLE(T) TO COLMEAN OF ROWS 1 TO N OF TABLE(T);
SET ROW N2 OF TABLE(T) TO COLSEM OF ROWS 1 TO N OF TABLE(T);
SET ROW N1 OF TABLE(T) TO ROW N1 - 0.025; /* correction for fixed error */

SET ROW N1 COL 5 OF TABLE(T) = MEAN OF COLS 1 TO 4 OF ROW N1 OF TABLE(T);
SET ROW N2 COL 5 OF TABLE(T) = SEM OF COLS 1 TO 4 OF ROWS 1 TO N OF TABLE(T);

SET ROW N3 OF TABLE(T) TO 30*ROW N1 OF TABLE(T);
SET ROW N4 OF TABLE(T) TO 30*ROW N2 OF TABLE(T);

SET ROW 0 COL 0 OF TABLE(T) TO 'File:
'.T;
SET ROW N1 COL 0 OF TABLE(T) TO 'MEAN(cor)'; /*flag to show correction done*/

```

Variable

09-SEP-89 18:31 Page 2

```

TYPE "done";

IF YESCOPY><EMPTY THEN BEGIN;
  IF YESCOPY THEN PRINT TABLE(T) COLWIDTH 12;
  IF NOT YESCOPY THEN DISPLAY TABLE(T) COLWIDTH 12 NONOTES;
END;

IF EMPTY(SEP) THEN
  SEP=YESANSWER("Do you want separate FANOVA analysis of A & B coeffs? ",TRUE);
TYPE "Doing analysis of variance of Fourier coefficients...";
CALL F_ANOVA(T,N,YESCOPY,FALSE,SEP);      /* do the analysis of variance */

IF MODEL_NAME = EMPTY THEN BEGIN;
  IF NOT YESANSWER('Shall we save these results in a MODEL? ') THEN RETURN;
  MODEL_NAME=GETTABLE('Name of model to put these data into: ');
END;

IF MODEL_NAME='NONE' THEN RETURN; /*short circuit requested noninteractively*/

DAT = ROW N7 COL 1 OF TABLE(T);          /* find the data */
DAT = "'".DAT."";                          /* and put in single quotes */
ECC = ROW N7 COL 2 OF TABLE(T);          /* find the eccentricity */
MER = ROW N7 COL 3 OF TABLE(T);          /* find the meridian */
TNAM= "'".T."";                          /* source tablename */
CALL ADD3COLS (MODEL_NAME);               /* expand the basic model */

/* -----
   SAVE THE DATA FOR MEANS
   ----- */
TYPE NOCR "Saving results in model ".MODEL_NAME." ... ";

ROWNAME= "mean '.INTEGER(ECC).'";          /* form the rowname for means */

CMD="SET COLS 1 TO 5 OF ROW ".ROWNAME." OF TABLE ".MODEL_NAME."
  TO COLS 1 TO 5 OF ROW ".N3." OF TABLE ".T;
/*TYPE "Now doing: ".CMD; */
EXEC(CMD);                                /* save the mean values */

CMD="SET COL 8 ROW ".ROWNAME." OF TABLE ".MODEL_NAME." TO "'".DAT."";
/*TYPE "Now doing: ".CMD; */
EXEC(CMD);                                /* save the date */

IF MER >< EMPTY THEN BEGIN;
CMD="SET COL 6 ROW ".ROWNAME." OF TABLE ".MODEL_NAME." TO ".MER;
/*TYPE "Now doing: ".CMD; */
EXEC(CMD);                                /* save the meridian */
END;

CMD="SET COL 17 ROW ".ROWNAME." OF TABLE ".MODEL_NAME." TO "'".TNAM."";
/*TYPE "Now doing: ".CMD; */
EXEC(CMD);                                /* save the source tablename */

ALPHA=0.05;                                /* pick a safe significance level */

IF NOT SEP THEN BEGIN; /* OLD CODE HANDLES THE "COMBINED" OPTION */

F_RATIO=ROW 2 COL 4 OF FANOVA;
SIGLEV=ROW 2 COL 5 OF FANOVA;
IF SIGLEV > ALPHA THEN F_RATIO = - F_RATIO; /* special convention: make
                                           F-ratio neg. if insignificant */
CMD="SET COL 18 ROW ".ROWNAME." OF TABLE ".MODEL_NAME." TO ".F_RATIO;
EXEC(CMD);                                /* save the F-ratio for fundamental */

```

Variable

09-SEP-89 18:32 Page 3

```

F_RATIO=ROW 3 COL 4 OF FANOVA;
SIGLEV=ROW 3 COL 5 OF FANOVA;
IF SIGLEV > ALPHA THEN F_RATIO = - F_RATIO;  /* special convention: make
                                           F-ratio neg. if insignificant */
CMD="SET COL 19 ROW ".ROWNAME." OF TABLE ".MODEL_NAME." TO ".F_RATIO;
EXEC(CMD);                                /* save the F-ratio for second harmonic*/

END;  /* END OF OLD CODE FOR "COMBINED OPTION" */

IF SEP THEN BEGIN;  /* NEW CODE TO SAVE A & B SEPARATELY */

END;  /* END OF NEW CODE FOR "SEPARATE" OPTION */

/* -----
                        SAVE THE DATA FOR ERRORS
----- */
ROWNAME= "sem ".INTEGER(ECC)." ";  /* form the rowname for sem's */

CMD="SET COLS 1 TO 5 OF ROW ".ROWNAME." OF TABLE ".MODEL_NAME."
    TO COLS 1 TO 5 OF ROW ".N4." OF TABLE ".T;
/*TYPE "Now doing: ".CMD; */
EXEC(CMD);                                /* save the sem values */

CMD="SET COL 8 ROW ".ROWNAME." OF TABLE ".MODEL_NAME." TO ".DAT." ";
/*TYPE "Now doing: ".CMD; */
EXEC(CMD);                                /* save the date */

IF MER >< EMPTY THEN BEGIN;
CMD="SET COL 6 ROW ".ROWNAME." OF TABLE ".MODEL_NAME." TO ".MER;
/*TYPE "Now doing: ".CMD; */
EXEC(CMD);                                /* save the meridian */
END;

CMD="SET COL 17 ROW ".ROWNAME." OF TABLE ".MODEL_NAME." TO ".TNAM." ";
/*TYPE "Now doing: ".CMD; */
EXEC(CMD);                                /* save the source tablename */

TYPE "done.";

END;  /* end of procedure rawstats */

```

Variable

09-SEP-89 18:34 Page 1

```

/*C1 FOURIER COEF FOR TUNING CURVE          */
/*PROCEDURE NAME = FC1_T                     */
/*USAGE: X = FC1_T(T,R,C,OPTION)            */
/*ARGUMENTS: T= TABLE NAME                 */
/*          R= CURRENT ROW                   */
/*          C= CURRENT COLUMN                */
/*          OPTION= "A", "B", OR "C"         */

/*LNT 21JUN85                               */
/*LNT 11JUL85; DISCOVERED & CORRECTED ERROR: MULTIPLY BY 2/N */
/*FEC 11SEPT86 PUT IN A1 AND B1 OPTION (ABSOLUTE NOT RELATIVE) */

PROCEDURE(T,R,C,OPTION);

A1=0.5*(T[R,1]-T[R,3]);
B1=0.5*(T[R,2]-T[R,4]);
C1=SQRT(A1*A1+B1*B1);

IF EMPTY(OPTION) THEN OPTION = "C"; /* DEFAULT */
IF OPTION="A" THEN RETURN A1;
IF OPTION="B" THEN RETURN B1;
IF OPTION="C" THEN RETURN C1;

END;

```

Variable

09-SEP-89 18:36 Page 1

```

/*FORMAT TUNING CURVES FROM ORIENTATION DATA TABLES          */
/*PROCEDURE NAME: DATA_TO_T                                     */
/*USAGE: CALL DATA_TO_T('DATA','TUNING')                       */
/*ARGUMENTS: RES = string variable containing name of           */
/*            'results of ...' table containing data            */
/*            TUN = string variable containing name of existing */
/*            table which is in 'DATA of G_TUNING' format        */
/*            that will be filled by this routine               */
/*ASSUMPTIONS: model G_FORMAT expects data to be in table D.    */
/*LNT 3JUL85                                                     */

PROCEDURE(RES,TUN);

IF TUN=EMPTY THEN RETURN; /*legality check on argument          */

TYPE '[DATA_TO_T: Beginning production of tuning curve table]';

IF TABLEEXISTS('D') THEN DELETE TABLE 'D';
MAKE TABLE 'D' FROM TABLE(RES);
COMPUTE MODEL G_FORMAT INTO TABLE(TUN);
TRANSPPOSE TABLE(TUN);
SET TITLE OF TABLE(TUN) = TITLE OF TABLE(RES);
SET NOTES OF TABLE(TUN) = 'G_TUNING format: orientation tuning curves.';

TYPE NOCR '[DATA_TO_T: Table ',TUN,' is ready for use.]';
TYPE ' ';

END;

```

Variable

09-SEP-89 18:46 Page 1

```

/*GRAPH FORMAT CONVERSION: TUNING TO ECCENTRICITY          */
/*PROCEDURE NAME = T_TO_E                                  */
/*USAGE: CALL T_TO_E('SOURCE','DESTINATION')              */
/*ARGUMENTS: TUN = string variable containing name of table in */
/*            tuning-curve format                          */
/*            ECC = string variable containing name of table  */
/*            in eccentricity format                        */
/*DEFAULT TEMPORARY TABLE IS CALLED PTEMP                */
/*LNT 20JUN85; 3JUL85;                                     */

PROCEDURE(TUN,ECC);

X = TABLEEXISTS(ECC);
IF NOT X THEN
  MAKE TABLE(ECC) FROM TABLE E_TEMPLATE;

/* first transpose means                                   */

IF TABLEEXISTS('PTEMP') THEN DELETE TABLE PTEMP;
MAKE TABLE PTEMP FROM ROWS 1 TO 4 OF COLS 2 TO 8 OF TABLE(TUN);
TRANSPOSE TABLE PTEMP;
SET ROWS 1 TO 7 OF COLS 2 TO 5 OF TABLE(ECC) TO
  ROWS 1 TO 7 OF COLS 1 TO 4 OF PTEMP;
TYPE NOCR '[T_TO_E: Step one complete,]';

/* next do low error bars                                 */

DELETE TABLE PTEMP;
MAKE TABLE PTEMP FROM ROWS 1 TO 4 OF COLS 9,11,13,15,17,19,21 OF TABLE(TUN);
TRANSPOSE TABLE PTEMP;
SET ROWS 1 TO 7 OF COLS 6,8,10,12 OF TABLE(ECC) TO
  ROWS 1 TO 7 OF COLS 1 TO 4 OF PTEMP;
TYPE NOCR 'step two complete,]';

/* now do high error bars                                 */

DELETE TABLE PTEMP;
MAKE TABLE PTEMP FROM ROWS 1 TO 4 OF COLS 10,12,14,16,18,20,22 OF TABLE(TUN);
TRANSPOSE TABLE PTEMP;
SET ROWS 1 TO 7 OF COLS 7,9,11,13 OF TABLE(ECC) TO
  ROWS 1 TO 7 OF COLS 1 TO 4 OF PTEMP;
TYPE NOCR 'step three complete.]';
TYPE ' ';

/* "DON'T FORGET TO SET TITLE OF THE NEW TABLE"          */
SET TITLE OF TABLE(ECC) = TITLE OF TABLE(TUN);

TYPE NOCR '[T_TO_E: Table ',ECC,' is ready for use.]';
TYPE ' ';

DELETE TABLE PTEMP;

END;

```


Variable

09-SEP-89 18:48 Page 1

```

/*A1 FOURIER ANGLE FOR TUNING CURVE          */
/*PROCEDURE NAME = FA1_T                      */
/*USAGE: X = FA1_T(T,R,C)                    */
/*ARGUMENTS: T= TABLE NAME                  */
/*          R= CURRENT ROW                   */
/*          C= CURRENT COLUMN                 */
/*LNT 18JUL85                                */

PROCEDURE (T,R,C);

tA1=(T[R,1]-T[R,3]);          /*don't bother to multiply by 2/N */
tB1=(T[R,2]-T[R,4]);          /*   when getting angle           */
THETA=ARCTN(tB1,tA1)/2.0;      /*divide by modality of tuning curve*/

RETURN THETA;

END;

```

Variable

09-SEP-89 18:49 Page 1

```

/*PROCESS ORIENTATION DATA TABLES FROM PSYCHOPHYSICAL EXPERIMENTS */
/*PROCEDURE NAME: PROCESS_DATA */
/*USAGE: CALL PROCESS_DATA('data model') */

/*VARIABLES: MOD = string variable containing name of model that */
/*             holds the raw data */
/*             RES = string variable containing name of data table in */
/*             'results of ...' format */
/*             TUN = string variable containing name of table to put */
/*             tuning curves into. */
/*             ECC = string variable containing name of table to put */
/*             eccentricity curves into. */
/*             A_BIAS= string variable containing name of table to put */
/*             absolute bias curves into. */
/*             R_BIAS= string variable containing name of table to put */
/*             relative bias curves into. */

/*LNT 08JUL85; LNT 11JUL85 add BIAS processing; */
/*LNT 28AUG85 add notes to tuning and eccentricity tables, graphs */
/*LNT 29OCT85 change convention for naming created tables */
/*LNT 03DEC85 add interactive queries for options */
/*LNT 03JAN86 change organization of orientation bias curves */
/*FEC 22JULY86 add graphs m_bias3 and m_bias4 */
PROCEDURE(MOD,Q1,Q2,Q3,Q4,Q5);

IF MOD=EMPTY THEN MOD=GETTEXT('Name of model containing data (omit quotes)? ');

IF Q1=EMPTY THEN Q1=YESANSWER('Do you want to compute the model? ',TRUE);
IF Q2=EMPTY THEN Q2=YESANSWER('Do you want to make tuning curves? ',TRUE);
IF Q3=EMPTY THEN Q3=YESANSWER('Do you want to make eccentricity curves? ',TRUE);
IF Q2=FALSE AND Q3=TRUE THEN TYPE '
Warning! Eccentricity curves are derived from tuning curves!
';
IF Q4=EMPTY THEN Q4=YESANSWER('Do you want to make orientation bias curves? ',
TRUE);
IF Q5=EMPTY THEN Q5=YESANSWER('Do you want an error analysis graph? ',TRUE);

SET STARTTIME = DATETIME();
TYPE STARTTIME; /* start time */

/*Set up variables containing table names */
RES = 'RESULTS OF ' .MOD; /*std RS1 convention for results*/
TUN = 'TUNING OF ' .MOD; /*borrow RS1 convention for others*/
ECC = 'ECCEN OF ' .MOD;
FUND = 'C1';
SECN = 'C2';
MERIDA1= 'A1';
MERIDB1= 'B1';
ERR = 'ERRORS OF ' .MOD;
SET T = TITLE OF TABLE(MOD); /*common title for new tables */

/*First step is to fill in results table. */
IF Q1=TRUE THEN BEGIN;
COMPUTE TABLE(MOD);
TYPE NOCR 'PROCESS_DATA: ',RES,' is ready.';
TYPE '';
END;

/*Second step is to generate an orientation tuning curve */
IF Q2=TRUE THEN BEGIN;

```

Variable

09-SEP-89 18:49 Page 2

```

SET M1 = COL 1 ROW 1 OF TABLE M;
SET N1 = 'Error bars are +/- ' ;
SET N2 = ' s.e.m.' ;
SET N3 = N1.M1.N2;

```

```

CALL DATA_TO_T(RES,TUN);
SET NOTES OF TABLE(TUN) TO N3;
COMPUTE TABLE(TUN) INTO TABLE 'DATA OF G_TUNING';
SET GRAPHTITLE OF G_TUNING TO T;
SET GRAPHNOTES OF G_TUNING TO N3;
TYPE 'PROCESS_DATA: Graph G_TUNING is ready to view';
END;

```

```

/*Third step is to generate an eccentricity curve */

```

```

IF Q3=TRUE THEN BEGIN;
CALL T_TO_E(TUN,ECC);
SET NOTES OF TABLE(ECC) TO N3;
COMPUTE TABLE(ECC) INTO TABLE 'DATA OF G_ECC';
SET GRAPHTITLE OF G_ECC TO T;
SET GRAPHNOTES OF G_ECC TO N3;
TYPE 'PROCESS_DATA: Graph G_ECC is ready to view';
END;

```

```

/*Fourth step is to generate orientation bias curves */

```

```

IF Q4=TRUE THEN BEGIN;
CALL DATA_TO_BIAS(RES,FUND,SECN);
SET COLS 2 TO 8 OF TABLE 'DATA OF M_BIAS1' TO COLS 1 TO 7 OF TABLE(FUND);
TYPE 'PROCESS_DATA: Graph M_BIAS1 is ready to view';
SET COLS 2 TO 8 OF TABLE 'DATA OF M_BIAS2' TO COLS 1 TO 7 OF TABLE(SECN);
TYPE 'PROCESS_DATA: Graph M_BIAS2 is ready to view';
SET COLS 2 TO 8 OF TABLE 'DATA OF M_BIAS3' TO COLS 1 TO 7 OF TABLE(MERIDA1);
TYPE 'PROCESS_DATA: Graph M_BIAS3 is ready to view';
SET COLS 2 TO 8 OF TABLE 'DATA OF M_BIAS4' TO COLS 1 TO 7 OF TABLE(MERIDB1);
TYPE 'PROCESS_DATA: Graph M_BIAS4 is ready to view';
END;

```

```

/*Fifth step is to generate error analysis curves */

```

```

IF Q5=TRUE THEN BEGIN;
CALL DATA_TO_ERRORS(RES,ERR);
SET ALL OF TABLE 'DATA OF ERRORS' TO ALL OF TABLE(ERR);
SET GRAPHTITLE OF ERRORS TO T;
TYPE 'PROCESS_DATA: Graph ERRORS is ready to view';
END;

```

```

/*Last step is to report elapsed time */

```

```

SET STOPTIME = DATETIME(); /* stop time */
TYPE NOCR 'Elapsed time = ',STOPTIME - STARTTIME,' seconds.';
TYPE '';

```

```

END;

```

Variable

09-SEP-89 18:51 Page 1

```

/*FORMAT ORIEN BIAS CURVES FROM DATA TABLES
PROCEDURE NAME: DATA_TO_BIAS
USAGE: CALL DATA_TO_BIAS('RESULTS OF LT0R','C1','C2')
ARGUMENTS: RES = string variable containing name of
             'results of ...' table containing data
             FUND = string variable containing name of table to be
                    filled with normalized fundamental harmonic amplitudes
             SECN = string variable containing name of table to be
                    filled with normalized second harmonic amplitudes
             MERIDA1 = string variable containing name of table to be
                      filled with normalized A1(merid, shifted) harmonic
                      amplitudes
             MERIDB1 = string variable containing name of table to be
                      filled with normalized B1(merid. shifted) harmonic
                      amplitudes

LNT 3jan86
fec 22july86
*/
PROCEDURE (RES,FUND,SECN,MERIDA1,MERIDA2); /* proc name = DATA_TO_BIAS */

IF FUND=EMPTY THEN FUND='C1'; /* default value */
IF SECN=EMPTY THEN SECN='C2'; /* default value */
IF MERIDA1=EMPTY THEN MERIDA1='A1'; /*default value */
IF MERIDB1=EMPTY THEN MERIDB1='B1'; /*default value */

IF NOT TABLEEXISTS(FUND) OR NOT TABLEEXISTS(SECN) OR NOT TABLEEXISTS(MERIDA1)
OR NOT TABLEEXISTS(MERIDB1) THEN BEGIN;
  TYPE "Data_to_bias: table C1,C2,A1 OR B1 do not exist. NO ACTION TAKEN";
  RETURN;
END;

MER=EMPTY; /* first find meridian */
DO R=3 TO 8 WHILE MER=EMPTY;
  MER = ROW R COL 6 OF TABLE (RES);
END;
MER=INTEGER(MER);

CMD="SET ROW 'm'=".MER." OF TABLE ' ".FUND." TO
ROWS 2 TO 8 OF COL 11 OF TABLE ' ".RES."";
EXEC (CMD);

CMD="SET ROW 'm'=".MER." OF TABLE ' ".SECN." TO
ROWS 2 TO 8 OF COL 12 OF TABLE ' ".RES."";
EXEC (CMD);

CMD="SET ROW 'm'=".MER." OF TABLE ' ".MERIDA1." TO
ROWS 2 TO 8 OF COL 22 OF TABLE ' ".RES."";
EXEC (CMD);

CMD="SET ROW 'm'=".MER." OF TABLE ' ".MERIDB1." TO
ROWS 2 TO 8 OF COL 23 OF TABLE ' ".RES."";
EXEC (CMD);

TYPE NOCR '[DATA_TO_BIAS: Tables ',FUND,', ',SECN,', ',MERIDA1,', ',MERIDB1,',
are ready for use.];
TYPE '';

END;

```

Variable

09-SEP-89 18:53 Page 1

```

/*ANOVA for Fourier Coefficients.          LNT 17dec85
23dec85: make anova table a temporary table portion
2jan86: make provision for special case because N=even number of points
FC11sept86: make A(i) and B(i) coefficients able to be evaluated
12SEP86, LT. Further mods to handle either A+B or C alone.
-----

```

Method is due to Hartley (1949), Biometrika v36, 194-201.

The method relies on not computing all of the harmonic coefficients which are allowed under the sampling theorem. The non-computed harmonics thus make up a 'residual' which serves as an independent estimate of noise variance.

This implementation of the algorithm is specific to the Fourier analysis of orientation tuning curves for 4 orientations. We think of the N-replications of data at each orientation as representing N repetitions of the basic cycle. The extra 4N-2-1 harmonic coefficients are of no interest and so are used to calculate the residual. In effect, we use the variance of data at each orientation to estimate the error variance in the underlying model:

$$R(q) = \text{mean} + A(1)\cos q + B(1)\sin q + A(2)\cos 2q + B(2)\sin 2q + \text{error}$$

where q = orientation, $A(i)$, $B(i)$ are Fourier coefficients.

If one has no prior reason to test a particular harmonic, then Hartley recommends that one should first test the largest harmonic amplitude for significance, then the second largest, etc. Because of the orthogonality of the harmonics, these tests can be done after the ANOVA without further computations. Note that because one has M chances of finding a significant component, the critical F-value for alpha significance level is in fact α/M for the largest harmonic, $\alpha/(M-1)$ for the second largest, etc. If $C(i) = \sqrt{A(i)^2 + B(i)^2}$ then the null hypothesis to be tested is: Largest $C(i)=0$. If this hypothesis is not rejected, stop. If it is rejected then go on to the next largest $C(i)$ and test it. Continue testing the harmonic coefficients in this way until null hypothesis is accepted.

In our case we have reason to suspect both the fundamental and second harmonics will be large because these represent meridional and oblique effects. Therefore, we may test each separately at the alpha level of significance.

The special case for last harmonic arises because a cosine is aliased by a constant. Consequently, its contribution to sum of squares is twice what would be expected from the Fourier coefficient. The test case verifying this is when only a second harmonic exists and there is no variance between trials.

*/

```

PROCEDURE (T,N,YESDIS,NEWTAB,SEP);      /* procedure name = F_anova

      T = name of data containing raw data.
      N = number of data rows.
      YESDIS = flag to allow auto display at end.
               Set to EMPTY to suppress output, TRUE to
               print output and FALSE to display on TTY.
      NEWTAB = name of table to put ANOVA results into.
               Set to FALSE to decline, EMPTY to query user.
      SEP = TRUE for separate analysis of A(i) & B(i)
             FALSE for combined analysis (=default
             for compatibility with previous version)

```

*/

```

IF NOT TABLEEXISTS('FANOVA') THEN BEGIN;
  TYPE "Table FANOVA is missing. No action taken";

```

Variable

09-SEP-89 18:53 Page 2

```

RETURN;
END;
IF SEP = EMPTY THEN SEP = FALSE; /* default is to combine A&B into C*/

IF T=EMPTY THEN T=GETTABLE("Name of table containing raw data: ");
IF N=EMPTY THEN N=GETNUMBER("Number of data rows: ",FALSE,5);

NP = 4.0*N; /* number of data points for 4-point tuning curve*/
N3 = N+3; /* row number for means in standard source table */
HMAX = 2; /* highest harmonic number to do*/

TPDAT=CAT("COLS 1 TO 4 OF ROWS 1 TO ",N," OF TABLE '",T,"'");
/* tableportion for data*/
TABPOR=TABLEPORTION(TPDAT);

SD= 30*STDEV OF TPREF(TABPOR); /* units are cyc/deg */
TOTAL_SS = SD*SD*(NP-1); /* easy way to get sum of squares */
RESID=TOTAL_SS; /* initialize residual sum of squares */
RESID_DF = NP-1; /* and degrees of freedom */
CLEAR ALL OF TABLE FANOVA;
CLEAR COL 0 OF FANOVA;

ROW 1 COL 0 OF FANOVA = "Total";
ROW 1 COL 1 OF FANOVA = TOTAL_SS;
ROW 1 COL 2 OF FANOVA = NP-1;

C=EMPTY;

AMP[1,1]=FC1_T(T,N3,C,"A"); /* get fundamental amplitude */
AMP[1,2]=FC1_T(T,N3,C,"B");
AMP[1,3]=FC1_T(T,N3,C,"C");

AMP[2,1]=FC2_T(T,N3,C,"A"); /* get second harmonic amplitude = A(2)/2 */
AMP[2,2]=FC2_T(T,N3,C,"B");
AMP[2,3]=FC2_T(T,N3,C,"C");

IF NOT SEP THEN BEGIN; /* ORIGINAL DO LOOP HANDLES "COMBINED" CASE */
M = 2;
DO H=1 TO HMAX; /* loop through harmonics getting sum of squares
and decrement residual along the way */
R= H+1; /* row number for destination table*/
SS=0.5*NP*AMP[H,3]*AMP[H,3]; /* sum of squares for each harmonic is */
/* 0.5*number of points*amplitude squared */

/* !! special case: number of sample points per period = 4 =even. Therefore,
contribution to sum of squares for last harmonic component must be doubled !
Also, only one degree of freedom for last harmonic in this special case. */

IF H=HMAX THEN BEGIN;
SS = 2.0*SS;
M = 1;
END;

ROW R COL 0 OF FANOVA = "C".H;
ROW R COL 1 OF FANOVA = SS;
ROW R COL 2 OF FANOVA = M; /* degrees of freedom per harmonic computed */

RESID = RESID - SS; /* decrement residual as we go */
RESID_DF = RESID_DF - M; /* and remaining degrees of freedom */
END;
END;

IF SEP THEN BEGIN; /* NEW DO LOOP HANDLES "SEPARATE" CASE */

```

Variable

09-SEP-89 18:53 Page 3

```

M = 1; /* df per calculation */
R = 1; /* init row number */

DO H=1 TO HMAX;      /* loop through harmonics getting sum of squares
                      and decrement residual along the way */

  DO J=1 TO 2;        /* loop through two cartesian components */
    R= R+1;           /* bump row number for destination table*/
    SS=0.5*NP*AMP[H,J]*AMP[H,J]; /* sum of squares for "A" or "B" component */

/* !! special case: number of sample points per period = 4 =even. Therefore,
contribution to sum of squares for last harmonic component must be doubled ! */

    IF H=HMAX THEN SS = 2.0*SS;

    IF J=1 THEN ROW R COL 0 OF FANOVA = "A".H;
    IF J=2 THEN ROW R COL 0 OF FANOVA = "B".H;
    ROW R COL 1 OF FANOVA = SS;
    ROW R COL 2 OF FANOVA = M; /* degrees of freedom per component */

    RESID = RESID - SS;          /* decrement residual as we go */
    RESID_DF = RESID_DF - M;     /* and remaining degrees of freedom */

    IF H=HMAX THEN DOEXIT;      /* skip last B */
  END; /* end of J loop */
END; /* end of H loop */
END;

LASTR = R + 1; /*find rownumber for residual */
ROW LASTR COL 1 OF FANOVA = RESID; /* and fill */
ROW LASTR COL 2 OF FANOVA = RESID_DF; /* it in */
ROW LASTR COL 0 OF FANOVA = "Residual";

COL 3 OF FANOVA = COL 1 / COL 2; /* calculate mean squares */

RESID_MS = COL 3 ROW LASTR OF FANOVA;
IF RESID_MS<0 THEN TYPE"
!!WARNING FROM F ANOVA: NEGATIVE RESIDUAL = ".RESID_MS;
IF RESID_MS<=0 THEN RESID_MS=1E-10; /* trap & fix small residuals */

COL 4 OF FANOVA = COL 3 / RESID_MS; /* calculate F-ratio */

DO R= 2 TO LASTR-1; /* look up alpha level in tables */
  F_VALUE= ROW R COL 4 OF FANOVA;
  SIG_LEVEL = PUBLIC $FSIGLEV(M,RESID_DF,F_VALUE);
  ROW R COL 5 OF FANOVA = SIG_LEVEL;
END;

TITLE OF FANOVA =
"Analysis of Variance for data table ".T." (non-meridionally shifted)";
IF NOTEMPTY(YESDIS) THEN BEGIN;
  IF YESDIS THEN PRINT TABLE FANOVA;
  IF NOT YESDIS THEN DISPLAY TABLE FANOVA NONOTES;
END;

IF NEWTAB=FALSE THEN RETURN;
IF NEWTAB=EMPTY THEN BEGIN;
  IF NOT YESANSWER("Do you wish to save the ANOVA table? ",FALSE) THEN RETURN;
  NEWTAB=GETTABLE("Name of table to save results into: ",TRUE);
END;
MAKE TABLE(NEWTAB) FROM TABLE FANOVA;

END; /* end of procedure F_ANOVA */

```

Variable

09-SEP-89 18:55 Page 1

```

/*C2 FOURIER COEF FOR TUNING CURVE  v12sep86          */
/*PROCEDURE NAME = FC2_T                      */
/*USAGE: X = FC2_T(T,R,C,OPTION)              */
/*ARGUMENTS:  T = TABLE NAME                 */
/*            R = CURRENT ROW                  */
/*            C = CURRENT COLUMN               */
/*            OPTION = "A","B", OR "C":        */
/*
/*LNT 21JUN85                                     */
/*LNT 11JUL85; DISCOVERED AND CORRECTED ERROR: MULTIPLY BY 2/N. */
/*            ALSO, OMIT SQRT TO SAVE TIME.    */
/* LNT 31DEC85: Discovered yet another error. Since number of data */
/* points is even, true amplitude is only half of computed coefficient. */
/*FEC 11SEPT86: ENABLED TO USE A2,B2, OR C2      */
/* LT 12sep86: corrected A2 as well.            */

PROCEDURE (T,R,C,OPTION);

A2 = 0.25*(T[R,1]+T[R,3]-T[R,2]-T[R,4]);
B2 = 0.0;                                     /*DOES NOT EXIST FOR 4 POINTS */
C2 = ABS(A2);

IF EMPTY(OPTION) THEN OPTION="C"; /* default */
IF OPTION ="A" THEN RETURN A2;
IF OPTION ="B" THEN RETURN B2;
IF OPTION ="C" THEN RETURN C2;

END;

```


Variable

09-SEP-89 18:57 Page 1

```

/*construct a table of relative tuning curves
parameters: m=model name containing data
             e=eccentricity
             t=tablename to put data into
*/

procedure();      /*procname = MAKE_REL_TUN */

do while true;

if notempty(m) then mtext=tpname($x2tp(m)); /*workaround but in gettable*/
m=gettable("Name of table containing data: ",empty,true,mtext);

n=getrow("Rownumber containing data: ",m,false,false,n);

if notempty(t) then ttext=tpname($x2tp(t));
t=gettable("Name of table to put the data into: ",empty,false,ttext);

do r=1 to 4;                                /*get relative orien */
  q="Relative stimulus orientation for data in col ".r." : ";
  col 0 row r of table(D) = gbndi(q,-91,91);
end;

col 1 of table(D) = cols 1 to 4 of row n of table(m); /* get data*/

do r=1 to 4;                                /*duplicate one point*/
  if col 0 row r of table(D) = 90 or
  col 0 row r of table(D) = -90 then
    add row to table(D) from row r of table(D);
end;

row 5 col 0 of table(D) = -1*row 5 col 0 of table(D); /*and change its sign*/
row 0 col 1 of table(D)=
  gettext("Column heading for these data (eg. meridian): ");

sort table(D) by col 0;                      /*get it in order*/

add col to table(T) from col 1 of table(D);    /*and put it away */

type "Data saved in table ".t;
del table(D);

if not yesanswer("Do another? ") then return;

end;      /* end of loop */

end;      /*end of proc make_rel_tun*/

```

10jul86

Variable

09-SEP-89 18:59 Page 1

```

/*somb(x)=2*J1(pi*x)/pi*x      procname=SOMB      24apr86
follows Gaskill conventions.
Formula for J1 is from Abramowitz & Stegun, eqn 9.44 & 9.46
(accuracy is about 4E-8)

somb(fd) = Fourier transform of disk of diameter=d and area=1.

*/

procedure(x);

/* define constants */

pi=3.1415927;

A1=-0.56249985;
A2= 0.21093573;
A3=-0.03954289;
A4= 0.00443319;
A5=-0.00031761;
A6= 0.00001109;

B1= 0.79788456;
B2= 0.00000156;
B3= 0.01659667;
B4= 0.00017105;
B5=-0.00249511;
B6= 0.00113653;
B7=-0.00020033;

C1=-2.35619449;
C2= 0.12499612;
C3= 0.00005650;
C4=-0.00637879;
C5= 0.00074348;
C6= 0.00079824;
C7=-0.00029166;

/* check for range of argument and branch accordingly */

y = abs(pi * x);

if (y) < 3.0 then begin;

    z = y * y / 9.0;

    s = 1.0 + 2.0*Z*(A1 + Z*(A2 + Z*(A3 + Z*(A4 + Z*(A5 + Z*A6)))));

    return s;

end;

else;      /* (y) > 3.0 */

    z = 3.0 / y;

    theta = y + C1 + Z*(C2 + Z*(C3 + Z*(C4 + Z*(C5 + Z*(C6 + Z*C7))));

    f = B1 + Z*(B2 + Z*(B3 + Z*(B4 + Z*(B5 + Z*(B6 + Z*B7))));

    s = 2.0 * f * cos(theta) / (y * sqrt (y));

    return s;

```

Variable

09-SEP-89 18:59 Page 2

end; /* end of proc SOMB */

APPENDIX VI

PUBLICATIONS RELATING TO THESIS RESEARCH.

Refereed Publications

1. Thibos, L.N. Walsh, D.J. and Cheney, F.E. (1987) Vision beyond the resolution limit: aliasing in the periphery. *Vision Res.* **27**, 2193-2197.
2. Thibos, L.N., Cheney, F.E. and Walsh, D.J. (1987) Retinal limits to the detection and resolution of gratings. *J. Opt. Soc. Amer. A* **4**, 1524-1529.

Published Abstracts

1. Cheney, F.E. and Thibos, L.N. (1986) Evidence of elongated receptive fields in human peripheral retina. *Invest. Ophthal. Vis. Sci.* **27** (suppl.), 341.
2. Thibos, L.N. and Cheney, F.E. (1986) Psychophysical evidence of a monosynaptic pathway in human peripheral vision. *Proc. Australian Physiol. Pharm. Soc.* **17**, 201P.
3. Cheney, F.E., Still, D.L., Thibos, L.N. and Walsh, D.J. (1987) What limits faithful encoding of spatial patterns in human peripheral vision? *J. Physiol.* **396**, 139P.
4. Cheney, F.E. and Thibos, L.N. (1987) Orientation anisotropy for the detection of aliased patterns by peripheral vision is optically induced. *J. Opt. Soc. Am.* **A4**, P79.

Manuscripts in Preparation

1. Cheney, F.E. and Thibos, L.N. Orientational anisotropy for detection of gratings in peripheral vision. (in preparation)

RESEARCH NOTE

VISION BEYOND THE RESOLUTION LIMIT: ALIASING IN THE PERIPHERY

L. N. THIBOS, D. J. WALSH* and F. E. CHENEY†

Department of Visual Science, School of Optometry, Indiana University, Bloomington, IN 47405, U.S.A.

(Received 20 October 1986; in revised form 25 June 1987)

Abstract—Pattern resolution is generally considered a prerequisite for spatial vision because details too fine to be resolved cannot be distinguished from a uniform field. However, our experiments using peripheral vision demonstrate that reliable pattern detection is possible for images far beyond the resolution limit. The visual percept which arises in this case is an illusion called aliasing in which the apparent spatial structure of the stimulus is quite different from that actually present. Aliasing begins at spatial frequencies just above the classical resolution limit, which is taken as evidence that peripheral resolution is limited by the coarse spacing of visual neurons rather than by increased size of their receptive fields. At a given eccentricity, the very finest pattern which produces aliasing has a spatial period which approaches the smallest anatomical dimension: the diameter of a single cone photoreceptor.

Aliasing Periphery Acuity Detection

INTRODUCTION

Visual processing begins with the sampling of a continuous retinal image by an array of discrete neurons to produce an internal representation of the stimulus that Troland (1924) termed the "neural image". This sampling process is of fundamental importance because it imposes a limit on the ability of the neural image to represent faithfully the retinal stimulus. Just as for photographic film, a sparse array of light-detecting elements can only represent the image coarsely and is incapable of accurately representing a fine image. These intuitive ideas may be stated more precisely by appealing to the sampling theorem of communication theory (Shannon, 1949): veridical representation of a retinal stimulus is possible only for components with spatial frequencies below a critical resolution limit, as set by the spacing between neurons. Retinal image components above this resolution limit may still be signalled by the neural array, but they will be misrepresented and appear as components below the resolution limit. This false representation of the stimulus is called "aliasing" and is due to the fact that a

sparse sampling array can only support coarse neural images.

Perceptually, aliasing is manifest as a kind of visual illusion that was first described for foveal vision over a century ago by Bergmann (1858; see appendix) and which has been characterized in detail recently by Williams (1985a, b). Ordinarily, the perceptual infidelity caused by aliasing would seem to be only a minor problem for central vision because ocular aberrations and diffraction will eliminate potentially troublesome, high-frequency components of the retinal image (Campbell and Gubish, 1966; Williams, 1985b). However, neurons in the peripheral retina are so coarsely spaced (Perry and Cowey, 1985) that even those image components of relatively low spatial frequency are beyond the resolution limit. As these images are probably passed by the eye's optics, (Green, 1970; Millodot *et al.*, 1975; Jennings and Charman, 1981) they should be detectable as an aliased pattern (Snyder *et al.*, 1986), which implies that aliasing may be important in determining the quality of peripheral vision.

Recently, the existence of aliasing in peripheral vision has been reported by several groups (Thibos and Walsh, 1985; Cheney and Thibos, 1986; Smith and Cas, 1986; Smith *et al.*, 1987; Coletta and Williams, 1986, 1987). Our purpose here is to report the range of spatial frequencies

*Present address: Ft Rucker, AL 36360, U.S.A.

†Present address: Brooks Air Force Base, TX 78235, U.S.A.

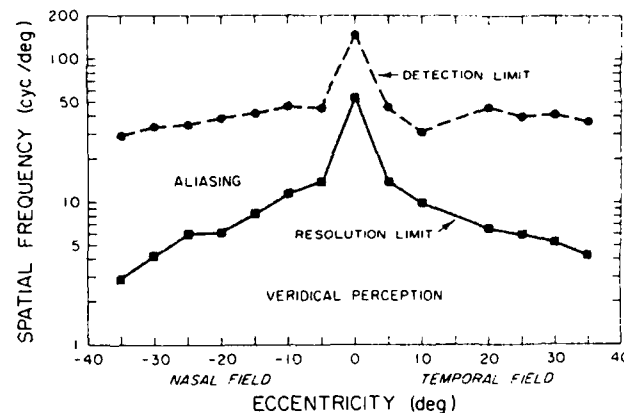


Fig. 1. The limiting spatial frequency for resolution (squares) and detection (circles) of sinusoidal, horizontal gratings varies with eccentricity from the fovea along the horizontal meridian in different ways for the same subject (L.N.T.). Symbols show the means of 5 determinations. Standard errors of the means are less than symbol radius in all cases. The detection value for central viewing is taken from Williams (1985b). The data separate the spectrum of visible spatial frequencies into a zone of veridical perception, which lies beneath the resolution limit, and a zone of aliasing, which extends from the resolution limit to the detection limit.

for which aliasing occurs and to assess the implications of these results for understanding the neural organization of the visual system.

METHODS AND RESULTS

Subjects viewed a white, sinusoidal grating of high contrast that was formed as interference fringes by an achromatic interferometer (Lotmar Visometer by Haag-Streit, Berne; see Lotmar, 1980) so as to avoid the defocusing effects of possible refractive errors. Lotmar's design is similar in principle to previously described, monochromatic interferometers (Le Grand, 1935; Westheimer, 1960) which image two coherent point sources near the nodal point of the eye so as to produce interference fringes directly on the retina. The enhancement provided by an achromatic interferometer is that pairs of coherent sources are produced for each wavelength of the visible spectrum, resulting in a multitude of interference patterns (all of the same spatial frequency and phase) which superimpose to produce a high-contrast, white grating (for further description see Thibos *et al.*, 1987). Stimulus diameter subtended 3.5 deg for all eccentricities except 5 deg, where it subtended 2.5 deg. The grating patch had a mean retinal illuminance of 4300 Trolands and was surrounded by a uniform, white field of the same illuminance. Stimuli were placed on the horizontal meridian of the visual field of the right eye with the left eye occluded. Stimulus orientation was

randomly selected to be either horizontal, vertical, left or right oblique. As performance was generally best for horizontal gratings, only these results are reported here.

Our initial goal was to replicate the classic study of Wertheim (1894) to determine, for four subjects, how resolution varies with stimulus eccentricity from the fovea. Subjects reduced the grating's spatial frequency until the stimulus orientation could just be identified confidently. The mean of 5 such determinations was taken as a measure of the limit to resolution. Representative results, presented in Fig. 1, are in agreement with previous reports (Wertheim, 1894; Kerr, 1971). The resolution limit fell rapidly from a central value of 54 c/deg for this subject to just 6 c/deg at 20 deg of eccentricity and only 3 c/deg at 35 deg. Such confirmation of earlier work verified that our subjects were normal and that our experimental methods yielded the conventional view of peripheral resolution.

The first indication that gratings beyond the resolution limit could be seen emerged during the resolution experiment just described. Occasionally, subjects would stop at a suspiciously high spatial-frequency and at the same time would misidentify the stimulus orientation. When informed of their error, subjects were mildly surprised but when invited to look directly at the stimulus with central vision they were genuinely astonished. The peripheral grating they "saw" had much lower spatial frequency and different orientation from the one

actually presented. Clearly these subjects had experienced a compelling demonstration of the aliasing phenomenon. The aliasing percept was not immediately apparent to all subjects, however, which may help to explain why the phenomenon has not been widely reported previously. Some individuals found it difficult at first to attend to peripheral images and only through training under controlled conditions did they begin to appreciate the ambiguity of their percepts.

Subsequent observations of gratings over a range of spatial frequencies higher than the resolution limit indicated that, although very robust, the aliasing percept is highly unstable. Subjects often reported seeing a cavalcade of relatively coarse gratings of rapidly changing spatial frequency, orientation or position. Sometimes there appeared to be two gratings present simultaneously to give the impression of a checkerboard-type pattern. At other times the overall impression was of a shimmering, shifting pattern that would not remain fixed long enough to ascertain its true nature. The spatial scale of these perceptions was reported to be similar to that of gratings which were at or below the resolution limit for the same retinal locus, as would be expected if subjects were perceived the coarse neural image carried by a sparse array of visual neurons. Apparent contrast was reported to be high and diminished only when the stimulus frequency was set far beyond the resolution limit. At these very high frequencies, contrast disappeared and subjects could no longer detect the presence of aliased patterns.

The subjective appearance of these spurious perceptions provided valuable insight into the nature of the resolution task itself. By gradually reducing grating frequency from an initially high value, where spatial contrast was not yet apparent, we found that aliased patterns were highly visible over a broad range of spatial frequencies. Eventually, when the frequency was reduced far enough, a sharp transition point was reached where the ambiguity of aliasing vanished and the true nature of the stimulus became evident. It was this distinct transition in appearance of the stimulus from the ambiguous to the veridical that we eventually adopted as a new method for experimentally determining the resolution limit. This limit could be precisely determined ($SEM < 5\%$ of the mean in Fig. 1) as even a slight increases of spatial frequency beyond the resolution limit gave rise to the

aliasing phenomenon. Since the apparent contrast was high for gratings just below and just above the resolution limit, it became clear that the ambiguity introduced by aliasing, rather than a loss of perceived contrast, is the factor which limits visual resolution in the periphery.

We next sought to determine the upper limit to the spectrum of spatial frequencies which elicits aliasing. Starting at a high spatial frequency for which aliasing was not visible, subjects were asked to reduce the frequency of the horizontal grating until the appearance of spatial contrast was clearly evident. The mean of 5 such determinations was taken as a measure of the limit to detection and representative results are shown in Fig. 1. Comparison of the two sets of data in Fig. 1, which are for the same individual, shows that gratings were detected at frequencies far beyond the resolution limit at all eccentricities tested. Although our subjects observed aliasing for gratings above the resolution limit using central vision, we were unable to determine the upper limit to detection there because of a limitation of our interferometer (maximum spatial frequency = 90 c/deg). Therefore, to complete the comparison we have re-plotted the detection limit reported by Williams (1985b) for foveal viewing of interference fringes.

Three quantitative features of the data in Fig. 1 deserve mention. First, in contrast to previous reports (Hiltz and Cavonius, 1974; Virsu and Rovamo, 1979) we find the limits to pattern detection are substantially higher than the limits to resolution at every eccentricity. Second, performance declines with eccentricity faster for resolution than for detection. As a result, the bandwidth of spatial frequencies subject to aliasing increases from about one octave for central vision to about one decade for peripheral vision. Third, variability of the data was small for both resolution and detection tasks. The standard errors of the means of 5 settings were in the range 2–5% for all data in Fig. 1. This high degree of repeatability indicates that although the aliased percept is often unstable, the frequency at which it completely disappears, at both the high and low end, is sharply defined.

DISCUSSION

Evidently, the spectrum of visible spatial frequencies is partitioned into a region of veridical pattern perception, where visual objects are faithfully represented by the visual system, and

a region of aliasing where patterns are misrepresented. In everyday central vision, the entire spectrum of visible spatial frequencies is in the veridical zone because of the filtering effect of optical aberrations and diffraction. In peripheral vision, however, not only is the veridical spectrum much narrower but the appreciation of low frequencies is likely to be hampered by spurious image components produced by aliasing of high frequencies. Since our interferometer produced retinal images with spatial frequencies higher than the optical cutoff of the eye's optical system, there remains uncertainty about how much of the aliasing spectrum shown in Fig. 1 is relevant to ordinary vision when the retinal image is formed naturally. Nevertheless, it must be that some portion of the aliasing spectrum is applicable to natural peripheral vision because we have verified with numerous observers that peripheral viewing of conventional gratings drawn on paper can produce the aliasing illusion. This observation of aliasing under normal viewing conditions provides direct proof of the widely accepted claim (Green, 1970; Millodot *et al.*, 1975) that the optical quality of the human eye is not a limiting factor for resolution acuity in the periphery.

If optical factors do not limit peripheral acuity, then neural factors must. Present results provide a basis for deciding between two currents, long-standing hypotheses which explain how the neural structure of the peripheral retina limits acuity. The first hypothesis is based on the sampling theorem and identifies the spacing of neural receptive fields, probably ganglion cells of the retina, as the limiting factor (Polyak, 1941; Ten Doeschette, 1946; Weymouth, 1958). The second idea is that the root cause of poor acuity in the periphery is increased size of receptive fields of individual ganglion cells (Westheimer, 1981). Spatial integration across these large receptive fields reduces contrast of the neural image to a level below the threshold for perception of spatial contrast. The critical experiment which discriminates between these two hypotheses is to present a stimulus with spatial frequency just beyond the resolution limit. According to the sampling theory hypothesis, the stimulus should be visible because of aliasing but according to the receptive field hypothesis, the stimulus should look like a uniform field. Our observation of aliasing for such stimuli is clear evidence that it is the spacing, not the size, of receptive fields which limits peripheral visual acuity. Furthermore, the

receptive fields in question are evidently not of cones because the cone array is packed too closely to cause aliasing of a peripheral stimulus which is just above the psychophysical resolution limit (Thibos *et al.*, 1987). Instead, the aliasing appears to be the result of undersampling by the array of ganglion cells since their spacing closely predicts the lowest frequencies for which aliasing occurs, i.e. the resolution limit.

To detect the spatial contrast of a grating requires retinal neurons which integrate light over a region smaller than the grating's period. Our experiments indicate that the maximum detectable period for achromatic gratings is in the range 1–2 min of arc, a dimension which matches the diameter of individual cones in the peripheral retina (Polyak, 1941). Evidently, human peripheral vision is capable of detecting the presence of spatial contrast which exists over the smallest of anatomical scales. This extraordinary level of performance raises a challenging question for future research: of what functional utility is vision beyond the resolution limit?

Acknowledgements—We thank S. L. Guth and A. Bradley for critical reviews of this paper, J. Kubley for graphics and H. Brown and staff for technical assistance. We are indebted to H. Cheney for translating Bergmann's paper and to the Division of Patient Care, School of Optometry, Indiana University for loan of the interferometer. F. C. was supported by the U.S. Air Force Institute of Technology and D. W. was supported by the U.S. Army. This work was supported in part by an NIH grant (EY5109) to L. T.

REFERENCES

- Bergmann C. (1858) Anatomisches und Physiologisches über die Netzhaut des Auges. *Z. ration. Medicin.* 2, 83–108.
- Campbell F. W. and Gubish R. W. (1966) Optical quality of the human eye. *J. Physiol., Lond.* 186, 558–578.
- Cheney F. E. and Thibos L. N. (1986) Evidence of elongated receptive fields in human peripheral retina. *Invest. Ophthalm. visual Sci. Suppl.* 27, 341.
- Coletta N. J. and Williams D. R. (1986) Psychophysical estimate of parafoveal cone spacing. *J. opt. Soc. Am.* A3, p92.
- Coletta N. J. and Williams D. R. (1987) Undersampling by cones reverses perceived direction of motion. *Invest. Ophthalm. visual Sci., Suppl.* 28, 232.
- Green D. G. (1970) Regional variations in the visual acuity for interference fringes on the retina. *J. Physiol., Lond.* 207, 351–356.
- Helmholtz H. von (1911) *Treatise on Physiological Optics*, Vol. 2. (Edited by Southall J. P. C.). Opt. Soc. Am. 1924.
- Hiltz R. and Cavonius C. R. (1974) Functional organization of the peripheral retina: sensitivity to periodic stimuli. *Vision Res.* 14, 1333–1338.
- Jennings J. A. M. and Charman W. N. (1981) Off-axis image quality in the human eye. *Vision Res.* 21, 445–455.

- Kerr J. L. (1971) Visual resolution in the periphery. *Percept. Psychophys.* 9, 375-378.
- Le Grand Y. (1935) Sur la mesure de l'acuité visuelle au moyen de franges d'interférence. *C. r. Seances Acad. Sci.* 200, 400.
- Lotmar W. (1980) Apparatus for the measurement of retinal visual acuity by moiré fringes. *Invest. Ophthalm. visual Sci.* 19, 393-400.
- Millodot M., Johnson A. L., Lamont A. and Leibowitz H. W. (1975) Effect of dioptrics on peripheral visual acuity. *Vision Res.* 15, 1357-1362.
- Perry V. H. and Cowey A. (1985) The ganglion cell and cone distributions in the monkey's retina: implications for central magnification factors. *Vision Res.* 25, 1795-1810.
- Polyak S. L. (1941) *The Retina*. Univ. Chicago Press, Chicago.
- Shannon C. E. (1949) Communication in the presence of noise. *Proc. I.R.E.* 37, 10-21.
- Smith R. A. and Cass P. (1986) Aliasing with incoherent-light stimuli. *J. opt. Soc. Am.* A3, P93.
- Smith R. A., Cass P. and Swift D. J. (1987) Aliasing with natural light in the parafovea. *Invest. Ophthalm. visual Sci. Suppl.* 28, 137.
- Snyder A. W., Bossomaier T. R. J. and Hughes A. (1986) Optical image quality and the cone mosaic. *Science, N.Y.* 231, 499-501.
- Ten Doesschate J. (1946) Visual acuity and distribution of perceptive elements on the retina. *Ophthalmologica* 112, 1-18.
- Thibos L. N., Cheney F. E. and Walsh D. J. (1987) Retinal limits to the detection and resolution of gratings. *J. opt. Soc. Am.* A4, 1524-1529.
- Thibos L. N. and Walsh D. J. (1985) Detection of high frequency gratings in the periphery. *J. opt. Soc. Am.* A2, P64.
- Troland L. T. (1924) The optics of the nervous system. *Am. J. Physiol. Opt.* 5, 127-153.
- Virsu V. and Rovamo J. (1979) Visual resolution, contrast sensitivity and the cortical magnification factor. *Expl Brain Res.* 37, 475-494.
- Wertheim Th. (1894) Peripheral visual acuity. Translated by Dunskey I. L. (1980). *Am. J. Optom. Physiol. Opt.* 57, 919-924.
- Westheimer G. (1960) Modulation thresholds for sinusoidal light distribution on the retina. *J. Physiol., Lond.* 152, 67-74.
- Westheimer G. (1981) Visual Acuity. In *Adler's Physiology of the Eye* (Edited by Moses R. A.), pp. 530-544. Mosby, St Louis, Mo.
- Weymouth F. W. (1958) Visual sensory units and the minimal angle of resolution. *Am. J. Ophthalm.* 46, 102-113.
- Williams D. R. (1985a) Visibility of interference fringes near the resolution limit. *J. Opt. Soc. Am.* A2, 1087-1093.
- Williams D. R. (1985b) Aliasing in human foveal vision. *Vision Res.* 25, 195-205.

APPENDIX

Historical Note

During the writing of this paper we traced the reference by Helmholtz (1911) to Bergmann's (1858) remarkable paper which gives perhaps the first report of the aliasing phenomenon. His careful observations and incisive explanations are evidently not widely known so are briefly summarized below.

Bergmann's stimulus was a circular patch (20 mm diameter) of square-wave grating (2 mm period). He found that he could repeatedly resolve the grating when viewed from 5 m, which indicates his resolution limit of 44 c/deg was not unduly limited by refractive errors (he was a corrected myope). When he stepped back to 5.5 m (48 c/deg), however, the target occasionally looked checkered (*scheckig*) or sometimes like a grating with the wrong orientation. A second observer, who did not know the stimulus was a grating, also reported that the target looked checkered (*gewurfelt*). This visual illusion was brief and intermittent. Bergmann recognized the importance of correctly identifying the grating's orientation as proof of resolution and so arranged for an assistant to vary the orientation between observations. With careful and repeated observation it became clear that at 5 m he could reliably identify the grating's orientation but that many mistakes occurred at 5.5 m.

Bergmann explained his visual illusion in terms of spatial sampling by the foveal cone mosaic. Based on his own light microscopy of fresh human retina, he gave a quantitative description of how the regular, hexagonal array of cones will falsely represent a high-frequency grating as a grating of lower spatial frequency and different orientation. He pointed out that the important factor for producing an illusory grating percept is the regularity of the cone mosaic rather than the shape of individual cones or the hexagonal symmetry of the cone mosaic. Bergmann's clear understanding of the phenomenon and its basis leaves little doubt that the illusion he discovered is what we call aliasing.

Retinal limits to the detection and resolution of gratings

L. N. Thibos, F. E. Cheney, and D. J. Walsh

School of Optometry, Indiana University, Bloomington, Indiana 47405

Received November 21, 1986; accepted March 2, 1987

The maximum spatial frequency for the detection and resolution of sinusoidal gratings was determined as a function of stimulus location across the visual field. Stimuli were produced directly on the retina as interference fringes, thus avoiding possible loss of image quality, which may occur when the optical system of the eye is used to form the retinal image. Contrary to earlier reports, we found that subjects could detect gratings with spatial frequencies much higher than the resolution limit. At 5° of eccentricity from the fovea, the detection limit was about three times the resolution limit, and this factor increased to about 10 as the test stimulus was moved 35° into the periphery. Quantitative comparison of the data with retinal anatomy and physiology suggests that pattern resolution is limited by the spacing of primate beta (midget) retinal ganglion cells, whereas pattern detection is limited by the size of individual cones.

INTRODUCTION

One of the goals of vision research is to account for limitations of visual performance by the underlying structure of the visual system. For example, textbooks typically offer cone spacing as the factor that limits pattern resolution in central vision. In peripheral vision, it is generally thought that pooling of receptor signals by retinal ganglion cells reduces the resolving capacity of the eye. Surprisingly, the equally important question of what limits our ability to detect patterns has not been so thoroughly debated, perhaps because previous experiments have failed to show any significant differences between the spatial-frequency limits to detection^{1,2} and to resolution.²⁻⁹

Two recent events indicate that a reexamination of these conventional views is timely. First, new experiments in humans and other primates are providing the detailed anatomical data necessary for a critical evaluation of the twin hypotheses that pattern detection and pattern resolution are limited by the neural architecture of the retina. Second, by generating interference fringes directly upon the retina so as to avoid optical limitations, it has been shown for both foveal^{10,11} and peripheral vision¹² that patterns may be reliably detected even though they are too fine to be resolved. Under ordinary viewing conditions, patterns beyond the neural resolution limit are eliminated from the foveal retinal image by the optical system of the eye.¹³ However, the peripheral retina may not be protected in the same way. Although optical quality declines in peripheral vision, the neural resolution limit appears to fall even more rapidly with eccentricity.^{5,14} Consequently, it seems likely that under normal circumstances the peripheral retina will be stimulated by images that it cannot resolve. The utility of such patterns is, at present, unknown, but their existence suggests the possibility of useful vision beyond the resolution limit.¹⁵⁻¹⁷

Our purpose here is to report on new measurements that quantify the relationship between the spatial-frequency limits to detection and to resolution of gratings across the visual field. A comparison of these results with the size and spacing of retinal neurons leads us to suggest that, when optical

factors are removed, grating resolution is limited by the spacing of beta (midget) retinal ganglion cells, whereas pattern detection is limited by the size of individual cones.

METHODS

Apparatus

A Lotmar visometer¹⁸ (Haag-Streit, Berne) was used to produce white, sinusoidal gratings directly upon the retina as interference fringes. The design of the visometer is similar in principle to that of previously described, monochromatic, Maxwellian-view interferometers.^{19,20} A diffraction grating illuminated by collimated light from a tungsten lamp produces a diffraction pattern from which two coherent point sources are isolated. A lens in the instrument then images these sources near the nodal point of the observer's eye. The angular period subtended at the nodal point of the eye by the resulting fringes is given by the ratio λ/s , where λ is the wavelength of light and s is the spacing of the point sources.

The enhancement offered by Lotmar's achromatic visometer is that, by diffracting white light, pairs of coherent sources are produced for each wavelength of the visible spectrum. It is a property of diffraction by a grating that the scale of the pattern so produced is proportional to wavelength.²¹ It therefore follows that the ratio λ/s , which defines the period of the interference fringes on the retina, will be invariant with wavelength. The resulting visual stimulus thus consists of a multitude of interference patterns, each of a different color but of the same spatial frequency and spatial phase. These superimpose to produce a high-contrast, white grating.

We verified that the different spectral components were proportionally spaced by direct microscopic measurement of the real image of the coherent sources in air. Narrow bands (5-nm half-width) of the spectrum were isolated by interposing a series of interference filters covering the range from 450 to 650 nm in steps of 50 nm. Separation of the sources was then measured, with accuracy of about 5%, using a calibrated graticule on the eyepiece of the microscope, and found to

agree with theory to within the accuracy of the measurements. Visual inspection of the interference gratings formed in air confirmed that the pattern was of high contrast and entirely white. Similarly, when the fringes were formed on the retina, observers reported the pattern to be of high contrast and achromatic.

The advantages of the achromatic interferometer include high retinal illumination, insensitivity to refractive errors, and absence of speckle noise associated with laser techniques. A potential limitation of the instrument arises, however, when it is positioned off the optic axis of the eye to produce stimuli in the peripheral visual field. This is because the prismatic effect of lateral chromatic aberration induces a wavelength-dependent shift of the grating. This, in turn, will reduce image contrast of peripherally viewed gratings that are oriented orthogonally to the visual meridian.^{22,23} To avoid introducing this optical effect into the present analysis, we report only on those results obtained with horizontal gratings located on the horizontal meridian, since this stimulus condition is unaffected by lateral chromatic aberration. For additional control experiments requiring monochromatic light, an interference filter (550 nm) was placed between the tungsten light source and the visometer.

A field stop limited the grating to a circular patch 3.5° in diameter for all stimulus eccentricities except 5°, where the stimulus diameter was reduced to 2.5°. The retinal illuminance of the grating patch was 3.6 log Td for white light and 2.4 log Td for monochromatic light. The stimulus was surrounded by a large, white uniform field with luminance adjusted by the subject to match that of the grating. Spatial frequency was continuously adjustable over the range 0–90 cycles/degree (cyc/deg) and was recorded during experiments to the nearest 0.3 cyc/deg.

The visometer was mounted on a gimbal that permitted the stimulus to be positioned at selected locations in the visual field while the subject maintained constant fixation on a 0.86° target consisting of concentric circles and radiating lines. This fixation target was 6 m straight ahead, the subject's head was held erect, and the eyes were in the primary position. The center of rotation of the gimbal coincided with the midpoint of the two coherent sources imaged by the visometer. This common reference point was placed near the pupil plane of the subject's eye, and final alignment was achieved by slight adjustment of the subject's bite bar.

Procedure

Three observers took part in the study, two who were experienced in making psychophysical judgments (LT and AB) and one who had no previous experience (FC). Visual stimuli were placed at selected positions along the horizontal meridian of the right eye with the left eye occluded. One subject (LT) was tested with gratings located on both the temporal and the nasal horizontal meridian, whereas the other two subjects (FC and AB) were tested only in the nasal visual field. Stimulus orientation was randomly selected to be either horizontal or vertical, left or right oblique. Only the results for horizontal gratings are presented here. Resolution thresholds were determined by having the subject reduce the grating's spatial frequency until the stimulus orientation could just be correctly identified with confidence. To determine detection thresholds, subjects re-

duced spatial frequency until the presence of spatial contrast was evident. For this detection task, there was no requirement that the percept be of a grating, although subjects often reported seeing patterns that resembled gratings.¹⁷ Each threshold value reported in the section entitled Results represents the mean of five such determinations.

RESULTS

Resolution and detection thresholds for three subjects are compared in Fig. 1 for the eccentricity range 0°–35°. Open symbols indicate mean ($n = 5$) cutoff spatial frequency for the resolution task, and filled symbols are for the detection task. In every case the standard error of the mean was less than 5% of the mean, which is slightly less than the diameter of the symbols used in Fig. 1. Data shown in Fig. 1 were obtained by using horizontal gratings located on the horizontal visual meridian. Values obtained for other stimulus orientations were typically less, a result possibly due to the contrast-degrading effects of lateral chromatic aberration²⁴ (see section entitled Methods). The main result, to be described in more detail below, is that detection performance far exceeds resolution performance throughout the visual field.

Maximum-resolvable spatial frequency for grating patterns fell rapidly with stimulus eccentricity. The initial steep decline over the parafoveal range 0°–5° was not measured in detail, as the main thrust of our study was to characterize peripheral vision. Over the eccentricity range from 5° to 35°, the average resolution threshold for our three subjects fell from 14 to 2.6 cyc/deg. When plotted on semilogarithmic coordinates, the average data for eccentricities beyond 5° were well fitted by a straight line, indicating an exponential decline of maximum-resolvable frequency with eccentricity. The rate of decline was such that resolution was halved for every 12° increase of eccentricity. Results

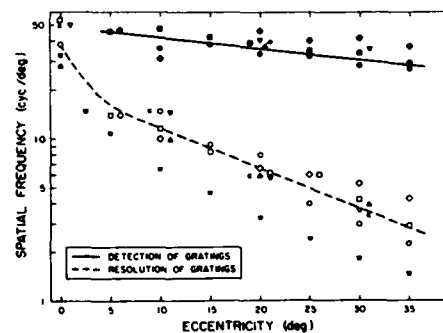


Fig. 1. Variation of maximum-resolvable (open symbols) and maximum-detectable (filled symbols) spatial frequency across the visual field. Each symbol represents the mean of five determinations for horizontal gratings located on the horizontal meridian. Subject LT was tested with white gratings located in either the nasal (squares) or temporal (inverted triangles) visual fields, while subjects FC (circles) and AB (triangles) were tested only in the nasal visual field. As a control against the possible effects of chromatic aberration, subjects LT (diamonds) and AB (asterisk) were also tested using monochromatic (550-nm) gratings. Smooth curves were drawn by eye through the means of the results for the three subjects viewing white-light gratings. Published data of Kerr⁶ (K) and of Wertheim³ (W) obtained with conventional visual stimuli are also shown.

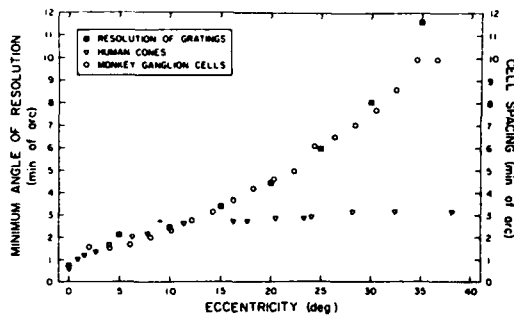


Fig. 2. Comparison of the MAR with spacing of retinal cells. Psychophysical data (filled squares; left ordinate) represent the mean results from Fig. 1 for three subjects viewing white gratings. Spacing of beta ganglion cells in monkey retina measured by Perry *et al.*²⁹ (circles; right ordinate) and cone spacing measured by Osterberg³³ (inverted triangles; right ordinate) were calculated from published data by assuming that spacing = $1/\sqrt{\text{density}}$.

about the same as the spacing of cones. That prediction is based, in turn, on anatomical evidence that foveal ganglion cells of the human retina are mainly of the midget class, a cell type characterized by one-to-one connectivity with cones through midget bipolar cells.³⁰ The above chain of inference gains some credence from the fact that the cone spacing,^{33,34} also shown in Fig. 2, and the MAR converge at the fovea to the common value of about 0.5 arcmin. Beyond about 10° into the periphery, however, the curves diverge with the psychophysical data following the spacing of ganglion cells, not cones. We therefore conclude that peripheral cones are spaced too closely to be a limiting factor for visual resolution.

Retinal Limits to Detection

If a visual neuron is to make a strong contribution to the detection of spatial contrast in a grating pattern, it should integrate light over a region that is small compared with the period of the gratings.³⁴ Each neural link in the chain from receptor to bipolar to ganglion cell provides an opportunity for convergence of signals and a broadening of the functional receptive field. Thus, if the retina limits pattern detection, then it will be because of the size of the largest receptive field in the sequence, presumably the ganglion cells. Although a precise theoretical assessment of the highest-detectable frequency will depend on signal-to-noise ratio considerations,^{15,35} a useful first approximation is to assume that the detection limit is met when one cycle of the grating just spans the center component of the neuron's receptive field. By analogy with the MAR measure of resolution, let the half-period of the finest-detectable grating be called the minimum angle of detection (MAD). If we let R be the radius of the center component of the receptive field, then the assumed relationship is

$$\text{MAD} = R. \quad (2)$$

This approximate relationship can be justified from first principles for the integrating receptive field of a cone photoreceptor^{34,35} and, according to physiological experiments in cat,³⁶ is not an unreasonable assumption for retinal ganglion cells.

Previous experiments have established that the minimum angle of detection for foveal vision¹¹ and the radius of foveal cones³⁴ are both about 0.25 arcmin. This match has been taken as evidence that foveal pattern detection is limited by the size of individual cones and is consistent with the argument that a midget ganglion cell of the fovea probably receives its primary input from a single cone.³⁰ Although it seemed unlikely that receptor size might also limit detection in peripheral vision, we tested this hypothesis by comparing in Fig. 3 the mean results for our three subjects with Polyak's measurements of human cone radius.³⁷ Surprisingly, a close agreement emerged that strongly suggests that, when optical factors are eliminated, human detection of spatial contrast in both central and peripheral vision is limited by the size of cone photoreceptors.

This conclusion leaves us with an intriguing puzzle. Why does subsequent pooling of receptor signals by retinal ganglion cells not increase the minimum angle of detection in peripheral vision? To estimate the expected increase in the MAD that is due to ganglion-cell pooling, available measurements of the radius of receptive fields in rhesus retina³⁸ and LGN³⁹ are included in Fig. 3. Many factors, including optical ones, tend to lower the detection limit of recorded cells, so it is believed that the smallest receptive fields encountered with the microelectrode give the best estimates for the population.³⁸ Accordingly, we have replotted in Fig. 3 only the smallest receptive-field dimensions reported. These physiological measurements indicate that, for cells within 5° of the foveal center, the smallest receptive fields have center components about the size of single cones, which is consistent with present psychophysical results. However, more peripherally the fields are much larger, and these individual neurons are unable to signal the presence of very fine patterns that human observers are still able to detect.

Also shown in Fig. 3 are measurements of dendritic-field radius for midget ganglion cells in human retina.⁴⁰ These anatomical data are plotted on the basis of the angular magnification of the Gullstrand schematic eye, 5 $\mu\text{m}/\text{arcmin}$.

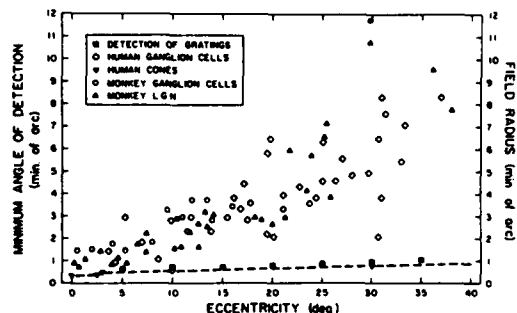


Fig. 3. Comparison of the MAD with the radius of retinal fields. Psychophysical data (filled squares; left ordinate) represent the mean results from Fig. 1 for three subjects viewing white gratings. Anatomical measurements of dendritic fields⁴⁰ (diamonds; right ordinate) and cones³⁷ (inverted triangles; right ordinate) are for human. Physiological measurements of the size of the center component of receptive fields of the smallest retinal ganglion cells³⁸ (circles; right ordinate) and LGN neurons³⁹ (triangles; right ordinate) are for rhesus monkey. Dashed curve is the predicted limit to detection if cone size is the limiting factor.

from our three subjects were in close agreement with one another and with previous results obtained when both interferometric^{7,8} and conventional^{6,9} gratings were used.

Maximum-detectable spatial frequency for the same observers fell slowly with stimulus eccentricity. Over the eccentricity range from 5° to 35°, the average detection threshold for our three subjects dropped from 46 to 28 cyc/deg. Average results fell exponentially with eccentricity at a rate such that detection was halved for every 43° increase of eccentricity. Because performance changed at a different rate for the two psychophysical tasks, the ratio of maximum-detectable frequency to maximum-resolvable frequency increased from about 3 at 5° to about 10 at 35°. We were unable to measure the maximum-detectable frequency for foveal vision, probably because of a limitation of the visual stimulator. Previous experiments¹¹ have indicated that the detection limit is about 150 cyc/deg for foveal vision, whereas the maximum spatial frequency that can be generated by the Lotmar visometer is 90 cyc/deg.

CONTROL FOR CHROMATIC ABERRATION

In this paper we are concerned with the maximum-achievable visual performance, unencumbered by optical aberrations. For this reason, only the results obtained with horizontal gratings are described here. Nevertheless, it might be argued that some residual degree of chromatic aberration could have caused the results of Fig. 1 to be spuriously low. As a control against this possibility, one subject (LT) was retested in the resolution experiment, and two subjects (LT and AB) were retested in the detection experiment using monochromatic (550-nm) light at selected locations along the horizontal meridian. As is shown in Fig. 1, the results for white and monochromatic light were in close agreement, which indicates that chromatic aberration did not significantly affect performance in these experiments.

DISCUSSION

Comparison with Previous Results

The classic study by Wertheim³ remains the standard of comparison for modern studies of peripheral grating resolution. Although Wertheim expressed his data relative to foveal resolution, sufficient information was given to plot the data on absolute scales, as shown in Fig. 1. Also shown in Fig. 1 are Kerr's measurements of grating resolution, which are representative of more modern results.^{2,4-9} Present results support Kerr's conclusion that peripheral resolution can be significantly better than that reported by Wertheim.

Although our results are in agreement with published values for visual resolution, they are quite different for visual detection. Previous experiments^{1,2} that required subjects merely to detect gratings without necessarily resolving them yielded results not much different from those obtained with the resolution criterion. By contrast, our data indicate that the limits to pattern detection are substantially higher than the limits to resolution. Indeed, all three observers were able reliably to detect peripheral gratings that, when seen foveally, were difficult to resolve. As a result of this new finding, we have been led to the following reconsideration of

the anatomical factors that may act to limit visual performance on these two psychophysical tasks.

Retinal Limits to Resolution

Since the time of Helmholtz it has been argued that the ability to resolve fine spatial details is limited by the spacing S of receptive fields of those visual neurons that sample the retinal image. Retinal sampling is a multistage process beginning with phototransduction by receptors, followed by convergence of receptor signals onto bipolar cells and further convergence onto ganglion cells. Thus, if the retina limits pattern resolution, then it will be because of the spacing of receptive fields of the coarsest array of the sequence, the ganglion cells.^{4,25} For a square array of cells of density D cells per unit area, the finest grating that can be resolved (i.e., the Nyquist limit) has a half-period equal to the spacing constant of the array, $S = 1/\sqrt{D}$. This visual angle is traditionally called the minimum angle of resolution (MAR), and so for this simple model of retinal sampling we may state that

$$\text{MAR} = S = 1/\sqrt{D}. \quad (1)$$

An alternative model assuming a hexagonal array predicts values of the MAR that differ from those of Eq. (1) by only a few percent.²⁶

Earlier attempts^{2,4,27} to link human visual resolution with ganglion-cell spacing were limited by several factors including (1) the discrepancy between Wertheim's classic data and more modern results, (2) apparent underestimation of ganglion-cell density in earlier anatomical experiments,²⁸ and (3) the uncertainty about which subpopulation of the ganglion-cell array is responsible for pattern resolution in peripheral vision. Recent advances in the anatomical classification of ganglion cells in monkey²⁹ have suggested that 80% of ganglion cells in the primate retina are of the beta class, which is believed to be the same as Polyak's midsize class³⁰ and is also thought to be the morphological substrate of the color-opponent X cells that project to the parvocellular layers of the lateral geniculate nucleus (LGN).²⁹ To test the idea that this is the population of ganglion cells that supports visual resolution, we calculated the spacing of beta ganglion cells in the horizontal temporal retina, assuming (1) a square array with density equal to 80% of that reported²⁹ for all ganglion cells and (2) an angular magnification for rhesus of 4.1 $\mu\text{m}/\text{arcmin}$.²⁸

The calculated spacing of beta ganglion cells is shown as a function of retinal eccentricity in Fig. 2. Also shown in Fig. 2 are the mean resolution data for the three subjects of Fig. 1 (white light, nasal visual field), replotted as MAR's (i.e., half-period of the maximum-resolvable frequency). The two sets of data may be directly compared, according to the relationship stated by Eq. (1). The close agreement that is evident supports the proposition that visual resolution is limited by the spacing of beta ganglion cells of the retina. Furthermore, while we are mindful of the limitations of cross-species comparisons, these results suggest that on-cells and off-cells may not function as independent arrays in primates, as has been suggested for cat.^{25,31,32}

Textbook accounts usually offer cone spacing as the factor that limits resolution in central vision. That view is acceptable only because the spacing of ganglion-cell receptive fields in the foveal region of the human retina is probably

These data provide indirect estimates of the sizes of the center components of receptive fields of retinal ganglion cells. It has been well established by physiological experiments on both X-type and Y-type ganglion cells in cat retina that the dendritic field is the neural substrate of the center component of the receptive field.⁴¹ If the same holds also for humans, then most of the midsize ganglion cells represented in Fig. 3 appear to be much too large to support the high level of detection performance measured in our experiments.

One possible explanation for the discrepancy between psychophysical performance and ganglion-cell fields is that the smallest fields might not have been encountered in the physiological and anatomical experiments summarized in Fig. 3. DeMonasterio and Gouras mentioned³⁸ that receptive-field size of color-opponent cells increased only slightly with eccentricity, and so a larger sample of peripheral neurons might have uncovered receptive fields small enough to account for the psychophysical data. Also, Rodieck *et al.* commented⁴⁰ that they did not observe any of the midsize ganglion cells with very restricted dendritic fields such as those previously revealed by different histological techniques.^{30,42,43}

If there exists in human peripheral retina a small population of ganglion cells that have functional receptive fields the size of single cones, then our psychophysical data could be easily explained. Polyak³⁰ attached special significance to this arrangement, calling it the "monosynaptic pathway" of vision. Although this pathway is of major importance for central vision, its role in peripheral vision has remained obscure in spite of accumulating evidence of its presence throughout the retina.^{30,42,43} A hypothesis that a monosynaptic pathway supports pattern detection in both central and peripheral vision is not incompatible with the traditional view that ganglion cells of the peripheral retina integrate light over large areas covering many cones. While it is acknowledged that cones outnumber ganglion cells in peripheral retina, the degree of neural convergence is likely to be different for each class of retinal ganglion cell in human just as it is in cat.⁴⁴ Consequently, it is possible that some retinal ganglion cells will pool only a few cones, perhaps just one, even though the majority may pool many.

Other neural arrangements are also consistent with our results. A small degree of convergence of cone signals onto ganglion cells could be present and not markedly limit performance because, unlike in the foveal region, in the periphery cones are not closely packed.^{30,34} Given a grating with a half-period smaller than the cone spacing yet larger than the cone radius, individual cones will act as functional subunits that sample the sinusoidal stimulus at random locations. If the number of subunits is small, the sum may still be substantial, but, if the number of subunits is large, the sum will tend to zero. On the basis of this argument, we can exclude the possibility that detection is limited by X ganglion cells with large receptive fields that linearly combine the signals from many cones. Nonlinear summation of cone signals, however, is not excluded by this argument. The Y-type ganglion cells of cat retina, for example, have large receptive fields containing many nonlinear subunits,⁴⁵ yet these cells are able to signal the presence of high-frequency gratings.^{46,47}

ACKNOWLEDGMENTS

We thank A. Bradley, D. R. Williams, A. Hughes, and A. Snyder for helpful discussions and J. Kubley for graphics. The research of F. E. Cheney was supported by the U.S. Air Force Institute of Technology, and that of D. J. Walsh was supported by the U.S. Army. This research was supported by a National Institutes of Health grant (EY5109) to L. N. Thibos and was reported at the 1985 Annual Meeting of the Optical Society of America, where it received valuable criticism.

REFERENCES AND NOTES

1. R. Hiltz and C. R. Cavonius, "Functional organization of the peripheral retina: sensitivity to periodic stimuli," *Vision Res.* **14**, 1333-1338 (1974).
2. V. Virsu and J. Rovamo, "Visual resolution, contrast sensitivity and the cortical magnification factor," *Exp. Brain Res.* **37**, 475-494 (1979).
3. Th. Wertheim, "Peripheral visual acuity" (1894) [translated by I. L. Dunskey, *Am. J. Optom. Physiol. Opt.* **57**, 919-924 (1980)]. Wertheim's normalized eccentricity curves (Table 2) were put on an absolute scale by using the data from a second experiment (Table 1).
4. F. W. Weymouth, "Visual sensory units and the minimal angle of resolution," *Am. J. Ophthalmol.* **46**, 102-113 (1958).
5. D. G. Green, "Regional variations in the visual acuity for interference fringes on the retina," *J. Physiol. (London)* **207**, 351-356 (1970).
6. J. L. Kerr, "Visual resolution in the periphery," *Percept. Psychophys.* **9**, 375-378 (1971).
7. J. M. Enoch and G. M. Hope, "Interferometric resolution determinations in the fovea and parafovea," *Doc. Ophthalmol.* **34**, 143-156 (1973).
8. L. Frisen and A. Glansholm, "Optical and neural resolution in peripheral vision," *Invest. Ophthalmol.* **14**, 528-536 (1975).
9. J. Rovamo, V. Virsu, P. Laurinen, and L. Hyvarinen, "Resolution of gratings oriented along and across meridians in peripheral vision," *Invest. Ophthalmol. Vis. Sci.* **23**, 666-670 (1982).
10. D. R. Williams, "Visibility of interference fringes near the resolution limit," *J. Opt. Soc. Am. A* **2**, 1087-1093 (1985).
11. D. R. Williams, "Aliasing in human foveal vision," *Vision Res.* **25**, 195-205 (1985).
12. L. N. Thibos and D. J. Walsh, "Detection of high frequency gratings in the periphery," *J. Opt. Soc. Am. A* **2**, P64 (1985).
13. F. W. Campbell and R. W. Gubish, "Optical quality of the human eye," *J. Physiol. (London)* **186**, 558-578 (1966).
14. M. Millodot, A. L. Johnson, A. Lamont, and H. W. Leibowitz, "Effect of dioptrics on peripheral visual acuity," *Vision Res.* **15**, 1357-1362 (1975).
15. A. W. Snyder, T. R. J. Bossomaier, and A. Hughes, "Optical image quality and the cone mosaic," *Science* **231**, 499-501 (1986).
16. D. R. Williams, "Seeing through the photoreceptor mosaic," *Trends Neurosci.* **9**, 193-198 (1986).
17. L. N. Thibos, D. J. Walsh, and F. E. Cheney, "Vision beyond the resolution limit: aliasing in the periphery," submitted to *Vision Res.*
18. W. Lotmar, "Apparatus for the measurement of retinal visual acuity by moiré fringes," *Invest. Ophthalmol. Vis. Sci.* **19**, 393-400 (1980).
19. Y. Le Grand, "La formation des images rétiniennes. Sur un mode de vision éliminant les défauts optiques de l'œil," presented at the 2e Reunion de l'Institut d'Optique, Paris, 1937.
20. G. Westheimer, "Modulation thresholds for sinusoidal light distributions on the retina," *J. Physiol. (London)* **152**, 67-74 (1960).
21. J. W. Goodman, *Introduction to Fourier Optics* (McGraw-Hill, New York, 1968).
22. L. N. Thibos, "Calculation of the influence of lateral chromatic

- aberration on image quality across the visual field," J. Opt. Soc. Am. A 4, 1673-1680 (1987).
23. L. N. Thibos, A. Bradley, D. Still, and P. Henderson, "Do white-light interferometers bypass the eye's optics? Clinical implications of decentering the optical beam in the pupil," in *Digest of the Conference on Noninvasive Assessment of the Visual System* (Optical Society of America, Washington, D.C., 1987), pp. 80-82.
 24. F. E. Cheney, "The effect of lateral chromatic aberration on the detection of gratings in peripheral vision," M.S. thesis (Indiana University, Bloomington, Ind., 1987).
 25. A. Hughes, "New perspectives in retinal organisation," *Prog. Retinal Res.* 4, 243-313 (1985).
 26. The center-to-center spacing of an hexagonal array of density D is given by the formula $S^2 = 2/(D\sqrt{3})$. The MAR of such an array is $MAR = 0.5S\sqrt{3}$. Combining these formulas leads to the result $MAR = 0.93/\sqrt{D}$, which is not much different from Eq. (1).
 27. N. Drasdo, "The neural representation of visual space," *Nature* 266, 554-556 (1977).
 28. E. T. Rolls and A. Cowey, "Topography of the retina and striate cortex and its relationship to visual acuity in rhesus monkeys and squirrel monkeys," *Exp. Brain Res.* 10, 298-310 (1970).
 29. V. H. Perry, R. Oehler, and A. Cowey, "Retinal ganglion cells that project to the dorsal lateral geniculate nucleus in the macaque monkey," *Neuroscience* 12, 1101-1123 (1984).
 30. S. L. Polyak, *The Retina* (U. Chicago Press, Chicago, 1941).
 31. A. Hughes, "Cat retina and the sampling theorem; the relation of transient and sustained brisk-unit cut-off frequency to alpha- and beta-mode cell density," *Exp. Brain Res.* 42, 196-202 (1981).
 32. H. Wässle, B. B. Boycott, and R.-B. Illing, "Morphology and mosaic of on- and off-beta cells in the cat retina and some functional considerations," *Proc. R. Soc. London Ser. B* 212, 177-195 (1981).
 33. G. Osterberg, "Topography of the layer of rods and cones in the human retina," *Acta Ophthalmol. Suppl.* 6, 1-103 (1935).
 34. W. H. Miller and G. D. Bernard, "Averaging over the foveal receptor aperture curtails aliasing," *Vision Res.* 23, 1365-1369 (1983).
 35. A. W. Snyder and W. H. Miller, "Photoreceptor diameter and spacing for highest resolving power," *J. Opt. Soc. Am.* 67, 696-697 (1977).
 36. B. G. Cleland, T. H. Harding, and U. Tulunay-Keesey, "Visual resolution and field size: examination of two kinds of cat retinal ganglion cell," *Science* 205, 1015-1017 (1979).
 37. S. L. Polyak, *The Vertebrate Visual System* (U. Chicago Press, Chicago, 1957).
 38. F. M. DeMonasterio and P. Gouras, "Functional properties of ganglion cells of the rhesus monkey retina," *J. Physiol. (London)* 251, 167-195 (1975).
 39. A. M. Derrington and P. Lennie, "Spatial and temporal contrast sensitivities of neurones in lateral geniculate nucleus in macaque," *J. Physiol. (London)* 357, 219-240 (1984).
 40. R. W. Rodieck, K. F. Binmoeller, and J. Dineen, "Parasol and midget ganglion cells of the human retina," *J. Comp. Neurol.* 233, 115-132 (1985).
 41. L. Peichl and H. Wässle, "Size, scatter and coverage of ganglion cell receptive field centres in the cat retina," *J. Physiol. (London)* 291, 117-141 (1979).
 42. B. B. Boycott and J. E. Dowling, "Organization of the primate retina: light microscopy," *Philos. Trans. R. Soc. London Ser. B* 255, 109-184 (1969).
 43. H. Kolb, K. A. Lineberg, and S. Fisher, "A Golgi study of ganglion cells in the human retina," *Invest. Ophthalmol. Vis. Sci. Suppl.* 27, 203 (1986).
 44. W. R. Levick and L. N. Thibos, "Receptive fields of cat ganglion cells: classification and construction," *Prog. Retinal Res.* 2, 267-319 (1983).
 45. S. Hochstein and R. M. Shapley, "Linear and nonlinear spatial subunits in Y cat retinal ganglion cells," *J. Physiol. (London)* 262, 265-284 (1976).
 46. S. Hochstein and R. M. Shapley, "Quantitative analysis of retinal ganglion cell classifications," *J. Physiol. (London)* 262, 237-264 (1976).
 47. L. N. Thibos and W. R. Levick, "Orientation bias of brisk-transient Y-cells of the cat retina for drifting and alternating gratings," *Exp. Brain Res.* 58, 1-10 (1985).

Supplement to:
Investigative Ophthalmology & Visual Science
Vol. 27, March 1986

ARVO abstracts 341

9

EVIDENCE OF ELONGATED RECEPTIVE FIELDS IN HUMAN PERIPHERAL RETINA.
F. E. Cheney*, L.N. Thibos, School of Optometry, Department of
Visual Sciences, Indiana University, Bloomington, IN. 47405,

Last year Thibos and Walsh (OSA, Digest Tech Papers, p.74, 1985) reported that peripheral gratings with spatial frequencies considerably higher than the resolution limit could elicit unusual and unexpected percepts. At very high frequencies subjects saw random noise which then became interspersed with brief percepts of grating-like patterns as the spatial frequency was reduced. As the subject continued to reduce the spatial frequency toward the resolution limit, the grating percepts became more persistent but they remained unstable. Subjects reported a sequence of gratings of rapidly changing orientation and relatively low spatial frequency. Thibos and Walsh concluded that the percepts were due to aliasing probably caused by the relatively low sampling density of ganglion cells in the peripheral retina.

Our study explored this aliasing phenomenon further by determining the highest spatial frequency which produced the percept of a persistent, grating-like pattern as a function of stimulus orientation. The stimulus was a high contrast achromatic grating formed on the retina as interference fringes (Lotmer Visometer, Invest. Oph. Vis. Sci. 19, p. 393, 1980). We used four different stimulus orientations (45°, 90°, 135°, 180°) in each of eight primary meridians at 20° eccentricity. Observers could consistently detect gratings oriented parallel to the visual meridian at higher spatial frequencies than they could for other stimulus orientations. These results suggest that receptive fields of retinal ganglion cells are elongated along meridians in humans as they are in cats.

*Captain, USAF, sponsored by Air Force Institute of Technology.

PSYCHOPHYSICAL EVIDENCE OF A MONOSYNAPTIC PATHWAY IN HUMAN PERIPHERAL VISION
*L.N. Thibos and F.E. Cheney, School of Optometry, Indiana University,
 Bloomington, IN., 47405, U.S.A.*

On the basis of his observations using light microscopy, Polyak (1941) described a "private" visual pathway from individual cones to individual midget ganglion cells. The key link of this "monosynaptic" pathway is the midget bipolar cell, which receives synaptic input from a single cone and delivers synaptic output to a single midget ganglion cell (Dowling & Boycott, 1966). This monosynaptic pathway provides foveal vision with fine spatial resolution and is generally thought to underlie a "point-to-point" representation of the visual world in the brain. Less certain is the role of the monosynaptic pathway in peripheral vision. Anatomical evidence clearly shows the pathway exists in peripheral retina, but until now a corresponding psychophysical demonstration of the pathway has been lacking.

Observers saw in Maxwellian view a sinusoidal grating of high contrast that was produced directly on the retina by an interferometer. The grating was limited to a patch 3.5 deg in diameter, was 3.6 log Td. in mean retinal illuminance, and was surrounded by a uniform field of the same illuminance. Stimulus location was varied from 5 to 35 deg in the peripheral visual field. The observer's task was to adjust the spatial frequency of the grating until luminance contrast was just detectable. Under these conditions, observers were able to detect gratings with spatial frequencies as much as an order of magnitude beyond the resolution limit. This occurs because spurious low frequency signals are generated by the sampling mosaic of retinal neurons, a phenomenon called aliasing.

The minimum detectable period for gratings falls only slightly with eccentricity from the fovea and is typically in the range 1-2 min of arc. This is about the diameter of individual cones of the peripheral retina (Polyak, 1941). Since grating detection requires neurons which integrate light over a region smaller than the grating's period, it appears that some optic nerve fibers serving human peripheral vision have receptive field units which approach the size of single cone photoreceptors. Thus present results are consistent with the hypothesis that detection of high-frequency patterns in the peripheral visual fields is mediated by the monosynaptic retinal pathway.

Dowling, J.E. & Boycott, B.B. (1966) *Proceedings of the Royal Society*, B166, 80-111.

Polyak, S.K. (1941) *The Retina*. Chicago: University Press.

P.C. 5

What limits faithful encoding of spatial patterns in human peripheral vision?

BY F. E. CHENEY, D. L. STILL, L. N. THIBOS and D. J. WALSH (introduced by COLIN BLAKEMORE). *School of Optometry, Indiana University, Bloomington, IN 47405, U.S.A.*

Three long-standing hypotheses are available to explain why grating resolution is worse for peripheral vision than for central vision. The first is that retinal image contrast is lost in the periphery because of off-axis aberrations. The second is that the root cause of poor acuity in the periphery is increased size of receptive fields of individual ganglion cells. Spatial integration across these large receptive fields reduces contrast of the neural image to a level below the threshold for perception. The third is based on the sampling theorem of communication theory and identifies the spacing of neural receptive fields, probably ganglion cells of the retina, as the limiting factor.

A critical experiment which discriminates the first two hypotheses from the third is to present a stimulus with spatial frequency just beyond the resolution limit. If contrast is lost because of optical blurring or because of spatial integration by receptive fields, the stimulus should look like a uniform field. However, according to the sampling-theory hypothesis, a stimulus which is not resolvable may still be visible because of aliasing.

We have performed this experiment for a 3 deg patch of high-contrast grating located anywhere from 10 to 30 deg of eccentricity along eight different meridians. Correct identification of stimulus orientation was taken as the criterion for resolution. In the first experiment we produced the grating stimulus as an interference pattern directly on the retina, thus avoiding optical limitations. The limiting spatial frequency for resolution was determined by method of adjustment. In the second experiment, gratings were formed on the face of a cathode-ray tube and viewed directly through spectacle lenses which corrected refractive errors. The limiting frequency for resolution was determined by a two-interval forced-choice comparison of two gratings identical except for their orientation.

The results of both experiments indicated that gratings just beyond the resolution limit are highly visible as aliases of the stimulus. Subjects reported that subjectively the stimulus appeared to be a high-contrast, coarse spatial pattern which sometimes resembled a grating of a different orientation. Although performance was at chance level for resolution, it was error-free for stimulus detection in another 2AFC experiment comparing grating with a uniform field. These observations of aliasing for stimuli just beyond the resolution limit indicate that peripheral resolution is not limited by a loss of contrast in the optical or neural image. Instead, it is the ambiguity of aliasing which limits pattern resolution as predicted by the sampling theorem.

Journal of the Optical Society of America, vol A4, page P79
(1987)

**WT1 Orientation anisotropy for the detection of
allased patterns by peripheral vision is optically
induced**

F. E. CHENEY, LARRY N. THIBOS, Indiana U.,
School of Optometry, Department of Visual Sci-
ences, Bloomington, IN 47405.

Detection of aliasing varies throughout the pe-
ripheral visual field in a systematic way we call
radial tuning; the cutoff spatial frequency is always
maximized when the grating is oriented radially.¹
Because this orientational anisotropy occurs for
grating stimuli produced as interference fringes
directly on the retina with an achromatic interfer-
ometer, we suggested previously that radial tuning
is of neural, not optical, origin. New theoretical
analysis has caused us to reconsider the basis of
radial tuning.

Lateral chromatic aberration of the eye induces
a wavelength-dependent phase shift which attenu-
ates retinal contrast even when the stimulus is
produced interferometrically.² This contrast at-
tenuation varies with stimulus orientation and is
minimal for radial fringes, thus accounting, per-
haps, for the radial bias found psychophysically.
To test this hypothesis, two new experiments were
devised to avoid the deleterious effects of chro-
matic aberration. The first was to translate the
interferometer so that its light rays were normal to
the corneal refracting surface. The second was to
filter the white light of the interferometer to make it
nearly monochromatic. In both cases the cutoff
frequency for detection became independent of
orientation, thus supporting the optical explanation
of radial tuning.

(12 min)

1. F. E. Cheney and L. N. Thibos, Invest. Ophthal-
mol. Visual Sci. Suppl. 27, 341 (1986).
2. L. N. Thibos *et al.*, in *Technical Digest, Topical
Meeting on Noninvasive Assessment of the Vi-
sual System* (Optical Society of America,
Washington, DC, 1987), pp. 80-82.

VITA

Frank E. Cheney, Jr.

Education:

Undergraduate: 1969 - B.A. University of Pennsylvania
1972 - B.S. Pennsylvania College of Optometry

Graduate: 1974 - O.D. Pennsylvania College of Optometry
1989 - M.S. Indiana University
(Physiological Optics)

Optometry Board Certification

New Jersey
Pennsylvania

Professional Experience

1974-1978 Raymond Adams, M.D. (Ophthalmologist)
Cherry Hill, New Jersey
Staff Optometrist

1978-1980 USAF Hospital
Fairchild AFB, Spokane, WA
Staff Optometrist

1980-1981 USAF Hospital
Fairchild AFB, Spokane WA
Chief, Optometry Services

1981-1984 USAF Hospital
Bitburg AB, Bitburg, Germany
Chief, Optometry Services

1984-1986 Indiana University
Bloomington Indiana
Graduate Studies, Physiological Optics

1986 USAF School of Aerospace Medicine
Brooks AFB, San Antonio, Texas
Research Optometrist